Structural Analysis of Regular Multi-Storey Buildings

KAROLY A. ZALKA

CRC Press
Taylor & Francis Group
A SPON BOOK

Structural Analysis of Regular Multi-Storey Buildings

This page intentionally left blank

Structural Analysis of Regular Multi-Storey Buildings

KAROLY A. ZALKA

CRC Press
Taylor & Francis Group
Boca Raton London New York

CRC Press is an imprint of the
Taylor & Francis Group, an **informa** business
A SPON PRESS BOOK

CRC Press
Taylor & Francis Group
6000 Broken Sound Parkway NW, Suite 300
Boca Raton, FL 33487-2742

Version Date: 20120625

International Standard Book Number-13: 978-0-203-84094-8 (eBook - PDF)

Visit the Taylor & Francis Web site at
http://www.taylorandfrancis.com

and the CRC Press Web site at
http://www.crcpress.com

Contents

Notations

CAPITAL LETTERS

A	cross-sectional area; area of plan of building; floor area; corner point
A_a	area of lower flange
A_b	cross-sectional area of beam
A_c	cross-sectional area of column
A_d	cross-sectional area of diagonal bar in cross-bracing
A_h	cross-sectional area of horizontal bar in cross-bracing
A_f	area of upper flange
A_g	area of web
A_o	area of closed cross-section defined by the middle line of the walls
B	plan breadth of the building (in direction y); constant of integration
B_l	local bending stiffness for sandwich model
B_o	global bending stiffness for sandwich model
C	centre of vertical load/mass; centroid; constant of integration
D	constant of integration
E	modulus of elasticity; constant of integration
E_c	modulus of elasticity of columns; modulus of elasticity of concrete
E_d	modulus of elasticity of diagonal bars in cross-bracing
E_h	modulus of elasticity of horizontal bars in cross-bracing
E_s	modulus of elasticity of steel
E_w	modulus of elasticity of shear wall
F	concentrated load (on top floor level); resultant of horizontal load
F_{cr}	critical concentrated load (on top floor level)
$F_{cr,}$	critical load for pure torsional buckling (for concentrated top load)
F_g	full-height (global) bending critical load (for concentrated top load)
F_l	full-height (local) bending critical load (for concentrated top load)
F_t	Saint-Venant torsional critical load (for concentrated top load)
F_ω	warping torsional critical load (for concentrated top load)
G	modulus of elasticity in shear
(GJ)	Saint-Venant torsional stiffness
$(GJ)_e$	effective Saint-Venant torsional stiffness
H	height of building/framework/coupled shear walls; horizontal force
I	second moment of area
I_{ag}	auxiliary constant
$I_{\omega g}$	auxiliary constant
I_b	second moment of area of beam
I_c	second moment of area of column

I_f sum of local and global second moments of area
I_g global second moment of area of the columns of the framework
$I_{g\omega}$ global warping torsional constant
I_o polar second moment of area
I_x, I_y second moments of area with respect to centroidal axes x and y
I_{xy} product of inertia with respect to axes x and y
I_w second moment of area of wall
I_Ω warping (bending torsional) constant
J Saint-Venant torsional constant
$\bar{J}$ supplementary Saint-Venant torsional constant
K shear stiffness of framework; shear critical load
K^* shear stiffness/shear critical load of coupled shear walls
K_b full-height global shear stiffness; global shear critical load
K_b^* full-height global shear stiffness/shear critical load of coupled shear walls
K_c local shear stiffness related to the columns; local shear critical load
K_d shear stiffness representing the effect of the diagonal bars in cross-bracing
K_e effective shear stiffness
K_h shear stiffness representing the effect of the horizontal bars in cross-bracing
L width of structure; plan length of building (in direction x)
M bending moment
M_i concentrated mass at the ith floor level
M_t torsional moment
N total applied uniformly distributed vertical load; normal force
N_{cr} critical load
$N_{cr,x}$ critical load for sway buckling in direction x
$N_{cr,y}$ critical load for sway buckling in direction y
$N_{cr,}$ critical load for pure torsional buckling
N_f local bending critical load of framework
N_h homogeneous solution
N_g full-height global bending critical load
N_l full-height local bending critical load
N_p particular solution
N_t Saint-Venant torsional critical load
N_w local bending critical load of shear wall
$N_{y\varphi}$ coupled sway-torsional critical load
N_ω warping torsional critical load
$N(z)$ total vertical load at z
O shear centre
Q uniformly distributed floor load per square metre
S lateral stiffness; shear stiffness for sandwich model
S_ω torsional stiffness

SMALL LETTERS

a length of wall section; stiffness ratio
$\bar{a}$ stiffness ratio for a system of bracing units
a_i local bending stiffness ratio
a_0, a_1, a_2 coefficients for cubic equation

$\underline{b}$ length of wall section; stiffness ratio
$\overline{b}$ stiffness ratio for a system of bracing units
b_i shear stiffness ratio
b_w width of diagonal strip for infill
b_0, b_1, b_2 coefficients for cubic equation
c length of wall section
c_i global bending stiffness ratio
c_1 stability coefficient/critical load factor
d length of wall section; length of diagonal; depth of beam; deflection
d_{ASCE} maximum deflection recommended by ASCE
dz length of elementary section
e location of shear centre; distance of upper flange from centroid
e^* distance of lower flange from centroid (with bracing cores)
f frequency; auxiliary constant; number of frames and coupled shear walls
f_b lateral frequency associated with local bending stiffness
f_f lateral frequency of framework
f_g lateral frequency associated with global bending stiffness
f_s lateral frequency associated with the effective shear stiffness
$f_{s'}$ lateral frequency associated with the "original" shear stiffness
f_w lateral frequency of shear wall/core
f_x lateral frequency in direction x
f_y lateral frequency in direction y
f_y coupled lateral-torsional frequency
f frequency of pure torsional vibration
g gravity acceleration
h height of storey; length of wall section
h^* different storey height between ground floor and first floor
i summation index for columns/bracing units
i_p radius of gyration
j summation index
k non-dimensional parameter
k_s non-dimensional parameter for stability analysis
k non-dimensional torsion parameter for frequency analysis
l width of bay
l^* distance between shear wall sections
m number of shear walls/cores/wall sections; mass; length of beam section
$\overline{m}$ torsional moment share on base unit
m_t total torsional moment on the bracing system
m_z torsional moment
n number of columns/walls; number of storeys
p intensity of uniformly distributed vertical load on beams
q intensity of uniform shear flow; intensity of axial load
q_i apportioner
q_ω torsional apportioner
q_1 apportioner for the base unit
r reduction factor for beam stiffness
r_f mass distribution factor for the frequency analysis
r_s load distribution factor for the stability analysis

s non-dimensional stiffness ratio for bracing unit; effectiveness factor; distance of connecting beams with partially closed U-core
$\bar{s}$ non-dimensional stiffness ratio for bracing system
s_i width of shear wall section
s_f effectiveness factor for frequency analysis
s_φ torsional effectiveness factor
t wall thickness; distance of shear centre and centroid; time; perpendicular distance of bracing unit from shear centre; distance of column from centroid of cross-sections with frameworks
t_b thickness of connecting beam with partially closed U-core
t_f wall thickness
t_i wall thickness
t_w wall thickness
u horizontal deflection of the shear centre in direction x
$u_{\max}$ maximum horizontal deflection in direction x
u_1 horizontal motion
v horizontal deflection in direction y
v_o horizontal deflection of the shear centre in direction y
$v_{\max}$ maximum horizontal deflection in direction y
v_φ horizontal deflection caused by torsional moment around the shear centre
w intensity of wind load
$\bar{w}$ intensity of wind load on base unit
x horizontal coordinate axis; horizontal coordinate
$\bar{x}$ horizontal coordinate axis; coordinate in coordinate system $\bar{x}-\bar{y}$
x_c coordinate of the centroid in the x-y coordinate system of the shear centre
x_i coordinate of the shear centre of the ith bracing unit
$x_{\max}$ location of maximum translation
$\bar{x}_i, \bar{y}_i$ coordinates of the shear centre of the ith bracing unit in the coordinate system $\bar{x}-\bar{y}$
$\bar{x}_o$ coordinate of the shear centre in coordinate system $\bar{x}-\bar{y}$
y horizontal coordinate axis; horizontal coordinate
$\bar{y}$ horizontal coordinate axis; coordinate in coordinate system $\bar{x}-\bar{y}$
y_b deflection due to bending deformation
y_c coordinate of the centroid in the x-y coordinate system of the shear centre
y_i coordinate of the shear centre of the ith bracing unit; deflection due to interaction
y_o location of shear centre
$\bar{y}_o$ coordinate of the shear centre in coordinate system $\bar{x}-\bar{y}$
y_s deflection due to shear deformation
z vertical coordinate axis; vertical coordinate

GREEK LETTERS

$$\lambda$$ eigenvalue; critical load parameter
λ_s eigenvalue; critical load parameter for the sandwich model with thin faces
κ part critical load ratio
κ_s part critical load ratio for the sandwich model with thin faces
Δ displacement

	frequency parameter for lateral vibration
$_{\varphi}$	frequency parameter for pure torsional vibration
γ	weight per unit volume
	stiffness parameter for a single bracing unit
$\bar{}$	stiffness parameter for a system of bracing units
	global critical load ratio
	Poisson ratio
Ω_1, Ω_2	auxiliary constants
Ω	circular frequency
	rotation
Ω_1, Ω_2	auxiliary constants
$_{\max}$	maximum rotation
Ψ	auxiliary constant
	mass density per unit volume; cross-sectional constant
$_x, _y$	eccentricity parameters for the three-dimensional analysis

This page intentionally left blank

1

Introduction

The book deals with the structural analysis of the bracing systems of multi-storey building structures and intends to offer useful tools to both researchers and practicing structural engineers. As a consequence, the material is divided into two parts: Part I presents the theoretical background and Part II gives worked examples.

A couple of decades ago approximate methods played a very important and normally dominant role in the structural design of large structures as often, because of the lack of computer power, it was not feasible, or practical, or sometimes possible, to carry out an "exact" analysis of big and complex structures. Then more and more powerful computers with more and more sophisticated programs started to become available to wider and wider structural engineering communities. Soon the debate started with questions like "Do we need old-fashioned approximate methods?" and "Should we rely on brainless number-crunching machines that cannot think?" and "Shall we just input all the data, press <Enter> and by tomorrow the structural analysis is done?" and "Computers in the design office: boon or bane" (Smart, 1997). This debate will perhaps go on for a long time. But one thing seems to be certain: simple analytical methods and closed-form approximate solutions do and will play an important role in practical structural engineering and theoretical research (Howson, 2006). Not only because they offer important independent checking possibilities to help to avoid CAD (Computer Aided Disaster) (Brohn, 1996) but also because the development and use of such methods help to understand the complex behaviour of large structures such as multi-storey buildings. They are also useful tools in developing structural engineering common sense and a feel for the behaviour of structures.

When multi-storey buildings are investigated, two main avenues are available for the structural engineer: sophisticated and powerful computer packages can be used or "conventional" calculations can be made. Perhaps the best way to tackle the task is to employ both approaches: at the preliminary design stage simple hand methods can quickly help to establish the main structural dimensions and to point to efficient bracing system arrangements. More detailed computer-based analyses can follow. Before the final decision is made, it is essential to check the results of the computer analysis and recheck the adequacy of the key elements of the bracing system. Here, again, suitable analytical methods can play a very useful part.

The fact that the methods in the book are all based on continuous models has another advantage. When the results of a finite element analysis (based on discrete models) are checked, it is advantageous to use a technique that is based on a different approach, i.e., on continuous media.

Structural analysis is normally carried out at two levels. The structural

engineer has to ensure that a) the individual elements (beams, columns, floor slabs, etc.) are of adequate size and material to carry their load and b) the structure as a whole has adequate stiffness and the bracing system fulfils its main role to provide sufficient stability to the building.

The book does not deal with individual structural elements. Its aim is to present simple analytical methods for the complex global analysis of whole structural systems in the three main structural engineering areas. Closed-form solutions will be given for the maximum rotation and deflection, the fundamental frequency and the critical load of the building, assuming three-dimensional behaviour.

The continuum method will be used which is based on an equivalent medium that replaces the whole building. The discreet load and stiffnesses of the building will be modelled by continuous load and stiffnesses that make it possible to use analytical tools to produce relatively simple, closed-form solutions to the resulting differential equations and eigenvalue problems.

It will be assumed that the structures are

- at least four storeys high with identical storey heights
- regular in the sense that their characteristics do not vary over the height
- sway structures with built-in lower end at ground floor level and free upper end

and that

- the floor slabs have great in-plane and small out-of-plane stiffness
- the deformations are small and the material of the structures is linearly elastic
- P-delta effects are negligible.

Structural engineering research and practice often see researchers/structural designers who have specialized in one area with limited knowledge elsewhere. Designers are often reluctant to deal with theoretical matters; researchers often have little practical knowledge (or attitude); those dealing with stress analyses are sometimes ignorant of stability matters; people engaged in earthquake engineering may not be very good at the optimisation of bracing systems, etc.

This book offers a unified treatment for the different structures (frameworks, coupled shear walls, shear walls and cores) and also for the different types of investigation (deflection, rotation, frequency, stability). The same terminology will be used throughout, and it will be shown that these seemingly independent areas (deformations, frequencies, critical loads—or stress, dynamic and stability analyses) are in fact very closely related. In addition, the global critical load ratio links them to the performance of the bracing system in a rather spectacular manner.

Numerous approximate methods have been published for structural analyses. However, it is surprising how few, if any, have been backed up with comprehensive accuracy analysis. Here, in this book, dozens/hundreds of bracing units/systems are used to demonstrate the applicability and accuracy of the methods presented.

Although real multi-storey buildings seldom develop planer deformation only, Chapter 2 (dealing with the planar analysis of individual bracing units) is probably the key chapter of the book in the sense that it introduces all the characteristic stiffnesses that will be used for the three-dimensional investigations

of whole systems later on. It is also shown here how the complex behaviour can be traced back to the local bending, global bending and shear deformation (and their torsional equivalents) of the bracing system. All the characteristic types of bracing unit are covered here: sway- and infilled frameworks, frameworks with cross-bracing, coupled shear walls, shear walls and cores.

Deflections and rotations are the subject of Chapter 3 where the main aim is to present simple, closed-form solutions for the maximum deflection and rotation of the building. The investigations spectacularly show the contribution of the two key (bending and shear) stiffnesses as well as the interaction between them. Chapter 4 deals with the frequency analysis of buildings. Closed form formulae and tables make it possible to calculate the lateral and torsional frequencies of the building. The coupling of the lateral and torsional modes can be taken into account by a simple summation formula or, if a more accurate result is needed, by calculating the smallest root of a cubic equation. The often neglected but very important area of stability is covered in Chapter 5. In using critical load factors, simple (Euler-like) formulae are presented for the lateral and torsional critical loads. The combined sway-torsional critical load is obtained as the smallest root of a cubic equation. Chapters 2, 3, 4 and 5 end with a demonstration of the accuracy of the method(s) presented in the chapter.

Chapter 6 introduces the global critical load ratio which is a useful tool for monitoring the “health” of the bracing system and indicates if the bracing system is adequate or more rigorous (second-order) analysis is needed. The global critical load ratio can also be used to assess different bracing system arrangements in minutes in order to chose the most economic one. The results of a comprehensive example illustrate the practical use of the global critical load ratio.

Part II presents sixteen examples worked out to the smallest details, with step-by-step instructions. The examples range from the deflection or frequency or stability analysis of individual bracing units to the complex deflection and frequency and stability analyses of bracing systems, considering both planar and spatial behaviour. Although most of the formulae in the book are of the back-of-the-envelope type, due to the complexity of global three-dimensional analyses, some of the calculations may still seem to be rather cumbersome to carry out by hand. It is very rare, however, that a structural engineer today would wish to do actual hand-calculations, however simple they may be. Convenient spreadsheets and calculation worksheets make it possible to do the structural analysis and document its result at the same time in minutes. All the methods presented in the book are suitable for this type of application; in fact the worksheet version of all the sixteen worked examples has been prepared and made available for download. These one-to-eight page long worksheets cover a very wide range of practical application and can also be used as templates for other similar structural engineering situations.

Part I: Theory

The widespread availability of powerful computers and sophisticated programs makes it possible to analyze even very large and complex structures with relatively little effort. This is very welcome. There is, however, a certain degree of danger that the structural engineer, in accepting the help of the computer, may get carried away and rely on the computer to a greater extent than would be desirable and pay less attention to the behaviour of the structure. It may be tempting to become complacent.

If the structural engineer's knowledge about the behaviour of complex structures is limited, then the temptation is even greater to accept the computer's solution to the structural engineering problem that has been fed to the computer. This is where "Part I: Theory" can be helpful. The continuum model of the multi-storey building is used repeatedly. The continuous medium approach makes it possible to handle complex structural engineering problems in a relatively simple way and to identify the key stiffness and geometrical characteristics that have a dominant role in shaping the behaviour of the structure.

In order for the accuracy analyses in Chapters 2, 3, 4 and 5 to correspond to the theoretical assumption that "the floor slabs have great in-plane and small out-of-plane stiffness" the floor slabs of the buildings are modelled using sets of bars interconnecting the vertical bracing units. The bars have very great cross-sectional areas and pinned ends. The shear walls are modelled by bar elements (cantilevers).

2

Individual bracing units: frames, (coupled) shear walls and cores

The bracing system of a multi-storey building is normally made up from different units: frameworks, shear walls, coupled shear walls and cores. They all contribute to the overall resistance of the system, but their contributions can be very different both in weight and in nature, so it is essential for the designer to know their behaviour in order that optimum bracing system can be produced.

Frameworks play a very important role in the structural analysis as they have all the three basic stiffness characteristics, i.e., they have local bending stiffness, global bending stiffness and shear stiffness. Their importance is underlined by the fact that the analysis of whole structures (consisting of frameworks, shear walls, coupled shear walls and cores) can often be traced back to the investigation of a single framework and its equivalent column. It is therefore advantageous to start the investigation with the analysis of frameworks.

2.1 DEFLECTION ANALYSIS OF SWAY-FRAMES UNDER HORIZONTAL LOAD

The behaviour of frameworks under lateral load is complex, mainly because they develop both bending and shear deformations. Due to the complexity of the problem, designers and researchers have made considerable efforts to develop approximate techniques and methods. Perhaps the best and most widespread method is the continuum method which is based on an equivalent medium that replaces the framework. It is difficult to pinpoint exactly who developed the first continuum model but the method probably surfaced in the 1940s. In her excellent paper, Chitty (1947) investigated parallel beams interconnected by cross bars, subjected to uniform lateral load, and established the governing differential equation of the problem. In a following paper she applied the method to tall buildings under horizontal load, however, she neglected the axial deformations of the columns (Chitty and Wan, 1948). Scientists from all over the world followed, many of them apparently unaware of the previous efforts, who created and sometimes reinvented and later further developed continuum models (Csonka, 1950; Beck, 1956; Rosman, 1960; MacLeod, 1971; Despeyroux, 1972; Stafford Smith *et al.*, 1981; Hoenderkamp and Stafford Smith, 1984; Coull, 1990). Perhaps the most comprehensive treatment of building structures under horizontal load is given by Stafford Smith and Coull (1991). The continuum model has also been applied successfully to the stability and dynamic analyses of buildings (Danay *et al.*, 1975; Rosman, 1981; Rutenberg, 1975; Kollár, 1986; Hegedűs and Kollár,

1999; Zalka, 2000; Potzta and Kollár, 2003).

The procedure presented in the following will result in a very simple and expressive formula for the deflection, identifying three distinctive parts: bending mode, shear mode and their interaction.

In addition to the general assumptions listed in the Introduction, it will also be assumed that the structures are subjected to uniformly distributed lateral load.

2.1.1 Basic behaviour; lateral deflection

In line with, and using the terminology established in the theory of sandwich structures (Plantema, 1961; Allen, 1969; Hegedűs and Kollár, 1999; Zalka, 2000), the behaviour of a framework may be characterised by three types of stiffness and the corresponding deflection types. The three types are: shear, global bending when the structure as a whole unit is considered and the bending of the unit occurs through the axial deformation of the columns, and local bending when the full-height bending of the individual columns of the framework is considered (Figure 2.1). From now on, these characteristics will be used, not only for the lateral deflection analysis in this Section but also for the rotation analysis later on as well as for the stability and frequency analyses in later chapters.

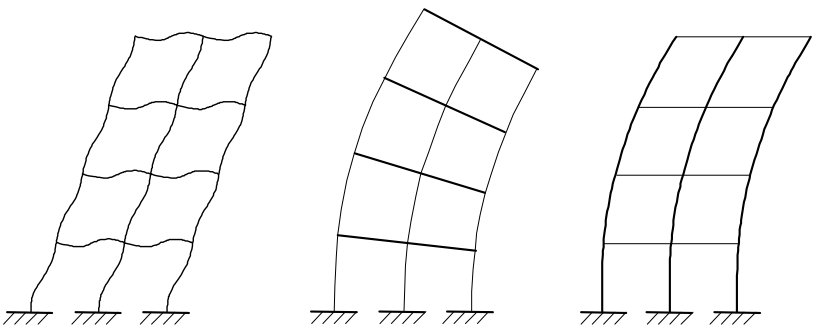

Figure 2.1 Characteristic deformations. a) shear, b) global bending, c) local bending.

For the deflection analysis, consider first the one-bay framework under horizontal load w, shown in Figure 2.2/a. In the usual manner with the continuum method, first the beams are cut at the vertical line of contraflexure. The resulting lack of continuity is compensated for by a shear flow of intensity q (Figure 2.2/b). It is assumed that there are “enough” beams so that they can be considered a continuous connecting medium between the columns. (As a rule, the technique can safely be applied to structures of at least four-storey height.) The shear flow is then transferred to the columns (Figure 2.2/c) in the form of normal forces (N) and bending moments (Nl_1 and Nl_2). Finally, after setting up a differential equation responsible for the lack of continuity in the following sections [c.f. Equation (2.9)], an equivalent column will be created as the continuum model for the problem

(Figure 2.2/d). The origin of the coordinate system is placed at and fixed to the top of the column.

If the beams are cut, relative vertical displacements develop along the line of contraflexure. Three different actions will cause displacement and they will now be considered, one by one, as if they occurred separately from each other.

The relative displacement due to the bending of the columns (Figure 2.3/a) is

$$\Delta_1 = ly'$$

The displacement is positive when the end of the beam-section belonging to the left column moves downward and the other upward.

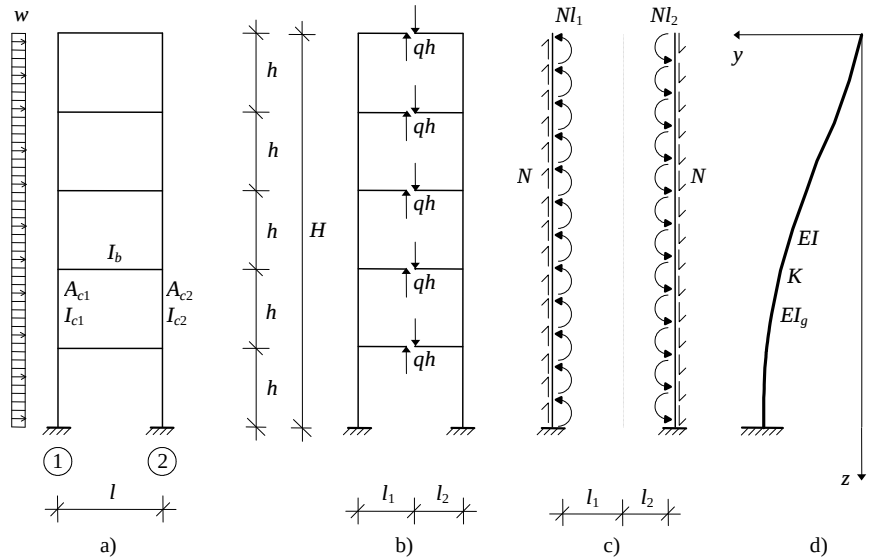

Figure 2.2 The continuum model. a) original frame, b) discontinuity along contraflexure line with shear force *qh*, c) the two columns with continuous forces, d) the equivalent column.

The axial deformation of the columns (Figure 2.3/b), due to the normal forces originating from the shear forces in the connecting beams, also contributes to the overall relative displacement

$$\Delta_2 = -\frac{1}{E}\left(\frac{1}{A_{c1}} + \frac{1}{A_{c2}}\right)\int_z^H N dz$$

where

$$N = \int_0^z q dz$$

is the normal force causing axial deformation in the columns, q is the intensity of the shear flow, A_{c1} and A_{c2} are the cross-sectional areas of the columns, H is the height of the structure and E is the modulus of elasticity.

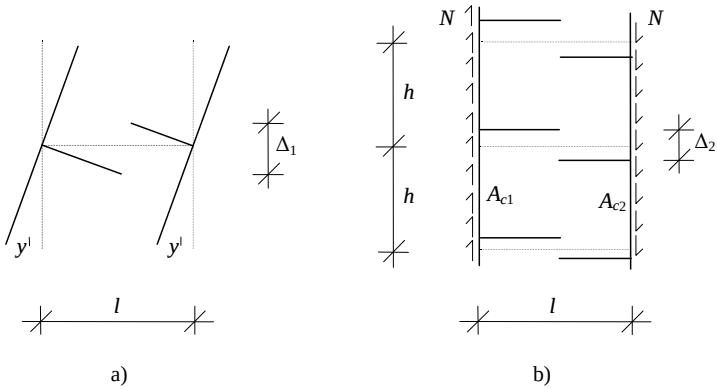

Figure 2.3 Vertical displacement at contraflexure point. a) due to the deflection of the columns, b) due to the axial deformation of the columns.

Due to the bending of the beams (Figure 2.4), the shear force at contraflexure also develops relative displacement. Assuming that the point of contraflexure is at mid-bay, this relative displacement is

$$\Delta_3^* = -2\frac{qh\left(\frac{l}{2}\right)^3}{3EI_b} = -\frac{ql^3h}{12EI_b} = -\frac{ql^2}{\frac{12EI_b}{lh}} = -\frac{ql^2}{K_b} \tag{2.1}$$

where I_b is the second moment of area of the beams, h is the storey height, l is the bay and

$$K_b = \frac{12EI_b}{lh} \tag{2.2}$$

is defined as the stiffness of the beams (distributed over the height).

Equation (2.1) only holds when the beams have horizontal tangent to the columns at the nodal points, i.e., when the columns are considered infinitely stiff (dashed line in Figure 2.4). This may be the case with coupled shear walls where the wall sections are often much stiffer than the connecting beams and can prevent the rotation of the beams at nodal points. However, this is not the case with frameworks where the columns develop double curvature bending between the beams (solid line in Figure 2.4). It follows that, due to the flexibility of the columns, in the case of frameworks, Equation (2.1) should be amended as the vertical displacement Δ_3^* increases:

$$\Delta_3 = -\left(\frac{ql^2}{\frac{12EI_b}{lh}} + \frac{ql^2}{\frac{12EI_c}{h^2}} \right) = -ql^2 \left(\frac{1}{K_b} + \frac{1}{K_c} \right)$$

where the stiffness of the columns (distributed over the height) is defined as

$$K_c = \frac{12EI_c}{h^2} \tag{2.3}$$

In the above equations I_c is the second moment of area of the columns.

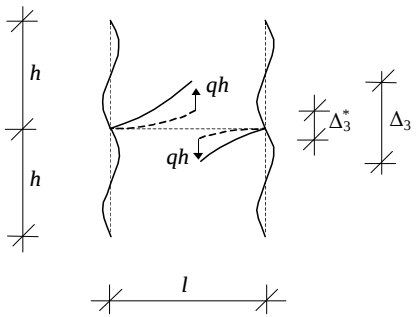

Figure 2.4 Vertical displacement at contraflexure point due to the bending of the beam.

The shear stiffness of the framework (distributed over the height) can now be defined as

$$K = \left(\frac{1}{K_b} + \frac{1}{K_c} \right)^{-1} = K_b \frac{K_c}{K_b + K_c} = K_b r \tag{2.4}$$

In Equation (2.4) the term

$$r = \frac{K_c}{K_b + K_c} \tag{2.5}$$

is also introduced. In relation to K_b, it can be considered as a reduction factor. This reduction factor will play an important role later on.

Replacing K_b in Equation (2.1) with K, the actual relative displacement of the framework, when the bending of both the beams and the columns is considered, emerges as

$$\Delta_3 = -\frac{ql^2}{K}$$

The above formulae are “exact” if the point of contraflexure is at mid-bay, i.e., if the structure is symmetric. However, their accuracy is considered adequate in most practical cases when the cross-sections of the columns are different. (When the stiffnesses of the columns are very different, e.g., the framework connects to a shear wall, a more accurate approach is needed. Formulae for such cases are given, e.g., in Stafford Smith and Coull, 1991.)

The above three relative displacements would develop if the beams are cut. However, the beams of the actual structure are not cut and therefore the sum of the relative displacements must equal zero for the real structure:

$$ly' - \frac{ql^2}{K} - \frac{1}{E}\left(\frac{1}{A_{c1}} + \frac{1}{A_{c2}}\right)\int_z^H N dz = 0 \tag{2.6}$$

With

$$N' = q \tag{2.7}$$

and introducing

$$I_g = A_{c1}l_1^2 + A_{c2}l_2^2 = \frac{A_{c1}A_{c2}}{A_{c1} + A_{c2}} l^2 \tag{2.8}$$

as the global second moment of area of the framework and after differentiating and some rearrangement, Equation (2.6) can be rewritten and the condition for continuity along the line of contraflexure assumes the form

$$y'' - \frac{l}{K} N'' + \frac{l}{EI_g} N = 0 \tag{2.9}$$

The bending of the two columns is considered next, based on the classical relationship for bending:

$$y''EI = -M$$

Because of the connecting beams, the two columns, with their combined second moments of area, are forced to assume the same deflection shape. The external moments (from the horizontal load) are now supplemented by the moments caused by the shear forces along the line of contraflexure (Figure 2.2/b,c) as

$$y''E(I_{c1} + I_{c2}) = -M - (l_1 + l_2)\int_z^0 q dz$$

Introducing the sum of the second moments of area of the columns

$$I_c = I_{c1} + I_{c2} \tag{2.10}$$

as the local second moment of area of the framework, and making use of

$$\int_z^0 q dz = -N$$

and with $Nl_1 + Nl_2 = N(l_1 + l_2) = Nl$, the equation can be rewritten as

$$y'' EI_c = -M + lN \tag{2.11}$$

The governing differential equation of deflection is obtained by combining Equations (2.9) and (2.11). Normal force N is obtained from Equation (2.11) as

$$N = \frac{1}{l}(y'' EI_c + M)$$

Substituting this and its second derivative for N and N'' in Equation (2.9) and some rearrangement lead to

$$y'''' - \left(\frac{K}{EI_c} + \frac{K}{EI_g}\right) y'' = \frac{1}{EI_c}\left(\frac{K}{EI_g} M - M''\right) \tag{2.12}$$

Before the solution of the problem is produced, a small modification has to be made. Detailed theoretical investigations (Hegedűs and Kollár, 1999) show and accuracy analyses (Zalka and Armer, 1992) demonstrate that in the above continuum model the bending stiffness of the columns is somewhat overrepresented. (For low-rise frameworks this overrepresentation may lead to unconservative results of up to 16%.) This overrepresentation can easily be corrected by introducing reduction factor r defined by Equation (2.5) in such a way that the second moment of area of the columns of the framework is adjusted by factor r:

$$I = I_c r \tag{2.13}$$

Accordingly, from this point on, this modified second moment of area will be used and

$$EI = EI_c r$$

will be defined as the local bending stiffness of the structure.

In order to shorten the formulae, the following—mostly temporary—notation will be used:

$$a = \frac{K}{EI_g}, \qquad b = \frac{K}{EI}, \qquad = \sqrt{a+b} = \sqrt{bs}\ ,$$

$$s = 1 + \frac{a}{b} = \frac{a+b}{b} = 1 + \frac{I_c r}{I_g} = \frac{I_g + I_c r}{I_g}, \qquad \frac{a}{a+b} = \frac{I_c r}{I_c r + I_g} \tag{2.14}$$

Using the above notation and with $M = wz^2/2$, the short version of Equation (2.12) is

$$y'''' - \ ^2y'' = \frac{w}{EI}\left(\frac{az^2}{2} - 1\right) \tag{2.15}$$

This is the governing differential equation of the framework that has now been replaced by a single cantilever with the corresponding local bending stiffness EI, global bending stiffness EI_g and shear stiffness K (Figure 2.2/d).

The deflection of the framework can be obtained in two ways. One possibility is to solve Equation (2.15) directly. Alternatively, the solution can be produced in two steps: first, the solution for the normal force is obtained then, using the formula for the normal force, the deflection is determined. Another aspect of the solution is the choice and placement of coordinate system. Although the actual result of the problem obviously does not depend on the solution process and the choice and placement of the coordinate system, the structure and complexity of the solution do. After solving the differential equation in the two different ways indicated above and using different coordinate systems, it turned out that the simplest result can be produced when the two-step approach is applied and when the coordinate system whose origin is fixed to the top of the equivalent column is used (Figure 2.2/d). The main steps of this procedure will now be presented.

In combining Equations (2.9) and (2.11), and with $M = wz^2/2$ and notation (2.14), the governing second order differential equation for the normal force emerges as

$$N'' - \ ^2N = -\frac{bwz^2}{2l} \tag{2.16}$$

Two boundary conditions accompany this differential equation. The first condition expresses the fact that the normal force at the top must assume zero:

$$N(0) = 0$$

The second condition is obtained using Equations (2.6) and (2.7). At the

bottom of the structure the tangent to the columns (y') is zero and the third term in Equation (2.6) also vanishes; hence

$$N'(H) = 0$$

The solution to differential equation (2.16) is sought in the form of

$$N = N_h + N_p$$

where

$$N_h = A\sinh\ z + B\cosh\ z$$

is the homogeneous solution and

$$N_p = Cz^2 + Dz + E$$

is a particular solution of the inhomogeneous problem.

In substituting N_p and its second derivative for N and N'' in Equation (2.16), constants C, D and E are determined by setting the coefficients of the powers of function z equal of the two sides. With the values of C, D and E now available, combining the homogeneous and particular solutions, and using the two boundary conditions, the normal force is obtained as

$$N = \frac{wb}{l^2}\left(\frac{\sinh\ H\sinh\ z}{^2\cosh\ H} - \frac{H\sinh\ z}{\cosh\ H} - \frac{\cosh\ z}{^2} + \frac{z^2}{2} + \frac{1}{^2}\right)$$

With the above equation of the normal force, Equation (2.11) can now be used to determine the deflection. After substituting for N, Equation (2.11) assumes the form:

$$y'' = \frac{w}{EI}\left(\frac{bz^2}{2\ ^2} + \frac{b}{^4} - \frac{z^2}{2} + \frac{b\sinh\ H\sinh\ z}{^4\cosh\ H} - \frac{bH\sinh\ z}{^3\cosh\ H} - \frac{b\cosh\ z}{^4}\right) \quad (2.17)$$

The boundary conditions for the equation express that there is no deflection at the top of the structure (as the origin of the coordinate system is fixed to the top) and that the tangent to the columns is vertical at the bottom (Figure 2.2/d):

$$y(0) = 0$$

and

$$y'(H) = 0$$

Integrating Equation (2.17) once and using the above boundary condition, then integrating again and using the other boundary condition give the formula of the deflection which, after lengthy rearrangement and returning to the original structural engineering notation, can be rearranged into a much simpler, meaningful and "user-friendly" form:

$$y = \frac{w}{EI_f}\left(\frac{H^3 z}{6} - \frac{z^4}{24}\right) + \frac{wz^2}{2Ks^2} - \frac{wEI}{K^2 s^3}\left(\frac{\cosh\ (H-z) + H\sinh\ z}{\cosh\ H} - 1\right) \tag{2.18}$$

or

$$y = y_b + y_s - y_i \tag{2.19}$$

where

$$y_b = \frac{w}{EI_f}\left(\frac{H^3 z}{6} - \frac{z^4}{24}\right) \tag{2.20}$$

$$y_s = \frac{wz^2}{2Ks^2} \tag{2.21}$$

and

$$y_i = \frac{wEI}{K^2 s^3}\left(\frac{\cosh\ (H-z) + H\sinh\ z}{\cosh\ H} - 1\right) \tag{2.22}$$

are the three key components of deflection: the bending and the shear deflections as well as the interaction between them.

In Equations (2.18) and (2.20)

$$I_f = I + I_g = I_c r + I_g \tag{2.23}$$

represents the sum of the local and the global second moments of area of the columns.

Maximum deflection develops at $z = H$:

$$y_{\max} = y(H) = \frac{wH^4}{8EI_f} + \frac{wH^2}{2Ks^2} - \frac{wEI}{K^2 s^3}\left(\frac{1 + H\sinh\ H}{\cosh\ H} - 1\right) \tag{2.24}$$

or

$$y_{\max} = y(H) = y_b(H) + y_s(H) - y_i(H) \tag{2.25}$$

where

$$y_b(H)=\frac{wH^4}{8EI_f},\quad y_s(H)=\frac{wH^2}{2Ks^2},\quad y_i(H)=\frac{wEI}{K^2s^3}\left(\frac{1+\ H\sinh\ H}{\cosh\ H}-1\right) \tag{2.26}$$

are the three characteristic parts of the top deflection.

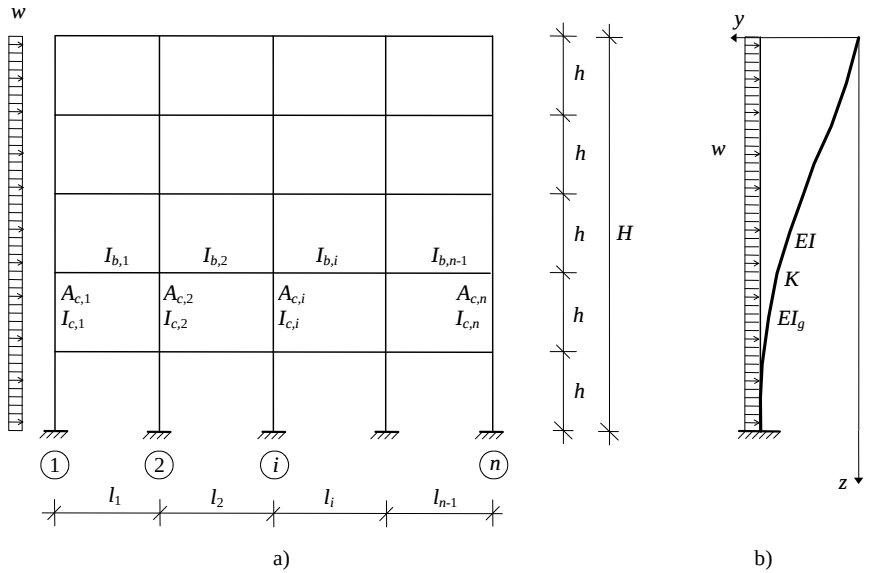

Figure 2.5 Multi-storey, multi-bay sway-frame and its equivalent column.

2.1.2 Multi-storey, multi-bay frameworks

Although the formulae in the previous section were derived for one-bay structures, their validity can be extended to cover multi-bay structures (Figure 2.5) as well.

The shear stiffness for the whole structure is obtained using

$$K=K_b r=K_b\frac{K_c}{K_b+K_c} \tag{2.27}$$

where the two contributors to the shear stiffness are

$$K_b=\sum_{i=1}^{n-1}\frac{12EI_{b,i}}{l_i h} \tag{2.28}$$

and

$$K_c = \sum_{i=1}^{n} \frac{12EI_{c,i}}{h^2} \tag{2.29}$$

and the reduction factor is

$$r = \frac{K_c}{K_b + K_c} \tag{2.30}$$

where n is the number of columns.

For the local bending stiffness ($EI = EI_c r$), the sum of the second moments of area of the columns should be produced (and multiplied by reduction factor r)

$$I = r \sum_{1}^{n} I_{c,i} \tag{2.31}$$

where the summation goes from $i = 1$ to $i = n$. When the cross-sections of the columns of the framework are identical (as is often the case), the second moment of area of the columns is simply multiplied by n and r (the reduction factor).

For the global bending stiffness (EI_g), the formula

$$I_g = \sum_{1}^{n} A_{c,i} t_i^2 \tag{2.32}$$

should be used, where $A_{c,i}$ is the cross-sectional area of the ith column and t_i is the distance of the ith column from the centroid of the cross-sections. It should be noted, however, that Equation (2.32) represents an approximation and its use for multi-bay frameworks may lead to slightly unconservative estimates for the deflection in the region of 0–3% for four-bay structures and up to 6% for ten-bay structures (Kollár, 1986).

2.1.3 Discussion

The evaluation of Equations (2.18) and (2.24) using the deflection data of 117 individual frameworks ranging in height from 4 to 80 storeys (c.f. Section 2.1.4: Accuracy) leads to the following observations:

a) The effect of interaction between the bending and shear modes is always beneficial as it reduces the deflection. The range of the reduction of the top deflection with the 117 frameworks was between 0% and 64%. Ignoring the effect of interaction leads to a very simple albeit conservative solution [with the first two terms in Equation (2.24)].
b) The effect of interaction significantly becomes smaller as the height of the

structures increases. For structures of height over 20 storeys, the reduction dropped below 20%. — Typical deflection shapes are shown in Figure 2.6.

c) The effect of interaction is roughly constant over the height of the structure.

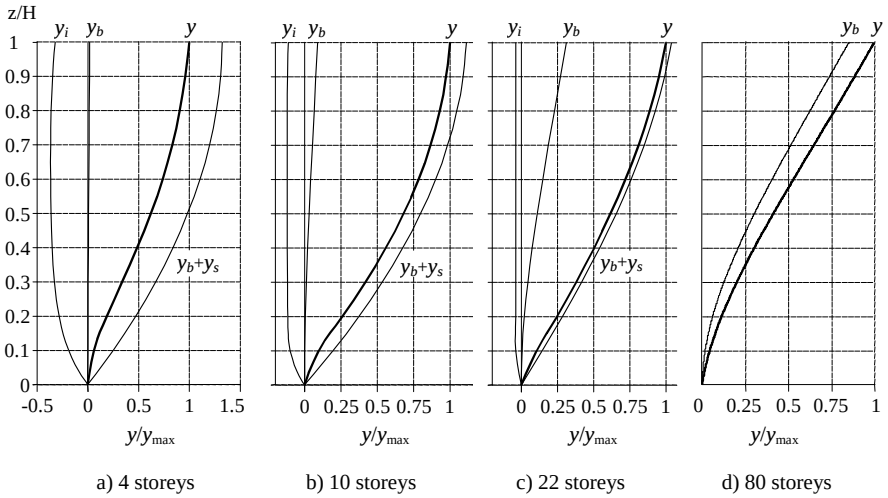

Figure 2.6 Typical deflection shapes with components y_b (bending), y_s (shear), y_i (interaction) and the overall deflection y for the 4-, 10-, 22- and 80-storey framework F1 shown in Figure 2.7/a.

To conclude the investigation of the behaviour of frameworks under lateral load, some special, sometimes theoretical, cases will now be considered.

a) Multi-bay, low-rise frameworks tend to develop predominantly shear-type overall deflection when the effect of the local and global bending may be negligible.

This case is characterised by $I_g >> I_c$, and consequently, $a \to 0$, $b \to \infty$. Governing differential equation (2.15) cannot be used directly because of singularity but, after some rearrangement, Equation (2.12) can, which then simplifies to

$$y'' = \frac{w}{K}$$

where $K \cong K_b$. This differential equation, together with the boundary conditions $y(0) = 0$ and $y'(0) = 0$, lead to the deflection and the top deflection as

$$y(z) = \frac{wz^2}{2K} \tag{2.33}$$

and

$$y_{max} = y(H) = \frac{wH^2}{2K} \tag{2.34}$$

The characteristic deflection shape is shown in Figure 2.1/a.

b) The connecting beams have no or negligible bending stiffness.

This case is characterized by $K_b = 0$. Consequently, the shear stiffness of the structure becomes zero ($K = 0$), which leads to $a = 0$, $b = 0$ and $\kappa = 0$. Governing differential equation (2.15) simplifies to

$$y'''' = -\frac{w}{EI}$$

and the solutions for the deflection and the top deflection are

$$y(z) = \frac{w}{EI_c}\left(\frac{H^3 z}{6} - \frac{z^4}{24}\right) \tag{2.35}$$

and

$$y_{\max} = y(H) = \frac{wH^4}{8EI_c} \tag{2.36}$$

where EI_c is the sum of the bending stiffnesses of the columns. This case is identified in Figure 2.1/c as one of the three characteristic types of behaviour of the framework, when the columns are linked by beams that can only pass on axial (horizontal) forces but no moments to the columns.

c) The structure is relatively slender (with great height/width ratio).

The structure develops predominantly (global) bending deformation. The second and third terms in Equations (2.18) and (2.24) tend to be by orders of magnitude smaller than the first term, and the solutions for the deflection and the top deflection effectively become

$$y(z) = \frac{w}{EI_f}\left(\frac{H^3 z}{6} - \frac{z^4}{24}\right) \tag{2.37}$$

and

$$y_{\max} = y(H) = \frac{wH^4}{8EI_f} \tag{2.38}$$

where $I_f = I_c r + I_g$. This case is illustrated in Figure 2.1/b.

d) The columns do not undergo axial deformations.

This case is characterised by $A_{c,i} \to \infty$, $I_g \to \infty$, $a = 0$, $\kappa^2 = b$ and $s = 1$. The governing differential equation, Equation (2.15), simplifies to

$$y'''' - by'' = -\frac{w}{EI}$$

The solutions of this equation for the deflection and the top deflection are

$$y(z) = \frac{wz^2}{2K} - \frac{wEI}{K^2}\left(\frac{\cosh\ (H-z) + \ H\sinh\ z}{\cosh\ H} - 1\right) \tag{2.39}$$

and

$$y_{\max} = y(H) = \frac{wH^2}{2K} - \frac{wEI}{K^2}\left(\frac{1 + \ H\sinh\ H}{\cosh\ H} - 1\right) \tag{2.40}$$

It is interesting to note that the above two formulae can be originated from Equations (2.18) and (2.24) by, in addition to setting $s = 1$, dropping the first term which is associated with the bending deformation of the structure. It follows that when the columns do not develop axial deformations the structure cannot—at least not directly—"utilise" its bending stiffness. (The bending stiffness does enter the picture, but indirectly, through the last term that is responsible for the interaction between the bending and shear modes.)

2.1.4 Accuracy

It is essential to examine the range of validity and accuracy for any respectable approximate method. To this end, a comprehensive validation exercise was carried out to check the accuracy of the formulae derived for the deflection. The results obtained using the approximate formulae were compared to the results of the Finite Element solution. The AXIS VM finite element package (Axis, 2003) was used for the comparison, whose results were considered "exact".

The top deflection of thirteen individual frameworks (F1 to F13 in Figure 2.7) was calculated. The height of the frameworks varied between 4 and 80 storeys in eight steps (4, 10, 16, 22, 28, 34, 40, 60 and 80 storeys), creating 117 test cases.

The bays of the one-, two- and three-bay reinforced concrete rigid frames were 6 m and the storey height was 3 m (F1 to F10 in Figure 2.7/a to 2.7/j). The rectangular cross-sections of the columns and beams are given in Figure 2.7/a to 2.7/j. With the one-, two- and three-bay steel braced frames (F11 to F13 in Figure 2.7/k to 2.7/m), both the bays and the storey height were 3 m. The cross-sections of the columns for the three braced frames were 305x305UC137.

The cross-sections of the beams and braces are given in Figure 2.7/k to 2.7/m. The moduli of elasticity for the concrete and steel frameworks were $E_c = 25$ kN/mm^2 and $E_s = 200$ kN/mm^2, respectively.

The cross-sections of the beams, columns and braces were chosen in such a way that the structures covered a wide range of stiffnesses and even represented extreme special cases.

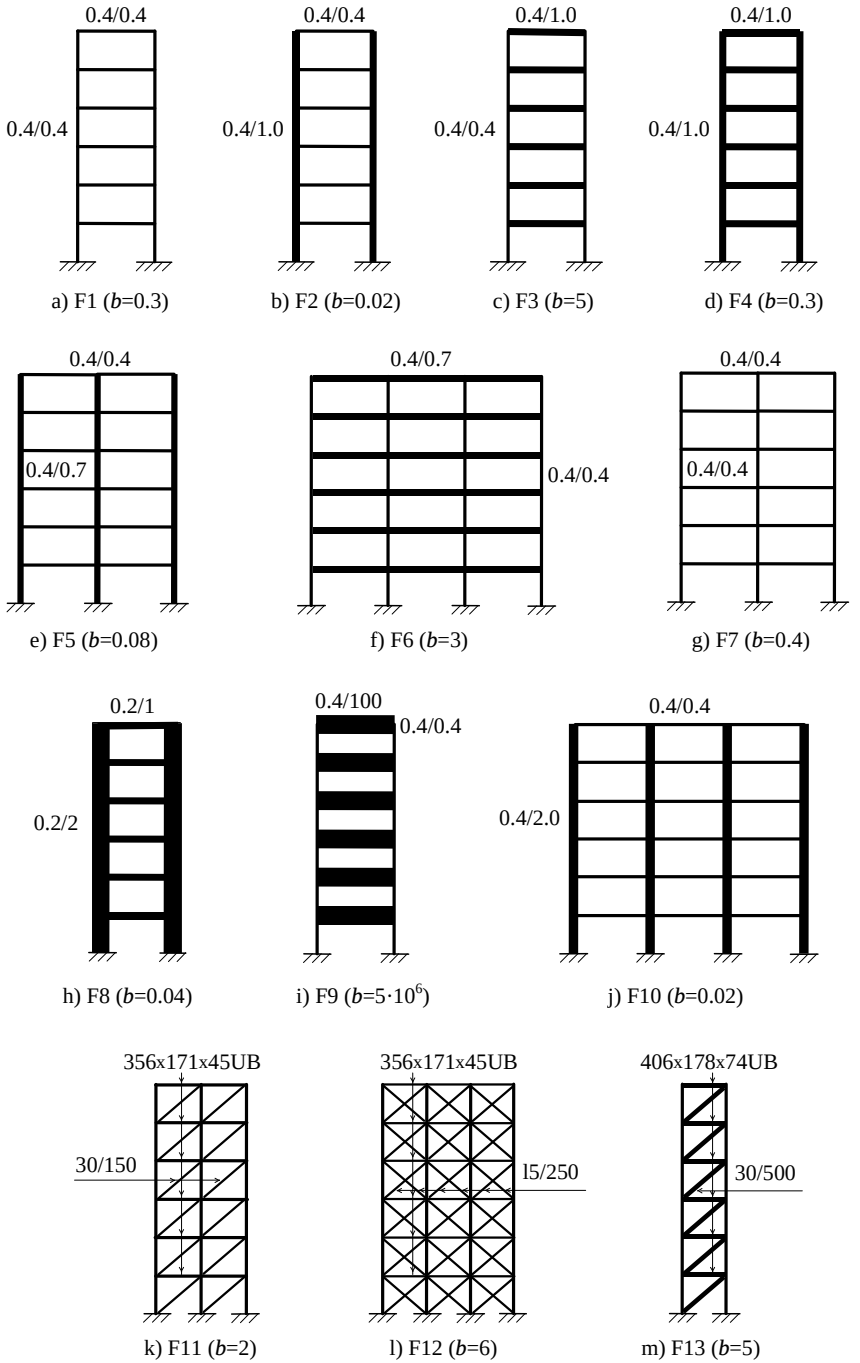

Figure 2.7 Frameworks (with parameter *b*=*K*/*EI*) for the accuracy analysis.

Even the highly theoretical case of a framework with beams with a depth of 100 m in Figure 2.7/i was included to model "pure" shear deformation. The deflected shapes represented predominant bending, mixed shear and bending, and predominant shear deformation. The summary of the accuracy analysis is given in Table 2.1 where "error" means the difference between the "exact" (FE) solution and the continuum solution by Equation (2.24), related to the "exact" solution.

Table 2.1 Accuracy of Equation (2.24) for the maximum deflection.

Method	Range of error (%)	Average absolute error (%)	Maximum error (%)
Continuum solution [Equation (2.24)]	–5 to 9	1.4	9

In addition to the data given in Table 2.1, it is also important to see how the error varies as the height of the structure changes. Figure 2.8 shows the error as a function of height for the thirteen frameworks.

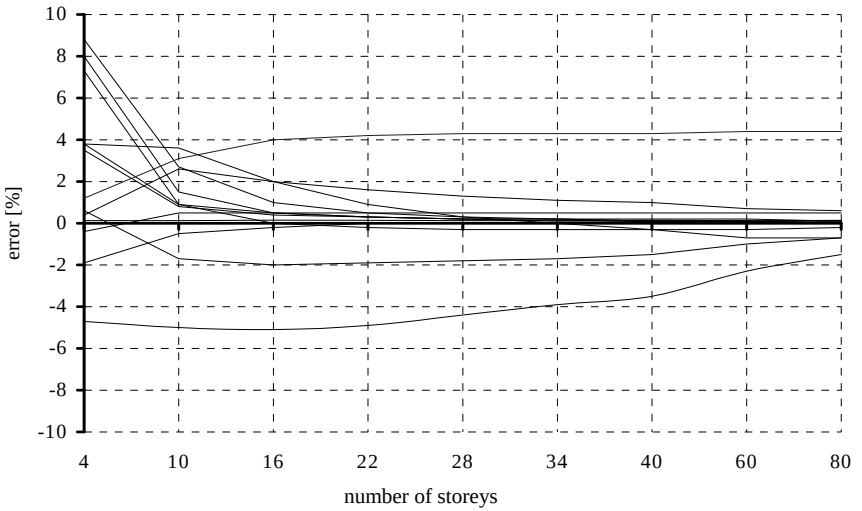

Figure 2.8 Accuracy of Equation (2.24) for maximum deflection for frameworks of different height.

The results summarised in Table 2.1 and shown in Figure 2.8 demonstrate the performance of the method. It can be stated that for practical purposes the continuum solution can be considered accurate enough: The error range of the method was between –5% (unconservative) and 9% (conservative). In the 117 cases, the average difference between the results of the continuum method and those of the finite element solution was 1.4%.

2.2 FREQUENCY ANALYSIS OF RIGID SWAY-FRAMES

Because of the complexity of the problem, a number of attempts have been made to develop approximate methods for the dynamic analysis of frameworks. Goldberg (1973) presented several simple methods for the calculation of the fundamental frequency of (uncoupled) lateral and pure torsional vibration. The effect of the axial deformation of the vertical elements was taken into account by a correction factor in his methods. The continuous connection method enabled the development of more rigorous analysis (Rosman, 1973; Coull, 1975; Kollár, 1992). However, most approximate methods are either still too complicated for design office use or restrict the scope of analysis or neglect one or more important characteristics. Another important factor in connection with the availability of good and reliable approximate methods is the fact that their accuracy has not been satisfactorily investigated. In two excellent publications, Ellis (1980) and Jeary and Ellis (1981) reported on accuracy matters in a comprehensive manner and their findings indicated that some widely used approximate methods were of unacceptable accuracy. The method to be presented here is not only simple and gives a clear picture of the behaviour of the structure, but its accuracy has also been comprehensively investigated.

In addition to the general assumptions made in Chapter 1, it will be assumed that the mass of the structures is concentrated at floor levels.

2.2.1 Fundamental frequency

As in the previous section, the multi-storey, multi-bay framework is characterised by its characteristic stiffnesses and the corresponding three characteristic deformations (Figure 2.1). The fundamental frequency for lateral vibration is determined using the three types of stiffness and the related vibration modes and frequencies. The three types are: shear, the bending of the framework as a whole unit (=global bending) and the full-height bending of the individual columns of the framework (=local bending). The deflected shape of the framework can be composed of the three deformation types and, in a similar manner, the frequency of the framework can be produced using the three “part” frequencies which are linked to the corresponding stiffnesses. These stiffnesses (K, EI_g and EI) are given in Section 2.1.2.

Vibration in shear (Figure 2.1/a) is defined by the shear stiffness of the framework. Based on the classical formula of a cantilever with uniformly distributed mass and shear stiffness (Vértes, 1985), the fundamental frequency of the framework due to shear deformation can be calculated from

$$f_{s'}^2 = \frac{1}{(4H)^2}\frac{r_f^2 K}{m} \tag{2.41}$$

where m is the mass density per unit length of the structure, K is the shear stiffness calculated using Equations (2.27), (2.28), (2.29) and (2.30) and H is the height. Mass distribution factor r_f is introduced into the formula to allow for the fact that

the mass of the structure is concentrated at floor levels (M_i in Figure 2.10/b) and is not uniformly distributed over the height (as assumed for the derivation of the classical formula). This phenomenon can easily be taken into account by the application of the Dunkerley theorem (Zalka, 2000). Values for r_f are given in Figure 2.9 for frameworks up to twenty storeys high. Table 4.1 can be used for more accurate values and/or for higher frameworks.

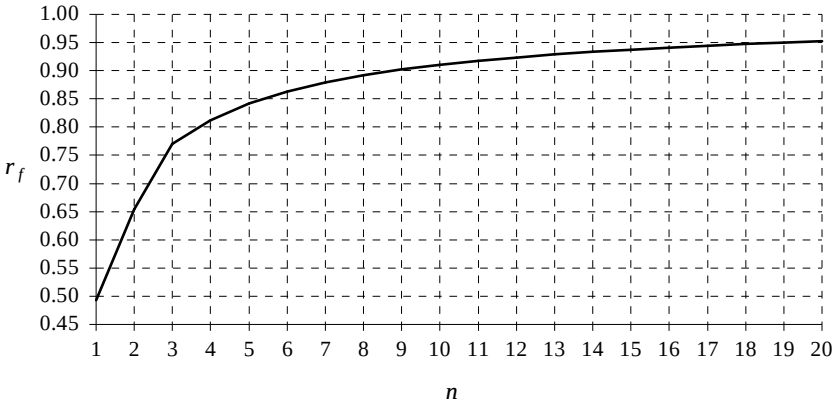

Figure 2.9 Mass distribution factor r_f as a function of n (the number of storeys).

The full-height bending vibration of the framework as a whole unit represents pure bending type deformation (Figure 2.1/b). In this case, the columns act as longitudinal fibres (in tension and compression) and the role of the beams is to transfer shear so as to make the columns work together in this fashion. The bending stiffness associated with this bending deformation is the global bending stiffness (EI_g) defined by Equation (2.32). The fundamental frequency that belongs to this global bending deformation is obtained using Timoshenko's (1928) classical formula, which is amended with factor r_f, as

$$f_g^2 = \frac{0.313 r_f^2 EI_g}{H^4 m} \tag{2.42}$$

Although frameworks are routinely associated with shear type deformation, reality is somewhat more complicated. As Figure 2.6 demonstrates, and the application of any FE package can confirm, as a function of height, a framework with the same (beam/column) stiffness characteristics may assume different types of deformation. Low frameworks tend to show a predominantly shear type vibration mode, in the case of medium-rise frameworks the vibration shape can be a mixture of bending and shear type deformations, and tall, "slender" structures normally vibrate in a predominantly bending mode. The reason for this type of behaviour lies in the fact that there is an interaction between sway in shear and in global bending. Low and/or wide (multi-bay) frameworks tend to undergo shear deformation while as the height of the framework increases, the effect of the axial

deformation of the columns becomes more and more important. The axial deformation of the columns can be interpreted as a "compromising" factor, as far as the shear stiffness is concerned. Because of the lengthening and shortening of the columns, there is less and less "scope" for the structure to develop shear deformation. As indeed is the case with narrow and very tall frameworks; very often they do not show any shear deformation at all.

This phenomenon can be easily taken into account by introducing the *effective* shear stiffness as follows. In applying the Föppl-Papkovich theorem (Tarnai, 1999) to the squares of the frequencies of an individual framework, related to the vibration mode in shear (subscript: *s'*) and the vibration mode in full-height global bending (subscript: *g*)

$$\frac{1}{f_s^2} = \frac{1}{f_{s'}^2} + \frac{1}{f_g^2}$$

the reduction in the value of the shear stiffness of the framework can be expressed as

$$f_s^2 = f_{s'}^2 \frac{f_g^2}{f_{s'}^2 + f_g^2} = \frac{1}{(4H)^2} \frac{r_f^2 K_e}{m} \tag{2.43}$$

where K_e is the effective shear stiffness, according to

$$K_e = s_f^2 K \tag{2.44}$$

and

$$s_f = \sqrt{\frac{f_g^2}{f_{s'}^2 + f_g^2}} = \sqrt{\frac{K_e}{K}} \tag{2.45}$$

is the effectiveness factor.

Finally, the framework may develop bending vibration in a different manner. The full-height bending vibration of the individual columns of the framework—also called local bending vibration—also represents pure bending type deformation (Fig. 1/c). The characteristic stiffness is defined by *EI* given by Equation (2.31). With the columns of the framework built in at ground floor level, the fundamental frequency which is associated with the local bending stiffness is again obtained using Timoshenko's formula for cantilevers under uniformly distributed mass:

$$f_b^2 = \frac{0.313 r_f^2 EI}{H^4 m} \tag{2.46}$$

The framework can now be characterised by its local bending stiffness and its effective shear stiffness (and the related frequencies). It follows that the complex behaviour of a framework in lateral vibration can now be analysed by using an equivalent column with stiffnesses EI and K_e (Figure 2.10/c).

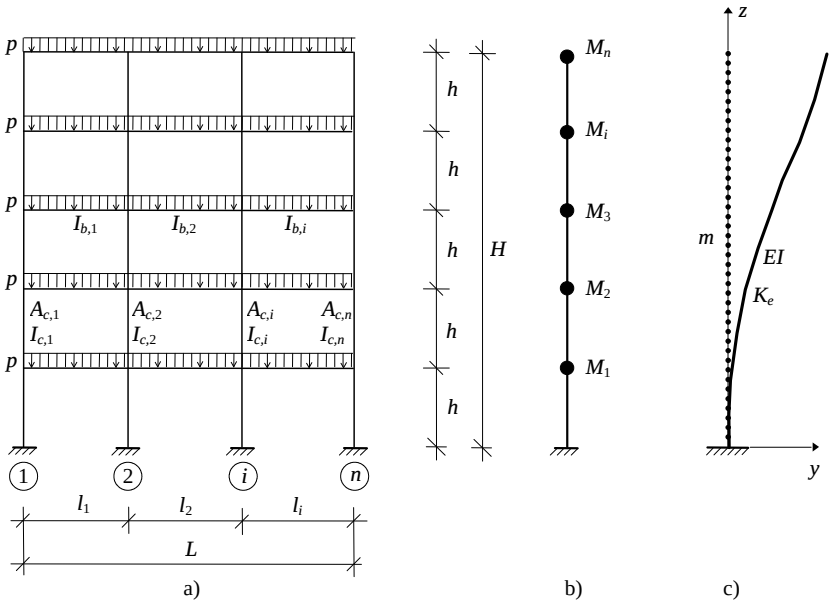

Figure 2.10 Multi-storey, multi-bay sway-frame and the origination of its equivalent column.

The governing differential equation of the equivalent column is obtained by examining the equilibrium of its elementary section. This leads to

$$r_f^2 EIu'''' - r_f^2 K_e u'' + m\ddot{u} = 0$$

where primes and dots mark differentiation by z and t (time), respectively. After seeking the solution in a product form, separating the variables and eliminating the time dependent functions, the above governing differential equation results in the boundary value problem

$$r_f^2 EIu_1'''' - r_f^2 K_e u_1'' - \Omega^2 m u_1 = 0 \tag{2.47}$$

If the origin of the coordinate system is at the lower built-in end of the equivalent column, the boundary conditions are as follows:

$$u_1(0) = 0$$

$$u_1'(0) = 0$$

$$u_1''(H) = 0$$

and

$$EIu_1'''(H) - K_e u_1'(H) = 0$$

In Equation (2.47) ω is the circular frequency and u_1 defines lateral motions. With the notation

$$\Omega = \frac{2}{H^2}\sqrt{\frac{EIr_f^2}{m}}$$

and the non-dimensional parameter

$$k = H\sqrt{\frac{K_e}{EI}} \tag{2.48}$$

and using trigonometric and hyperbolic functions, the solution is obtained after some rearrangement as

$$f^2 = \left(\frac{2}{0.313} - \frac{k^2}{5}\right) f_b^2 + f_s^2 \tag{2.49}$$

Values for frequency parameter η (the eigenvalue of the problem) are given in Figure 2.11 as a function of parameter k for $0 \le k \le 10$. Table 4.2 can also be used if a more accurate value of η or a wider range of k is needed. Values of parameter η for the second and third frequencies are tabulated in (Zalka, 2000).

Before this solution is used for the lateral vibration analysis, however, a small modification has to be made. The first term in Equation (2.49) stands for the bending contribution of the individual columns *and* it also represents the increase of the lateral frequency of the framework, due to the interaction between the bending and shear modes. However, because of the fact that the effectiveness of the shear stiffness is normally smaller than 100% [c.f. Equation (2.45) where $s_f \le 1$ holds], these two contributions have to be separated and the effectiveness factor should be applied to the part which is responsible for the interaction. When this amendment is made, the formula for the lateral vibration assumes the form

$$f = \sqrt{f_b^2 + f_s^2 + \left(\frac{2}{0.313} - \frac{k^2}{5} - 1\right) s_f\, f_b^2} \tag{2.50}$$

In the right-hand side of the above equation, the first two terms stand for the lateral frequency associated with bending and shear deformations, respectively,

while the third term represents the effect of the interaction between the bending and shear modes.

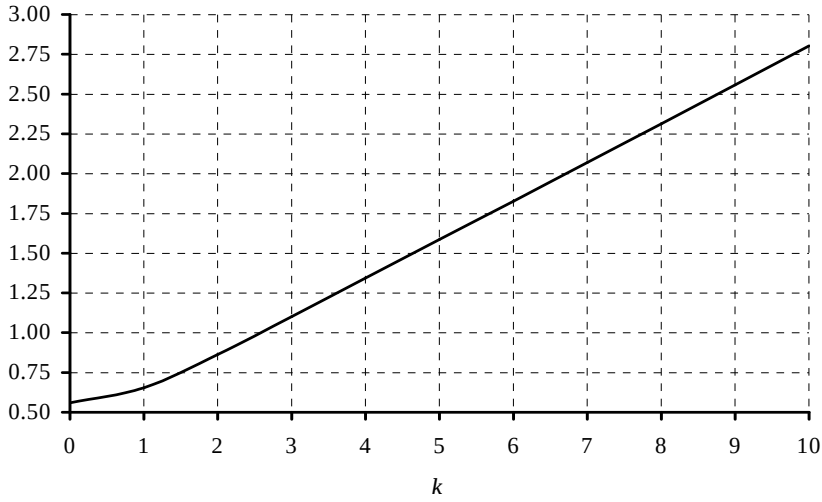

Figure 2.11 Frequency parameter η as a function of non-dimensional parameter k.

2.2.2 Discussion

The evaluation of Equation (2.50) using the values of the fundamental frequencies of 117 frameworks ranging in height from 4 to 80 storeys (c.f. Section 2.2.3: Accuracy) leads to the following observations:

a) As is the case with frameworks subjected to horizontal load, the interaction between the bending and shear modes is always beneficial. Bearing in mind that $(\eta^2/0.313 - k^2/5) \geq 1$ always holds, the evaluation of the third term in Equation (2.50) demonstrates that the effect of the interaction increases the value of the lateral frequency of the framework. According to the data given in Table 4.2, the maximum increase is 62%, at $k = 3.2$.

b) The effect of interaction significantly becomes smaller as the height of the framework increases. For structures of height over 20 storeys, the increase dropped below 20% in the test cases.

2.2.3 Accuracy

A comprehensive accuracy analysis was carried out to check the accuracy of Equation (2.50) for the fundamental frequency of multi-storey frameworks. The frameworks used for the accuracy analysis were the same used in Section 2.1.4 for the accuracy analysis of Equation (2.24) for the maximum deflection. Details of the frameworks are given in Figure 2.7 in Section 2.1.4. The fundamental frequency of the thirteen frameworks (F1 to F13 in Figure 2.7)—each of 4-, 10-,

16-, 22-, 28-, 34-, 40-, 60- and 80-storey height—was calculated and compared to the Finite Element solution. The AXIS VM finite element package (AXIS, 2003) was used for the comparison, whose results were considered "exact". The error of the continuum solution was defined as the difference between the "exact" and the approximate solutions, related to the "exact" solution. When the frequency given by Equation (2.50) was smaller than the "exact" one, it was considered conservative (and the "error" was defined positive).

Table 2.2 Accuracy of Equation (2.50) for the fundamental frequency.

Method	Range of error (%)	Average absolute error (%)	Maximum error (%)
Continuum solution [Equation (2.50)]	–3 to 8	1.5	8

The bays of the one-, two- and three-bay sway-frames were 6 metres (F1 to F10 in Figure 2.7) and 3 metres (F11 to F13) and the storey height was 3 metres for all structures. The cross-sections of the beams and columns were chosen in such a way that the structures covered a wide range of stiffnesses. The deflected shapes represented predominant bending, mixed shear and bending, and predominant shear deformation. The results are summarised in Table 2.2.

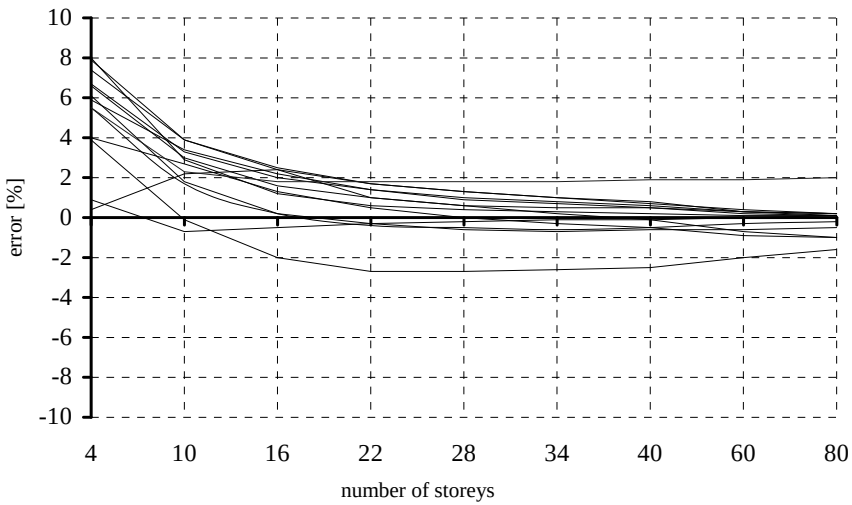

Figure 2.12 Accuracy of Equation (2.50) for the fundamental frequency as a function of height.

The results given in Table 2.2 and shown in Figure 2.12 as a function of height demonstrate the excellent performance of Equation (2.50). In the 117 cases, the average difference between the results of the continuum method and those of the finite element solution was 1.5%. The maximum error of Equation (2.50) was 8%.

2.3 STABILITY ANALYSIS OF RIGID SWAY-FRAMES

If the dynamic analysis of complex bar structures is said to be complex, then the stability analysis certainly presents an even greater challenge as numerical difficulties may further aggravate the situation in the course of the solution of the eigenvalue problem. The determination of the critical load of even a small framework may be a formidable task using conventional methods. It would be impossible to list all the approximate methods that are worth mentioning as the field has been more than well cultivated and it would be unjust to chose one or two.

The method to be presented here is of general validity. It is certainly very simple and probably the most accurate one, as it will be demonstrated in Section 2.3.2.

2.3.1 Critical load

In addition to the general assumptions made in Chapter 1, it will be assumed that

a) the frameworks are subjected to uniformly distributed vertical load at storey levels (Figure 2.13)
b) the critical load defines the bifurcation point

The best way, perhaps, towards a simple and still accurate solution is the application of the continuum method. If the structure is considered a continuous medium, as shown in the previous sections, the analysis can be carried out in a relatively simple way. In doing so, a closed-form solution can be produced for the critical load, which can then directly be used in practical structural design (see Chapter 6 on the global critical load ratio).

Investigating sandwich columns, Hegedűs and Kollár (1984) derived the governing differential equation of a sandwich column with thick faces as

$$\frac{B_0 B_l}{S}\,\varphi'''' - (B_0 + B_l)\,\varphi'' + N(z)\left(\frac{B_0}{S}\,\varphi'' - \varphi\right) = 0$$

where φ is the rotation of the normal to the cross-section of the sandwich column, $N(z)$ is the axial load and B_0, B_l and S are the global bending, local bending and shear stiffnesses of the sandwich column. For a sandwich column with a free upper end and a fixed lower end and using a coordinate system whose origin is fixed at the upper end, the boundary conditions are

$$\varphi(H) = \varphi''(H) = 0$$

and

$$\varphi'(0) = \varphi'''(0) = 0$$

Hegedűs and Kollár (1984 and 1999) solved the above differential equation

for different load cases. The solution for the uniformly distributed axial load [when $N(z) = qz$ holds and q is the intensity of the load] assumes the form

$$N_{cr} = qH = c_1 \frac{B_0 + B_l}{H^2} \tag{2.51}$$

where coefficient c_1 is obtained using a table as a function of $B_l/(B_0 + B_l)$ and $SH^2/(B_0 + B_l)$.

Table 2.3 Values for coefficient c_1.

$\frac{KH^2}{E(I+I_g)r_s}$	$\frac{I}{I+I_g}$													
	0	0.001	0.005	0.01	0.05	0.1	0.2	0.3	0.4	0.5	0.6	0.7	0.8	1
0.00	0.000	0.0078	0.039	0.078	0.392	0.784	1.567	2.351	3.135	3.918	4.702	5.486	6.269	7.837
0.05	0.050	0.099	0.161	0.211	0.535	0.928	1.712	2.496	3.279	4.062	4.844	5.626	6.405	7.837
0.1	0.100	0.171	0.255	0.320	0.668	1.064	1.850	2.632	3.414	4.195	4.974	5.750	6.519	7.837
0.2	0.200	0.304	0.412	0.500	0.904	1.314	2.102	2.882	3.658	4.432	5.219	5.957	6.698	7.837
0.5	0.500	0.665	0.815	0.933	1.465	1.917	2.717	3.486	4.238	5.025	5.691	6.378	7.015	7.837
1	1.000	1.222	1.403	1.536	2.142	2.642	3.449	4.185	4.887	5.551	6.179	6.757	7.265	7.837
2	2.000	2.289	2.483	2.574	3.094	3.589	4.366	5.026	5.618	6.178	6.679	7.111	7.473	7.837
5	4.211	4.364	4.475	4.524	4.858	5.057	5.637	6.117	6.532	6.892	7.202	7.458	7.655	7.837
10	5.597	5.600	5.626	5.655	5.861	6.080	6.457	6.773	7.052	7.279	7.466	7.620	7.736	7.837
20	6.570	6.572	6.584	6.599	6.706	6.828	7.045	7.230	7.388	7.522	7.632	7.719	7.783	7.837
50	7.287	7.288	7.292	7.298	7.344	7.395	7.485	7.574	7.641	7.700	7.749	7.787	7.815	7.837
100	7.554	7.555	7.557	7.560	7.583	7.609	7.657	7.700	7.736	7.767	7.792	7.812	7.826	7.837
∞	7.837	7.837	7.837	7.837	7.837	7.837	7.837	7.837	7.837	7.837	7.837	7.837	7.837	7.837

With some modification, the above simple formula can also be used for determining the global critical load of multi-storey, multi-bay frameworks. First, the stiffnesses that correspond to those of the sandwich column should be identified. This procedure is presented in the following, with most of the characteristics shown in Figure 2.13, using the terminology common in structural engineering. The stiffnesses are very similar to those introduced in Section 2.1.

The shear stiffness of a framework (K) is composed using two parts. The first part is associated with the beams of the framework as

$$K_b = \sum_{i=1}^{n-1} \frac{12EI_{b,i}}{l_i h} \tag{2.52}$$

where

E is the modulus of elasticity
$I_{b,i}$ is the second moment of area of the ith beam
h is the storey height
l_i is the width of the ith bay
n is the number of columns

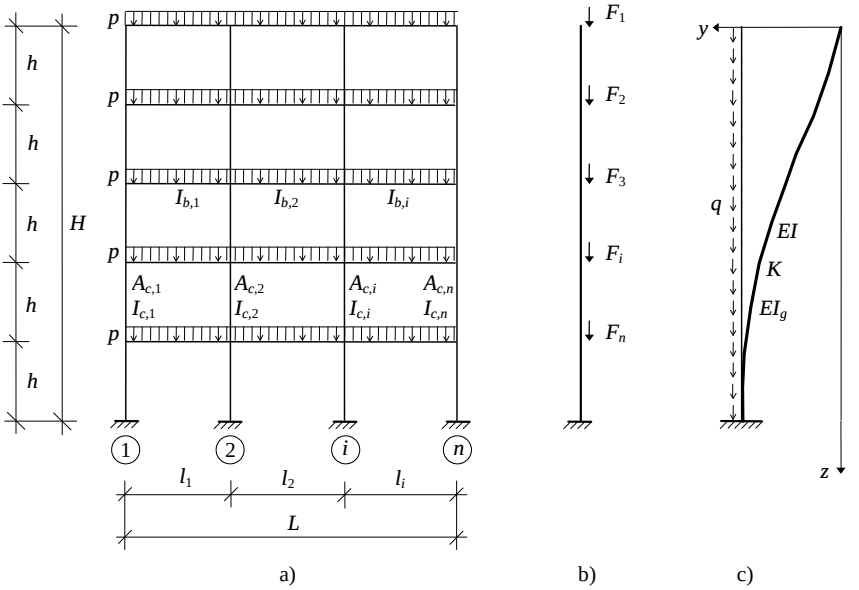

Figure 2.13 Origination of the equivalent column for the stability analysis.

The second part of the shear stiffness is associated with the columns and the local sway of the framework between two storeys:

$$K_c = \sum_{i=1}^{n} \frac{^2EI_{c,i}}{h^2} \tag{2.53}$$

where $I_{c,i}$ is the second moment of area of the ith column. With the two components, the shear stiffness of the framework assumes the form

$$K = K_b r = K_b \frac{K_c}{K_b + K_c} \tag{2.54}$$

where the reduction factor r is also introduced as

$$r = \frac{K_c}{K_b + K_c} \tag{2.55}$$

Note the similarity to—and the difference from—the shear stiffness that was used for the deflection and frequency analyses in Section 2.1 and Section 2.2, respectively. For more detailed explanation regarding the components of the shear stiffness, see Chapter 5 where the stability analysis of whole systems is carried out.

The global bending stiffness (EI_g) is associated with the full-height bending of the framework when the columns act as longitudinal fibres of a solid body in bending. It is calculated in the same way as in Section 2.1, with

$$I_g = \sum_{1}^{n} A_{c,i} t_i^2 \tag{2.56}$$

where $A_{c,i}$ is the cross-sectional area of the ith column and t_i is the distance of the ith column from the centroid of the cross-sections.

The local bending stiffness (EI) of the framework is associated with the full-height bending of the individual columns. Again, it is obtained in the same way as in Section 2.1, with

$$I = r \sum_{1}^{n} I_{c,i} \tag{2.57}$$

where $I_{c,i}$ is the second moment of area of the ith column and r is the reduction factor [Equation (2.55)].

Having identified the stiffnesses for the use of the sandwich solution above, the way the framework is loaded should now be considered. The sandwich solution was produced for a cantilever subjected to a uniformly distributed axial load. The load of multi-storey frameworks, however, is not uniformly distributed over the height but it consists of floor loads (Figure 2.13/a). When the framework is modelled for the continuum method by an equivalent column, the floor load can be considered as a system of concentrated forces at floor levels (Figure 2.13/b). This load system can then be distributed over the height of the column (Figure 2.13/c). This procedure represents an approximation and this approximation is unconservative as the distribution of the load occurs ***downwards*** at each storey and the centroid of the load also moves downwards. The lower the framework, the greater the approximation. For a four-storey structure, for example, this approximation can lead to a critical load that is up to 40% greater than the exact one, therefore this phenomenon cannot be ignored.

This unfavourable phenomenon, however, can easily be taken into account by using Dunkerley's summation theorem (Zalka, 2000) and introducing a load distribution factor into the formula of the critical load. Accordingly, based on the sandwich solution, the critical load of the framework can be produced as

$$N_{cr} = qH = c_1 \frac{E(I + I_g) r_s}{H^2} \tag{2.58}$$

where EI is the local bending stiffness, EI_g is the global bending stiffness and r_s is

the load distribution factor whose values are given in Figure 2.14. Based on the Hegedűs-Kollár solution (1984 and 1999), values for the critical load factor c_1 are given in Table 2.3 as a function of

$$\frac{I}{I+I_g} \tag{2.59}$$

and

$$\frac{KH^2}{E(I+I_g)r_s} \tag{2.60}$$

where K is the shear stiffness.

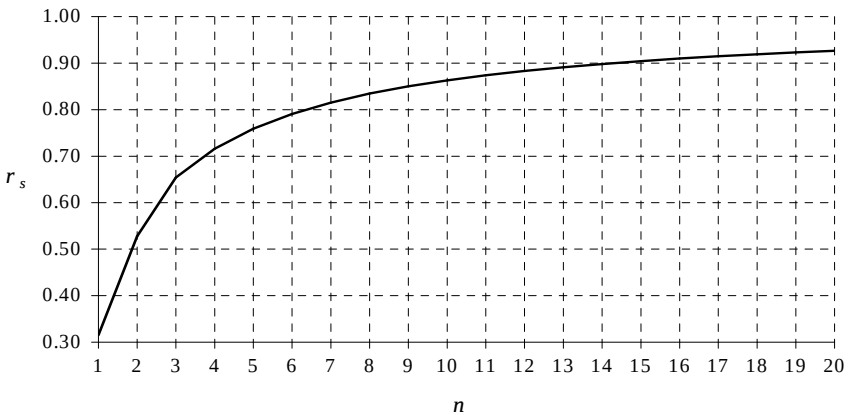

Figure 2.14 Load distribution factor r_s as a function of n (number of storeys).

Values for r_s are given in Figure 2.14 for frameworks up to twenty storeys high. Table 5.1 can be used for more accurate values and/or for higher frameworks.

When the framework is very wide and/or the effect of the local second moment of area of the columns is very small [i.e., when ratio (2.59) is very small], an even simpler method, to be presented in Section 2.4.1, can be used for the determination of the critical load.

2.3.2 Accuracy

A comprehensive accuracy analysis was carried out to check the accuracy of Equation (2.58) for the critical load of multi-storey frameworks. The frameworks used for the accuracy analysis were the same used in Section 2.1.4 for the accuracy analysis of Equation (2.24) for the maximum deflection and of Equation (2.50) in

Section 2.2.1 for the fundamental frequency. Details of the frameworks are given in Figure 2.7 in Section 2.1.4. The critical load of the thirteen frameworks (F1 to F13 in Figure 2.7) was calculated and compared to the Finite Element solution. The height of the frameworks varied from 4 storeys to 80 storeys in eight steps resulting in 117 test cases. The AXIS VM finite element package (AXIS, 2003) was used for the comparison, whose results were considered "exact". The error of the continuum solution was defined as the difference between the "exact" and the approximate solutions, related to the "exact" solution. The bays of the frameworks were 6 and 3 metres; 6 metres for the one-, two- and three-bay concrete sway-frames (F1 to F10 in Figure 2.7) and 3 metres for the steel braced frames (F11 to F13). The storey height was 3 metres for all structures.

Table 2.4 Accuracy of Equation (2.58) for the stability analysis.

Method	Range of error (%)	Average absolute error (%)	Maximum error (%)
Continuum solution [Equation (2.58)]	–8 to 17	3.1	17

The cross-sections of the beams and columns were chosen in such a way that the structures covered a wide range of stiffnesses. The deflected shapes represented predominant bending, mixed shear and bending, and predominant shear deformation. The results are summarised in Table 2.4.

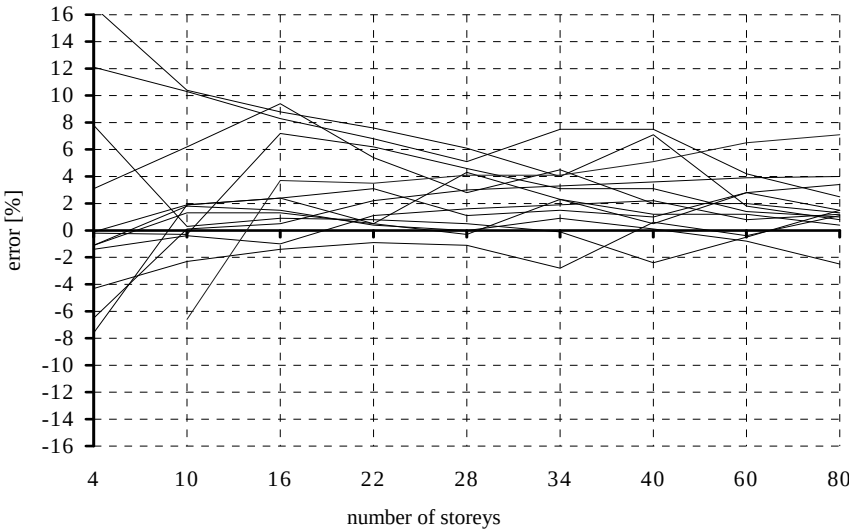

Figure 2.15 Accuracy of Equation (2.58) for the critical load for frameworks of different height.

In addition to the data given in Table 2.4, it is also important to see how the error varies as the height of the framework changes. Figure 2.15 shows the error as a function of height for the thirteen frameworks. In Figure 2.15 and Table 2.4 positive error represents conservative critical load.

The results summarised in Table 2.4 and Figure 2.15 demonstrate the performance of the method. It can be stated that for practical purposes the continuum solution can be considered accurate enough: The error range of the method was between –8% (unconservative) and 17% (conservative). In 116 cases, the average difference between the results of the continuum method and the finite element solution was 3.1%. (It should be noted that the 4-storey framework F12 did not develop global sway buckling and its critical load was omitted from the accuracy analysis as—in line with the basic assumptions—only sway-frames were considered.)

2.4 OTHER TYPES OF FRAMEWORK

The investigations in the previous sections centred on rigid sway-frames. However, the methods can also be used for the deflection, frequency and stability analyses of other types of framework, sometimes with some modification, if the three characteristic stiffnesses (local and global bending and shear) are known. In some cases, a solution even simpler than the one presented in Section 2.3.1, can be used.

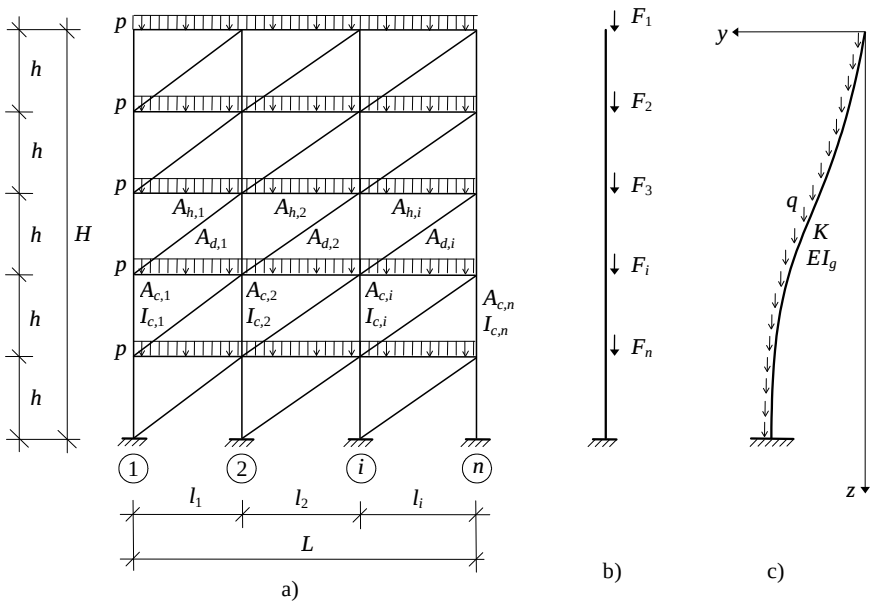

Figure 2.16 Framework with cross-bracing. a) basic characteristics, b) equivalent column with concentrated load at floor levels, c) equivalent column with uniformly distributed load.

2.4.1 Frameworks with cross-bracing

With multi-storey frameworks with cross-bracing (Figure 2.16/a), their local bending stiffness is calculated directly as the sum of the bending stiffnesses of the columns [Equation (2.31)], but with $r = 1$, i.e., $EI = EI_c$. The calculation of the global bending stiffness EI_g is identical to that of the rigid frames, i.e., according to Equation (2.32).

Their behaviour in shear is somewhat different from that of unbraced frames and depends on the arrangement of the bracing. Formulae for different bracing arrangements are given in Table 2.6.

Table 2.5 Critical load parameter $_s$ as a function of parameter β_s.

s	s	s	s	s	s	s	s
0.0	1.0000	2.2	0.3711	4.2	0.2135	17	0.05722
0.3	1.0000	2.3	0.3579	4.3	0.2090	18	0.05413
0.4	0.9972	2.4	0.3457	4.4	0.2047	19	0.05135
0.5	0.9325	2.5	0.3342	4.5	0.2006	20	0.04884
0.6	0.8663	2.6	0.3235	5.0	0.1824	25	0.03926
0.7	0.8051	2.7	0.3134	5.5	0.1672	30	0.03282
0.8	0.7501	2.8	0.3039	6.0	0.1543	35	0.02819
0.9	0.7011	2.9	0.2950	6.5	0.1433	40	0.02471
1.0	0.6575	3.0	0.2866	7.0	0.1337	45	0.02199
1.1	0.6186	3.1	0.2787	7.5	0.1253	50	0.01981
1.2	0.5838	3.2	0.2711	8.0	0.1179	55	0.01803
1.3	0.5526	3.3	0.2640	8.5	0.1114	60	0.01654
1.4	0.5243	3.4	0.2572	9.0	0.1055	65	0.01527
1.5	0.4988	3.5	0.2508	10	0.09544	70	0.01419
1.6	0.4755	3.6	0.2447	11	0.08713	80	0.01243
1.7	0.4543	3.7	0.2389	12	0.08015	90	0.01105
1.8	0.4349	3.8	0.2333	13	0.07420	100	0.00995
1.9	0.4170	3.9	0.2280	14	0.06908	200	0.00499
2.0	0.4005	4.0	0.2230	15	0.06462	300	0.00333
2.1	0.3852	4.1	0.2181	16	0.06069	>300	1/ $_s$

Regarding stability analysis, the procedure presented in Section 2.3.1 for the stability analysis of rigid frameworks can still be used but an even simpler method is available. Of the three characteristic stiffness contributors (local bending, global bending and shear), the effect of the local bending stiffness tends to become very small compared to that of the other two stiffnesses. If this contribution is therefore neglected, then a very simple model can be used for the analysis. This simple model (Figure 2.16/c) is the equivalent sandwich column with thin faces

(Zalka, 1999). The analysis of the equilibrium of an elementary section of the column leads to the differential equation

$$y''''\left(1-\frac{zq}{K}\right)-\frac{3q}{K}y'''+\frac{q}{r_s EI_g}(zy''+y')=0$$

where critical load intensity q is the eigenvalue of the problem.

The boundary conditions are

$$y(0)=0\,, \qquad y'(H)\left(1-\frac{qH}{K}\right)=0$$

$$y''(0)-\frac{q}{K}y'(0)=0\,, \qquad y'''(0)-\frac{2q}{K}y''(0)=0$$

and the solution for the critical load is obtained as

$$N_{cr} = {}_sK \tag{2.61}$$

where K is the shear stiffness of the framework.

Critical load parameter ${}_s$ is given in Figure 2.17 and in Table 2.5 as a function of part critical load ratio ${}_s$, defined by

$${}_s=\frac{K}{N_g} \tag{2.62}$$

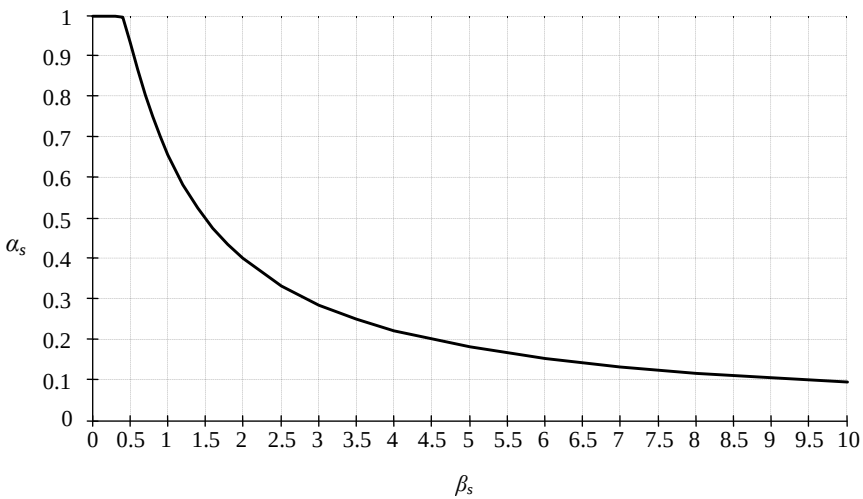

Figure 2.17 Critical load parameter α_s as a function of parameter β_s.

Table 2.6 Shear stiffness K for different cross-bracing arrangements.

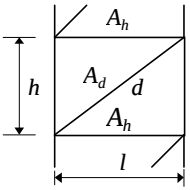	$K = \left(\frac{1}{K_d} + \frac{1}{K_h}\right)^{-1} = \left(\frac{d^3}{A_d E_d h l^2} + \frac{l}{A_h E_h h}\right)^{-1}$	Bracing type: single
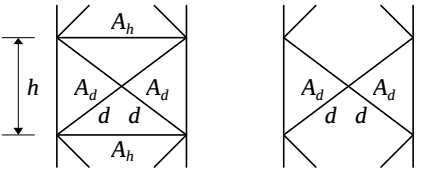	$K = 2A_d E_d \frac{hl^2}{d^3}$	double
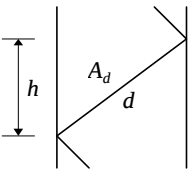	$K = A_d E_d \frac{hl^2}{d^3}$	continuous
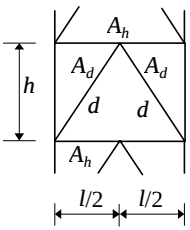	$K = \left(\frac{2d^3}{A_d E_d h l^2} + \frac{l}{4A_h E_h h}\right)^{-1}$	K-bracing
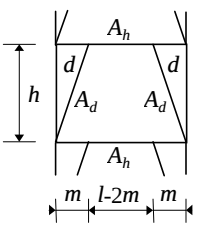	$K = \left(\frac{d^3}{2A_d E_d m^2 h} + \frac{m}{2A_h E_h h} + \frac{h(l-2m)^2}{12 I_h E_h l}\right)^{-1}$	K-bracing
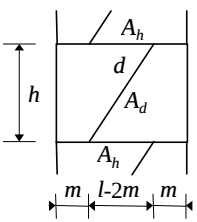	$K = \left(\frac{d^3}{A_d E_d h (l-2m)^2} + \frac{l-2m}{A_h E_h h} + \frac{hm^2}{3 I_h E_h l}\right)^{-1}$	knee-bracing

In equation (2.62) N_g is the part critical load characterizing the full-height global buckling of the framework as a whole:

$$N_g = \frac{7.837 r_s E I_g}{H^2} \tag{2.63}$$

where I_g is the global bending second moment of area defined by Equation (2.32) and r_s is the load distribution factor whose values are given in Figure (2.14) and in Table 5.1.

As Equations (2.61) and (2.62) show, the value of the critical load depends on the two part critical loads K and N_g and its value increases as the value of the shear critical load (K) and that of the global bending critical load (N_g) increase. However, it is important to know how these part critical loads compare and influence the value of the critical load. Based on the Föppl-Papkovich summation theorem (Tarnai, 1999), Figure 2.18 demonstrates that the most efficient case arises when the two part critical loads are equal (Figure 2.18/c). In this case, the critical load of the framework is maximum and its value increases in direct proportion with the increase of the part critical loads, i.e., doubling the part critical loads leads to a critical load which is twice as much as the original critical load. Figure 2.18 also demonstrates that, for unequal part critical loads, there is no point in increasing the greater part critical load as the overall critical load is always governed by the value of the smaller part critical load (Figures 2.18/a and 2.18/b).

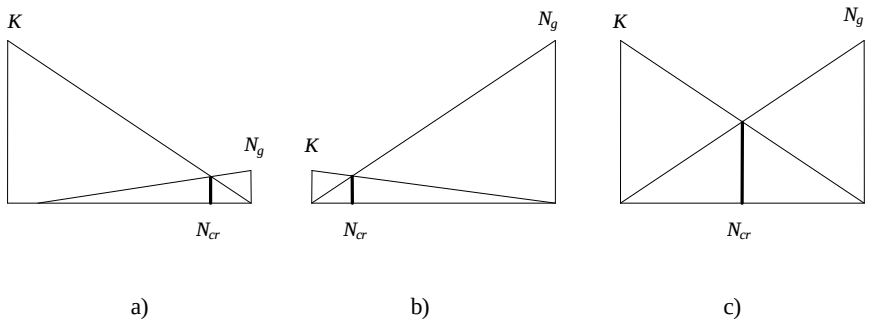

Figure 2.18 The effect of the relative values of the part critical loads on the critical load. a) $K >> N_g$, b) $N_g >> K$, c) $K = N_g$.

2.4.2 Frameworks on pinned support

Frameworks on pinned supports (Figure 2.19/a) have full-height columns that, because of the pinned support, would not be stable by themselves and therefore the critical load that would belong to their local bending stiffness is zero. It follows that the sandwich model with thin faces (used in the previous section) can be used again to produce a simple and good estimate of the global critical load of the

framework.

The critical load is obtained using

$$N_{cr} = {}_{s}K \tag{2.64}$$

where K is the shear stiffness of the framework.

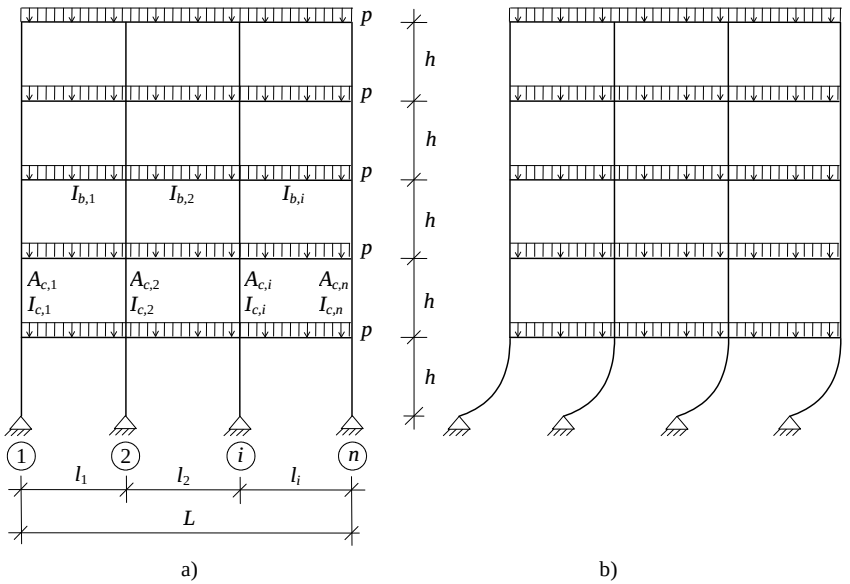

Figure 2.19 Frameworks on pinned support. a) geometrical characteristics, b) local sway at ground floor level.

The shear stiffness originates from two sources. The global part of the shear stiffness (K_b) depends on the stiffness of the beams and its value is not affected by the type of support of the columns so it is defined by Equation (2.52) as with frameworks on fixed support. The other component of the shear stiffness depends on the columns of the framework and the local sway of the framework between two storeys. With frameworks on pinned supports, the most vulnerable level is ground floor level (Figure 2.19/b) and the local shear stiffness is associated with sway buckling between ground floor and first floor level (Zalka and Armer, 1992). The local shear stiffness is therefore defined by

$$K_c = \sum_{j=1}^{n} \frac{{}^{2}EI_{c,j}}{(2h)^2} = \sum_{j=1}^{n} \frac{{}^{2}EI_{c,j}}{4h^2} \tag{2.65}$$

With this local shear stiffness, the shear stiffness of the framework on pinned support is given by Equation (2.54). Critical load parameter ${}_{s}$ in Equation (2.64)

is again given in Figure 2.17 and in Table 2.5 as a function of part critical load ratio $_s$, defined by Equation (2.62), where the value of N_g does not depend on the type of support of the framework; therefore Equation (2.63) can be used.

2.4.3 Frameworks with columns of different height at ground floor level

If the framework has columns that are of different height at ground floor level—normally higher than those above—then the corresponding equations can be used if the value of the local shear stiffness is determined according to the greater storey height, i.e. Equations (2.53) or (2.65) should be used but with storey height h^* (Figure 2.20) instead of h.

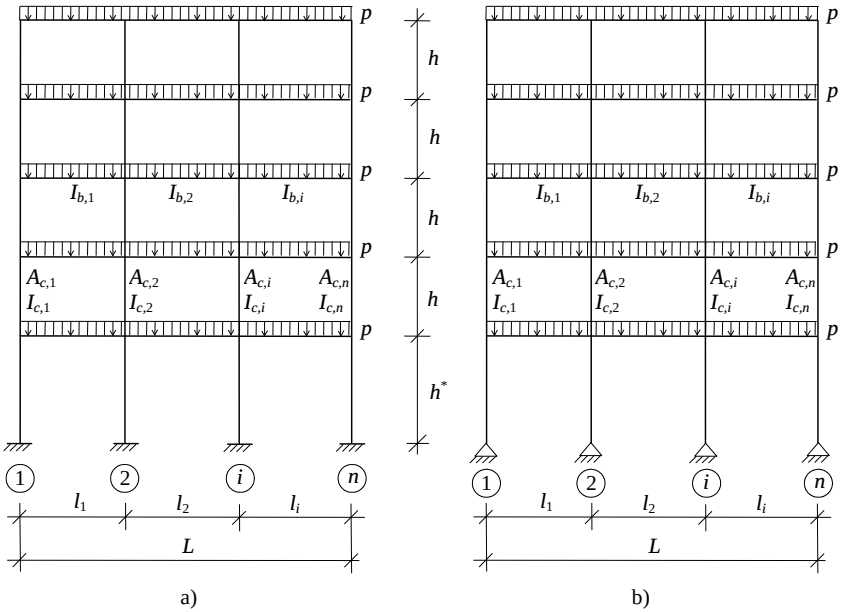

Figure 2.20 Frameworks with ground floor columns of different height. a) on fixed support, b) on pinned support.

2.4.4 Infilled frameworks

Frameworks filled with masonry walls (Figure 2.21/a) have increased resistance to lateral movement. Theoretical investigations (Polyakov, 1956; Madan *et al.*, 1997; Mainstone and Weeks, 1972) and experimental evidence (Mainstone and Weeks, 1972; Riddington and Stafford Smith, 1977) show that the complex behaviour of the composite structure can be handled in a relatively simple way. The contribution of the masonry infill panel to the response of the infilled framework can be modelled by replacing the panel with two equivalent struts: one in tension and the other in compression. The tensile strength of masonry is negligible and can

therefore be safely neglected, leading to the model shown in Figure 2.21/b. As for the diagonal in compression, the cross-section is

$$A_d = tb_w \tag{2.66}$$

where

t is the thickness of the masonry wall
b_w is the effective width of the diagonal strip (Figure 2.21/c)

Experimental evidence shows that the value of the effective width varies in a relatively wide range (Mainstone and Weeks, 1972; Riddington and Stafford Smith, 1977; Achyutha *et al.*, 1994): $0.10 \leq b_w/d \leq 0.40$, with d being the length of the diagonal strut. Design charts have been made available offering values for the effective width, as a function of stiffness parameters and panel proportions (Stafford Smith, 1966; Stafford Smith and Carter, 1969). Alternatively, the value of the effective width can be approximated by

$$b_w = 0.15d \tag{2.67}$$

which normally leads to a conservative estimate.

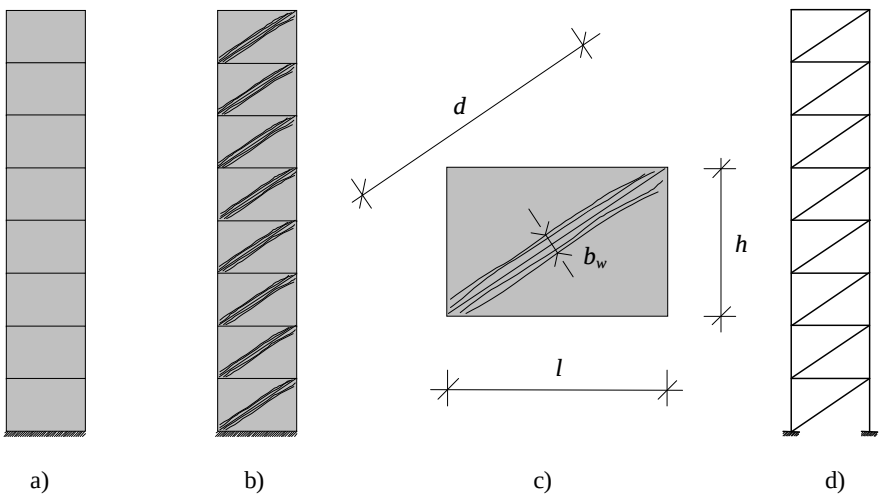

Figure 2.21 Model for infilled framework.

This leads to a framework with single bracing as a possible model for the structural analysis (Figure 2.21/d), whose shear stiffness, based on the first equation in Table 2.6, is composed of two parts, depending on the diagonals (K_d)

and the horizontal beams (K_h), as

$$K = \left(\frac{1}{K_d} + \frac{1}{K_h} \right)^{-1} = \left(\frac{d^3}{A_d E_d h l^2} + \frac{l}{A_h E_h h} \right)^{-1} \tag{2.68}$$

where

E_d is the modulus of elasticity of the masonry wall
E_h is the modulus of elasticity of the beams
A_h is the cross-sectional area of the beams

Equation (2.68) stands for single-bay infilled frameworks. For multi-bay frameworks, the shear stiffness is obtained by adding up the shear stiffnesses of the bays:

$$K = \sum_{i=1}^{n-1} K_i \tag{2.69}$$

where n is the number of columns and K_i refers to the shear stiffness of the ith bay.

By definition, K is also the shear critical load of the framework and has a very important contribution to the overall performance of the framework.

The critical load is then obtained using Equation (2.61) with K and N_g as described in Section 2.4.1.

As for increasing the values of the part critical loads K and N_g, the following rules apply. The value of the shear stiffness depends on two parts: the shear stiffness of the diagonal struts—the first term between the brackets in Equation (2.68)—and the shear stiffness of the beams of the framework (the second term). The bigger K_d and K_h, the bigger the overall shear stiffness K. The shear stiffness is optimized when K_d and K_h are equal. (What was said about the part critical loads in Section 2.4.1—with regard to K and N_g—is also valid here for K_d and K_h.)

The value of K_d is directly proportional to the cross-sectional area A_d and the modulus of elasticity E_d of the diagonals. As for the geometry of the structure, maximum shear stiffness associated with the diagonals is achieved (Figure 2.22) at

$$\frac{h}{l} = 0.708$$

where h is the height of the storeys and l is the bay of the framework.

The situation is simpler with the second part of the shear stiffness K_h which reflects the contribution of the beams. Its value is in direct proportion to the cross-sectional area A_h and the modulus of elasticity E_h of the beams and the height of the storeys and in inverse proportion to the length of the beams.

Finally, the value of the global bending critical load N_g can be increased in different ways: by increasing the cross-sectional area and the modulus of elasticity of the columns and, most importantly, by increasing the distance between the

columns.

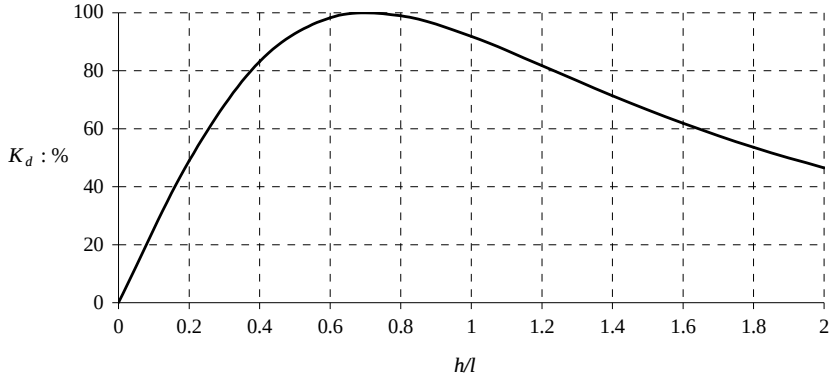

Figure 2.22 Optimum geometrical arrangement for part shear stiffness K_d associated with the diagonals.

2.5 COUPLED SHEAR WALLS

Coupled shear walls can be treated as special frameworks if two phenomena are taken into account. Coupled shear walls normally have relatively wide columns and beams with relatively great depth (Figure 2.23). Consequently, the straight-line section of the beams has to be considered when the relative displacement at the contraflexure point (Δ_3) and consequently the formula for the shear stiffness are derived—see Section 2.1.1 for details. The shear deformation of the beams also has to be taken into account.

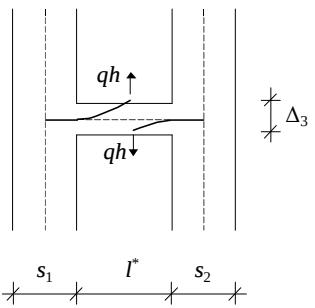

Figure 2.23 Vertical displacement Δ_3 at contraflexure point due to the bending of the connecting beam.

These amendments can be made in a relatively simple way (Zalka and Armer, 1992) and the resulting relative displacement at the contraflexure point of the beams (Figure 2.23) is obtained as

$$\Delta_3 = -\frac{ql^2}{K^*}$$

where

$$K^* = K_b^* r^* = K_b^* \frac{K_c}{K_b^* + K_c} \tag{2.70}$$

and

$$K_b^* = \frac{6EI_b\left((l^* + s_1)^2 + (l^* + s_2)^2\right)}{l^{*3}h\left(1 + 12\dfrac{EI_b}{l^{*2}GA_b}\right)} \tag{2.71}$$

for one bay, where

G	is the modulus of elasticity in shear of the beams
A_b	is the cross-sectional area of the beams
s_1, s_2	are the width of the wall sections of the coupled shear walls
ρ	is a constant depending on the shape of the cross-section of the beams ($\rho = 1.2$ for rectangular cross-sections)
h	is the storey height
l^*	is the distance between the two wall sections (Figure 2.23)

It follows that all the formulae for the lateral deflection, fundamental frequency and the critical load can be used if, according to Equation (2.70), K_b and r are replaced by K_b^* and r^* for coupled shear walls. For multi-bay coupled shear walls the shear stiffnesses of the bays should be added up using Equation (2.69), where n is now the number of walls.

2.6 SHEAR WALLS

In the case of shear walls, the situation is very simple as they can be considered (very) simple frameworks. Of the three characteristic stiffnesses only their bending stiffness EI should be considered that corresponds to the local bending stiffness of a framework. (Their resistance to global bending and shear—using frame-terminology—can be considered infinitely great.) The well-known formulae for the deflection, maximum deflection, the fundamental frequency and the critical load are as follows.

Deflection:

$$y(z) = \frac{w}{EI}\left(\frac{H^3 z}{6} - \frac{z^4}{24}\right) \qquad \text{and} \qquad y_{\max} = y(H) = \frac{wH^4}{8EI} \tag{2.72}$$

where w is the intensity of the uniformly distributed horizontal load and z is measured from ground floor level.

Fundamental frequency:

$$f = \frac{0.56 r_f}{H^2}\sqrt{\frac{EI}{m}} \tag{2.73}$$

where m is the mass density per unit length of the shear wall and r_f is the mass distribution factor according to Figure 2.9 and Table 4.1.

Critical load:

$$N_{cr} = qH = \frac{7.837 EI r_s}{H^2} \tag{2.74}$$

where r_s is the load distribution factor given in Figure 2.14 and in Table 5.1.

2.7 CORES

Shear walls are often built together to create three dimensional units. Prime example is the U-shaped elevator core but many different shapes exist in building structures. The second moments of area of a reinforced concrete core are normally large and a small number of cores are often sufficient to provide the building with the necessary stiffness to resist lateral loading. In the two principal directions they act as shear walls and, knowing the second moments of area, Equations (2.72), (2.73) and (2.74) can be readily used to calculate the deflection, the maximum top deflection, the fundamental frequency and the critical load of a core.

As opposed to shear walls (and frameworks), however, cores are three-dimensional structures and they also have torsional resistance which may constitute a significant part of the overall torsional resistance of the building. In the case of the five-storey building investigated in detail in Section 12.2, for example, the torsional resistance of the building is solely provided by a single U-core.

2.7.1 Torsional stiffness characteristics

As far as torsional behaviour is concerned, in view of their dimensions (height of core, thickness of the wall sections of the cross-section of the core), cores can be considered thin-walled columns and their torsional resistance originates from two sources: the pure (Saint-Venant) torsional stiffness (GJ) and the warping torsional stiffness (EI_ω).

For cores of open cross-section (Figure 2.24/a), the Saint-Venant torsional constant is obtained from

$$J = \frac{1}{3}\sum_{i=1}^{m} h_i t_i^3 \tag{2.75}$$

where

h_i is the length of the *i*th wall section
t_i is the thickness of the *i*th wall section
m is the number of wall sections

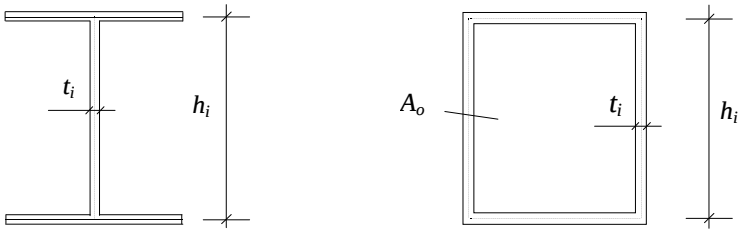

a) b)

Figure 2.24 Cores of thin-walled wall sections. a) open cross-section, b) closed cross-section.

On the rare occasion when the core has a closed cross-section (or its openings are so small that they can be ignored), Bredt's formula should be used:

$$J = \frac{4A_o^2}{\sum_{i=1}^{m} \frac{h_i}{t_i}} \tag{2.76}$$

where A_o is the area enclosed by the mean centre lines of the wall sections (Figure 2.24/b) and again:

h_i is the length of the *i*th wall section
t_i is the thickness of the *i*th wall section
m is the number of wall sections

The relationship between Young's modulus and the modulus of elasticity in shear is

$$G = \frac{E}{2(1+\ )} \tag{2.77}$$

where v is the Poisson ratio.

Warping torsion is associated with the bending of the wall sections of the core—c.f. Section 3.2.1—but the determination of the stiffness associated with it is much more complicated than with pure torsion (Vlasov, 1961; Zbirohowski-Koscia; 1967, Kollbrunner and Basler, 1969). No simple procedure of general validity is available for the calculation of the warping constant (I_ω) but closed form solutions exist for several cross-sections. Some of these formulae are collected in Table 2.7 where, in addition to the warping constant, formulae for the pure torsional constant and the location of the shear centre are also presented for the most commonly used cores. Tables 2.8 and 2.9 cover more complex (or

unsymmetric) cases.

Table 2.7 Torsional characteristics for common bracing cores of simple cross-section.

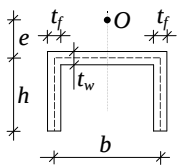

$$e = \frac{3t_f h^2}{6t_f h + t_w b}, \qquad J = \frac{1}{3}(2ht_f^3 + bt_w^3)$$

$$I_\Omega = \frac{t_f h^3 b^2}{12} \frac{3t_f h + 2t_w b}{6t_f h + t_w b}$$

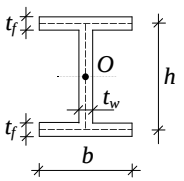

$$J = \frac{1}{3}(2bt_f^3 + ht_w^3)$$

$$I_\Omega = \frac{t_f b^3 h^2}{24}$$

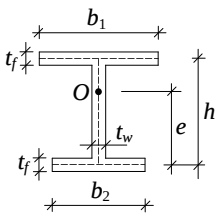

$$e = h\frac{b_1^3}{b_1^3 + b_2^3}, \qquad J = \frac{1}{3}\left((b_1 + b_2)t_f^3 + ht_w^3\right)$$

$$I_\Omega = \frac{t_f h^2}{12} \frac{b_1^3 b_2^3}{b_1^3 + b_2^3}$$

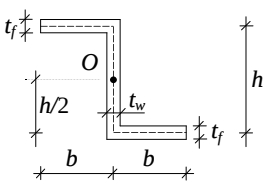

$$J = \frac{1}{3}(2bt_f^3 + ht_w^3)$$

$$I_\Omega = \frac{b^3 h^2}{12(2b+h)^2}[2t_f(b^2 + bh + h^2) + 3t_w bh]$$

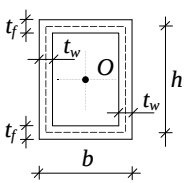

$$J = \frac{2b^2 h^2 t_f t_w}{ht_f + bt_w}$$

$$I_\Omega \cong 0$$

Typical bracing cores are shown in Figure 2.25 where the warping stiffness of the first four cores (Figure 2.25/a) is so small that it can safely be ignored for practical calculations.

a)

b)

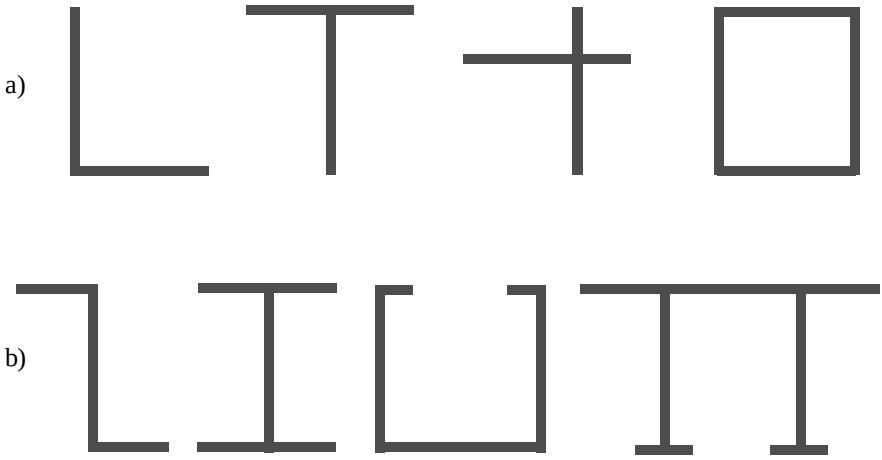

Figure 2.25 Cores. a) with $I_\omega \approx 0$, b) with considerable I_ω.

Table 2.8 Cross-sectional characteristics for TT-sections.

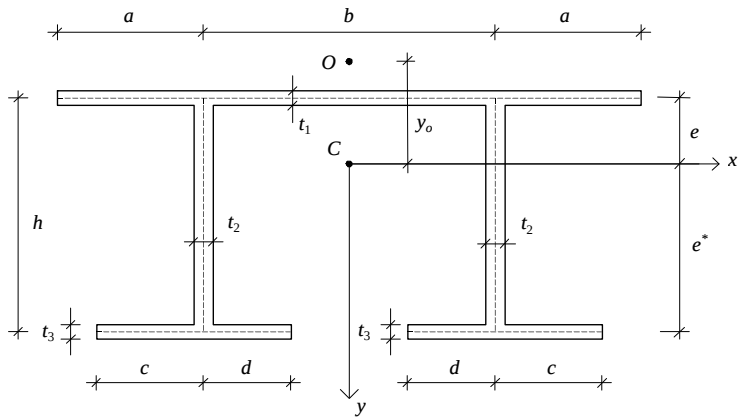

$$A = A_f + 2A_g + 2A_a \qquad \text{with}$$

$$A_f = t_1(2a+b), \quad A_g = t_2(h - \frac{t_1}{2} - \frac{t_3}{2}), \quad A_a = t_3(c+d)$$

$$e = \frac{1}{A}\left(2A_a h + 2A_g(\frac{h}{2} - \frac{t_3}{4} + \frac{t_1}{4})\right), \quad e^* = h - e$$

$$y_o = -e - \frac{eAb^2}{4I_y} + \frac{2hI_{ag}}{I_y} \qquad \text{where} \qquad I_{ag} = \frac{t_3}{3}(c^3 + d^3)$$

Table 2.8 Continued. Cross-sectional characteristics for TT-sections.

$$I_x = \frac{1}{12}\left(A_f t_1^2 + 2A_a t_3^2 + 2A_g (h - \frac{t_1}{2} - \frac{t_3}{2})^2 \right) + A_f e^2 + 2A_a e^{*2} + 2A_g \left(\frac{h}{2} - \frac{t_3}{4} + \frac{t_1}{4} - e \right)^2$$

$$I_y = \frac{1}{12}\left(A_f (2a+b)^2 + t_3(b+2c)^3 - t_3(b-2d)^3 + 2A_g t_2^2 \right) + \frac{b^2}{2} A_g$$

$$I_{xy} = 0, \qquad J = \frac{1}{3}\left(A_f t_1^2 + 2A_g t_2^2 + 2A_a t_3^2 \right)$$

$$I_\Omega = \frac{b^2 I_x}{4} + \frac{b^2 e^2 A}{4}\left(1 - \frac{b^2 A}{4 I_y} \right) + 2h^2 I_{ag} - 2bfh^2 A_a + b^2 ehA \frac{I_{ag}}{I_y} - 4h^2 \frac{I_{ag}^2}{I_y}$$

where $f = \dfrac{c-d}{2}$

Table 2.9 Cross-sectional characteristics for □-sections.

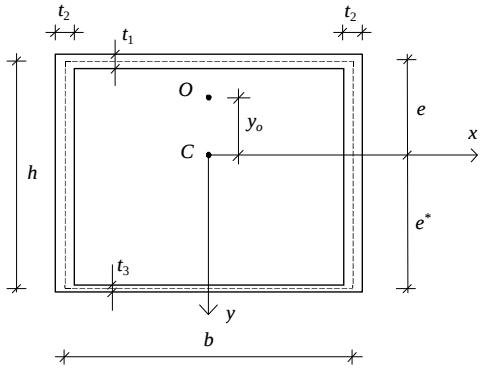

$$A = A_f + 2A_g + A_a \qquad \text{with}$$

$$A_f = t_1(b+t_2), \quad A_g = t_2(h - \frac{t_1}{2} - \frac{t_3}{2}), \quad A_a = t_3(b+t_2)$$

$$e = \frac{1}{A}\left(A_a h + A_g (h - \frac{t_3}{2} + \frac{t_1}{2}) \right), \quad e^* = h - e$$

$$I_x = \frac{1}{12}\left(A_f t_1^2 + A_a t_3^2 + 2A_g (h - \frac{t_1}{2} - \frac{t_3}{2})^2 \right) + A_f e^2 + A_a e^{*2} + 2A_g \left(\frac{h}{2} - \frac{t_3}{4} + \frac{t_1}{4} - e \right)^2$$

$$I_y = \frac{1}{12}\left((A_f + A_a)(b+t_2)^2 + 2A_g t_2^2 \right) + \frac{b^2}{2} A_g, \qquad I_{xy} = 0$$

Table 2.9 Continued. Cross-sectional characteristics for □-sections.

$$y_o = -e - \frac{I_{\Omega x}}{I_y} \qquad \text{where} \qquad I_{\Omega x} = \frac{b^2}{6}(\Omega_1 t_1 + \Omega_2 t_3) + \frac{bht_2}{2}(\Omega_1 + \Omega_2)$$

$$\Omega_1 = -\Psi\frac{b}{2t_1}, \qquad \Omega_2 = \frac{bh}{2} - \Psi\left(\frac{b}{2t_1} + \frac{h}{t_2}\right), \qquad \Psi = \frac{2A_o}{\int \frac{ds}{t}} = \frac{2hb}{\frac{b}{t_1} + \frac{b}{t_3} + \frac{2h}{t_2}}$$

$$J = 2A_o\Psi = \frac{4h^2b^2}{\frac{b}{t_1} + \frac{b}{t_3} + \frac{2h}{t_2}}, \qquad I_\Omega = \frac{2}{3}\left(ht_2(\Omega_1^2 + \Omega_1\Omega_2 + \Omega_2^2) + \frac{1}{2}b(\Omega_1^2 t_1 + \Omega_2^2 t_3)\right)$$

where $\Omega_1 = -\frac{bI_{\Omega x}}{2I_y} + \Omega_1$, $\Omega_2 = -\frac{bI_{\Omega x}}{2I_y} + \Omega_2$ and $A_o = bh$

U-cores are perhaps the most commonly used types (for elevator and service shafts) but they are in most cases partially closed at storey levels by floor slabs or beams (Figure 2.26). The effect of the connecting elements can always be safely ignored but their contribution is normally significant and the structural engineer may wish to take it into consideration for economic reasons. The connecting elements restrain the core section from warping and increase its torsional stiffness. Vlasov's (1961) investigations show that the phenomenon can be taken into account by amending the governing differential equation of torsion [Equation (2.84), to be discussed later on] in the form of

$$EI_\Omega\, \theta'''' - G(J + \bar{J})\, \theta'' = m_z \tag{2.78}$$

where

$$\bar{J} = \frac{4A_o^2}{\frac{l^3 sG}{12EI_b} + \frac{1.2ls}{A_b}} \tag{2.79}$$

represents the effect of the connecting beams and J is defined by Equation (2.76). In the above equation

A_o	is the area enclosed by the mean centre lines of the wall sections (Figure 2.26/b)
b and h	are the lengths of the wall sections of the U-core
l	is the span of the connecting beams
s	is the vertical distance of the connecting beams (storey height in most cases)
E	is the modulus of elasticity of connecting beam
G	is the modulus of elasticity in shear of connecting beam

and

$$A_b = t_b d \qquad \text{and} \qquad I_b = \frac{t_b d^3}{12}$$

are the area and the second moment of area of the cross-section of the connecting beams with t_b and d being the thickness and depth of the connecting beams.

If the amended torsional stiffness ($J + \bar{J}$) is used, then all the formulae originating from the governing differential equation (2.84) and given in this Section later on can be used for the determination of the rotation, fundamental frequency and critical load of the partially closed core.

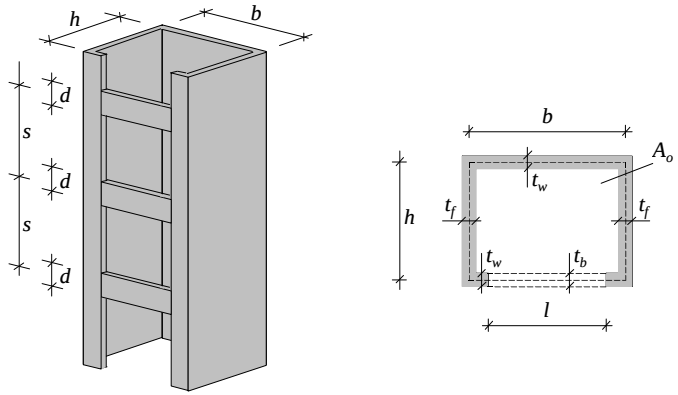

a) b)

Figure 2.26 Partially closed U-core.

Numerical investigations show that when the depth of the connecting beam (d) is relatively great, Equation (2.79) tends to overestimate the effect of the connecting beams and may result in a value for the torsional stiffness that is greater than that of an entirely closed section—which is clearly impossible. In such cases, the approximation

$$\bar{J} = \frac{4h^2 b^2}{\dfrac{2b-l}{t_w} + \dfrac{l}{t_w^*} + \dfrac{2h}{t_f}} \tag{2.80}$$

may be used where the equivalent thickness is determined using

$$t_w^* = \frac{d}{s} t_b \tag{2.81}$$

where, again, d is the depth of the connecting beams and s is the vertical distance of the connecting beams.

2.7.2 Deflection and rotation under uniformly distributed horizontal load

When the horizontal load passes through the shear centre axis, Equations (2.72) can be applied, using the relevant second moment of area, for the determination of the deflection and maximum deflection of the core:

$$u(z) = \frac{w_x}{EI_y}\left(\frac{H^3 z}{6} - \frac{z^4}{24}\right) \qquad \text{and} \qquad u_{\max} = u(H) = \frac{w_x H^4}{8EI_y} \tag{2.82}$$

$$v(z) = \frac{w_y}{EI_x}\left(\frac{H^3 z}{6} - \frac{z^4}{24}\right) \qquad \text{and} \qquad v_{\max} = v(H) = \frac{w_y H^4}{8EI_x} \tag{2.83}$$

When the torsional behaviour of a core subjected to uniformly distributed torsional moment is investigated (Figure 2.27), the governing differential equation assumes the form

$$EI_\Omega \, \varphi'''' - GJ \, \varphi'' = m_z \tag{2.84}$$

with the boundary conditions

$$\varphi(0) = 0\,, \qquad \varphi'(0) = 0 \tag{2.85}$$

and

$$\varphi''(H) = 0\,, \qquad EI_\Omega \, \varphi'''(H) - GJ \, \varphi'(H) = 0 \tag{2.86}$$

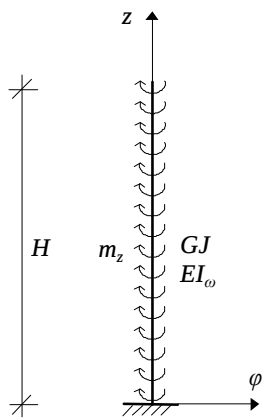

Figure 2.27 Bracing core for the torsional analysis, subjected to uniformly distributed torsional moment.

The solution can be expressed in closed form:

$$(z) = \frac{m_z}{GJ \cosh k}\left[\frac{H^2}{k^2}\left(\cosh\frac{kz}{H} + k\sinh(k - \frac{kz}{H}) - k\sinh k - 1\right)\right.$$

$$\left. + z(H - \frac{z}{2})\cosh k\right] \tag{2.87}$$

where

$$k = H\sqrt{\frac{GJ}{EI_\Omega}} \tag{2.88}$$

is the torsion parameter.

Maximum rotation develops at the top:

$$_{\max} = \quad (H) = \frac{m_z H^2}{GJ}\left(\frac{\cosh k - 1}{k^2 \cosh k} - \frac{\tanh k}{k} + \frac{1}{2}\right) \tag{2.89}$$

Two special cases will now be considered. In most practical cases the effect of the Saint-Venant torsional stiffness (GJ) is small compared to the effect of the warping stiffness (EI_ω) and

$$k << 1$$

holds. In such cases, keeping in mind that $GJ/EI_\omega \approx 0$ holds, the governing differential equation of the torsional problem simplifies to

$$'''' = \frac{m_z}{EI_\Omega}$$

and the formula for the maximum rotation is obtained as

$$_{\max} = \quad (H) = \frac{m_z H^4}{8EI_\Omega} \tag{2.90}$$

When the core has no warping stiffness (Figure 2.25/a), the above solutions cannot be used as the denominator in Equations (2.88) and (2.90) vanishes. In such cases the original governing differential equation simplifies to

$$'' = -\frac{m_z}{GJ}$$

whose solution results in

$$_{\max} = \quad (H) = \frac{m_z H^2}{2GJ} \tag{2.91}$$

for the maximum rotation.

2.7.3 Critical load

When the stability of a core is investigated, three things have to be considered: lateral buckling in the two principal directions and pure torsional buckling. For lateral buckling, Equation (2.74) given for shear walls can be used and the critical loads in the principal directions can be calculated from

$$N_{cr,x} = \frac{7.837 EI_y r_s}{H^2} \qquad \text{and} \qquad N_{cr,y} = \frac{7.837 EI_x r_s}{H^2} \tag{2.92}$$

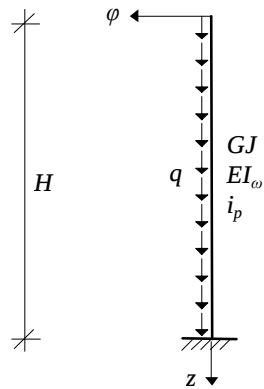

Figure 2.28 Bracing core for the analysis of pure torsional buckling.

The situation with pure torsional buckling is more complicated. It is advantageous for the origin of the coordinate system to be placed at and attached to the upper free end of the core (Figure 2.28). The governing differential equation in this coordinate system assumes the form

$$r_s EI_\Omega \; ''''+\left[\left(N(z) i_p^2 - GJ\right) \; '\right]' = 0$$

with the boundary conditions

$$(0) = 0\,, \qquad ''(0) = 0$$

and

$$'(H) = 0, \qquad EI_{\Omega}\ '''(H) - GJ\ '(H) = 0$$

where

$$i_p = \sqrt{\frac{I_x + I_y}{A}} \tag{2.93}$$

is the radius of gyration of the cross-section of the core, r_s is the load distribution factor (Figure 2.14 or Table 5.1) and $N(z) = qz$.

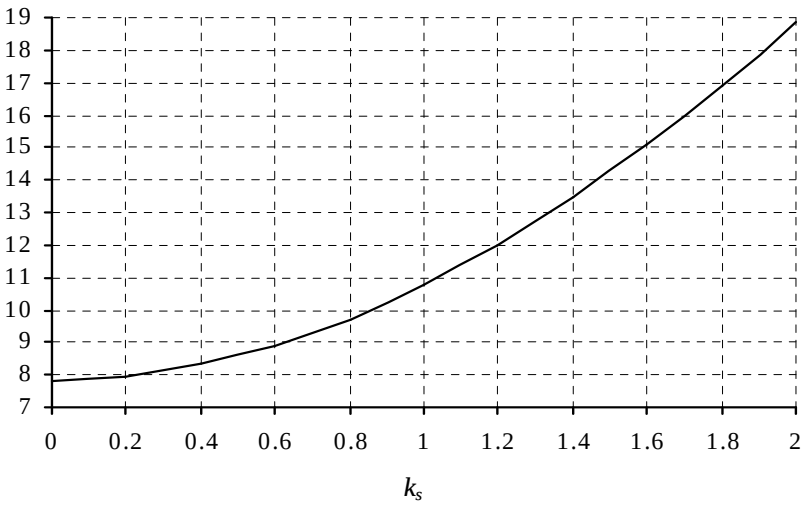

Figure 2.29 Critical load parameter α as a function of parameter k_s.

The solution of the above governing differential equation gives the critical load for pure torsional buckling as

$$N_{cr,} = \frac{r_s EI_{\Omega}}{i_p^2 H^2} \tag{2.94}$$

where α is the critical load factor. Its function is shown in Figure 2.29 and its values are given in Table 2.10 as a function of

$$k_s = \frac{k}{\sqrt{r_s}} = H\sqrt{\frac{GJ}{r_s EI_{\Omega}}} \tag{2.95}$$

It is important to point out that when Equation (2.94) is used for the stability analysis of a ***building*** braced by a single core, then the radius of gyration refers to the layout of the building (rather than to the cross-section of the core).

When the warping stiffness of the core is zero, Equations (2.94) and (2.95) cannot be used. Instead,

$$N_{cr,} = \frac{GJ}{i_p^2} \tag{2.96}$$

should be used. It is interesting to note that in this case the value of the critical load does not depend on the height of the structure.

It should be noted here that cores normally behave in a true three-dimensional fashion and the above three critical loads can only be considered ***basic*** critical loads. The basic critical loads ($N_{cr,x}$, $N_{cr,y}$ and $N_{cr,\varphi}$) may, and normally will, combine during buckling resulting in the global critical load of the core. This combination is very important as the actual critical load of the core is always smaller than (or equal to) the smallest one of the three basic critical loads. For the coupling of the basic critical loads, see Chapter 5 that deals with three-dimensional behaviour.

Table 2.10 Critical load parameter α as a function of parameter k_s.

k_s	α	k_s	α	k_s	α	k_s	α
0.00	7.837	1.3	12.72	2.8	28.03	50	2984.7
0.01	7.838	1.4	13.47	2.9	29.30	60	4209.3
0.05	7.845	1.5	14.27	3.0	30.59	70	5640.9
0.10	7.867	1.6	15.11	4.0	44.69	80	7278.1
0.20	7.957	1.7	15.99	5.0	60.75	90	9120.7
0.30	8.107	1.8	16.91	6.0	78.80	100	11168
0.40	8.316	1.9	17.87	7.0	98.94	200	42864
0.50	8.583	2.0	18.87	8.0	121.2	300	94863
0.60	8.909	2.1	19.91	9.0	145.7	400	167093
0.70	9.291	2.2	20.98	10	172.4	500	259498
0.80	9.730	2.3	22.08	15	338.6	1000	1023750
0.90	10.22	2.4	23.21	20	558.6	2000	4059499
1.00	10.77	2.5	24.38	25	831.8	3000	9101926
1.10	11.37	2.6	25.57	30	1157.8	4000	16149383
1.20	12.02	2.7	26.79	40	1967.1	>4000	k_s^2

2.7.4 Fundamental frequency

When the vibration of the core is investigated, the frequencies for the lateral vibration can again be readily obtained using the solution given for shear walls:

$$f_x = \frac{0.56 r_f}{H^2}\sqrt{\frac{EI_y}{m}} \qquad \text{and} \qquad f_y = \frac{0.56 r_f}{H^2}\sqrt{\frac{EI_x}{m}} \tag{2.97}$$

where m is the mass density per unit length of the material of the core and r_f is the mass distribution factor by Figure 2.9 or Table 4.1.

The analysis of pure torsional vibration is carried out by investigating the equilibrium of an elementary section of the core (Figure 2.30). Its governing differential equation emerges as

$$r_f^2 EI_\Omega \, '''' - r_f^2 GJ \, '' + m i_p^2 \, \ddot{} = 0$$

where primes and dots mark differentiation by z and t (time). After seeking the solution in a product form, separating the variables and eliminating the time dependent functions, the above governing differential equation leads to the boundary value problem

$$r_f^2 EI_\Omega \, {}_1'''' - r_f^2 GJ \, {}_1'' - \Omega^2 m i_p^2 \, {}_1 = 0$$

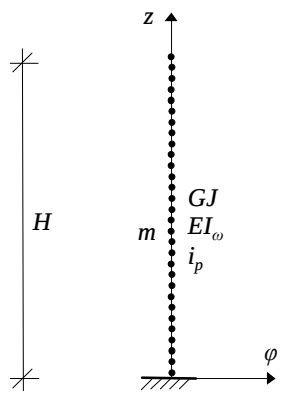

Figure 2.30 Bracing core for the analysis of pure torsional vibration.

This differential equation is identical to Equation (2.47) in structure, has the same boundary conditions, and so the solution to Equation (2.47) can be used if the stiffness characteristics in Equation (2.47) are replaced with those in the above equation. In doing so, the formula for the pure torsional frequency is obtained as

$$f = \frac{r_f}{i_p H^2}\sqrt{\frac{EI_\Omega}{m}} \tag{2.98}$$

where values for η are given in Figure 2.11 and in Table 4.2 as a function of k [Equation (2.88)]:

$$k = H\sqrt{\frac{GJ}{EI_\Omega}}$$

Equation (2.98) for the fundamental frequency of pure torsional vibration cannot be used for cores with zero warping stiffness. For such cores the fundamental frequency for pure torsion is calculated from

$$f = \frac{1}{4Hi_p}\sqrt{\frac{GJ}{m}} \tag{2.99}$$

It is important to point out that when Equations (2.98) and (2.99) are used for the frequency analysis of a ***building*** braced by a single core, then the radius of gyration refers to the layout of the building (rather than to the cross-section of the core).

As with the stability investigation of the core, it should be noted here that cores normally behave in a true three-dimensional fashion and the above three fundamental frequencies (f_x, f_y and f_φ) can only be considered ***basic*** fundamental frequencies and they normally combine during vibration resulting in the fundamental frequency of the core. This combination is very important as the fundamental frequency of the core is always smaller than (or equal to) the smallest one of the three basic frequencies. For the coupling of the basic modes see Chapter 4 that deals with three-dimensional behaviour.

3

Deflection and rotation analysis of buildings under horizontal load

Based on the deflection analysis of a single framework, the characteristic unit of a bracing system, whole structures braced by frameworks, coupled shear walls, shear walls and cores will now be investigated. The task is made more complicated than with a simple unit as, in addition to the interaction among the elements of a framework, interaction also occurs among the bracing units themselves. Approximate methods have been developed for the investigation of bracing systems under horizontal load (Pearce and Matthews, 1971; Dowrick, 1976; Schueller, 1977; Irwin, 1984; Stafford-Smith and Coull, 1991; Coull and Wahab, 1993) but they often have restrictive assumptions and their accuracy and reliability have not been comprehensively investigated. Sporadic checks indicate that in certain cases they lead to unconservative estimates of unacceptable magnitude (up to 70%).

A building under horizontal load can, and normally will, develop lateral deflection in two planes and rotation. One of the most important pieces of information regarding the building as a whole unit is its maximum deflection and the aim of this chapter is to offer a relatively simple solution for the top deflection as well as for the rotation of the building. The solutions to be presented in this chapter are not only simple but their structure is such that they show how the different stiffness characteristics influence the deflection and rotation of the building. The summary of a comprehensive accuracy analysis involving 279 structures of different height and stiffness characteristics, with both reinforced concrete and steel bracing units, demonstrates the accuracy and reliability of the methods.

It will be shown that the deflection of the building is defined by three distinctive parts: bending deflection, shear deflection and the interaction between the bending and shear modes. It is demonstrated that the interaction is always beneficial as it reduces the deflection of the structure. Similar conclusions are made regarding the rotation of the building.

3.1 LATERAL DEFLECTION ANALYSIS OF BUILDINGS UNDER HORIZONTAL LOAD

Consider a *system* of frameworks and coupled shear walls ($i = 1, \ldots, f$), subjected to a uniformly distributed lateral load of intensity w, shown in Figure 3.1. (Shear walls and cores will be incorporated into the system later on.) Unlike in Section 2.1, for the following derivation let l_i and I_i denote the bays of the frameworks and

the sums of the second moments of area of the columns of the units, respectively. Although the bracing units act independently from each other, the connecting floor slabs make them deflect together assuming the same deflection shape. Each unit takes horizontal load and bending moment according to its stiffness

$$w_i = q_i w \qquad \text{and} \qquad M_i = q_i M \tag{3.1}$$

where factor q_i is an apportioner that is responsible for distributing the total load among the bracing units.

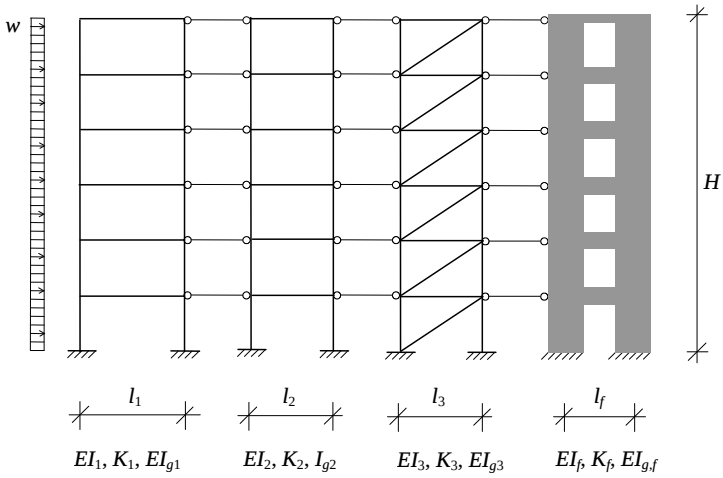

Figure 3.1 A system of f bracing units.

Each unit may have three stiffnesses (EI, EI_g and K, as defined in Section 2.1.2) and all three influence its behaviour. The best way to take into account the combined effect of the stiffnesses is to consider the deflection of the unit. Accordingly, the "governing" stiffness of each unit is defined as

$$S_i = \frac{1}{y_i} \tag{3.2}$$

where y_i is the top deflection of the ith unit, calculated using Equation (2.24) in Section 2.1.1. With the above unit-stiffness, the apportioners are calculated from

$$q_i = \frac{S_i}{\sum S_i} \tag{3.3}$$

The summation in Equation (3.3) covers *all* the bracing units—see remark above Equation (3.15). During deflection, the columns and the beams of the

frameworks assume their bending deformation and the columns develop their axial deformation, utilising their individual bending and axial stiffnesses. Consequently, Equation (2.9) holds for each framework. Because of the identical deflection shapes, in the equations expressing continuity along the lines of contraflexure of the frameworks, the function of deflection is the same for each framework ($y_i \equiv y$) while the other characteristics are unit-specific:

$$y'' - \frac{l_i}{K_i} N_i'' + \frac{l_i}{EI_{g,i}} N_i = 0 \tag{3.4}$$

In order to determine normal force N_i for substitution in the above equation, the bending/deflection of the frameworks is considered next. Based on Equation (2.11), the bending of the frameworks is defined by

$$y'' EI_i = -M_i + l_i N_i \tag{3.5}$$

Rearranging Equation (3.5) and making use of Equation (3.1) result in the normal forces as

$$N_i = \frac{1}{l_i}(y'' EI_i + q_i M) \tag{3.6}$$

Substituting for N_i in Equation (3.6) leads to the following differential equation for the *i*th unit of the system:

$$y'' - \frac{1}{K_i}\left(y'' EI_i + q_i M\right)'' + \frac{1}{EI_{g,i}}\left(y'' EI_i + q_i M\right) = 0 \tag{3.7}$$

Making use of the fact that the floor slabs make the bracing units assume the same deflection, a single differential equation can be obtained for the whole system by adding up the above equations from $i = 1$ to $i = f$. Using the first, second and last bracing units for clarity, the differential equation for the whole system assumes the form:

$$\begin{aligned} f y'' - y'''' \left(\frac{EI_1}{K_1} + \frac{EI_2}{K_2} + \cdots + \frac{EI_f}{K_f} \right) + y'' \left(\frac{EI_1}{EI_{g1}} + \frac{EI_2}{EI_{g2}} + \cdots + \frac{EI_f}{EI_{g,f}} \right) \\ = M'' \left(\frac{q_1}{K_1} + \frac{q_2}{K_2} + \cdots + \frac{q_f}{K_f} \right) - M \left(\frac{q_1}{EI_{g1}} + \frac{q_2}{EI_{g2}} + \cdots + \frac{q_f}{EI_{g,f}} \right) \end{aligned} \tag{3.8}$$

The equation can be written in a more general form if one of the units is considered the "base unit" (with *EI*, *K* and EI_g) and the stiffness characteristics of the others are expressed by those of the base unit. Let Unit 1 be the base unit.

Introducing the notation

$$\begin{array}{llll} EI_1 = EI & K_1 = K & EI_{g1} = EI_g & q_1 \\ EI_2 = a_1 EI & K_2 = b_1 K & EI_{g2} = c_1 EI_g & q_2 = a_1 q_1 \\ \vdots & \vdots & \vdots & \vdots \\ EI_f = a_{f-1} EI & K_f = b_{f-1} K & EI_{g,f} = c_{f-1} EI_g & q_f = a_{f-1} q_1 \end{array} \tag{3.9}$$

and after some rearrangement Equation (3.8) turns into

$$y'''' \frac{EI}{K}\left(1+\frac{a_1}{b_1}+\cdots+\frac{a_{f-1}}{b_{f-1}}\right) - y'' \frac{EI}{EI_g}\left(1+\frac{a_1}{c_1}+\cdots+\frac{a_{f-1}}{c_{f-1}}+f\frac{EI_g}{EI}\right)$$

$$= M\frac{q_1}{EI_{g1}}\left(1+\frac{a_1}{c_1}+\cdots+\frac{a_{f-1}}{c_{f-1}}\right) - M''\frac{q_1}{K}\left(1+\frac{a_1}{b_1}+\cdots+\frac{a_{f-1}}{b_{f-1}}\right)$$

which, after re-introducing a and b from Equation (2.14) and with $M = wz^2/2$, can be rearranged as:

$$y'''' - \left(a\frac{1+\sum_{i=1}^{f-1}\frac{a_i}{c_i}}{1+\sum_{i=1}^{f-1}\frac{a_i}{b_i}} + b\frac{f}{1+\sum_{i=1}^{f-1}\frac{a_i}{b_i}} \right) y'' = \frac{wq_1}{EI}\left(\frac{z^2}{2} a\frac{1+\sum_{i=1}^{f-1}\frac{a_i}{c_i}}{1+\sum_{i=1}^{f-1}\frac{a_i}{b_i}} - 1 \right) \tag{3.10}$$

It is easily seen that the above equation is in the form of

$$y'''' - {}^{-2}y'' = \frac{\bar{w}}{EI}\left(\frac{\bar{a}z^2}{2}-1\right) \tag{3.11}$$

and therefore it is, in structure, identical to Equation (2.15). It follows that the solution of Equation (2.15) for a single bracing unit can be generalized and used for the determination of the deflection of a system of frameworks and coupled shear walls (Zalka, 2009):

$$y(z) = \frac{\bar{w}}{EI_f}\left(\frac{H^3 z}{6}-\frac{z^4}{24}\right) + \frac{\bar{w}z^2}{2K\bar{s}^2} - \frac{\bar{w}EI}{K^2\bar{s}^3}\left(\frac{\cosh{}^{-}(H-z)+{}^{-}H\sinh{}^{-}z}{\cosh{}^{-}H}-1\right) \tag{3.12}$$

where $\overline{w} = q_1 w$ is the wind load on the base unit, and

$$\bar{} = \sqrt{\bar{a} + \bar{b}} \qquad \text{and} \qquad \bar{s} = 1 + \frac{\bar{a}}{\bar{b}} \tag{3.13}$$

Maximum deflection develops at $z=H$:

$$y_{\max} = y(H) = \frac{\overline{w} H^4}{8EI_f} + \frac{\overline{w} H^2}{2K\bar{s}^2} - \frac{\overline{w} EI}{K^2 \bar{s}^3}\left(\frac{1 + \bar{} H \sinh \bar{} H}{\cosh \bar{} H} - 1\right) \tag{3.14}$$

Stiffnesses EI, K and EI_g are those of the "base unit" (and $I_f = I + I_g$).

The derivation presented above assumed a system of f rigid frames with EI, K and EI_g. For coupled shear walls, stiffnesses EI, K^* and EI_g are used. [See Equation (2.70) for K^*.] The bracing system may also contain braced frames, infilled frames, shear walls and cores.

Braced frames and infilled frames should be handled in a similar way, keeping in mind the following small differences. Their shear stiffness K should be determined according to the different types of bracing. Ready-to-use formulae are given in Table 2.6. Equations (2.68) and (2.69) can be used for infilled frames. When the bending stiffness of braced and infilled frames is calculated, their local bending stiffness is calculated directly as the sum of the bending stiffnesses of the columns, with $r = 1$, i.e., $EI = EI_c$. The calculation of the global bending stiffness EI_g is identical to that of the rigid frames, i.e., according to Equation (2.32).

Assume now that the system also contains m shear walls and cores. The situation is different (and much simpler) with shear walls and cores. They only have bending stiffness EI (the torsional stiffness of the cores is irrelevant for the time being), which corresponds to the local bending stiffness of rigid frames. In terms of frame-behaviour, their resistance against shear deflection and global bending deflection is considered infinitely great and they do not participate in "normal" frame-type interaction. This has two important consequences:

a) When the apportioner of the base unit q_1 is established, the shear walls and cores are also included when the total stiffness of the bracing system (ΣS_i) is calculated, i.e., $i = f + m$ in Equation (3.3). When the deflection of a shear wall/core is calculated (for determining its characteristic stiffness S_i), only its bending stiffness is considered, i.e.,

$$y(z) = \frac{w}{EI}\left(\frac{H^3 z}{6} - \frac{z^4}{24}\right) \qquad \text{and} \qquad y_{\max} = y(H) = \frac{wH^4}{8EI} \tag{3.15}$$

b) When a shear wall/core is incorporated into a bracing system, it is assumed that their shear and global bending stiffnesses are infinitely great in the sense frame terminology interprets these stiffnesses. It follows that they would not appear in Equation (3.10) where f stands for the number of frameworks.

With the above considerations, parameters $\bar{a}$ and $\bar{b}$ for a system of frames

and shear walls/cores are determined as follows:

$$\bar{a} = \frac{K}{EI_g}\frac{1+\sum_{i=1}^{f-1}\frac{a_i}{c_i}}{1+\sum_{i=1}^{f-1}\frac{a_i}{b_i}}, \qquad \bar{b} = \frac{K}{EI}\frac{f}{1+\sum_{i=1}^{f-1}\frac{a_i}{b_i}}, \qquad \bar{w} = wq_1$$

$$\text{with} \qquad a_i = \frac{EI_{i+1}}{EI_1}, \qquad b_i = \frac{K_{i+1}}{K_1} \qquad c_i = \frac{EI_{g,i+1}}{EI_{g,1}} \tag{3.16}$$

where f is the number of frameworks and coupled shear walls.

The above derivation and formulae spectacularly demonstrate how complicated and delicate the interaction among the stiffness characteristics of the bracing units is. As a rule, it is certainly not possible to create an equivalent structure for the analysis by simply adding up the corresponding stiffnesses (EI, EI_g and K) as is widely circulated in the literature. Simple addition of the stiffnesses might work in some cases, but only in some special cases (e.g. when the bracing system only consists of a single framework and one or more shear walls), and in the majority of other cases it leads to highly unreliable results.

A key element of the procedure is the "base" unit. Choosing a "base" unit makes it possible to reduce the problem of $f + m$ bracing units to the problem of a single unit. In other words, choosing a base unit is equivalent to incorporating the bracing elements into a single equivalent column. This equivalent column is based on the "base unit" (with its load share wq_1) but (through $\Sigma a_i/b_i$ and $\Sigma a_i/c_i$) the effects of interaction among the bracing units are also taken into consideration.

Theoretically, it is not important which unit is chosen as base unit. Practically, however, the choice of a base unit is important as it has an "influence" on how "quickly" (height-wise) the continuum model works. With a "good" choice, the method works perfectly well even for low-rise (say, four-storey) structures. On the other hand, with a "worse" choice, the method may not be accurate enough for low-rise structures. Luckily, there is always a "good" choice and, after the determination of the stiffness characteristics of the bracing units (which are needed anyway), an extremely simple answer can be given to the question "How to choose the 'base unit'?" The derivation in the previous section is based on the ***bending*** analysis of the system. The resulting formulae for the deflection consist of three parts: the bending part, the shear part and the interaction part. The more shear-sensitive a unit, the more important the interaction part is. As the derivation is based on bending analysis, a base unit as different from the bending-dominant case as possible should be chosen in order to offer the biggest "scope" for interaction. It follows that the rule for choosing the base unit is this:

<u>The bracing unit with the highest $b=K/EI$ value must be chosen as the base unit</u>.

As the ratio K/EI has no meaning with shear walls and cores, a shear wall or core cannot be a base unit.

If the structure is under horizontal load whose distribution is not uniform (but triangular, for example), the method can still be used. In such cases, the first and

second terms in Equations (3.12) and (3.14) should be replaced by the closed-form solutions of the relevant load cases, available from textbooks. As an approximation, the third term responsible for the interaction may remain unchanged. As the effect of interaction is of secondary nature, this approximation is considered acceptable for most structural engineering purposes.

3.2 TORSIONAL ANALYSIS OF BUILDINGS UNDER HORIZONTAL LOAD

The torsional analysis of multi-storey building structures braced by frameworks, (coupled) shear walls and cores, subjected to lateral load represents a formidable task. The main difficulty is caused by the fact that the different bracing units with different deflection shapes interact with each other, and this time in a three-dimensional manner.

Because of the complexity of the torsional behaviour, not many authors deal with the problem. Considerable efforts have been made regarding the torsional behaviour of individual structural elements (Council..., 1978; Seaburg and Carter, 2003) but the global torsional behaviour of whole structural systems is a less cultivated area. There are some excellent publications that offer relatively simple solution for the global torsional problem (Council..., 1978; Irwin, 1984; Schueller, 1990; Coull and Wahab, 1993; Hoenderkamp, 1995; Nadjai and Johnson, 1998; Howson and Rafezy, 2002) but they are either still too complicated or of limited applicability and neither of them is backed up with a comprehensive accuracy analysis.

To handle this three-dimensional problem in a simple way seems to be hopeless using conventional tools. However, by relying on an analogy between bending and torsion, a relatively simple solution can be produced (Zalka, 2010). The aim of this section is threefold:

a) to establish a new model for the analysis using the bending-torsion analogy
b) to produce a simple closed-form solution for the rotation of the building that clearly shows the contribution of the different stiffness characteristics to the torsional resistance
c) to show how this new method can be used for the determination of the maximum deflection of multi-storey asymmetrical building structures

It will be demonstrated that the torsional behaviour is defined by three distinctive phenomena: warping torsion, Saint-Venant torsion and the interaction between the two basic modes. It will be seen that the interaction between the warping and Saint-Venant types of torsion is always beneficial as it always reduces the rotation of the system.

3.2.1 Torsional behaviour and basic characteristics

As with thin-walled bars, multi-storey building structures react to torsion by utilizing their torsional resistance. As with thin-walled bars, the torsional resistance of multi-storey buildings originates from two sources. The warping stiffness is associated with the in-plane bending stiffness of the individual bracing units,

which is “activated” by their moment arm (perpendicular distance) measured from the shear centre of the bracing system. This phenomenon is best demonstrated by the torsional behaviour of a single I-column on a fixed base and with a free upper end, whose warping stiffness EI_ω is calculated by multiplying the (in-plane) bending stiffness of its flanges and the square of the perpendicular distance of the flanges from the shear centre of the column (Figure 3.2/a):

$$EI_\Omega = EI_{flange}\left(\frac{h}{2}\right)^2 2 = E\frac{tb^3}{12}\frac{h^2}{4}2 = E\frac{tb^3h^2}{24}$$

where E is the modulus of elasticity of the material of the column. Point O marks the shear centre of the cross-section and axis z passing through the shear centre is the axis of rotation.

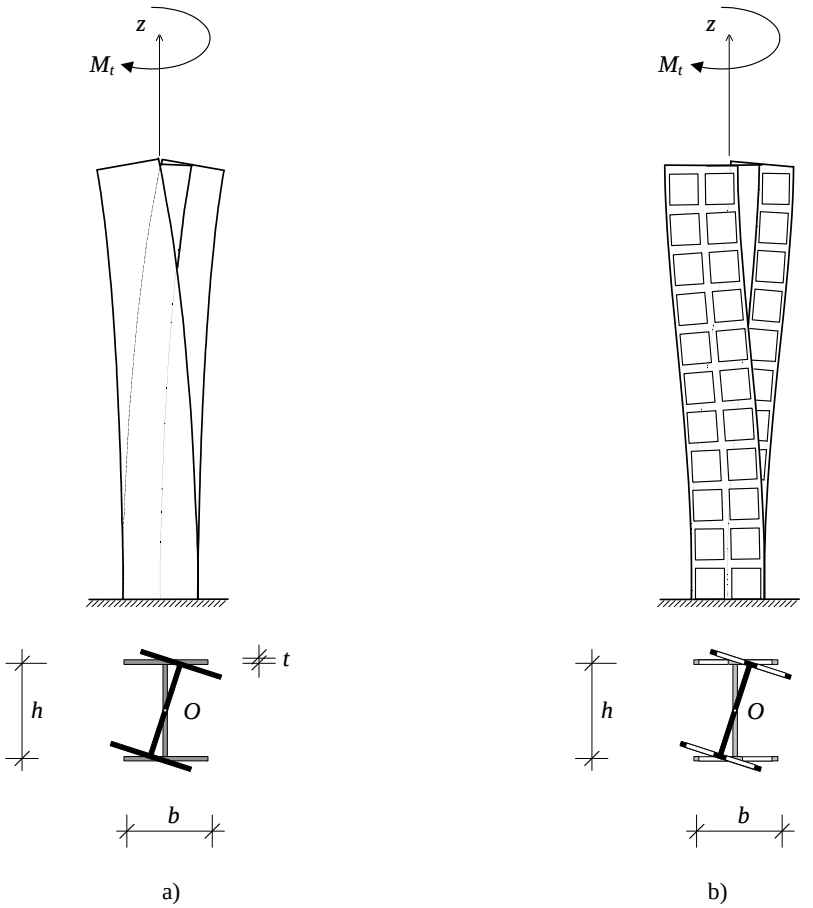

Figure 3.2 Rotation of an I-column on a fixed base. a) with solid flanges, b) with flanges with openings.

The Saint-Venant torsional stiffness of the bracing system is associated with the in-plane shear stiffness of the bracing units, which is "activated" by its moment arm (perpendicular distance) measured from the shear centre of the bracing system. For its demonstration and using the same I-column as above, assume that the flanges are pierced with big openings of rectangular shape (they are in fact frames). The Saint-Venant torsional stiffness (GJ) is calculated by multiplying the shear stiffness of the flanges (i.e. the frames) and the square of the perpendicular distance of the flanges from the shear centre of the column (Figure 3.2/b):

$$(GJ) = 2K\left(\frac{h}{2}\right)^2 = \frac{Kh^2}{2}$$

where K is the shear stiffness of the flanges. It is easy to see that in building structures the floor slabs of the building (with their great in-plane stiffness) play the role of the web of the I-column in making the bracing elements (the flanges) work together.

It follows that the bending and shear stiffnesses of the individual bracing units as well as the distance of the bracing units from the shear centre of the building are the key players in the torsional behaviour.

According to Section 2.1, in the case of a framework (the most characteristic bracing unit) the characteristic stiffnesses are the local and global bending stiffnesses [EI and EI_g by Equations (2.31) and (2.32)] and the shear stiffness as given by Equation (2.27).

In addition to the stiffnesses of the bracing units, their distance from the shear centre is also needed. The location of the shear centre is defined as the centre of stiffnesses of the bracing units. The stiffness of each bracing unit is defined by Equation (3.2) as the reciprocal of the top (in-plane) deflection of the unit.

With the stiffnesses of the units, the calculation of the location of the shear centre is carried out in the co-ordinate system $\bar{x} - \bar{y}$ whose origin lies in the upper left corner of the plan of the building and whose axes are aligned with the sides of the building (Figure 3.3):

$$\bar{x}_o = \frac{\sum_{1}^{f+m} S_{y,i}\bar{x}_i}{\sum_{1}^{f+m} S_{y,i}} \quad \text{and} \quad \bar{y}_o = \frac{\sum_{1}^{f+m} S_{x,i}\bar{y}_i}{\sum_{1}^{f+m} S_{x,i}} \tag{3.17}$$

where

$\bar{x}_i, \bar{y}_i$ are the perpendicular distances of the ith bracing unit from $\bar{y}$ and $\bar{x}$
f is the number of frameworks and coupled shear walls
m is the number of shear walls and cores
$S_{x,i}, S_{y,i}$ are the "governing" stiffnesses by Equation (3.2) in directions x and y

For the calculation of the location of the shear centre, only the in-plane stiffness of the frameworks and shear walls needs to be taken into account. Once

the location of the shear centre is determined, coordinate system $\bar{x}-\bar{y}$ has fulfilled its role and a new coordinate system $x-y$ is established with its origin in the shear centre (Figure 3.3).

It is easily seen that Equations (3.17) simplify to

$$\bar{x}_o = \frac{\sum_{1}^{f+m} I_{x,i}\bar{x}_i}{\sum_{1}^{f+m} I_{x,i}} \quad \text{and} \quad \bar{y}_o = \frac{\sum_{1}^{f+m} I_{y,i}\bar{y}_i}{\sum_{1}^{f+m} I_{y,i}} \tag{3.18}$$

when the units of the bracing system only have bending stiffness (and no or negligible shear stiffness) as is the case with shear walls/cores and the task of establishing the location of the shear centre simplifies considerably.

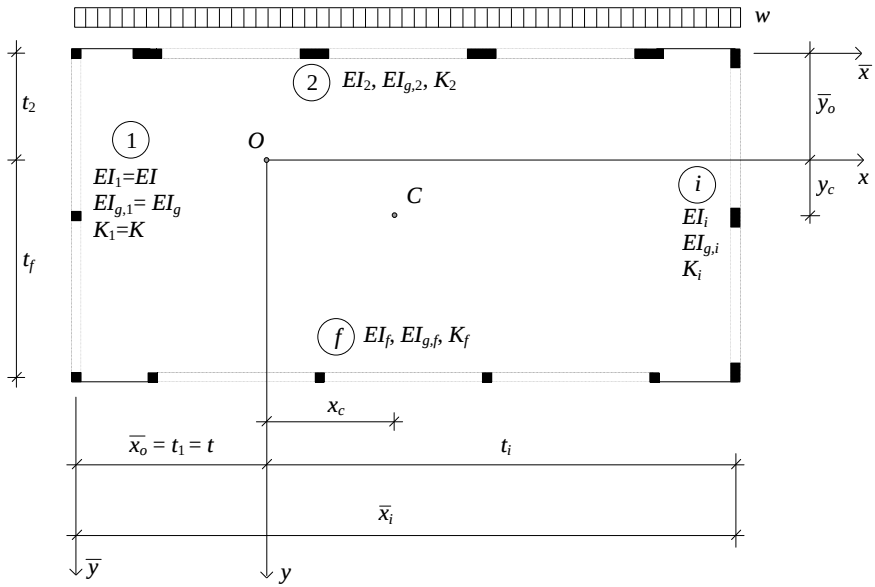

Figure 3.3 Plan arrangement of the bracing system of frameworks for the torsional analysis.

3.2.2 Torsional analysis

Knowing the stiffness characteristics of the individual bracing units as well as their perpendicular distance from the shear centre, it is now possible to carry out the torsional analysis of the bracing system of the building. The torsional analysis is based on an analogy well-known in the stress analysis of thin-walled structures in bending and torsion (Kollbrunner and Basler, 1969; Vlasov, 1961). According to

the analogy, translations, bending moments and shear forces correspond to rotation, warping moments and torsional moments, respectively. It follows from the analogy that the results of the deflection analysis of a system of frameworks, (coupled) shear walls and cores can be used for the torsional analysis if the characteristic stiffnesses of the deflection analysis are "matched" with stiffnesses that characterise the torsional problem.

Stiffness EI is the local bending stiffness of the base unit with the deflection analysis. The corresponding stiffness with the torsional analysis is the local warping torsional stiffness

$$EI_{\Omega} = EIt^2 \tag{3.19}$$

where t is the perpendicular distance of the unit from the shear centre (Figure 3.3).

Stiffness EI_g is the global bending stiffness with the deflection analysis. The corresponding stiffness now is the global warping torsional stiffness

$$EI_{g\Omega} = EI_g t^2 \tag{3.20}$$

Stiffness K is the shear stiffness with the deflection analysis. The corresponding stiffness here is the Saint-Venant torsional stiffness

$$(GJ) = Kt^2 \tag{3.21}$$

With the above analogous characteristics the governing differential equation of torsion assumes the form

$$''''_{} - {}^{-2}\ ''_{} = \frac{\overline{m}}{EI_{\Omega}}\left(\frac{\bar{a}z^2}{2} - 1\right) \tag{3.22}$$

The solution of the differential equation is given by

$$(z) = \frac{\overline{m}}{E(I_{\Omega} + I_{g\Omega})}\left(\frac{H^3 z}{6} - \frac{z^4}{24}\right) + \frac{\overline{m}z^2}{2(GJ)\bar{s}^2}$$

$$- \frac{\overline{m}EI_{\Omega}}{(GJ)^2\bar{s}^3}\left(\frac{\cosh\ ^{-}(H-z) + {}^{-}H\sinh\ ^{-}z}{\cosh\ ^{-}H} - 1\right) \tag{3.23}$$

Maximum rotation develops at $z = H$:

$$_{\max} = \frac{\overline{m}H^4}{8E(I_{\Omega} + I_{g\Omega})} + \frac{\overline{m}H^2}{2(GJ)\bar{s}^2} - \frac{\overline{m}EI_{\Omega}}{(GJ)^2\bar{s}^3}\left(\frac{1 + {}^{-}H\sinh\ ^{-}H}{\cosh\ ^{-}H} - 1\right) \tag{3.24}$$

Instead of the lateral load on the base unit ($\overline{w}$) in Equations (3.12), (3.14)

and (3.16), Equations (3.22), (3.23) and (3.24) contain the torsional moment $\overline{m}$ that the base unit takes of the total torsional moment. Its value is determined as follows.

Each of the bracing units takes torsional moment according to their torsional stiffness. The torsional stiffness of the *i*th unit is defined as

$$S_{\Omega i} = S_i t_i^2 = \frac{t_i^2}{y_i(H)} \tag{3.25}$$

where t_i is the perpendicular distance of the *i*th bracing unit from the shear centre and $y_i(H)$ is the (in-plane) top deflection of the *i*th unit. Thus, the torsional apportioner related to the base unit assumes the form

$$q_\Omega = \frac{S_\Omega}{\sum_{i=1}^{f+m} S_{\Omega i}} \tag{3.26}$$

where S_ω is the torsional stiffness of the base unit as

$$S_\Omega = \frac{t^2}{y(H)} = t^2 S \tag{3.27}$$

and $f + m$ is the total number of bracing units (with f frames/coupled shear walls and m shear walls/cores). The torsional moment the base unit takes is therefore

$$\overline{m} = m_t q_\Omega = w x_c q_\Omega \tag{3.28}$$

where

$$m_t = w x_c \tag{3.29}$$

is the total torsional moment on the bracing system.

Equivalents of coefficients $\bar{}$ and $\bar{s}$ in Equations (3.12), (3.13) and (3.14) also have to be established for use in Equations (3.23) and (3.24). Careful investigation of Equations (3.13) and (3.16) shows that if the torsional equivalents —stiffness×(moment-arm)^2 —are substituted for the relevant stiffnesses, the moment-arms drop out of the formulae. It follows that the coefficients defined by Equations (3.13) and (3.16) remain unchanged and could be used for the torsional analysis as well. It should be pointed out here that when these coefficients are determined, f refers to the number of frameworks and coupled shear walls that are ***effective*** against torsion, i.e. to those whose line of action do not pass through the shear centre.

The evaluation of Equations (3.23) and (3.24) using the rotational data of 126 bracing systems ranging in height from 4 to 80 storeys (c.f. Section 3.4: Accuracy)

leads to the following observations:

a) The torsional behaviour of the building can be separated into three distinctive parts. The bending stiffness of the individual bracing units (activated through rotation around the shear centre) is associated with warping torsion—first term in Equation (3.24). The shear stiffness of the bracing units (activated through rotation around the shear centre) results in pure, Saint-Venant-type torsion—second term in Equation (3.24). Because of the different ("bending-type" and "shear-type") rotation shapes (Figure 3.2), there is an interaction between the two modes, defined by the third term in Equation (3.24). Figure 3.4 shows the characteristic types of rotation of a 40-storey building braced by frameworks.
b) The effect of interaction between the warping and Saint-Venant modes (Figure 3.4/c) is always beneficial as it reduces the rotation of the structure.
c) The effect of interaction significantly becomes smaller as the height of the structures increases.
d) For a structure of given height, the effect of interaction is roughly constant over the height of the structure (Figure 3.4/c).

To conclude the investigation of the torsional behaviour, some special cases will now be considered as their analysis leads to extremely simple solutions in many practical cases.

Case A: The horizontal elements of the bracing system (including the connecting beams in the frameworks and the floor slabs) have negligibly small bending stiffness.

This case is characterized by $K_b \to 0$ (for the frameworks). Consequently, the shear stiffness of the system tends to zero ($K \to 0$), which leads to $\bar{a} \to 0$ and $\bar{b} \to 0$ and $\bar{} \to 0$. Governing differential equation (3.22) simplifies to

$$'''' = \frac{m_t}{EI_\Omega}$$

and the solutions for the rotation and top rotation assume the form

$$(z) = \frac{m_t}{EI_\Omega}\left(\frac{H^3 z}{6} - \frac{z^4}{24}\right) \tag{3.30}$$

and

$$_{\max} = \quad (H) = \frac{m_t H^4}{8EI_\Omega} \tag{3.31}$$

where EI_ω is the local warping stiffnesses. This case is identified in Figure 3.4/a.

The use of Equations (3.30) and (3.31) should be considered when the shear stiffness of the bracing units is very small and/or when the bracing system consists of shear walls/cores only. It should be noted that in this case m_t is the *total*

torsional moment and I_ω represents the ***sum*** of the warping stiffnesses of the shear walls/cores. There is no need for a base unit in this case.

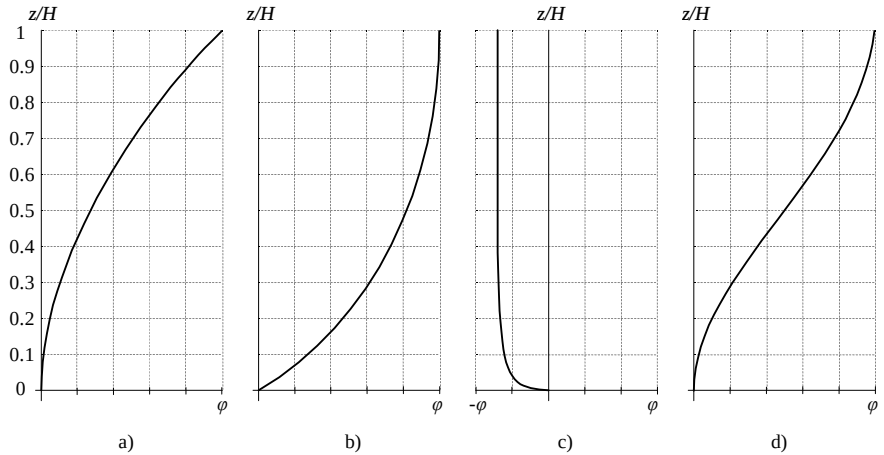

Figure 3.4 Typical rotation shapes. a) warping, b) Saint-Venant, c) interaction, d) combined.

Case B: Bracing systems comprising multi-bay, low-rise frameworks tend to develop predominantly Saint-Venant-type rotation and the effect of the warping stiffness becomes insignificant.

This case is characterised by $\bar{a} \to 0$ and $\bar{b} \to \infty$ and governing differential equation (3.22) cannot be used directly. However, after some rearrangement, the original derivation leads to

$$'' = \frac{\bar{m}}{(GJ)}$$

where $(GJ) = K_b t^2$. This differential equation, together with the boundary conditions $\varphi(0) = 0$ and $\varphi'(0) = 0$, lead to the rotation and the top rotation as

$$(z) = \frac{\bar{m} z^2}{2(GJ)} \tag{3.32}$$

and

$$_{\max} = \quad (H) = \frac{\bar{m} H^2}{2(GJ)} \tag{3.33}$$

The characteristic rotation shape is shown in (Figure 3.4/b). It is certainly worth considering the use of Equations (3.32) and (3.33) when the building is relatively low and the bracing system only consists of (mainly multi-bay) frameworks.

Case C: The structure is relatively slender (with great height/width ratio). The structure develops predominantly (global) warping rotation. The second and third terms in Equations (3.23) and (3.24) tend to be by orders of magnitude smaller than the first term and the solutions for the rotation and the top rotation effectively become

$$(z) = \frac{\overline{m}}{E(I_{\Omega} + I_{g\Omega})}\left(\frac{H^3 z}{6} - \frac{z^4}{24}\right) \tag{3.34}$$

and

$$_{\max} = \quad (H) = \frac{\overline{m}H^4}{8E(I_{\Omega} + I_{g\Omega})} \tag{3.35}$$

This case is illustrated in Figure 3.4/a. It is interesting to note that both Case A and Case C are characterised by warping-type rotation.

3.3 MAXIMUM DEFLECTION

Multi-storey buildings under horizontal load never develop torsion only. When the bracing system of the building is doubly symmetric, the shear centre of the bracing system (*O*) and the centre of the plan of the building (*C*) coincide (Figure 3.5/a).

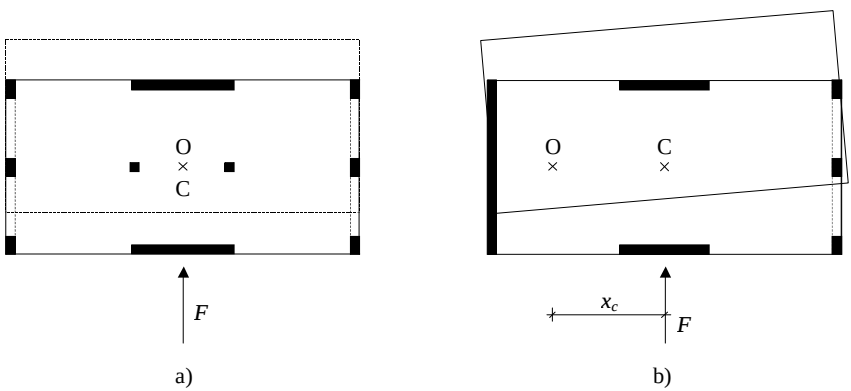

Figure 3.5 Plan arrangement. a) symmetric, b) asymmetric.

Under horizontal load—represented by its resultant *F* in Figure 3.5—the building develops lateral displacement and no rotation occurs. Equation (3.14) gives the maximum deflection of the building.

When the building is asymmetric, the shear centre of the bracing system and the centroid of the plan of the building do not coincide (Figure 3.5/b). The external load passing through the centroid causes two things: lateral displacement in the

direction of the load and rotation around the shear centre (Figure 3.6).

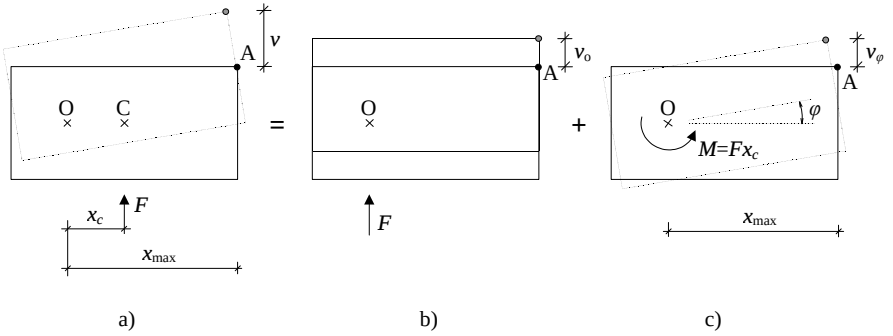

Figure 3.6 Displacements. a) v: maximum displacement, b) v_o: displacement due to force F, c) v_φ: displacement due to torsional moment M.

The behaviour of the building is best analysed by transferring the load to the shear centre. This procedure results in a horizontal load passing through the shear centre and a torsional moment $M = Fx_c$, where x_c is the distance between the shear centre and the centroid. Force F develops lateral displacements only (v_o in Figure 3.6/b) and torsional moment M develops rotation (φ) around the shear centre (Figure 3.6/c), which causes additional displacement (v_φ). At any given location the total displacement is obtained by adding up the two components:

$$v = v_o + v$$

The maximum displacement of the building develops at the top at a corner of the plan of the building (point A in Figure 3.6) and, making use of the angle of rotation, is obtained from

$$v_{max} = v(H) = v_o + \quad x_{max} \tag{3.36}$$

where x_{max} is the distance of the corner point (where maximum deflection occurs) from the shear centre. The first term (v_o) on the right-hand side in the above equation can be obtained using Equation (3.14) and the angle of rotation is determined by Equation (3.24).

3.4 ACCURACY

The results obtained using the approximate formulae derived in this chapter were compared to the results of the Finite Element solution. The AXIS VM finite element package (Axis, 2003) was used for the comparison, whose results were considered “exact”. The “error” of the method was defined as the difference between the “exact” and approximate results, related to the “exact” solution. Positive error meant conservative estimates.

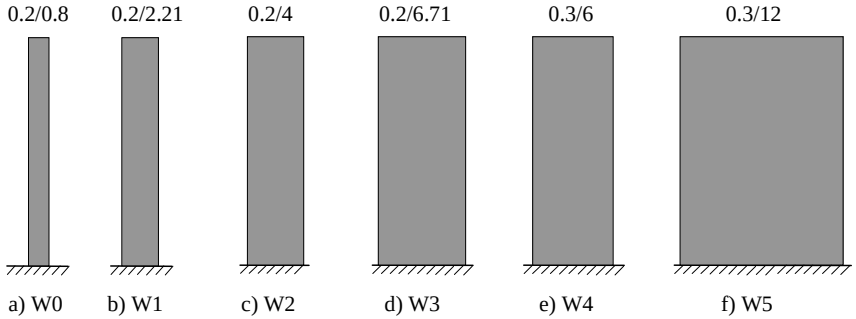

Figure 3.7 Shear walls for the accuracy analysis (with thickness/width in metres).

The frameworks used in Sections 2.1.4 for checking the accuracy of the methods for individual frameworks (Figure 2.7) were used again. The bays of the one-, two- and three-bay reinforced concrete rigid frames were 6 m and the storey height was 3 m. The rectangular cross-sections of the beams and columns (in metres) are given in Figure 2.7 for frameworks F1 ... F10. The modulus of elasticity for these frameworks was $E = 25$ kN/mm^2. Frameworks F11, F12 and F13 were one-, two- and three-bay steel braced frames whose bays and storey height were 3 m. The cross-sections of the columns for the three braced frames were 305x305UC137; the cross-sections of the beams and braces are given in Figure 2.7/k to 2.7/m. The modulus of elasticity for the steel frameworks was $E_s = 200$ kN/mm^2.

The thirteen frameworks (Figure 2.7) were supplemented by three shear walls (W1, W2 and W3 in Figure 3.7) and seventeen two-dimensional bracing *systems* were created:

F1+F7+F13, F1+F7+F13+W2, F2+F3, F2+F3+W1, F5+F6+F8, F5+F6+F8+W2, F2+F3+F5+F6, F3+F6+F9, F3+F6+F9+W3, F2+F5+F9+F10, F2+F3+F5+F6+W2, F1+F2+F3+F4+F5+F6+F7+F8, F1+F2+F3+F4+F5+F6+F7+F8+W3, F5+F11, F5+F11+W3, F6+F12 and F6+F12+W3.

The base unit in each system is underlined; the *b*-value of each frame is given in Figure 2.7 The combination of the bracing units was determined in such a way that the widest possible range of stiffness could be covered in the most varied way.

First, the results of a comprehensive accuracy analysis regarding the formula for maximum deflection [Equation (3.14)] is given here.

The height of the structures in the seventeen systems varied from 4 to 80 storeys in eight steps, leading to 153 test cases. The structures were subjected to a uniformly distributed horizontal load of $w = 10$ kN/m. The top deflection of the 153 test systems was calculated using Equation (3.14) and then compared to the Finite Element solution.

The summary of the results (range of error, average absolute error and maximum error) is given in Table 3.1. In addition to the data given in Table 3.1, it is also important to see how the error varies as the height of the building changes. Figure 3.8 shows the error as a function of height. The results summarised in

Table 3.1 and Figure 3.8 demonstrate the performance of the continuum solution.

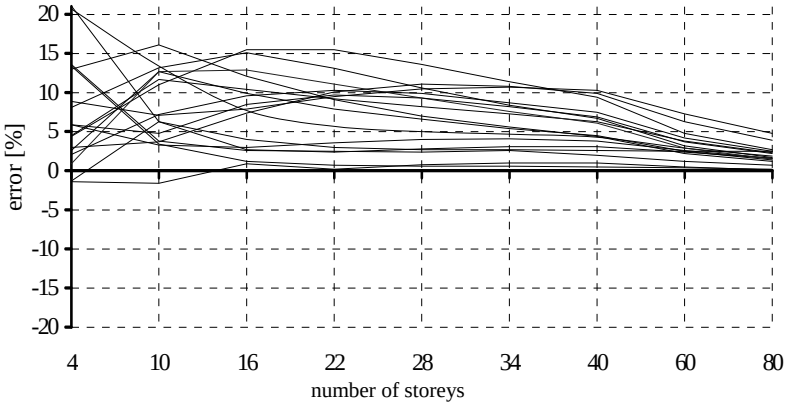

Figure 3.8 Accuracy of Equation (3.14) for the lateral deflection as a function of height.

It can be stated that for practical purposes the method can be considered conservative: The error range of the method was between –2% (unconservative) and 21% (conservative). In the 153 cases, the average difference between the results of the analytical method and the finite element solution was around 6% (conservative).

Table 3.1 Accuracy of Equation (3.14) for the lateral deflection.

Method	Range of error (%)	Average absolute error (%)	Maximum error (%)
Continuum solution [Equation (3.14)]	-2 to 21	6.0	21

The accuracy of Equation (3.24) derived for the maximum rotation was also investigated.

Frameworks F1, F3, F5, F6, F7 and F10 shown in Figure 2.7 were chosen and supplemented with shear walls W1, W3, W4 and W5 (Figure 3.7) and with a U-core. The wall sections for the U-core were $h = 4.0$ and $b = 4.0$ with a wall thickness of $t = 0.3$. Fourteen bracing systems were created (Figure 3.9).

Again, the height of the structures varied between 4 and 80 storeys in eight steps (4, 10, 16, 22, 28, 34, 40, 60 and 80 storeys), creating 126 test cases. The stiffness characteristics and the arrangements of the bracing units were chosen in such a way that the structures covered a wide range of stiffnesses.

The top rotation of the fourteen bracing systems under uniformly distributed torsional load was calculated and the error of the method (the difference between the continuum and the “exact” solutions, related to the “exact” solution) was

determined. Again, the error was defined positive if it represented conservative approximation.

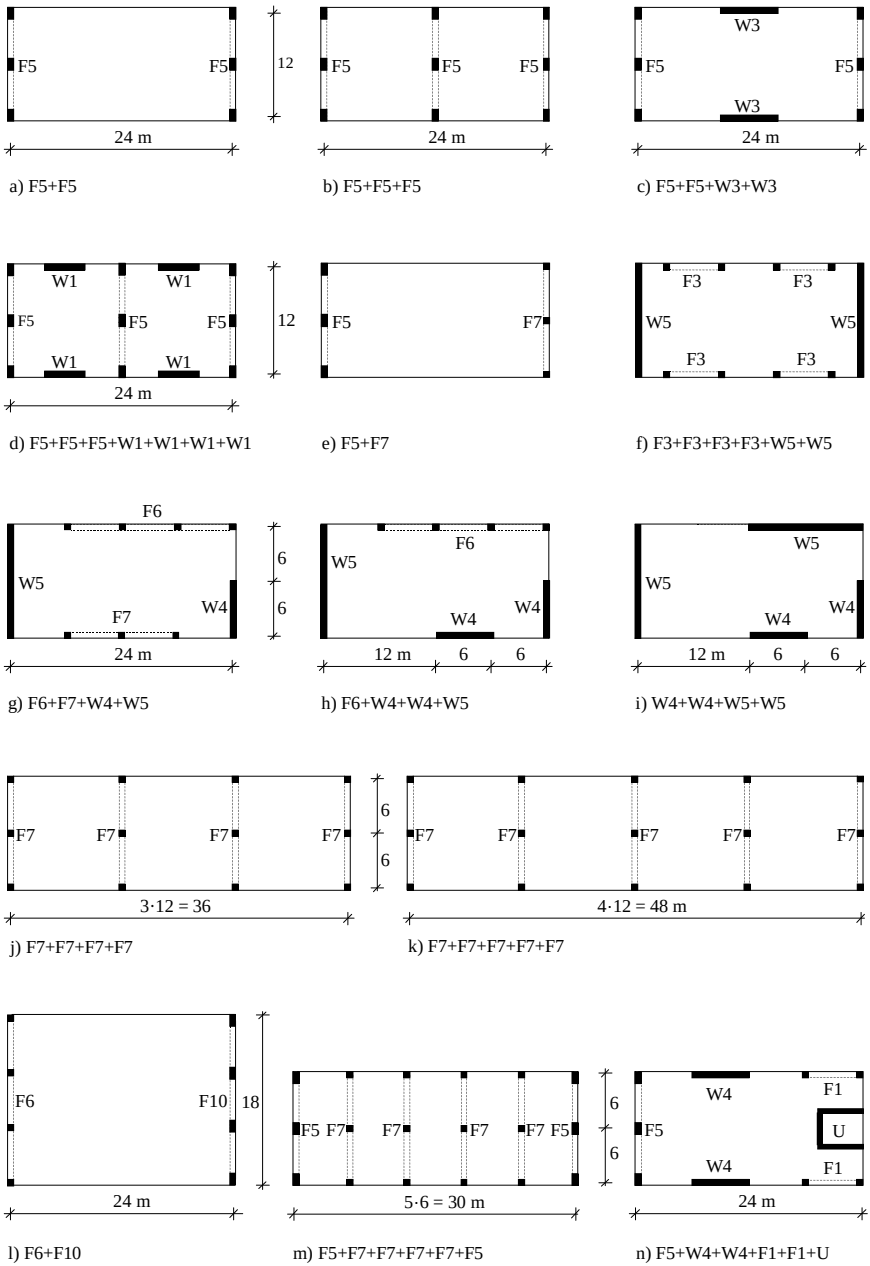

Figure 3.9 Fourteen bracing systems for the torsional analysis.

The torsional shapes represented predominant warping-type, mixed warping-type and Saint-Venant type, and predominant Saint-Venant type deformation. The summary of the results (range of error, average absolute error and maximum error) is given Table 3.2.

Table 3.2 Accuracy of Equation (3.24) for maximum rotation.

Method	Range of error (%)	Average absolute error (%)	Maximum error (%)
Continuum solution [Equation (3.24)]	0 to 25	9.0	25

The results summarized in Table 3.2 demonstrate the performance of the method. It should be emphasized that the method produced conservative estimates in every test case. The error range of the method was between 0% and 25%. In the 126 cases, the average difference between the results of the proposed analytical method and the finite element solution was around 9%. Figure 3.10 shows the error as a function of height.

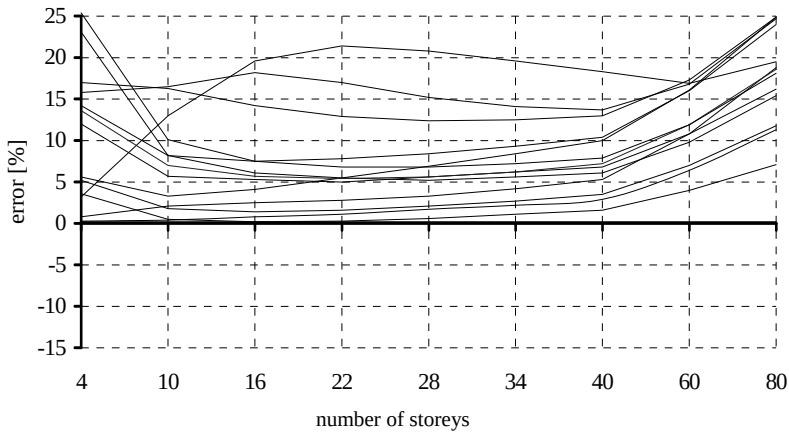

Figure 3.10 Accuracy of Equation (3.24) for the maximum rotation as a function of height.

It is interesting to note that the magnitude of the error does not decrease as the height of the structures increases, as is normally the case with continuum models of multi-storey structures. The reason for this peculiar phenomenon probably lies with the computer modelling of the floor slabs (see page 4): although the pinned bars represent the great in-plane and small out-of-plane stiffness of the floors reasonably well, with their great cross-sectional area they somewhat restrict the warping deformation, effectively increasing the torsional resistance of the bracing system. This increase in not present in the continuum model; thus the more conservative results for the higher structures where the effect of the warping stiffness is dominant.

4

Frequency analysis of buildings

A great number of methods have been developed for the dynamic analysis of individual frameworks, coupled shear walls and shear walls. Fewer methods are available to deal with a *system* of these bracing elements. This follows from the fact that the interaction among the elements (beams/lintels and columns/walls) of a single framework or coupled shear walls is complex enough but then the bracing units interact with one another not only in planar behaviour but normally also in a three-dimensional fashion. This is why the available analytical methods make one or more simplifying assumptions regarding the characteristic stiffnesses of the bracing units or the geometry of the building.

Based on drift calculations and assuming a doubly symmetric structural arrangement, Goldberg (1973) presented several simple methods for the calculation of the fundamental frequency of (uncoupled) lateral vibration and pure torsional vibration. The effect of the axial deformation of the vertical elements was taken into account by a correction factor in his method. The continuous connection method enabled more rigorous analyses (Coull, 1975; Rosman, 1973 and 1981; Kollár, 1992). Using a single-storey torsional analogy, Glück *et al*. (1979) developed a matrix-based solution for buildings having uncoupled stiffness matrixes. A simple procedure with design tables was made available for asymmetrical buildings developing predominantly bending deformation (Zalka, 2000). Ng and Kuang (2000) presented a simple method for the triply coupled vibration of asymmetric wall-frame structures. However, their method is only applicable to buildings whose vertical bracing elements develop no or negligible axial deformation.

In taking into consideration all the characteristic stiffnesses of the bracing frameworks, shear walls and cores, as well as the interaction among the elements of the bracing structures and among the bracing units themselves (Zalka, 2001), the aim of this chapter is to introduce a simple analytical method for the calculation of the natural frequencies of regular multi-storey buildings braced by a system of frameworks, (coupled) shear walls and cores.

In addition to the general assumptions made in Chapter 1, it is also assumed for the analysis that the mass of the building is uniformly distributed over the floors of the building and that the location of the shear centre only depends on geometrical characteristics.

The equivalent column approach shall be used for the analysis. The equivalent mass and stiffnesses shall be established first, considering deformations due to bending, shear, the lengthening and shortening of the vertical elements and torsion. Closed-form solutions shall then be given for lateral, pure torsional and coupled vibration.

The method is simple and accurate enough to be used both at the concept design stage and for final analysis. It can also be useful to verify the results of the FE method, where the time consuming procedure of handling all the data can always be a source of error.

A multi-storey building may develop lateral vibrations in the two principal directions and torsional vibration around its vertical shear centre axis. All the three corresponding frequencies have to be calculated before their coupling can be considered. The investigation here starts with the lateral vibration of the bracing system, which can be based on the vibration analysis of a single framework presented in Section 2.2.

4.1 LATERAL VIBRATION OF A SYSTEM OF FRAMEWORKS, (COUPLED) SHEAR WALLS AND CORES

Consider a *system* of frames and coupled shear walls ($i = 1...f$) and shear walls and cores ($k = 1...m$) shown in Figure 4.1/a. Based on the analysis of a single framework in Section 2.2.1, the whole bracing system can be characterised by the shear stiffness of the frameworks and coupled shear walls, the global bending stiffness of the frameworks and coupled shear walls and the local bending stiffness of the individual columns/wall sections, shear walls and cores.

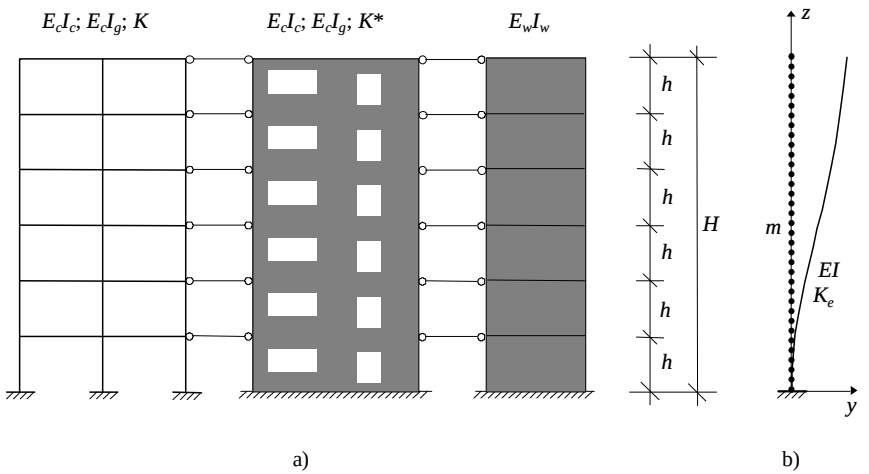

Figure 4.1 Model for the lateral vibration analysis. a) bracing system consisting of frames, coupled shear walls, shear walls and cores, b) equivalent column.

By combining the individual bracing elements, linked by the floor slabs, to form a single cantilever, an equivalent system can be established with shear stiffness K, global bending stiffness EI_g and local bending stiffness EI. The shear stiffness and the global bending stiffness are not independent of each other and can be incorporated into an effective shear stiffness, leading to a single equivalent column with effective shear stiffness K_e and bending stiffness EI. These

characteristics shall be established as follows.

The shear stiffness of the system originates from the shear stiffnesses of the frameworks and coupled shear walls. Based on Equation (2.27), the "original" shear stiffness of the *i*th framework is

$$K_i = K_{b,i} r_i = K_{b,i} \frac{K_{c,i}}{K_{b,i} + K_{c,i}} \tag{4.1}$$

where the two contributors to the shear stiffness are

$$K_{b,i} = \sum_{j=1}^{n-1} \frac{12 E_b I_{b,j}}{l_j h} \tag{4.2}$$

and

$$K_{c,i} = \sum_{j=1}^{n} \frac{12 E_c I_{c,j}}{h^2} \tag{4.3}$$

where

E_c is the modulus of elasticity of the columns of the frameworks
E_b is the modulus of elasticity of the beams of the frameworks
$I_{c,j}$ is the second moments of area of the *j*th column of the *i*th framework
$I_{b,j}$ is the second moments of area of the *j*th beam of the *i*th framework
h is the storey height
l_j is the *j*th bay of the *i*th framework
n is the number of columns of the *i*th framework

Factor r_i is introduced as a reduction factor:

$$r_i = \frac{K_{c,i}}{K_{b,i} + K_{c,i}} \tag{4.4}$$

The total "original" shear stiffness of f bracing frameworks is

$$K = \sum_{i=1}^{f} K_i \tag{4.5}$$

[If coupled shear walls are also included in the system, their shear stiffness is determined using Equation (2.70).]

The square of the frequency of shear vibration associated with the "original" shear stiffness of the *i*th unit is

$$f_{s,i}^2 = \frac{1}{(4H)^2} \frac{r_f^2 K_i}{m} \tag{4.6}$$

where m is the mass density per unit length [kg/m].

For regular multi-storey buildings, the mass density per unit length is calculated using

$$m = A \tag{4.7}$$

where A is the plan area of the building and

$$= \frac{}{g}$$

is the mass density per unit volume. Constant g is the gravity acceleration, with $g = 9.81$ m/s^2, and γ [kN/m^3] is the weight per unit volume of the building.

Factor r_f is included in Equation (4.6). It is responsible for taking into account the fact that the mass of the original structures is concentrated at floor levels and is not uniformly distributed over the height (as assumed for the model used for the original derivation, shown in Figure 4.1/b). Values for r_f are given in Table 4.1.

Table 4.1 Mass distribution factor r_f as a function of n (the number of storeys).

n	1	2	3	4	5	6	7	8	9	10	11
r_f	0.493	0.653	0.770	0.812	0.842	0.863	0.879	0.892	0.902	0.911	0.918
n	12	13	14	15	16	18	20	25	30	50	>50
r_f	0.924	0.929	0.934	0.938	0.941	0.947	0.952	0.961	0.967	0.980	$\sqrt{n/(n+2.06)}$

The full-height global bending vibration of the ith framework or coupled shear walls as a whole unit represents pure bending type vibration. The square of the fundamental frequency that is associated with this vibration is

$$f_{g,i}^2 = \frac{0.313 r_f^2 E_c I_{g,i}}{H^4 m} \tag{4.8}$$

where I_g is the global second moment of area of the cross-sections of the columns:

$$I_{g,i} = \sum_{j=1}^{n} A_{c,j} t_j^2 \tag{4.9}$$

with

$A_{c,j}$ the cross-sectional area of the jth column
t_j the distance of the jth column from the centroid of the cross-sections

According to the dynamic analysis carried out in Section 2.2.1, there is an

interaction between the shear and global bending modes that reduces the effectiveness of the shear stiffness. The factor of effectiveness for the *i*th unit can be calculated using the two relevant frequencies as

$$s_{f,i}^2 = \frac{f_{g,i}^2}{f_{g,i}^2 + f_{s,i}^2} \tag{4.10}$$

and using the effectiveness factor, the effective shear stiffness for the whole system is obtained as

$$K_e = \sum_1^f s_{f,i}^2 K_i \tag{4.11}$$

Using the "original" and the effective shear stiffnesses, the effectiveness for the whole system is obtained as

$$s_f = \sqrt{\frac{K_e}{K}} \tag{4.12}$$

The actual lateral frequency of the system which is associated with shear deformation can now be determined using the effective shear stiffness:

$$f_s^2 = \frac{1}{(4H)^2} \frac{r_f^2 K_e}{m} \tag{4.13}$$

If higher frequencies are needed, the factor 4 in Equation (4.13) should be replaced by 4/3 and 4/5, respectively, for the calculation of the second and third frequencies.

When the lateral frequency that is associated with the local bending deformation is considered, the bending stiffnesses of the columns of the frameworks and coupled shear walls, the shear walls and the cores have to be taken into consideration:

$$EI = E_c I_c + E_w I_w = E_c \sum_1^f I_{c,i} r_i + E_w \sum_1^m I_{w,k} \tag{4.14}$$

In Equation (4.14)

E_w is the modulus of elasticity of the shear walls/cores
$I_{c,i}$ is the sum of the second moments of area of the columns of the *i*th framework
r_i is the reduction factor for the *i*th framework [Equation (4.4)]
$I_{w,k}$ is the second moment of area of the *k*th shear wall/core

When the system has mixed bracing units—both frameworks and shear walls/cores—the contribution of the columns of the frameworks [first term in Equation (4.14)] is normally very small compared to that of the shear walls/cores and can safely be ignored.

With the above bending stiffness, the lateral frequency of the system in bending is obtained from

$$f_b^2 = f_f^2 + f_w^2 = \frac{0.313 r_f^2}{H^4 m}\left(E_c \sum_1^f I_{c,i} r_i + E_w \sum_1^m I_{w,k} \right) = \frac{0.313 r_f^2 EI}{H^4 m} \tag{4.15}$$

where

f_f fundamental frequency of the frameworks/coupled shear walls
f_w fundamental frequency of the shear walls/cores

If higher frequencies are needed, the factor 0.313 in Equation (4.15) should be replaced by 12.3 and 96.4, respectively, for the calculation of the second and third frequencies.

In Equations (4.14) and (4.15), the bending stiffness of the columns of the frameworks and coupled shear walls is adjusted by combination factor r_i. Theoretical investigations (Hegedűs and Kollár, 1999) demonstrate that this adjustment is necessary to prevent the over-representation of the second moments of area of the columns in the equivalent column where they are also represented in K_e [through K_c—c.f. Equations (4.3) and (4.11)].

The whole system is now modelled by a single equivalent column with bending stiffness EI and effective shear stiffness K_e (Figure 4.1/b). The governing differential equation of the equivalent column is obtained by examining the equilibrium of its elementary section. This leads to

$$r_f^2 EI u'''' - r_f^2 K_e u'' + m\ddot{u} = 0$$

where primes and dots mark differentiation by z and t (time). After seeking the solution in a product form, separating the variables and eliminating the time dependent functions, this equation results in the boundary value problem

$$r_f^2 EI u_1'''' - r_f^2 K_e u_1'' - \Omega^2 m u_1 = 0 \tag{4.16}$$

where ω is the circular frequency and u_1 defines lateral motions.

If the origin of the coordinate system is at the lower built-in end of the equivalent column (Figure 4.1/b), the boundary conditions are as follows:

$$u_1(0) = 0$$

$$u_1'(0) = 0$$

$$u_1''(H) = 0$$

and

$$EIu_1'''(H) - K_e u_1'(H) = 0$$

Governing differential equation (4.16) is identical in form to Equation (2.47). As the boundary conditions are also identical, the solution to Equation (2.47) in Section 2.2.1 can be used, bearing in mind that the stiffnesses now refer to the whole system of bracing units (not to an individual framework). With the notation

$$\Omega = \frac{2}{H^2}\sqrt{\frac{EIr_f^2}{m}}$$

and the non-dimensional parameter

$$k = H\sqrt{\frac{K_e}{EI}} \tag{4.17}$$

the solution emerges as

$$f^2 = \left(\frac{^2}{0.313} - \frac{k^2}{5}\right) f_b^2 + f_s^2$$

Table 4.2 Frequency parameters η and η_φ as a function of k and k_φ.

k or k_φ	η or η_φ	k or k_φ	η or η_φ	k or k_φ	η or η_φ	k or k_φ	η or η_φ	k or k_φ	η or η_φ
0.00	0.5596	4.5	1.465	9.5	2.680	14.5	3.913	20	5.278
0.10	0.5606	5.0	1.586	10.0	2.803	15.0	4.036	30	7.769
0.50	0.5851	5.5	1.706	10.5	2.926	15.5	4.160	40	10.26
1.00	0.6542	6.0	1.827	11.0	3.049	16.0	4.284	50	12.76
1.50	0.7511	6.5	1.949	11.5	3.172	16.5	4.408	60	15.26
2.00	0.8628	7.0	2.070	12.0	3.295	17.0	4.532	70	17.76
2.50	0.9809	7.5	2.192	12.5	3.418	17.5	4.656	80	20.26
3.00	1.1014	8.0	2.313	13.0	3.542	18.0	4.781	90	22.76
3.50	1.2226	8.5	2.435	13.5	3.665	18.5	4.905	100	25.26
4.00	1.3437	9.0	2.558	14.0	3.789	19.0	5.029	>100	$\frac{k}{4}$ or $\frac{k}{4}$

The above equation needs some modification as the first term in the right hand side contains ***both*** the bending part of the vibration of the system ***and*** also the effect of the interaction between the bending and shear vibrations. Proceeding as in

Section 2.2.1 and separating the two parts, then applying the effectiveness factor to the part that is responsible for the interaction, and assuming a bracing system in the *y*-*z* plane (as in Figure 4.1), the formula for the fundamental frequency is obtained as

$$f_y = \sqrt{f_b^2 + f_s^2 + \left(\frac{2}{0.313} - \frac{k^2}{5} - 1 \right) s_f \, f_b^2} \tag{4.18}$$

where f_b, f_s, k and s_f are calculated by taking into account the bracing elements in the relevant direction, i.e. in direction *y*. In replacing subscript *y* with *x* and considering the bracing elements in direction *x*, Equation (4.18) can also be used for the calculation of the lateral frequency in direction *x*.

Values for frequency parameter η are given in Table 4.2 as a function of parameter *k*. Values of parameter η for the second and third frequencies are tabulated in (Zalka, 2000).

It is interesting to note that when the global bending stiffness is incorporated into the (original) shear stiffness resulting in a (smaller) effective shear stiffness for the frequency analysis, then the equivalent column can be created simply by adding up the effective shear stiffnesses and the local bending stiffnesses, respectively, of the individual bracing units. This simple approach does not work in the case of the deflection and rotation analyses of systems. This is the reason why in Chapter 3 a "base unit" was created (with its load share) for the deflection and rotation analyses and the effects of the other bracing units were taken into account through additional stiffness parameters (a_i, b_i, c_i).

4.2 PURE TORSIONAL VIBRATION

Although the torsional vibration problem is more complex than that of lateral vibration, a solution may be obtained in a relatively simple way, due to an analogy between the three-dimensional torsional problem and the two-dimensional lateral vibration problem (discussed in the previous section). This analogy is well known in the stress analysis of thin-walled structures in bending and torsion (Vlasov, 1961; Kollbrunner and Basler, 1969). According to the analogy, translations, bending moments and shear forces correspond to rotations, warping moments and torsional moments, respectively. It will be demonstrated in the following that the analogy can be extended to the lateral vibration of an elastically supported cantilever (discussed in the previous section) and the pure torsional vibration of a cantilever of thin-walled cross-section (to be investigated in this section).

The model which is used for the pure torsional vibration analysis of the building is an equivalent cantilever of thin-walled, open cross-section which replaces the bracing system of the building for the torsional analysis (Figure 4.2). This equivalent cantilever is situated in the shear centre and has effective Saint-Venant torsional stiffness $(GJ)_e$ and warping torsional stiffness EI_ω (Figure 4.3). The governing differential equation of the cantilever (whose lumped masses M_i at floor levels are replaced by uniformly distributed mass *m* over the height) is obtained by examining the equilibrium of its elementary section as

$$r_f^2 EI_\Omega \varphi_1'''' - r_f^2 (GJ)_e \varphi_1'' + i_p^2 m \ddot{\varphi}_1 = 0$$

where primes and dots mark differentiation by z and t (time).

After seeking the solution in a product form, separating the variables and eliminating the time dependent functions, this equation results in the boundary value problem

$$r_f^2 EI_\Omega \varphi_1'''' - r_f^2 (GJ)_e \varphi_1'' - \Omega^2 i_p^2 m \varphi_1 = 0 \tag{4.19}$$

where ω is the circular frequency, i_p is the radius of gyration and φ_1 defines rotational motions.

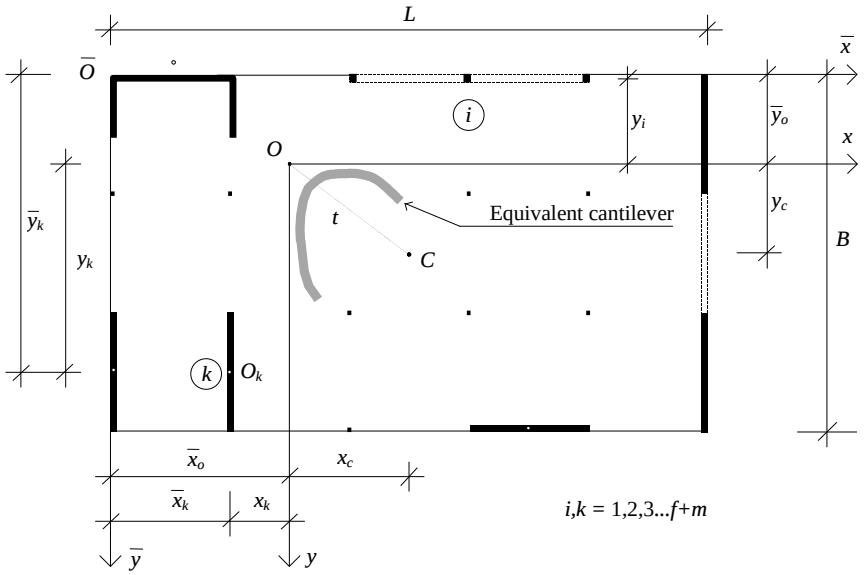

Figure 4.2 Typical layout with the equivalent column of open, thin-walled cross-section.

As the origin of the coordinate system is fixed at the bottom of the equivalent column (Figure 4.3), the boundary conditions are

$$\varphi_1(0) = 0$$

$$\varphi_1'(0) = 0$$

$$\varphi_1''(H) = 0$$

$$EI_\Omega \varphi_1'''(H) - (GJ)_e \varphi_1'(H) = 0$$

Eigenvalue problem (4.19) is clearly analogous with the one defined by the

governing differential equation (4.16) and its boundary conditions. Bending stiffness EI and the elastic support defined by the effective shear stiffness K_e in Equation (4.16) correspond to warping stiffness EI_ω and effective Saint-Venant torsional stiffness $(GJ)_e$, divided by i_p^2 in Equation (4.19), respectively.

As the derivation of Equation (4.19) demonstrates (Zalka, 1994), the radius of gyration is related to the distribution of the mass of the building. For regular multi-storey buildings of rectangular plan-shape and subjected to a uniformly distributed mass at floor levels, the radius of gyration is obtained from

$$i_p = \sqrt{\frac{L^2 + B^2}{12} + t^2} \tag{4.20}$$

where L and B are the plan length and breadth of the building and t is the distance between the geometrical centre of the plan of the building and the shear centre of the bracing system (Figure 4.2). For arbitrary plan-shapes and/or other types of mass distribution, formulae for the radius of gyration are available elsewhere (Kollár, 1999; Zalka, 2000). It is important to note that the value of i_p depends on the geometrical characteristics of the plan of the building, rather than the stiffness characteristics of the bracing system.

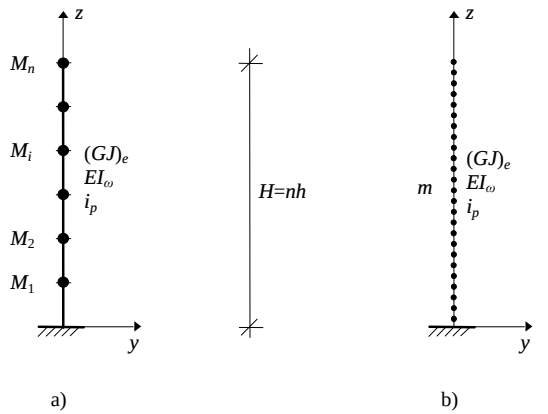

Figure 4.3 Equivalent column with: a) lumped masses M_i, b) uniformly distributed mass m.

Once the corresponding stiffnesses are established, the solution to Equation (4.16) can be used and converted to represent the solution of Equation (4.19).

The effective Saint-Venant torsional stiffness of the system may come from two sources: the Saint-Venant torsional stiffness of the shear walls and cores and from the effective shear stiffness of the frameworks as

$$(GJ)_e = \sum_1^m GJ_k + \sum_1^f \left((K_{e,i})_x y_i^2 + (K_{e,i})_y x_i^2 \right) \tag{4.21}$$

where

J_k	is the Saint-Venant constant of the kth wall/core
G	is the modulus of elasticity in shear of the walls/cores
$(K_{e,i})_x$, $(K_{e,i})_y$	are the effective shear stiffnesses of ith framework/coupled shear walls in directions x and y, respectively
x_i, y_i	are the perpendicular distances of the ith framework/coupled shear walls from the shear centre in directions x and y, respectively

If the bracing system consists of frameworks, (coupled) shear walls and cores of open cross-section, the first term in Equation (4.21) is normally negligible compared to the contribution of the frameworks.

The warping stiffness of the system may originate from three sources: the own warping stiffness of the cores, the bending stiffness of the walls and cores and the bending stiffness of the columns of the frameworks/wall sections of the coupled shear walls:

$$EI_\Omega = E_w \sum_1^m \left(I_{\Omega k} + (I_{w,k})_x y_k^2 + (I_{w,k})_y x_k^2 \right) + E_c \sum_1^f \left((I_{c,i} r_i)_x y_i^2 + (I_{c,i} r_i)_y x_i^2 \right) \tag{4.22}$$

where

$I_{\omega,k}$	is the warping constant of the kth wall/core
$E_w(I_{w,k})_x$, $E_w(I_{w,k})_y$	are the bending stiffnesses of the kth wall/core in directions x and y, respectively
$E_c(I_{c,i}r_i)_x$, $E_c(I_{c,i}r_i)_y$	are the bending stiffnesses of the columns/wall sections of the ith framework in directions x and y, respectively
x_k, y_k	are the perpendicular distances of the kth wall/core from the shear centre in directions x and y, respectively
x_i, y_i	are the perpendicular distances of the ith framework/coupled shear walls from the shear centre in directions x and y, respectively

The warping stiffness of a well-balanced bracing system is normally dominated by the contribution of the shear walls and cores (if their perpendicular distance from the shear centre is great enough). The contribution of the cores through their own warping stiffness [first term in Equation (4.22)] tends to be much smaller and the effect of the columns of the frames (last two terms) is generally negligible.

To facilitate the easy calculation of the warping constant I_Ω, closed-form formulae for cross-sections widely used for bracing cores are given in Tables 2.7, 2.8 and 2.9. More formulae are available in (Zalka, 2000). For bracing elements of special (irregular) cross-sections where no closed-form solution is available, the excellent computer program PROSEC (1994) can be used, whose accuracy has been established and proved to be within the range required for structural

engineering calculations.

With the above stiffnesses, and making use of the analogy, the fundamental frequency for pure torsional vibration is obtained in the same manner as Equation (4.18):

$$f = \sqrt{f_{\Omega}^2 + f_t^2 + \left(\frac{2}{0.313} - \frac{k^2}{5} - 1 \right) s \; f_{\Omega}^2} \tag{4.23}$$

where the pure torsional frequency associated with the warping torsional stiffness is obtained from

$$f_{\Omega}^2 = \frac{0.313 r_f^2 E I_{\Omega}}{i_p^2 H^4 m} \tag{4.24}$$

and the formula for the pure torsional frequency associated with the Saint-Venant torsional stiffness is

$$f_t^2 = \frac{r_f^2 (GJ)_e}{(4H)^2 i_p^2 m} \tag{4.25}$$

The effectiveness of the Saint-Venant torsional stiffness is expressed by the factor

$$s = \sqrt{\frac{(GJ)_e}{(GJ)}} \tag{4.26}$$

where the “original” Saint-Venant torsional stiffness is

$$(GJ) = \sum_1^m GJ_k + \sum_1^f \left((K_i)_x y_i^2 + (K_i)_y x_i^2 \right) \tag{4.27}$$

Values of vibration parameter η_{φ} are given in Table 4.2 as a function of torsion parameter k_{φ}:

$$k = H \sqrt{\frac{(GJ)_e}{EI_{\Omega}}} \tag{4.28}$$

Values for the second and third frequencies are given in (Zalka, 2000).

4.3 COUPLED LATERAL-TORSIONAL VIBRATION

When the shear centre of the bracing system and the centre of the mass coincide (e.g. doubly symmetric arrangement), the three basic frequencies f_x, f_y and f_φ are independent of each other and the smallest one is the fundamental frequency of the building.

When the system is not doubly symmetric and the shear centre does not coincide with the centre of the mass of the building, two things have to be considered. First, for the calculation of the frequency of pure torsional vibration, the location of the shear centre has to be determined. (The value of the lateral frequencies is not affected.) Second, the question of interaction among the basic modes has to be addressed.

For bracing systems developing predominantly bending deformation, the location of the shear centre is calculated using the bending stiffness of the bracing elements [Equations (3.18)]. However, with bracing systems having frameworks and coupled shear walls as well, the shear deformation of some of the bracing elements may be of considerable magnitude (in addition to their bending deformation). The behaviour of such systems is complex (and the location of the shear centre may even vary over the height). No exact solution is available for this case but, as a good approximation, the formulae given below can be used to determine the location of the shear centre.

As the lateral frequency of a bracing unit reflects both its bending and shear stiffnesses, the location of the shear centre is calculated using the lateral frequencies (f_x and f_y) of the bracing units:

$$\bar{x}_o = \frac{\sum_{1}^{f+m} f_{y,i}^2 \bar{x}_i}{\sum_{1}^{f+m} f_{y,i}^2}, \qquad \bar{y}_o = \frac{\sum_{1}^{f+m} f_{x,i}^2 \bar{y}_i}{\sum_{1}^{f+m} f_{x,i}^2} \tag{4.29}$$

where $\bar{x}_i$ and $\bar{y}_i$ are the perpendicular distances of the frameworks/coupled shear walls, shear walls and cores from axes $\bar{y}$ and $\bar{x}$, respectively (Figure 4.2). Any suitable method can be used for the calculation of the lateral frequencies in Equation (4.29), including Equation (4.18) given in Section 4.1. The repeated application of the Southwell formula (1922) and the Föppl-Papkovich formula (Tarnai, 1999) offers another very simple alternative for the calculation of the fundamental lateral frequencies. According to this approach, a lower bound to the lateral frequency of a bracing unit is obtained from the summation formula

$$f = \sqrt{f_b^2 + \frac{f_g^2 f_{s'}^2}{f_g^2 + f_{s'}^2}} \tag{4.30}$$

where $f_{s'}$, f_g and f_b relate to the bracing unit. Their values are given by Equations (2.41), (2.42) and (2.46) in Section 2.2.1.

Knowing the location of the shear centre, the Saint-Venant and warping

torsional stiffnesses can be calculated in the coordinate system whose origin is in the shear centre (Figure 4.2) using Equations (4.21) and (4.22) and the frequency of pure torsional vibration is obtained from Equation (4.23).

Assuming unsymmetric bracing system arrangement, interaction occurs among the two lateral and pure torsional modes. There are two possibilities to take into account the effect of interaction: "exactly" or approximately. The "exact" method automatically covers all the three coupling possibilities (triple-, double and no-coupling) with an error range of 0-2%. This method is given first.

When the basic frequencies f_x, f_y and f_φ are known, their coupling can be taken into account in a simple way by using the cubic equation

$$\left(f^2\right)^3 + a_2\left(f^2\right)^2 + a_1 f^2 - a_0 = 0 \tag{4.31}$$

whose smallest root yields the combined lateral-torsional frequency of the building. The coefficients in the above cubic equation are

$$a_0 = \frac{f_x^2 f_y^2 f^2}{1 - {}^2_x - {}^2_y}, \qquad a_1 = \frac{f_x^2 f_y^2 + f^2 f_x^2 + f^2 f_y^2}{1 - {}^2_x - {}^2_y},$$

$$a_2 = \frac{f_x^2 {}^2_x + f_y^2 {}^2_y - f_x^2 - f_y^2 - f^2}{1 - {}^2_x - {}^2_y} \tag{4.32}$$

where τ_x and τ_y are eccentricity parameters:

$$_x = \frac{x_c}{i_p} \quad \text{and} \quad _y = \frac{y_c}{i_p} \tag{4.33}$$

In Equations (4.33) i_p is given by Equation (4.20) and x_c and y_c are the coordinates of the geometrical centre (Figure 4.2):

$$x_c = \frac{L}{2} - \bar{x}_o \quad \text{and} \quad y_c = \frac{B}{2} - \bar{y}_o \tag{4.34}$$

If a quick solution is needed or a cubic equation solver is not available or if one of the basic frequencies is much smaller than the others, the following approximate method based on the Föppl-Papkovich theorem (Tarnai, 1999) may be used.

For unsymmetric bracing systems when the centroid of the mass of the building does not lie on either principal axis of the bracing system, triple coupling occurs and the resulting fundamental frequency is obtained using the reciprocal summation

$$\frac{1}{f^2} = \frac{1}{f_x^2} + \frac{1}{f_y^2} + \frac{1}{f^2}$$

as

$$f = \left(\frac{1}{f_x^2} + \frac{1}{f_y^2} + \frac{1}{f^2} \right)^{-\frac{1}{2}} \tag{4.35}$$

If the arrangement of the bracing system is monosymmetric and the centroid of the mass of the building lies on one of the principal axes of the bracing system (say, axis x), then two things may happen. Vibration may develop in direction x (defined by f_x) or vibration in direction y (f_y) couples with pure torsional vibration around axis z (f_φ). The frequency of this coupled vibration is obtained from

$$f_y = \left(\frac{1}{f_y^2} + \frac{1}{f^2} \right)^{-\frac{1}{2}} \tag{4.36}$$

The fundamental frequency of the building is the smaller one of f_x and $f_{y\varphi}$, i.e.:

$$f = \text{Min! } f_x,\ f_y \tag{4.37}$$

If the arrangement of the bracing system is doubly symmetric and the centroid of the mass of the building coincides with the shear centre of the bracing system, then no coupling occurs and the fundamental frequency of the building is the smallest one of f_x, f_y and f_φ, i.e.:

$$f = \text{Min! } f_x,\ f_y,\ f \tag{4.38}$$

The value of the coupled frequency of the building is basically depends on two factors: the values of the basic frequencies (f_x, f_y and f_φ) and the eccentricities of the bracing system (τ_x and τ_y). The great disadvantage of using the summation equations for determining the coupled frequency may be that they totally ignore the eccentricity of the system. If the system has relatively small eccentricity, then the summation equations tend to result in very conservative estimates.

The natural frequencies of buildings are also affected by other factors, such as foundation flexibility, reduced stiffness due to cracking, damping, etc. The treatment of such “secondary” effects is outside the scope of this book; more detailed information is available elsewhere (Barkan, 1962; Rosman, 1973; Fintel, 1974; Ellis, 1986).

4.4 ACCURACY

The reliability of the continuum method has already been demonstrated in Section 2.2.3 when the accuracy of Equation (2.50) was investigated. As Equations (4.18) and (4.23) are originated from Equation (2.50), it is not expected that the accuracy analysis to be presented here would lead to conclusions that are very different from those in Section 2.2.3. Indeed, the results are similar.

Table 4.3 Accuracy of Equation (4.18) for the fundamental frequency.

Method	Range of error (%)	Average absolute error (%)	Maximum error (%)
Continuum solution [Equation (4.18)]	-6 to 5	2.1	6

As Equations (4.18) and (4.23) are analogous in structure, and identical at theoretical level, the accuracy of Equation (4.18) was investigated only. Using eight of the frameworks shown in Figure 2.7 in Section 2.1.4 (F1 to F8) and supplementing them with four shear walls (W0 to W3 in Figure 3.7), eight planar systems were created (Figure 4.5). The height of the structures in the eight systems varied from 4 to 80 storeys in eight steps creating 72 bracing systems. The lateral frequency of the 72 bracing systems was calculated and compared to the Finite Element solution. The AXIS VM finite element package (AXIS, 2003) was used for the comparison, whose results were considered “exact”.

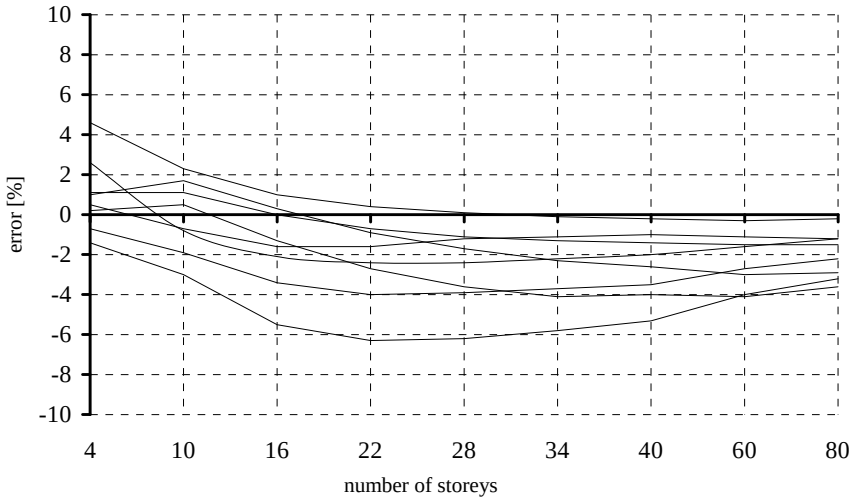

Figure 4.4 Accuracy of Equation (4.18) for the fundamental frequency for bracing systems of different heights.

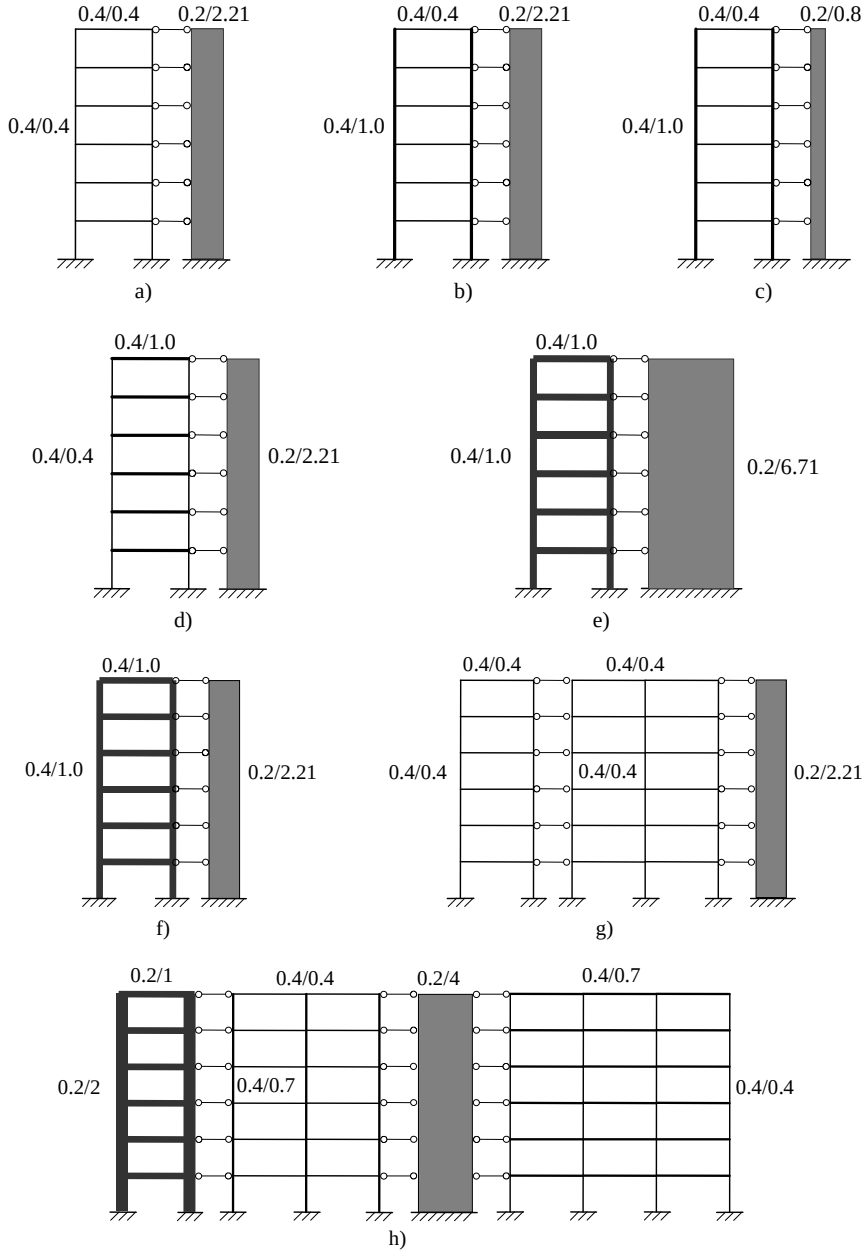

Figure 4.5 Bracing systems for the accuracy analysis. a) F1-W1: frame–shear wall, b) F2-W1: frame with high column/beam stiffness ratio–shear wall, c) F2-W0: frame with high column/beam stiffness ratio–slender shear wall, d) F3-W1: frame with high beam/column stiffness ratio-shear wall, e) F4-W3: coupled shear walls–wide shear wall, f) F4-W1: coupled shear walls–shear wall, g) F1-F7-W1: one- and two-bay frames with a shear wall, h) F8-F5-W2-F6: one-, two- and three-bay frames with a shear wall.

The bays of the one-, two- and three-bay frameworks were 6 m and the storey height was 3 m. The cross-sections of the beams and columns were chosen in such a way that the structures covered a wide range of stiffnesses.

The deflected shapes represented predominant bending, mixed shear and bending, and predominant shear deformation. The "error" was defined as the difference between the "exact" (FE) and the continuum solutions, related to the "exact" solution. When the frequency given by Equation (4.18) was smaller than the "exact" one, it was considered conservative (and the "error" was defined positive).

The results are given in Table 4.3. The variation of the error over the height of the systems is shown in Figure 4.4.

The results summarised in Table 4.3 and Figure 4.4 demonstrate the excellent performance of Equation (4.18). In the 72 cases, the average difference between the results of the continuum solution and the finite element solution was around 2%. The maximum error of Equation (4.18) was 6%.

5

Stability analysis of buildings

The stability of a building can, and should be, assessed by looking at the stability of its individual elements as well as examining its stability as a whole. National codes have detailed instructions for the first case but the buckling analysis of whole structures is not so well regulated and therefore this chapter intends to address the second case. The designer basically has two possibilities to tackle whole building behaviour in either using finite element packages or relying on analytical methods. The analytical approach is used here.

A great number of methods have been developed for the stress analysis of individual frameworks, coupled shear walls and shear walls. Fewer methods are available to deal with a *system* of these bracing units. The availability of methods for the *stability* analysis of a system of frameworks, coupled shear walls and shear walls is even more limited. This follows from the fact that the interaction among the elements (beams/lintels and columns/walls) of a single framework or coupled shear walls is complex enough but then the bracing units interact with one another not only in planar behaviour but normally also in a three-dimensional fashion. This is why the available analytical methods make one or more simplifying assumptions regarding the characteristic stiffnesses of the bracing units, the geometry of the building, or loading.

In using an equivalent Timoshenko-beam, Goschy (1970) developed a simple hand-method for the stability analysis of buildings under top-level load. Goldberg (1973) concentrated on plane buckling and presented two simple approximate formulae which can be used in the two extreme cases when the building develops pure shear mode or pure bending mode buckling. The interaction of the two modes is taken into account by applying the Föppl-Papkovich summation formula to the flexural and shear mode critical loads. Using the continuum approach (Gluck and Gellert, 1971; Rosman, 1974), Stafford Smith and Coull (1991) presented a more rigorous analysis for the sway and pure torsional buckling analysis of doubly symmetric multi-storey buildings whose vertical elements develop no or negligible axial deformations. Based on the top translation of the building (obtained from a plane frame analysis) and assuming a straight line deflection shape, MacLeod and Marshall (1983) derived a simple formula for the sway critical load of buildings. In using simple closed-form solutions for the critical loads of the individual bracing frames and coupled shear walls, Southwell's summation theorem results in a lower bound for the sway critical load of multi-storey buildings (Zalka and Armer, 1992). Even when the critical loads of the individual bracing units are not available, the repeated application of summation formulae leads to conservative estimates of the critical load in a simple manner (Kollár, 1999). In replacing the bracing units of a building with sandwich columns with thick faces, Hegedűs and Kollár (1999)

developed a simple method for calculating the critical load of multi-storey buildings with bracing shear walls and frameworks in an arbitrary arrangement, subjected to concentrated top load. All these methods restrict the scope of analysis in one way or another and none were backed up with a comprehensive accuracy analysis.

In taking into consideration all the characteristic stiffnesses of the bracing frameworks and shear walls as well as the interaction among the elements of the bracing structures and among the bracing units themselves (Zalka, 2002), the aim of this chapter is to introduce a simple analytical method for the calculation of the critical load of buildings braced by a system of frameworks, (coupled) shear walls and cores.

In addition to the general assumptions made in Chapter 1, it is also assumed for the analysis that the load of the building is uniformly distributed over the floors and that the location of the shear centre only depends on geometrical characteristics. The critical load of the structures defines the bifurcation point.

The procedure for establishing the method for the determination of the critical load of the building will be very similar to the way the method for the calculation of the fundamental frequency was developed in the previous chapter. First, the basic stiffness characteristics will be established for the analysis. The effective shear stiffness will be introduced, which, as in the previous chapter, makes it possible to create an equivalent column by the simple summation of the relevant stiffnesses. Second, based on the equivalent column, the eigenvalue problems characterising the sway buckling and pure torsional buckling problems will be set up and solved. Third, the coupling of the basic (sway and pure torsional) modes will be taken into account. Finally, a comprehensive accuracy analysis will demonstrate the reliability of the method.

5.1 SWAY BUCKLING OF A SYSTEM OF FRAMEWORKS, (COUPLED) SHEAR WALLS AND CORES

Consider a *system* of frameworks and coupled shear walls ($i = 1...f$) and shear walls and cores ($k = 1...m$), shown in Figure 5.1. The whole bracing system can be characterised by the shear stiffness of the frameworks and coupled shear walls, the global bending stiffness of the frameworks and coupled shear walls and the local bending stiffness of the individual columns/wall sections, shear walls and cores. They are the key characteristics of the equivalent cantilever that will replace the whole system, enabling a relatively simple analysis.

The shear stiffness of the equivalent column shall be determined first. The "original" shear stiffness consists of two parts. The *global* shear stiffness of the *i*th framework corresponds to the global (full-height) shear resistance of the framework and it is associated with the beams of the framework, assuming that the beams are continuously distributed over the height of the framework, resulting in full-height shear deformation (Figure 5.2/a). It is defined as

$$K_{b,i} = \sum_{j=1}^{n-1} \frac{12 E_b I_{b,j}}{l_j h} \tag{5.1}$$

where

E_b	is the modulus of elasticity of the beams of the framework
$I_{b,j}$	is the second moments of area of the *j*th beam of the *i*th framework
h	is the storey height
l_j	is the *j*th bay of the *i*th framework
n	is the number of columns of the *i*th framework

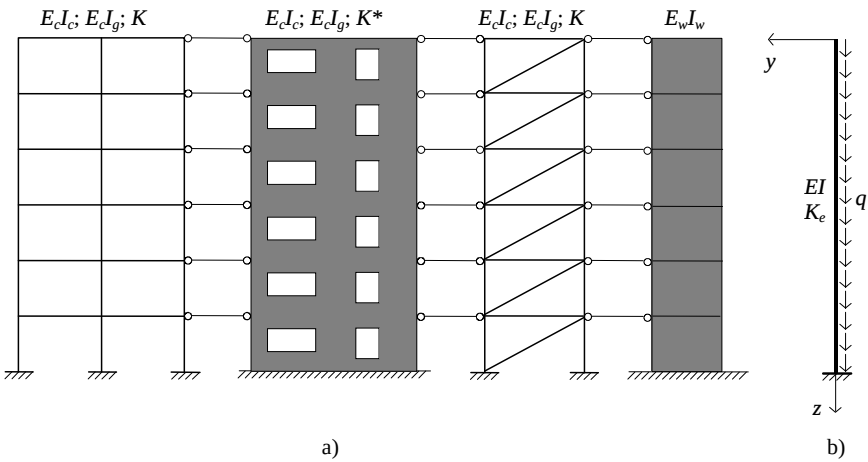

Figure 5.1 A system of frameworks and (coupled) shear walls for the lateral stability analysis.

However, the beams are not distributed continuously over the height of the framework and only contribute to the shear resistance at floor levels. Between two floor levels, it is the responsibility of the storey-height columns to resist sway locally. It follows that the *local* shear stiffness is associated with the storey-height shear resistance of the structure (Figure 5.2/b) and —assuming fixed supports—is defined as

$$K_{c,i} = \sum_{j=1}^{n} \frac{^2E_c I_{c,j}}{h^2} \tag{5.2}$$

where

E_c	is the modulus of elasticity of the columns of the framework
$I_{c,j}$	is the second moments of area of the *j*th column of the *i*th framework

Note that $\pi^2 EI/h^2$ is the critical load of a column (with stiffness EI) of height h, with two built-in ends when the lateral movement of the upper end is not restricted. The fact that the local part of the shear stiffness is linked to the storey-height buckling makes it possible to handle frameworks with non-uniform storeys and also frameworks on pinned supports—see Sections 2.4.2 and 2.4.3.

Using the above two components, the shear stiffness of the *i*th framework is obtained using the Föppl-Papkovich theorem in the form of

$$\frac{1}{K_i} = \frac{1}{K_{b,i}} + \frac{1}{K_{c,i}}$$

as

$$K_i = K_{b,i} r_i = K_{b,i} \frac{K_{c,i}}{K_{b,i} + K_{c,i}} \tag{5.3}$$

where factor r_i is introduced (for later use) as a reduction factor:

$$r_i = \frac{K_{c,i}}{K_{b,i} + K_{c,i}} \tag{5.4}$$

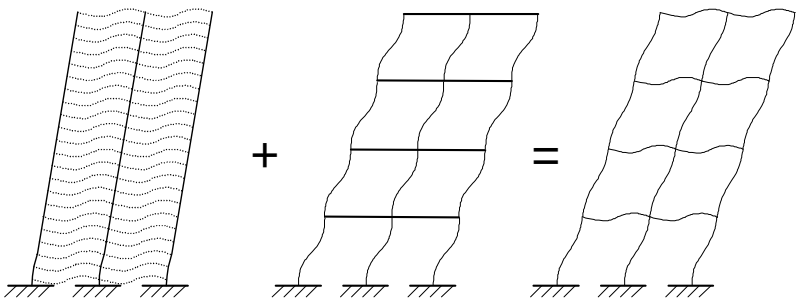

Figure 5.2 Shear deformation. a) global (full-height) component, b) local (storey-height) component, c) actual shear deformation.

The total shear stiffness of f bracing frameworks is

$$K = \sum_{i=1}^{f} K_i \tag{5.5}$$

The deformation that is associated with this “original” shear stiffness is shown in Figures 2.1/a and 5.2/c. Equation (5.5) also defines the “original” shear critical load of a system of *f* frameworks. It is called “original”, as during buckling the system also develops bending type deformations. In fact, the system develops two types of bending deformation, of which the global bending deformation (Figure 2.1/b) is worth paying attention to now, as it interacts with the above “original” shear deformation and tends to erode the original shear resistance of the system. [If coupled shear walls are also included in the system, then Equation (2.71) should be used for the calculation of the global shear stiffness, instead of

Equation (5.1).]

Global bending deflection is resisted by the global second moment of area of the cross-sections of the columns. Its value for the *i*th framework is given by

$$I_{g,i} = \sum_{j=1}^{n} A_{c,j} t_j^2 \tag{5.6}$$

just like in previous chapters. In Equation (5.6)

$A_{c,j}$ is the cross-sectional area of the *j*th column of the framework
t_j is the distance of the *j*th column from the centroid of the cross-sections

With the global second moment of area, the global bending critical load of the *i*th framework is

$$N_{g,i} = \frac{7.837 r_s E_c I_{g,i}}{H^2} \tag{5.7}$$

where H is the height of the framework and r_s is the same load distribution factor that was used earlier to allow for the fact that the load of the structure is not uniformly distributed over the height but consists of concentrated forces at floor levels (Figure 5.4). Values for r_s are given in Figure 2.14 for structures up to twenty storeys high; alternatively, if the structure is higher or more precise values are needed, Table 5.1 can be used.

Table 5.1 Load distribution factor r_s as a function of n (the number of storeys).

n	1	2	3	4	5	6	7	8	9	10	11
r_s	0.315	0.528	0.654	0.716	0.759	0.791	0.815	0.834	0.850	0.863	0.874
n	12	13	14	15	16	18	20	25	30	50	>50
r_s	0.883	0.891	0.898	0.904	0.910	0.919	0.926	0.940	0.950	0.969	$n/(n+1.588)$

During buckling there is an interaction between the shear mode and the global bending mode. This interaction is detrimental as the resulting critical load is smaller than either the shear or the global bending critical load. This phenomenon can be taken into account using the Föppl-Papkovich theorem

$$\frac{1}{K_{e,i}} = \frac{1}{K_i} + \frac{1}{N_{g,i}}$$

and the role of global bending can be interpreted as an eroding effect which leads to a reduced shear stiffness. In doing so, this shear stiffness is expressed as

$$K_{e,i} = K_i \frac{N_{g,i}}{K_i + N_{g,i}} = K_i s_i \tag{5.8}$$

where $K_{e,i}$ is defined as the *effective* shear stiffness of the *i*th framework and

$$s_i = \frac{N_{g,i}}{K_i + N_{g,i}} \tag{5.9}$$

is the effectiveness factor related to the shear stiffness of the *i*th framework.

It follows that the effective shear stiffness of the whole system (and of the equivalent column) is

$$K_e = \sum_1^f K_i s_i \tag{5.10}$$

and the effectiveness factor for the whole system is

$$s = \frac{K_e}{K} \tag{5.11}$$

where K is the "original" shear stiffness [Equation (5.5)].

The other characteristic stiffness of the system (and of the equivalent column) is the local bending stiffness. As all the columns of the frameworks, wall sections of the coupled shear walls, the shear walls and the cores have bending stiffness and all these structural items are made to work together by the floor slabs (and the beams of the frameworks), the total bending stiffness of the system is obtained by adding up the local bending stiffness of the vertical structural units:

$$EI = E_c I_c + E_w I_w = E_c \sum_1^f I_{c,i} r_i + E_w \sum_1^m I_{w,i} \tag{5.12}$$

where

E_w is the modulus of elasticity of the shear walls/cores
$I_{w,i}$ is the second moment of area of the *i*th shear wall/core

When the system has mixed bracing units—both frameworks and shear walls/cores—the contribution of the columns of the frameworks [first term in Equation (5.12)] is normally very small compared to that of the shear walls/cores and can safely be ignored.

In Equation (5.12), the bending stiffness of the columns of the frameworks are adjusted by combination factor r_i. Theoretical and numerical investigations (Hegedűs and Kollár, 1999; Zalka and Armer, 1992) demonstrate that this adjustment is necessary to prevent the over-representation of the second moments of area of the columns in the equivalent column where they are also represented in the shear stiffness.

With the above bending stiffness—that is identical to the one used for the frequency analysis—the local bending critical load of the system of frameworks and shear walls/cores can now be presented as

$$N_l = N_f + N_w = \sum_1^f N_{f,i} r_i + \sum_1^m N_{w,i}$$

$$= \frac{7.837 r_s}{H^2}\left(E_c \sum_1^f I_{c,i} r_i + E_w \sum_1^m I_{w,i} \right) = \frac{7.837 r_s EI}{H^2} \tag{5.13}$$

With N_l and K_e (the shear critical load), an approximation of the critical load of the system can already be given. According to the Southwell theorem, the two part critical loads simply have to be added up:

$$N_{cr} = N_l + K_e \tag{5.14}$$

The beauty of this formula is that it is extremely simple and also it is conservative. However, it does not take into account the interaction between the (local) bending and shear modes.

This interaction can now be taken into account as the equivalent column of the bracing system (Figure 5.1/b) is now established with bending stiffness *EI* and effective shear stiffness K_e. The governing differential equation of the equivalent column is obtained by examining the equilibrium of an elementary section of the column. This leads to the eigenvalue problem

$$r_s EI y'''' + \left[\left(N(z) - K_e \right) y' \right]' = 0 \tag{5.15}$$

where $N(z) = qz$ is the vertical load at z. The origin of the coordinate system is placed at and fixed to the top of the equivalent column, so the boundary conditions are as follows:

$$y(0) = 0$$

$$y'(H) = 0$$

$$y''(0) = 0$$

and

$$y'''(H) = 0$$

This kind of eigenvalue problem can be solved relatively easily using the generalized power series method (Zalka and Armer, 1992). After introducing the critical load parameter

$$= \frac{N_{cr}}{N_l} \tag{5.16}$$

and the part critical load ratio

$$= \frac{K_e}{N_l} \tag{5.17}$$

some rearrangement and the application of the power series method, the solution for the sway buckling of the equivalent column is obtained as

$$N_{cr} = (\quad - \quad) N_l + K_e$$

Values of critical load parameter α are given in Table 5.2 as a function of part critical load ratio β.

Table 5.2 Critical load parameters α and α_φ as a function of part critical load ratios β and β_φ.

β or β_φ	α or α_φ	β or β_φ	α or α_φ	β or β_φ	α or α_φ	β or β_φ	α or α_φ
0.0000	1.0000	0.05	1.1487	2	5.624	80	106.44
0.0005	1.0015	0.06	1.1782	3	7.427	90	118.38
0.001	1.0030	0.07	1.2075	4	9.100	100	130.25
0.002	1.0060	0.08	1.2367	5	10.697	200	246.24
0.003	1.0090	0.09	1.2659	6	12.241	300	359.51
0.004	1.0120	0.10	1.2949	7	13.749	400	471.29
0.005	1.0150	0.20	1.5798	8	15.227	500	582.06
0.006	1.0180	0.30	1.8556	9	16.682	1000	1127.5
0.007	1.0210	0.40	2.1226	10	18.118	2000	2199.1
0.008	1.0240	0.50	2.3817	20	31.820	5000	5360.5
0.009	1.0270	0.60	2.6333	30	44.862	10000	10567
0.010	1.0300	0.70	2.8780	40	57.545	100000	102579
0.020	1.0598	0.80	3.1163	50	69.991	1000000	1011864
0.030	1.0896	0.90	3.3488	60	82.265	2000000	2018802
0.040	1.1192	1.00	3.5758	70	94.405	>2000000	β or β_φ

Before this solution is used for the sway buckling analysis of the whole bracing system, however, a small modification has to be made. The first term in the above equation stands for the bending contribution of the individual columns/wall sections, shear walls and cores in the system *and* it also represents the increase of the critical load of the system, due to the interaction between the bracing units in bending and the bracing units in shear. However, because of the fact that the effectiveness of the shear stiffness is normally smaller than 100% [c.f. Equation (5.11) where $s \leq 1$ holds], these two contributions have to be separated and the

effectiveness factor should be applied to the part which is due to the interaction. The formula for the sway critical load then emerges as

$$N_{cr} = N_l + K_e + (\quad - \quad - 1)sN_l \tag{5.18}$$

In the right-hand side of the above equation, the first two terms stand for the bending and shear critical loads of the system—compare Equation (5.18) and the approximate solution represented by Equation (5.14)—while the third term represents the effect of the interaction between the bending and shear deformations. As is the case with systems subjected to horizontal load (MacLeod, 1971), the interaction is beneficial. Bearing in mind that $(\alpha - \beta - 1) \geq 1$ always holds, the evaluation of the third term demonstrates that the effect of the interaction increases the critical load of the system. The evaluation of the data in Table 5.2 shows that the maximum increase is 87%, at $\beta = 2.1$.

The method can also be used when the building is subjected to a concentrated force on top of the building—e.g., a swimming pool on the top floor. In such a case N_l and N_g in the relevant formulae are to be replaced by the corresponding Euler critical loads. It is interesting to note that the interaction in this load case does not increase the value of the critical load; the value of the term in brackets in Equation (5.18) becomes zero and Equation (5.14)—with the Euler critical loads—becomes the exact solution. See Section 5.5 for details.

A building may develop sway buckling in the two principal directions and both critical loads have to be calculated. These critical loads are obtained using Equation (5.18) where N_l, K_e, β and s are calculated by taking into account the bracing elements in the relevant principal directions, say, in x and y.

5.2 SWAY BUCKLING: SPECIAL BRACING SYSTEMS

The following—idealised—special cases of bracing systems are worth considering (where the term “framework” refers to frameworks and coupled shear walls and the term “wall” covers both shear walls and cores).

5.2.1 Bracing systems consisting of shear walls only

In this special case, there is no shear stiffness in the sense it is used in this chapter. This translates to $K = 0$, $\beta = 0$ and $\alpha = 1$. As $N_f = 0$ in Equation (5.13), Equation (5.18) simplifies to

$$N_{cr} = N_l = N_w = \frac{7.837 r_s E_w I_w}{H^2} \tag{5.19}$$

which is the standard solution for the sway buckling of a bracing system in pure bending.

5.2.2 Bracing systems consisting of frameworks only

Equations (5.13) and (5.18) hold with $E_w I_w = 0$; everything else is unchanged.

If, furthermore, the beam/column stiffness ratio is very high, then the formula for the critical load further simplifies. In this special case, $K_b >> K_c$ and $N_g \approx \infty$ hold. Consequently, $r_i \approx 0$, $K \approx K_c$, $s_i \approx 1$, $K_e \approx K_c$ and $s \approx 1$. This leads to

$$N_{cr} = \sum_1^f K_{c,i} = \sum_1^f \left(\sum_1^n \frac{^2E_c I_{c,j}}{h^2} \right) \tag{5.20}$$

showing that the building loses stability through storey-high sway (shear failure from the point of view of the whole building), which is resisted by the stiffness of the columns. Equation (5.20) can also be used for checking stability when there is a loss of stiffness at a particular storey, making that storey vulnerable to local shear buckling (Zalka, 2000).

5.2.3 Bracing systems consisting of shear walls and frameworks with very high beam/column stiffness ratio

Three sub-cases are worth considering.

First, assume that the axial deformations of the columns are negligible. The practical case that belongs here is the case of low-rise buildings. In this special case, $K_b >> K_c$ and $N_g \approx \infty$ hold. Consequently, $r_i \approx 0$, $K \approx K_c$, $s_i \approx 1$, $K_e \approx K_c$ and $s \approx 1$. $\beta \approx K_c/N_w > 0$ and $\alpha > 1$. This leads to

$$N_{cr} = (\quad - \quad) N_w + K_c = \quad N_w = \quad \frac{7.837 E_w I_w r_s}{H^2} \tag{5.21}$$

showing that the critical load is based on the bending critical load of the shear walls and cores. This value is increased (through $\alpha > 1$) due to the interaction between the bracing elements in shear (frameworks with stiff beams) and the bracing elements in bending (walls and cores). The shear stiffness is characterised by the weakest link (i.e. by the stiffness of the columns).

Second, assume that the axial deformations of the columns are not negligible. The practical case that belongs here is the case of medium-rise buildings. In this case, $K_b >> K_c$ and $N_g \neq \infty$ hold. Consequently, $r_i \approx 0$, $K \approx K_c$, $s_i < 1$, $K_e \approx \sum K_{c,i} s_i < K_c$ and $s < 1$. $\beta \approx sK_c/N_w > 0$ and $\alpha > 1$. This results in

$$N_{cr} = N_l + sK_c + (\quad - \quad - 1) s N_l = [s(\quad - \quad - 1) + 1 + \quad] \frac{7.837 E_w I_w r_s}{H^2} \tag{5.22}$$

As $[s(\alpha - \beta - 1) + 1 + \beta] > 1$ always holds, due to the supporting effect of the shear stiffness of the frameworks, the overall critical load is again greater than that of the shear walls/cores. However, the magnitude of the increase in this case is

more difficult to estimate as, in addition to the effect of the columns as in the previous case, it also depends on the "eroding" effect of the axial deformations of the columns (through parameter s).

Third, assume that the axial deformations of the columns are very great. The practical case that belongs here is the case of medium/high-rise buildings with columns of relatively small cross-section. In this special case, $K_b >> K_c$ and $N_g \approx 0$ hold. Consequently, $r_i \approx 0$, $K \approx K_c$, $s_i \approx 0$, $K_e \approx 0$ and $s \approx 0$. $\beta \approx 0$ and $\alpha \approx 1$. This results in

$$N_{cr} = [s(\quad - \quad) + 1 - s]N_w = N_w = \frac{7.837 E_w I_w r_s}{H^2} \tag{5.23}$$

Due to the excessive axial deformation of the columns, all the shear capacity of the frameworks is eroded and the shear walls and cores act as individual bracing elements in bending—c.f. Section 5.2.1 and Equation (5.19).

5.2.4 Bracing systems consisting of shear walls and frameworks with very high column/beam stiffness ratio

Again, three characteristic cases can be distinguished.

First, assume that the axial deformations of the columns are negligible. Practical case: low/medium-rise buildings.

In this special case, $K_b << K_c$ and $N_g \approx \infty$ hold. Consequently, $r_i \approx 1$, $K \approx K_b$, $s_i \approx 1$, $K_e \approx K_b$ and $s \approx 1$. $\beta \approx K_b/N_l > 0$ and $\alpha > 1$. This leads to

$$N_{cr} = (\quad - \quad)N_l + K_b = \quad (N_f + N_w) = \quad \frac{7.837 r_s (E_c I_c + E_w I_w)}{H^2} \tag{5.24}$$

showing that the critical load is based on the bending critical load of the columns, shear walls and cores; this value is presumably slightly increased (through $\alpha > 1$) due to the interaction between the bracing elements in shear (frameworks) and the bracing elements in bending (walls and cores). The shear stiffness is characterised by the weakest link, i.e., by the stiffness of the beams.

Second, assume that axial deformations of the columns are not negligible. Practical case: low/medium-rise buildings.

In this case, $K_b << K_c$ and $N_g \neq \infty$ hold. Consequently, $r_i \approx 1$, $K \approx K_b$, $s_i < 1$, $K_e \approx \sum K_{b,i} s_i < K_b$ and $s < 1$. $\beta \approx sK_b/N_l > 0$ and $\alpha > 1$. This results in

$$N_{cr} = [s(\quad - \quad - 1) + 1 + \quad] \frac{7.837 r_s (E_c I_c + E_w I_w)}{H^2} \tag{5.25}$$

As $[s(\alpha - \beta - 1) + 1 + \beta] > 1$ always holds, due to the supporting effect of the shear stiffness of the frameworks, the overall critical load is greater than that of the shear walls/cores. However, the magnitude of the increase in this case is more difficult to estimate as, in addition to the effect of the columns as in the previous

case, it also depends on the "eroding" effect of the axial deformations of the columns (through parameter s). The stiffness of the columns (E_cI_c) is in most practical cases negligible compared to the stiffness of the shear walls and cores (E_wI_w).

Third, assume that the axial deformations of the columns are very great. Practical case: high-rise buildings with frameworks of great global slenderness.

In this special case, $K_b << K_c$ and $N_g \approx 0$ hold. Consequently, $r_i \approx 1$, $K \approx K_b$, $s_i \approx 0$, $K_e \approx 0$ and $s \approx 0$. $\beta \approx 0$ and $\alpha \approx 1$. This results in

$$N_{cr} = [s(\quad - \quad) + 1 - s](N_f + N_w) = \frac{7.837 r_s (E_c I_c + E_w I_w)}{H^2} \tag{5.26}$$

Due to the excessive axial deformation of the columns, all the shear capacity of the frameworks is eroded and the shear walls and cores work as individual bracing elements in bending. The stiffness of the columns (E_cI_c) is in most practical cases negligible compared to the stiffness of the shear walls and cores (E_wI_w).

5.3 PURE TORSIONAL BUCKLING

Although the torsional buckling problem is more complex than that of sway buckling, the solution is obtained in a relatively simple way, due to an analogy between the three-dimensional torsional problem and the two-dimensional sway buckling problem (discussed in the previous section). This analogy is well known in the stress analysis of thin-walled structures in bending and torsion (Vlasov, 1961; Kollbrunner and Basler, 1969). (The same analogy was used in Chapter 4 for the analysis of pure torsional vibration.) According to the analogy, translations, bending moments and shear forces correspond to rotations, warping moments and torsional moments, respectively. It will be demonstrated in the following that the analogy can be extended to the sway buckling of an elastically supported cantilever (discussed in the previous section) and the pure torsional buckling of a cantilever of thin-walled cross-section (to be investigated in this section).

The model which is used for the pure torsional buckling analysis of the building is an equivalent cantilever of thin-walled, open cross-section which replaces the bracing system of the building for the torsional analysis (Figure 5.3). This equivalent column is situated in the shear centre and has effective Saint-Venant torsional stiffness $(GJ)_e$ and warping torsional stiffness EI_ω. The governing differential equation of the cantilever is obtained by examining the equilibrium of its elementary section as

$$\frac{r_s EI_\Omega}{i_p^2} \quad '''' + \left[\left(N(z) - \frac{(GJ)_e}{i_p^2} \right) \quad ' \right]' = 0 \tag{5.27}$$

where $N(z)$ is the vertical load at z and i_p is the radius of gyration.

If the origin of the coordinate system is placed and fixed to the cross-section

at the top of the equivalent column (Figure 5.4/d), the boundary conditions are:

$$(0) = 0$$

$$'(H) = 0$$

$$''(0) = 0$$

$$'''(H) = 0$$

This eigenvalue problem is clearly analogous with the one defined by the governing differential equation (5.15) and its boundary conditions. Bending stiffness EI and the elastic support defined by the effective shear stiffness K_e in Equation (5.15) correspond to warping stiffness EI_ω and effective Saint-Venant torsional stiffness $(GJ)_e$, divided by i_p^2 in Equation (5.27), respectively.

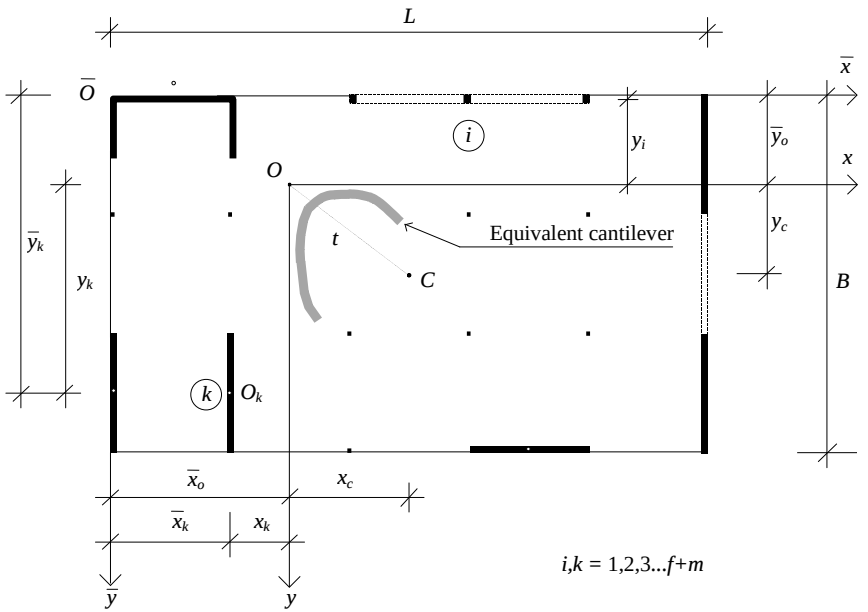

Figure 5.3 Typical layout with the equivalent column of open, thin-walled cross-section in the shear centre.

As the derivation of an equation identical in structure to Equation (5.27) demonstrates (Zalka and Armer, 1992), the radius of gyration is related to the vertical load of the building. For regular multi-storey buildings of rectangular plan-shape that are subjected to a uniformly distributed load on the floors, the radius of gyration is obtained from

$$i_p = \sqrt{\frac{L^2 + B^2}{12} + t^2} \tag{5.28}$$

where L and B are the plan length and breadth of the building and t is the distance between the geometrical centre of the plan of the building and the shear centre of the bracing system (Figure 5.3). [For arbitrary plan-shapes and/or other types of load distribution, formulae for the radius of gyration are available elsewhere (Kollár, 1999; Zalka, 2000).] It is important to note that the value of i_p depends on the geometrical characteristics of the plan of the building, rather than the stiffness characteristics of the bracing system.

Once the corresponding stiffnesses are established, the solution to Equation (5.15) can be used and converted to represent the solution of Equation (5.27). The effective Saint-Venant torsional stiffness of the system may come from two sources: the Saint-Venant torsional stiffness of the shear walls and cores and from the effective shear stiffness of the frameworks as

$$(GJ)_e = \sum_1^m GJ_k + \sum_1^f \left((K_{e,i})_x y_i^2 + (K_{e,i})_y x_i^2 \right) \tag{5.29}$$

where

J_k	is the Saint-Venant constant of the kth wall/core
G	is the modulus of elasticity in shear of the walls/cores
$(K_{e,i})_x$, $(K_{e,i})_y$	are the effective shear stiffnesses of the ith framework/coupled shear walls in directions x and y, respectively
x_i, y_i	are the perpendicular distances of the ith framework/coupled shear walls from the shear centre in directions x and y, respectively

If the bracing system consists of frameworks, (coupled) shear walls and cores of open cross-section, the first term in Equation (5.29) is normally negligible compared to the contribution of the frameworks.

The warping stiffness of the system may originate from three sources: the own warping stiffness of the cores, the bending stiffness of the walls and the bending stiffness of the columns of the frameworks/wall sections of the coupled shear walls:

$$EI_\Omega = E_w \sum_1^m \left(I_{\Omega,k} + (I_{w,k})_x y_k^2 + (I_{w,k})_y x_k^2 \right) + E_c \sum_1^f \left((I_{c,i} r_i)_x y_i^2 + (I_{c,i} r_i)_y x_i^2 \right) \tag{5.30}$$

where

$I_{\omega,k}$	is the warping constant of the kth wall/core

$E_w(I_{w,k})_x$, $E_w(I_{w,k})_y$ are the bending stiffnesses of the kth wall/core in directions x and y, respectively

$E_c(I_{c,i}r_i)_x$, $E_c(I_{c,i}r_i)_y$ are the bending stiffnesses of the columns/wall sections of the ith framework in directions x and y, respectively

x_k, y_k are the perpendicular distances of the kth wall/core from the shear centre in directions x and y, respectively

x_i, y_i are the perpendicular distances of the ith framework/coupled shear walls from the shear centre in directions x and y, respectively

The warping stiffness of a well-balanced bracing system is normally dominated by the contribution of the shear walls and cores (if their perpendicular distance from the shear centre is great enough). The contribution of the cores through their own warping stiffness [first term in Equation (5.30)] tends to be much smaller and the effect of the columns of the frames (last two terms) is generally negligible.

To facilitate the easy calculation of the warping constant I_Ω, closed-form formulae for cross-sections widely used for bracing cores are given in Tables 2.7, 2.8 and 2.9. More formulae are available in (Zalka, 2000). For bracing elements of special (irregular) cross-sections where no closed-form solution is available, the excellent computer program PROSEC (1994) can be used, whose accuracy has been established and proved to be within the range required for structural engineering calculations.

With the above stiffnesses, and making use of the analogy, the critical load of pure torsional buckling is obtained in the same manner as with Equation (5.18):

$$N_{cr,} = N_\Omega + N_t + (\quad - \quad -1)s\ N_\Omega \tag{5.31}$$

where the warping torsional critical load of the system is

$$N_\Omega = \frac{7.837 r_s E I_\Omega}{i_p^2 H^2} \tag{5.32}$$

and the Saint-Venant torsional critical load is

$$N_t = \frac{(GJ)_e}{i_p^2} \tag{5.33}$$

It is interesting to note that the value of the Saint-Venant torsional critical load does not depend on the height of the building.

The effectiveness of the Saint-Venant torsional stiffness is expressed by the factor

$$s = \frac{(GJ)_e}{(GJ)} \tag{5.34}$$

where the “original” Saint-Venant torsional stiffness is

$$(GJ) = \sum_{1}^{m} GJ_k + \sum_{1}^{f} \left((K_i)_x y_i^2 + (K_i)_y x_i^2 \right) \tag{5.35}$$

Values for the critical load parameter α_φ are given in Table 5.2 as a function of parameter β_φ:

$$= \frac{N_t}{N_\Omega} \tag{5.36}$$

In making use of the analogy, special cases can be investigated in the same manner as in Section 5.2.

In the special case when the bracing system only consists of a single bracing unit with no warping stiffness—e.g. a closed or partially closed U-core—the above procedure cannot be used as the denominator in Equation (5.36) vanishes. This case is covered in Section 2.7.3 which deals with the stability of a single core. Section 12.2 also deals with this case in great detail.

5.4 COMBINED SWAY-TORSIONAL BUCKLING

When the shear centre of the bracing system and the centre of the vertical load coincide, the three basic critical loads $N_{cr,x}$, $N_{cr,y}$ and $N_{cr,\varphi}$ are independent of each other and the smallest one is the overall critical load of the building.

When the system is not doubly symmetric and the shear centre does not coincide with the geometrical centre of the building, two things have to be considered. First, for the calculation of the critical load of pure torsional buckling, the location of the shear centre has to be determined. (The value of the sway buckling critical loads is not affected.) Second, as sway buckling in the two principal directions combines with pure torsional buckling (Figure 5.4/d), the question of interaction among the three basic modes has to be addressed.

For bracing systems developing bending deformation only, the location of the shear centre is calculated using the bending stiffness of the bracing units. However, with bracing systems having frameworks and coupled shear walls as well, the shear deformation of the bracing units may be of considerable magnitude (in addition to their bending deformation). The behaviour of such systems is complex (and the location of the shear centre may even vary over the height). No exact solution is available for this case but, as a good approximation, the formulae given below can be used to determine the location of the shear centre.

As the critical load of a bracing unit reflects both its bending and shear stiffnesses, the location of the shear centre is calculated using the critical loads of the bracing units:

$$\bar{x}_o = \frac{\sum_{1}^{f+m} N_{y,i} \bar{x}_i}{\sum_{1}^{f+m} N_{y,i}}, \qquad \bar{y}_o = \frac{\sum_{1}^{f+m} N_{x,i} \bar{y}_i}{\sum_{1}^{f+m} N_{x,i}} \tag{5.37}$$

where $\bar{x}_i$ and $\bar{y}_i$ are the perpendicular distances of the bracing units from axes $\bar{y}$ and $\bar{x}$ and f and m are the number of frameworks/coupled shear walls and shear walls/cores, respectively (Figure 5.3). Any suitable method can be used for the calculation of the critical loads in Equations (5.37), including Equation (5.18) given in Section 5.1—c.f. special cases discussed in Sections 5.2.

When the bracing system consists of shear walls (and cores) only, Equations (5.37) for the location of the shear centre simplify and the shear centre coordinates can be determined using

$$\bar{x}_o = \frac{\sum_1^m I_{x,i}\bar{x}_i}{\sum_1^m I_{x,i}}, \qquad \bar{y}_o = \frac{\sum_1^m I_{y,i}\bar{y}_i}{\sum_1^m I_{y,i}} \tag{5.38}$$

Equations (5.38) can also be used for the frequency and deflection calculations for systems that only have bending stiffness.

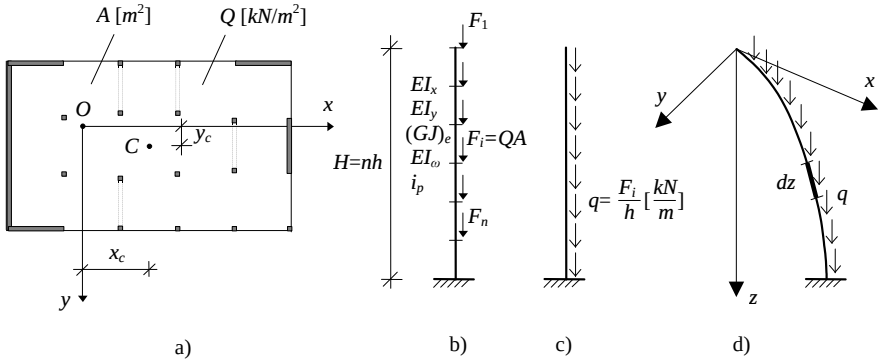

Figure 5.4 Sway-torsional buckling. a) layout, b) equivalent column with its stiffness characteristics and load at floor levels, c) equivalent column with its uniformly distributed load, d) model for the analysis.

When the location of the shear centre is known, the Saint-Venant and warping torsional stiffnesses can be calculated in the coordinate system whose origin is in the shear centre using Equations (5.29) and (5.30) and the critical load of pure torsional buckling is obtained from Equation (5.31).

Assuming unsymmetric bracing system arrangement, interaction occurs among the two lateral and pure torsional modes. The situation is very similar to that of the frequency analysis. Accordingly, there are two possibilities to take into account the effect of interaction: exactly or approximately. The exact method automatically covers all the three coupling possibilities (triple-, double and no-coupling). This method is given first.

The critical load is obtained by solving the cubic equation

$$(N)^3 + b_2(N)^2 + b_1 N - b_0 = 0 \tag{5.39}$$

whose smallest root yields the combined global critical load of the building. In the case of buildings subjected to uniformly distributed floor load, Equation (5.39) is exact, as far as the effect of the coupling of the three modes is concerned.

The coefficients in the above cubic equation are

$$b_0 = \frac{N_{cr,x} N_{cr,y} N_{cr,}}{1 - {}^2_x - {}^2_y}, \qquad b_1 = \frac{N_{cr,x} N_{cr,y} + N_{cr,}\ N_{cr,x} + N_{cr,}\ N_{cr,y}}{1 - {}^2_x - {}^2_y},$$

$$b_2 = \frac{N_{cr,x}\ {}^2_x + N_{cr,y}\ {}^2_y - N_{cr,x} - N_{cr,y} - N_{cr,}}{1 - {}^2_x - {}^2_y} \tag{5.40}$$

where τ_x and τ_y are eccentricity parameters:

$${}_x = \frac{x_c}{i_p} \quad \text{and} \quad {}_y = \frac{y_c}{i_p} \tag{5.41}$$

Radius of gyration i_p is given by Equation (5.28) and x_c and y_c are the coordinates of the geometrical centre:

$$x_c = \frac{L}{2} - \bar{x}_o \quad \text{and} \quad y_c = \frac{B}{2} - \bar{y}_o \tag{5.42}$$

If a quick solution is needed or a cubic equation solver is not available or if one of the basic critical loads is much smaller than the others, the Föppl-Papkovich theorem (Tarnai, 1999) offers a simple albeit approximate solution.

If the bracing system is unsymmetric and the centroid of the vertical load of the building does not lie on either principal axis of the bracing system, triple coupling occurs and an approximation of the resulting combined critical load is obtained using the reciprocal summation as

$$N_{cr} = \left(\frac{1}{N_{cr,x}} + \frac{1}{N_{cr,y}} + \frac{1}{N_{cr,}} \right)^{-1} \tag{5.43}$$

If the arrangement of the bracing system is monosymmetric and the centroid of the vertical load of the building lies on one of the principal axes of the bracing system (say, axis x), then two things may happen. Sway buckling may develop in

direction x (defined by $N_{cr,x}$) or buckling in direction y ($N_{cr,y}$) couples with pure torsional buckling ($N_{cr,\varphi}$). The critical load of this coupled buckling is obtained from

$$N_y = \left(\frac{1}{N_{cr,y}} + \frac{1}{N_{cr,}} \right)^{-1} \tag{5.44}$$

The global critical load of the building is the smaller one of $N_{cr,x}$ and $N_{y\varphi}$, i.e.:

$$N_{cr} = \text{Min!}\, N_{cr,x}, N_y \tag{5.45}$$

If the arrangement of the bracing system is doubly symmetric and the centroid of the vertical load of the building coincides with the shear centre of the bracing system, then no coupling occurs and the global critical load of the building is the smallest one of $N_{cr,x}$, $N_{cr,y}$ and $N_{cr,\varphi}$, i.e.:

$$N_{cr} = \text{Min!}\, N_{cr,x}, N_{cr,y}, N_{cr,} \tag{5.46}$$

Simplicity and the fact that the above Föppl-Papkovich equations are always conservative may justify the use of the approximate solutions. However, their application may lead to rather uneconomic structural solutions as they cannot take into consideration the degree of eccentricity of the bracing system. The (conservative) error of Equation (5.43) can be as much as 67%.

When the global critical load of the system is calculated, the global critical load ratio can be used to assess the effectiveness of the bracing system. It also indicates whether or not a more sophisticated second order analysis needs to be carried out. The application of the global critical load ratio is discussed in the next chapter and it is only mentioned here that the greater the global critical load ratio, the greater the level of safety against buckling.

5.5 CONCENTRATED TOP LOAD

In certain cases, concentrated load on top of the building may need to be considered. A panorama restaurant, a swimming pool or a water tank may represent some extra load that is not covered by the uniformly distributed floor load, considered to be the same at each floor level over the height of the building. The critical load for the concentrated top case can be determined relatively easily using (and amending) the equations presented in the previous sections for the uniformly distributed load case.

The critical concentrated load for sway buckling, based on Equation (5.18), assumes the form

$$F_{cr} = F_l + K_e \tag{5.47}$$

where F_l is the local bending critical load and K_e is the effective shear stiffness for

concentrated top load case. The effective shear stiffness is determined as

$$K_e = \left(\frac{1}{K} + \frac{1}{F_g} \right)^{-1} \tag{5.48}$$

where F_g is the global bending critical load. Note that for the part critical loads F_l and F_g, the corresponding Euler critical loads should be used:

$$F_l = \frac{^2EI}{4H^2} \tag{5.49}$$

and

$$F_g = \frac{^2EI_g}{4H^2} \tag{5.50}$$

To calculate the sway critical loads in directions x and y ($F_{cr,x}$ and $F_{cr,y}$), the relevant bracing units (with their stiffnesses) should be used.

For pure torsional buckling, Equation (5.31) leads to

$$F_{cr,} = F_\Omega + F_t \tag{5.51}$$

where the warping torsional critical load of the system is

$$F_\Omega = \frac{^2EI_\Omega}{4H^2 i_p^2} \tag{5.52}$$

where the warping torsional stiffness is given by Equation (5.30).

The Saint-Venant torsional critical load is obtained from

$$F_t = \frac{(GJ)_e}{i_p^2} \tag{5.53}$$

The effective Saint-Venant torsional stiffness $(GJ)_e$ in Equation (5.53) consists of two parts, as seen in Equation (5.29). The first term is identical to the first term in Equation (5.29). However, the second term (that depends on the contribution of the frameworks) is calculated using K_e according to Equation (5.48).

It is interesting to note that when the load is concentrated on top of the building, there is no interaction (that would increase the critical load) between the bending and shear modes.

Once the basic critical loads $F_{cr,x}$, $F_{cr,y}$ and $F_{cr,\varphi}$ are available, the coupling of the basic modes is taken into account exactly as with $N_{cr,x}$, $N_{cr,y}$ and $N_{cr,\varphi}$ in

Section 5.4 above, i.e. applying Equations (5.39), (5.40), (5.41) and (5.42) for the exact analysis or Equations (5.43), (5.44), (5.45) and (5.46) for the approximate analysis, using the Euler basic critical loads.

5.6 ACCURACY

A comprehensive accuracy analysis was carried out to check the accuracy of the method. As the key element of the method is the calculation of the critical load of sway buckling of a system of frameworks, (coupled) shear walls and cores, the analysis centred on checking the accuracy of Equation (5.18). The sway critical load of 72 bracing systems was calculated and compared to the Finite Element solution. The AXIS VM finite element package (AXIS, 2003) was used for the comparison, whose results were considered "exact". The "error" was defined as the difference between the results obtained using Equation (5.18) and from the FE analysis, related to the "exact" solution. Positive error meant conservative estimates.

The test structures were identical to those used for the accuracy analysis of the method presented in Chapter 4 for the frequency analysis of buildings. Eight frameworks/coupled shear walls (F1 to F8 in Figure 2.7) and four shear walls (W0, W1, W2 and W3 in Figure 3.7) were used as bracing units. Using these bracing units, eight bracing systems were created (Figure 4.5) to cover a wide range of stiffness characteristics, representing buildings developing predominantly bending deformation, a mixture of bending and shear deformations and predominantly shear deformation. The height of the buildings varied between 4 and 80 storeys in eight steps, creating 72 test cases. The bays of the frameworks were 6 m and the storey height was 3 m.

Table 5.3 Accuracy of approximate methods for the sway-critical load of buildings.

Method	Range of error (%)	Average absolute error (%)	Maximum error (%)
Summation formulae (Kollár, 1999)	1 to 44	24	44
Southwell's formula (Zalka and Armer, 1992)	-3 to 34	16	34
Stafford Smith – Coull formula (Stafford Smith and Coull, 1991)	-1 to -1596	231	1596
MacLeod-Marshall formula (MacLeod and Marshall, 1983)	-4 to -64	17	64
Continuum solution [Equation (5.18)]	-15 to 19	6	19

The summary of the results is given in the last row in Table 5.3. The

performance of the method over the height of the structures is shown in Figure 5.5. The results summarised in Table 5.3 and shown in Figure 5.5 demonstrate the general performance of Equation (5.18). In the 72 cases, the average difference between the results of the continuum solution and the finite element solution was around 6%. The maximum error of Equation (5.18) was 19%.

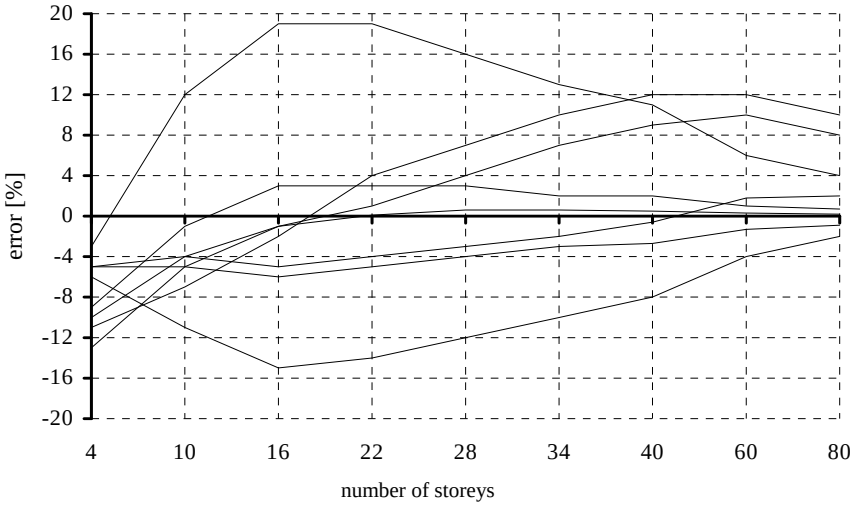

Figure 5.5 Accuracy of Equation (5.18) for the critical load of bracing systems of different height.

The results are not as good as those obtained in the case of the frequency analysis. They may even be considered disappointing. However, a comparison with other approximate methods mentioned in the introduction (given in the first four rows in Table 5.3) puts them in perspective. (It is well-known in structural engineering research that some complex stability problems are notoriously difficult to solve as the structural engineering modelling difficulties often combine with ill-conditioned mathematical problems.)

6

The global critical load ratio

Stability problems concerning multi-storey buildings can be investigated on two levels. An element-based “local” analysis can be carried out, step by step, aimed at certain key structural members. Codes of practice normally follow this avenue and have detailed instructions for the analysis. This approach makes it possible to carry out the analysis in a relatively simple way but has disadvantages. It leaves the designer with the task of identifying all the key members and it cannot address the full-height, three-dimensional global behaviour of the multi-storey building. The “local” approach may also lead to uneconomic solutions as the elements of the whole structure tend to work together and, with the local approach, the possibility to take into account the effects of interaction is normally limited to the neighbouring members only.

The other approach is the global approach. The concept of the global critical load ratio has been around for some time. Around but not in use. Or at least not in use to such an extent as it should have been. As the results of an illustrative example given in this chapter will demonstrate, the global critical load ratio is far more than a stability parameter: It is a generic characteristic with which the designer can monitor the overall performance of the whole bracing system. It also links the three important areas of analysis: the stress, stability and dynamic analyses. The way the structure responds to the loads—in two or three-dimensional manner—is automatically taken into account and made clear to the designer.

Around the middle of the last century Chwalla (1959) emphasized the importance of the global approach and recommended the introduction of a “global factor”. Halldorsson and Wang (1968) suggested that a “general safety factor” should be used for building structures, and its importance was comparable to that of the “overturning factor” used in the design of dams. Dowrick (1976) drew attention to the importance of the overall stability of structures. Dealing with plane structures Stevens (1983) linked theory and practice and underlined the importance of the critical load in the design of frameworks. The idea of a global safety factor also surfaced in connection with the structural design of large structures (Zalka and Armer, 1992). MacLeod and Zalka (1996) and MacLeod (2005) advocated the use of the critical load ratio emphasizing its ability to handle torsional behaviour in a relatively simple way. The importance of torsional behaviour cannot be overemphasized, especially considering the fact that up to the emergence of the personal computer, relatively little attention had been paid to the three-dimensional behaviour of complex structures in university textbooks and in national and international codes of practice.

However, the situation seems to be changing. More and more powerful computers, sophisticated software packages and advanced guidelines on modelling

complex structures (MacLeod, 1990 and 2005) make it easier to carry out true three-dimensional analyses. The global approach and methods developed with the global aspect in mind have also been emerging in structural designer handbooks and in codes of practice themselves (EN 1992, 2004; EN 1993, 2004; Martin and Purkiss, 2008). Applying the global approach, the structural engineer can rely on two types of technique: full-blown, albeit time consuming, analyses can be performed using advanced computer modelling, or quick, less accurate, but more descriptive investigations may be carried out that use specialized but simpler models (Howson, 2006) like those presented in this book.

Depending on which direction the situation is looked at from, the global critical load ratio can be defined in two ways. First, it can be defined as

$$\frac{N}{N_{cr}} \tag{6.1}$$

where

$$N = LBQn \tag{6.2}$$

is the total vertical load of the regular multi-storey building with

N_{cr}	global elastic critical load for buildings subjected to uniformly distributed floor load
L, B	plan length and breadth of the building
Q	intensity of the uniformly distributed floor load
n	number of storeys

Practicing structural engineers may prefer the reciprocal definition when the global critical load ratio is the ratio of the global elastic critical load and the total vertical load:

$$= \frac{N_{cr}}{N} \tag{6.3}$$

as it carries a practical meaning that is easy to relate to the safety of the structure.

Somewhat confusingly, codes of practice use both definitions. In this book, from now on, the reciprocal definition [Equation (6.3)] will be used.

When there is significant extra load at top floor level (e.g., a swimming pool), its detrimental effect cannot be ignored. For such cases Equation (6.3) can be amended and the global critical load ratio can be obtained using

$$\frac{1}{} = \frac{N}{N_{cr}} + \frac{F}{F_{cr}} \tag{6.4}$$

where

F is the extra concentrated load at top floor level
F_{cr} is the critical load for the concentrated top load case

The global critical load can be determined carrying out a full-blown second order analysis using a computer program or by approximate analytical solutions e.g., the ones presented in Chapter 5.

The global critical load ratio can be used in different ways. Codes of practice normally concentrate on its use as an indicator whether or not second order analysis is needed. If the condition

$$\geq 10 \tag{6.5}$$

is satisfied, then the suitability of the bracing system is proved and the vertical load bearing elements can be considered as braced (by the bracing system) and neglecting the second-order effects (due to sway and torsion) may result in a maximum 10% error.

If condition (6.5) is not satisfied, the stability of the building may still be acceptable but it must be demonstrated using a second-order analysis. However, there is a warning here: it is widely accepted in practical structural engineering that the absolute minimum for a critical load ratio is four.

Another simple use of the global critical load ratio may be as a global safety factor: the greater the value of the global critical load ratio, the greater the safety of the multi-storey building against buckling.

The global critical load ratio can also be used as a performance indicator. As its value is calculated using the basic (sway and pure torsional) critical loads and taking into account the coupling of the basic modes, any weakness either in the bending/shear and torsional stiffnesses or in the geometrical arrangement of the bracing units (on which the detrimental coupling depends) is picked up automatically. As it happens, any weakness detected during the course of the stability analysis leads to unfavourable behaviour when the fundamental frequency and the maximum deflection of the building are calculated. This is demonstrated below when the structural performance of a building is monitored using the global critical load ratio.

The case study concentrates on a 10-storey building whose detailed global analysis is presented in Section 12.1 and only the main results are summarised here. The plan length of the building is 15 metres and the breadth is 9 metres, resulting in a plan area of 135 m^2 (Figure 6.1).

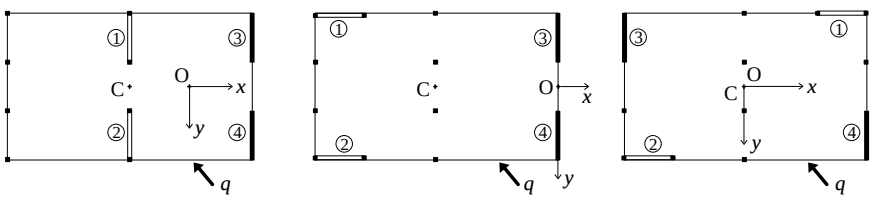

Figure 6.1 Ten-storey building braced by four bracing units. a) Case 1, b) Case 2, c) Case 3.

Four bracing units are available for making the building stable enough: two steel frameworks with cross-bracing and two reinforced concrete shear walls. Their location and orientation inside the layout are arbitrary. Three different arrangements are considered. Three analyses are carried out for each arrangement: for the deflection analysis it is assumed that the building is subjected to a uniformly distributed wind load of intensity q = 17 kN/m, making 50° with axis x. The uniformly distributed floor load for the global stability analysis is Q = 10 kN/m^2. The weight per unit volume for the determination of the fundamental frequency of the building is assumed to be γ = 3 kN/m^3. In the three cases, the following characteristics are determined:

φ_{max}	maximum rotation of the building (in degrees) at top level [°]
d_{max}	maximum deflection of the building (in metres) at top level [m]
d_{max}/d_{ASCE}	ratio of the maximum and recommended deflection
f	fundamental frequency of the building [Hz]
N_{cr}	global critical load of the building [MN]
λ	global critical load ratio of the building

The main results are collected in Table 6.1.

Case 1 is an arrangement that is obviously unacceptable (Figure 6.1/a) and the fact is spectacularly picked up by the global critical load ratio which (being smaller than 1.0) shows the unstable nature of the system. In line with the very small critical load ratio, the calculated maximum deflection is huge, the fundamental frequency and the critical loads are very small. The fatal weakness of the system is the lack of sufficient bracing in direction x. In addition, the torsional resistance of the structure is far from optimum.

Table 6.1 The global critical load ratio as a performance indicator.

	Case 1	Case 2	Case 3
φ_{max} [°]	n/a	1.0	0
d_{max} [m]	5.65	0.313	0.060
$\frac{d_{max}}{d_{ASCE}}$	94	5.2	1.0
f [Hz]	0.039	0.213	0.468
N_{cr} [MN]	1.5	41.6	211.4
λ	0.1	3.1	15.7

By rotating the two frameworks by 90 degrees, the bracing system of Case 2 addresses the main problem with the previous arrangement and provides the building with sufficient bracing in direction x (Figure 6.1/b). The results clearly

show the improvement. The global critical load ratio defines a theoretically stable structure (albeit the margin is not considered sufficient enough in structural engineering practice); the maximum deflection is much smaller and the fundamental frequency and the critical load are much greater. However, as the details in Section 12.1 show, the torsional resistance is relatively small. This is due to the fact that the perpendicular distance of the two shear walls from the shear centre is zero.

By exchanging bracing units 1 and 3 for Case C (without changing their orientation), the shear centre of the system moves to the geometrical centre of the building without changing the value of the lateral stiffness in directions x and y (Figure 6.1/c). The hugely beneficial consequence of the alteration is that all four bracing units can now contribute to the torsional resistance of the system as all four units now "have" perpendicular distance from the shear centre. In addition, as the bracing units are now placed along the sides of the layout ***and*** the farthest from the shear centre, their torsion arms are the longest and their efficiency is the greatest against torsion. The results reflect the beneficial change in the arrangement. The system is not only stable but the global critical load ratio now exceeds the recommended value ($\lambda = 15.7 > 10$). The maximum deflection of the building is much smaller than with the previous arrangement and now it does not exceed the recommended value ($H/500$). The value of the fundamental frequency has also increased.

The results in Table 6.1 (together with the details of the calculations given in Section 12.1) and the results of dozens of other examples show that the global critical load ratio is a reliable and sensitive indicator regarding the overall performance of the structural system. It may be advantageous to determine the value of the global critical load ratio for different arrangements and the arrangement that belongs to the greatest value is normally the best arrangement also when the maximum deflection and the fundamental frequency of the building are calculated. However, the global critical load ratio should not be too big—compared to 10—as it could easily lead to uneconomic structural arrangements.

Part II
Practical application: worked examples

The equations in Part I were derived and presented in the order that the theoretical background demanded. However, for practical structural engineering applications, when the equations have to be applied to real structures, their order can be, and often is, different from the theoretical order. The worked examples here in Part II reflect this fact and show the best order the equations should be used to produce the maximum rotation and deflection, the fundamental frequency and the global critical load of individual bracing units and whole structural systems.

The demonstrative examples are worked out to the smallest details for the sake of completeness. The same calculations in most cases can be considerably simplified and the amount of work can be spectacularly reduced as in structural engineering practice some of the stiffness characteristics are normally neglected as their value is small compared to the dominant ones. These circumstances are mentioned in the theoretical part at the relevant formulae. In addition, once determined, some of the characteristics can be reused repeatedly.

Although the methods and formulae are simple—some easily fall into the back-of-the-envelope category—some may still look too cumbersome for hand calculations. However, there is no need for hand calculations as all the procedures can easily be worked into handy worksheets. The worksheet version of each worked example has been prepared and the files are available for download.

7

Individual bracing units

Five worked examples are given here for the deflection, frequency and stability analyses of individual bracing units. The calculations are based on the material presented in Chapter 2, and the numbers of the equations used will be given on the right-hand side in curly brackets.

7.1 THE MAXIMUM DEFLECTION OF A THIRTY-FOUR STOREY FRAMEWORK

Determine the maximum deflection of framework F6, used for the accuracy analysis in Section 2.1.4 (Figure 2.7/f), using the equations given in Sections 2.1.1 and 2.1.2. The thirty-four storey structure is subjected to a uniformly distributed wind load of intensity $w = 5.0$ kN/m (Figure 7.1). The modulus of elasticity is $E = 25 \cdot 10^6$ kN/m^2. The cross-sections of the columns and beams are 0.4 m/0.4 m and 0.4 m/0.7 m, respectively, where the first number stands for the width (perpendicular to the plane of the structure) and the second number is the depth (in-plane size of the member). The three bays are identical at 6.0 m and the storey height is 3.0 m.

The part of the shear stiffness which is associated with the beams is

$$K_b = \sum_{i=1}^{n-1} \frac{12EI_{b,i}}{l_i h} = 3\frac{12 \cdot 25 \cdot 10^6 \cdot 0.4 \cdot 0.7^3}{12 \cdot 6 \cdot 3} = 571667 \text{ kN} \qquad \{2.28\}$$

The part of the shear stiffness which is associated with the columns is

$$K_c = \sum_{i=1}^{n} \frac{12EI_{c,i}}{h^2} = 4\frac{12 \cdot 25 \cdot 10^6 \cdot 0.4^4}{12 \cdot 3^2} = 284444 \text{ kN} \qquad \{2.29\}$$

The above two parts define reduction factor r as

$$r = \frac{K_c}{K_b + K_c} = \frac{284444}{571667 + 284444} = 0.33225 \qquad \{2.30\}$$

The shear stiffness of the framework can now be determined:

$$K = K_b r = K_b \frac{K_c}{K_b + K_c} = 571667 \cdot 0.33225 = 189936\,\text{kN} \qquad \{2.27\}$$

For the local bending stiffness (EI=$EI_c r$), the sum of the second moments of area of the columns should be produced (and multiplied by reduction factor r). As the bays of the framework are identical, the second moment of area of one column is simply multiplied by n and r (the reduction factor):

$$I = r\sum_{1}^{n} I_{c,i} = 0.33225 \cdot 4 \cdot \frac{0.4^4}{12} = 0.0028352\,\text{m}^4 \qquad \{2.31\}$$

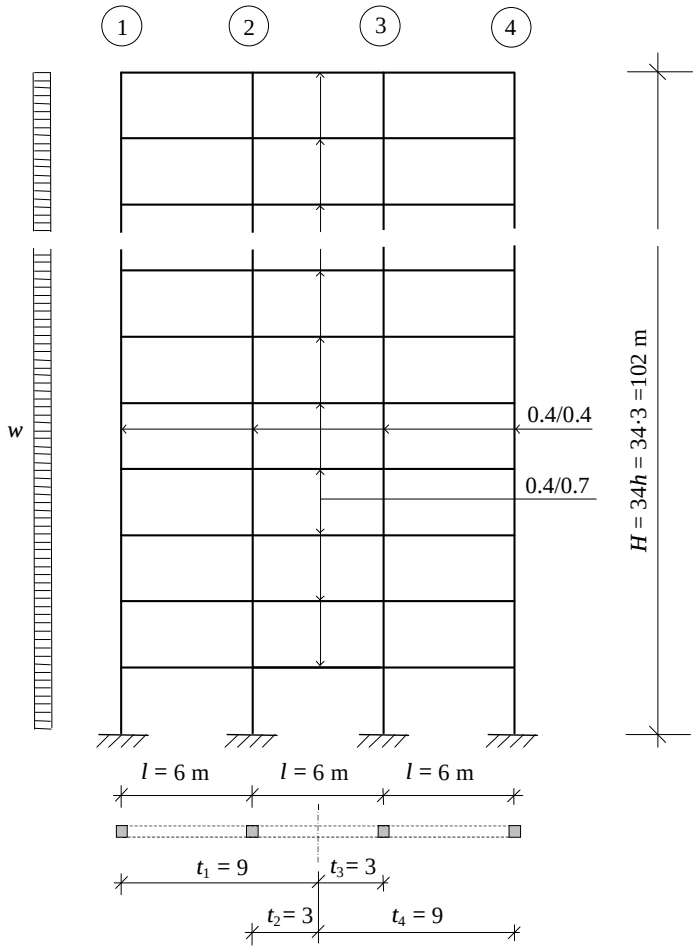

Figure 7.1 Three-bay, thirty-four storey framework F6 for the deflection analysis.

The global second moment of area is

$$I_g = \sum_1^n A_{c,i} t_i^2 = 0.4 \cdot 0.4(9^2 + 3^2 + 3^2 + 9^2) = 28.8\,\text{m}^4 \qquad \{2.32\}$$

The total second moment of area for the bending stiffness is

$$I_f = I + I_g = I_c r + I_g \cong 28.80\,\text{m}^4 \qquad \{2.23\}$$

Parameters s, and H are also needed for the calculation of the maximum deflection:

$$s = 1 + \frac{I_c r}{I_g} = 1 + \frac{0.0028352}{28.8} = 1.000098 \approx 1.0 \qquad \{2.14\}$$

$$= \sqrt{bs} = \sqrt{\frac{K}{EI}} = \sqrt{\frac{189936}{25 \cdot 10^6 \cdot 0.0028352}} = 1.637 \quad \text{and} \quad H=167 \qquad \{2.14\}$$

With the above auxiliary quantities, the maximum top deflection of the framework can now be calculated:

$$y_{\max} = y(H) = \frac{wH^4}{8EI_f} + \frac{wH^2}{2Ks^2} - \frac{wEI}{K^2 s^3}\left(\frac{1 + H\sinh H}{\cosh H} - 1\right) \qquad \{2.24\}$$

$$= \frac{5 \cdot 102^4}{8 \cdot 25 \cdot 10^6 \cdot 28.8} + \frac{5 \cdot 102^2}{2 \cdot 189936} - \frac{5 \cdot 25 \cdot 10^6 \cdot 0.0028352}{189936^2}\left(\frac{1 + 167\sinh 167}{\cosh 167} - 1\right)$$

$$y_{\max} = 0.094 + 0.137 - 0.002 = 0.229\ \text{m}$$

The "exact" (FEM) solution (Axis, 2003) is

$$y_{\max}(\text{FEM}) = 0.238\ \text{m}$$

The continuum solution is conservative and the difference between the continuum and FEM solutions is 3.8%.

As indicated in Section 2.1.3, the effect of interaction tends to be negligible for frameworks over 20 storeys high and indeed, the third term responsible for the interaction is very small compared to the first and second terms (responsible for the bending and shear deflection) and can safely be ignored, leading to a very simple back-of-the-envelope calculation involving the first two terms only.

7.2 THE FUNDAMENTAL FREQUENCY OF A FORTY-STOREY FRAMEWORK

Determine the fundamental frequency of framework F5 used for the accuracy analysis in Section 2.2.3, shown in Figure 7.2, using the equations given in Sections 2.1.2, 2.2.1 and 4.1. The forty-storey structure is subjected to a mass of $m = 0.8495$ kg/m. The modulus of elasticity is $E = 25 \cdot 10^6$ kN/m^2. The cross-sections of the columns and beams are 0.4 m/0.7 m and 0.4 m/0.4 m, respectively, where the first number stands for the width (perpendicular to the plane of the structure) and the second number is the depth (in-plane size of the member). The two bays are identical at 6.0 m and the storey height is 3.0 m.

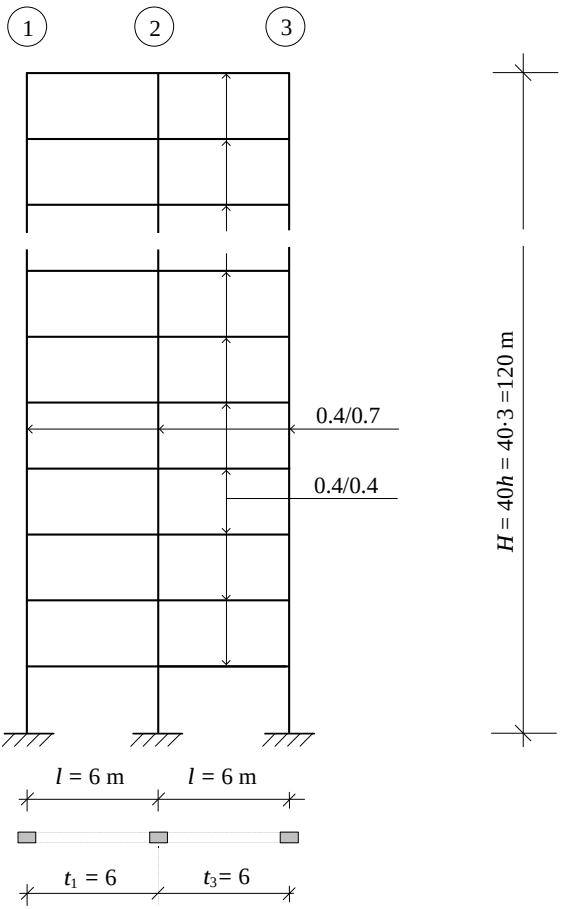

Figure 7.2 Two-bay, forty-storey framework F5 for the frequency analysis.

The part of the shear stiffness which is associated with the beams is

$$K_b = \sum_{i=1}^{n-1} \frac{12EI_{b,i}}{l_i h} = 2\frac{12 \cdot 25 \cdot 10^6 \cdot 0.4^4}{12 \cdot 6 \cdot 3} = 71111\,\text{kN} \qquad \{2.28\}$$

The part of the shear stiffness which is associated with the columns is

$$K_c = \sum_{i=1}^{n} \frac{12EI_{c,i}}{h^2} = 3\frac{12 \cdot 25 \cdot 10^6 \cdot 0.4 \cdot 0.7^3}{12 \cdot 3^2} = 1143333\,\text{kN} \qquad \{2.29\}$$

The above two parts define reduction factor r as

$$r = \frac{K_c}{K_b + K_c} = \frac{1143333}{71111 + 1143333} = 0.9414 \qquad \{2.30\}$$

The "original" shear stiffness of the framework can now be determined:

$$K = K_b r = K_b \frac{K_c}{K_b + K_c} = 71111 \cdot 0.9414 = 66947\ \text{kN} \qquad \{2.27\}$$

With the above shear stiffness, the square of the fundamental frequency of the framework due to shear deformation can be calculated as

$$f_s^2 = \frac{1}{(4H)^2}\frac{r_f^2 K}{m} = \frac{0.9752^2 \cdot 66947}{(4 \cdot 120)^2 \cdot 0.8495} = 0.3253\,\text{Hz}^2 \qquad \{2.41\}$$

where mass distribution factor r_f was obtained using Table 4.1:

$$r_f = \sqrt{\frac{n}{n + 2.06}} = \sqrt{\frac{40}{40 + 2.06}} = 0.9752 \qquad \{\text{Table 4.1}\}$$

The global second moment of area is

$$I_g = \sum_{1}^{n} A_{c,i} t_i^2 = 0.4 \cdot 0.7(6^2 + 6^2) = 20.16\,\text{m}^4 \qquad \{2.32\}$$

The square of the fundamental frequency that belongs to this global second moment of area is

$$f_g^2 = \frac{0.313 r_f^2 EI_g}{H^4 m} = \frac{0.313 \cdot 0.9752^2 \cdot 25 \cdot 10^6 \cdot 20.16}{120^4 \cdot 0.8495} = 0.8517\,\text{Hz}^2 \qquad \{2.42\}$$

The effectiveness factor shows the extent the global bending deformation erodes the shear stiffness:

$$s_f = \sqrt{\frac{f_g^2}{f_s^2 + f_g^2}} = \sqrt{\frac{0.8517}{0.3253 + 0.8517}} = \sqrt{0.7236} = 0.8507 \qquad \{2.45\}$$

With the effectiveness factor, the effective shear stiffness is

$$K_e = s_f^2 K = 0.7236 \cdot 66947 = 48443\,\text{kN} \qquad \{2.44\}$$

The square of the fundamental frequency that belongs to the effective shear stiffness can now be calculated:

$$f_s^2 = \frac{1}{(4H)^2}\frac{r_f^2 K_e}{m} = \frac{1}{(4 \cdot 120)^2}\frac{0.9752^2 \cdot 48443}{0.8495} = 0.2354\,\text{Hz}^2 \qquad \{2.43\}$$

For the local bending stiffness (EI=$EI_c r$), the sum of the second moments of area of the columns should be produced (and multiplied by reduction factor r). As the bays of the framework are identical, the second moment of area of one column is simply multiplied by n and r (the reduction factor):

$$I = r\sum_{1}^{n} I_{c,i} = 0.9414 \cdot 3 \cdot \frac{0.4 \cdot 0.7^3}{12} = 0.0323\,\text{m}^4 \qquad \{2.31\}$$

The fundamental frequency which is associated with the local bending stiffness is defined by

$$f_b^2 = \frac{0.313 r_f^2 EI}{H^4 m} = \frac{0.313 \cdot 0.9752^2 \cdot 25 \cdot 10^6 \cdot 0.0323}{120^4 \cdot 0.8495} = 0.00136\,\text{Hz}^2 \qquad \{2.46\}$$

As a function of the non-dimensional parameter

$$k = H\sqrt{\frac{K_e}{EI}} = 120\sqrt{\frac{48443}{25 \cdot 10^6 \cdot 0.0323}} = 29.39 \qquad \{2.48\}$$

the frequency parameter is obtained using Table 4.2 as

$$= 5.278 + \frac{7.769 - 5.278}{30.0 - 20.0}(k - 20.0) = 7.617 \qquad \{\text{Table 4.2}\}$$

Finally, the fundamental frequency is

$$f = \sqrt{f_b^2 + f_s^2 + \left(\frac{^2}{0.313} - \frac{k^2}{5} - 1\right) s_f\, f_b^2} \qquad \{2.50\}$$

$$= \sqrt{0.00136 + 0.2354 + \left(\frac{7.617^2}{0.313} - \frac{29.39^2}{5} - 1\right) 0.8507 \cdot 0.00136} = 0.500 \text{ Hz}$$

The "exact" (FEM) solution (Axis, 2003) is

$$f\,(\text{FEM}) = 0.503\,\text{Hz}$$

The difference between the continuum and FEM solutions is 0.6%.

7.3 THE CRITICAL LOAD OF A SEVEN-BAY, TWELVE-STOREY FRAMEWORK

Determine the critical load of the large framework FFSH1 shown in Figure 7.3, using the equations given in Sections 2.3.1 and 5.1. The seven-bay, twelve-storey structure is subjected to uniformly distributed load on the beams. The modulus of elasticity is $E = 29{\cdot}10^6$ kN/m^2. The cross-sections of the columns and beams are 0.4 m/0.4 m and 0.4 m/0.5 m, respectively, where the first number stands for the width (perpendicular to the plane of the structure) and the second number is the depth (in-plane size of the member). The seven bays are identical at 6.0 m and the storey height is 2.9 m.

The shear stiffness of a framework is composed using two parts. The first part is associated with the beams of the framework:

$$K_b = \sum_{i=1}^{n-1} \frac{12EI_{b,i}}{l_i h} = 7\frac{12 \cdot 29 \cdot 10^6 \cdot 0.4 \cdot 0.5^3}{12 \cdot 6 \cdot 2.9} = 583333\,\text{kN} \qquad \{2.52\}$$

The second part of the shear stiffness is associated with the columns:

$$K_c = \sum_{i=1}^{n} \frac{^2 EI_{c,i}}{h^2} = 8\frac{^2 \cdot 29 \cdot 10^6 \cdot 0.4^4}{12 \cdot 2.9^2} = 580832\ \text{kN} \qquad \{2.53\}$$

With the two components, the shear stiffness is

$$K = K_b r = K_b \frac{K_c}{K_b + K_c} = 583333\frac{580832}{583333 + 580832} = 291040\,\text{kN} \qquad \{2.54\}$$

where the reduction factor r is

$$r = \frac{K_c}{K_b + K_c} = \frac{580832}{583333 + 580832} = 0.499 \qquad \{2.55\}$$

The global second moment of area is

$$I_g = \sum_1^n A_{c,i} t_i^2 = 0.4 \cdot 0.4(21^2 + 15^2 + 9^2 + 3^2)2 = 241.92\ \mathrm{m}^4 \qquad \{2.56\}$$

The local second moment of area of the framework, amended by r, making use of the fact that the eight columns have the same cross-section, is

$$I = r \sum_1^n I_{c,i} = 0.499 \cdot 8 \frac{0.4^4}{12} = 0.008516\ \mathrm{m}^4 \qquad \{2.57\}$$

Load distribution factor r_s is obtained from Table 5.1 as $r_s = 0.883$.

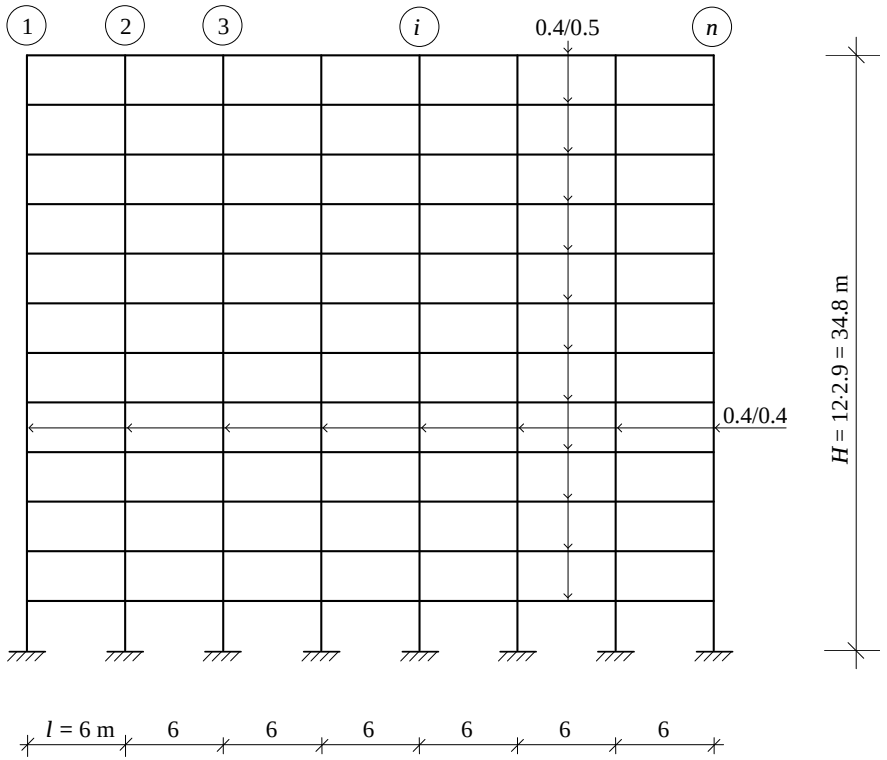

Figure 7.3 Seven-bay, twelve-storey framework FFSH1 for the stability analysis.

Parameter c_1 is needed for the calculation of the critical load. Its value is obtained from Table 2.3 as a function of

$$\frac{I}{I+I_g}=\frac{0.008516}{0.008516+241.92}=0.0000352 \qquad \{2.59\}$$

and

$$\frac{KH^2}{E(I+I_g)r_s}=\frac{291040\cdot 34.8^2}{29\cdot 10^6\cdot 241.9285\cdot 0.883}=0.0569 \qquad \{2.60\}$$

With the relevant values from Table 2.3

	0.000	0.001
0.05	0.050	0.099
0.10	0.100	0.171

parameter c_1 is obtained either as an "intelligent guess", $c_1 = 0.057$, for example, based on {2.60}, or after three interpolations

1: $$0.050+\frac{0.099-0.050}{0.001}0.0000352=0.0517248$$

2: $$0.100+\frac{0.171-0.100}{0.001}0.0000352=0.1024992$$

3: $$c_1=0.0517248+\frac{0.1024992-0.0517248}{0.10-0.05}(0.0569-0.05)=0.05873$$

The critical load of the framework can now be calculated:

$$N_{cr}=c_1\frac{E(I+I_g)r_s}{H^2}=0.05873\frac{29\cdot 10^3\cdot 241.9285\cdot 0.883}{34.8^2}=300.4 \text{ MN} \qquad \{2.58\}$$

The "exact" (FEM) solution (Axis, 2003) is

$$N_{cr}(\text{FEM})=300.0 \text{ MN}$$

The difference between the continuum and FEM solutions is negligible.

It is mentioned in Section 2.3.1 that when the local second moment of area of the columns/shear wall sections is small compared to the global second moment of area, then an even simpler method, presented in Section 2.4.1, can be used for the determination of the critical load. This is the case now, as ratio {2.59} above is

very small, so the method in Section 2.4.1 can safely be used.

The global bending part critical load is

$$N_g = \frac{7.837 E I_g r_s}{H^2} = \frac{7.837 \cdot 29 \cdot 10^3 \cdot 241.92 \cdot 0.883}{34.8^2} = 40089 \text{ MN} \qquad \{2.63\}$$

As a function of the shear critical load and the global bending critical load

$$_s = \frac{K}{N_g} = \frac{291.04}{40089} = 0.007 \qquad \{2.62\}$$

the critical load parameter is obtained from Table 2.5 as

$$_s = 1.0 \qquad \{\text{Table 2.5}\}$$

and the critical load is

$$N_{cr} = \ _sK = 1.0 \cdot 291 = 291 \text{ MN} \qquad \{2.61\}$$

The difference between the continuum and FEM solutions now is 3%.

7.4 THE CRITICAL LOAD OF AN EIGHT-STOREY FRAMEWORK WITH CROSS-BRACING

Determine the critical load of framework SR-X shown in Figure 7.4. The one-bay, eight-storey structure is subjected to uniformly distributed load on the beams. The modulus of elasticity for the beams, columns and cross-bracing is $E = 200 \cdot 10^6$ kN/m^2. The framework represents a bracing unit of the Cardington Steel Building which was constructed in 1993 at the Building Research Establishment's Large Building Test Facility in Cardington (Armer and Moore, 1994) and its geometrical characteristics are given in Table 7.1. The size of the bay and the storey height are both 3.0 m.

The critical load can be determined by using the methods presented in Section 2.3.1 and Section 2.4.1. The procedure given in Section 2.4.1 will be used here.

The shear stiffness of the structure is

$$K = \left(\frac{d^3}{A_d E_d h l^2} + \frac{l}{A_h E_h h} \right)^{-1} = \qquad \{\text{Table 2.6}\}$$

$$= \left(\frac{4.243^3}{3.75 \cdot 10^{-3} \cdot 2 \cdot 10^8 \cdot 3 \cdot 3^2} + \frac{3}{5.73 \cdot 10^{-3} \cdot 2 \cdot 10^8 \cdot 3} \right)^{-1} = 215295 \text{ kN}$$

The global second moment of area is

$$I_g = \sum_{1}^{n} A_{c,i} t_i^2 = 1.74 \cdot 10^{-2} \cdot 1.5^2 \cdot 2 = 0.0783\,\text{m}^4 \qquad \{2.32\}$$

Table 7.1 Cross-sectional characteristics for framework SR-X.

Characteristics	Columns	Beams	Diagonals
Cross-section	305×305UC137	356×171×45UB	250/15
Area [m^2]	$1.74 \cdot 10^{-2}$	$5.73 \cdot 10^{-3}$	$3.75 \cdot 10^{-3}$
Second moment of area [m^4]	$3.281 \cdot 10^{-4}$	$1.207 \cdot 10^{-4}$	$1.953 \cdot 10^{-5}$

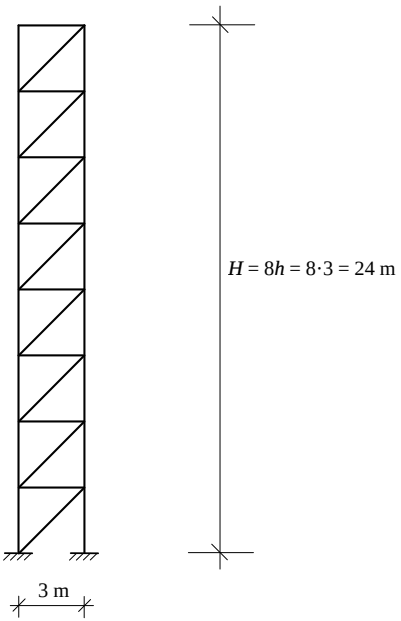

Figure 7.4 Eight-storey framework SR-X with cross-bracing.

Load distribution factor r_s is obtained from Table 5.1 as $r_s = 0.834$. The global bending critical load is

$$N_g = \frac{7.837 r_s E I_g}{H^2} = \frac{7.837 \cdot 0.834 \cdot 2 \cdot 10^8 \cdot 0.0783}{24^2} = 177699\ \text{kN} \qquad \{2.63\}$$

As a function of

$$_s = \frac{K}{N_g} = \frac{215295}{177699} = 1.21 \qquad \{2.62\}$$

the critical load parameter is obtained from Table 2.5 as

$$_s = 0.5838 - \frac{0.5838 - 0.5526}{1.3 - 1.2}(\ _s - 1.2) = 0.581 \qquad \{\text{Table 2.5}\}$$

Finally, the critical load of the framework is

$$N_{cr} = \ _sK = 0.581 \cdot 215.295 = 125.1\,\text{MN} \qquad \{2.61\}$$

The "exact" (FEM) solution (Axis, 2003) is

$$N_{cr}(\text{FEM}) = 126.9\ \text{MN}$$

The continuum solution is conservative and the difference between the continuum and FEM solutions is 1.4%.

7.5 THE CRITICAL LOAD OF EIGHTEEN-STOREY COUPLED SHEAR WALLS

Determine the critical load of coupled shear walls CSWSH3 shown in Figure 7.5, using the equations given in Sections 2.3.1, 2.4 and 2.5. The structure is eighteen-storey high and consists of three shear walls that are connected by beams at every floor level. The story height is h = 3.0 m and the total height of the structure is H = 54.0 m. The wall thickness is t = 0.20 m and the cross-section of the beams is 0.2 m/1.5 m. The cross-sectional area and the second moment area of the beams are A_b = 0.3 m^2 and I_b = 0.05625 m^4, respectively. The modulus of elasticity of the structure is E = 30000 MN/m^2. The modulus of elasticity in shear is G = 12500 MN/m^2.

Taking into consideration that the two sets of beams are of identical characteristics, the part of the shear stiffness of the coupled shear walls that is associated with the beams is

$$K_b^* = \frac{6EI_b\left((l_1^* + s_1)^2 + (l_1^* + s_2)^2\right)}{l_1^{*3}h\left(1 + 12\dfrac{EI_b}{l_1^{*2}GA_b}\right)}(n-1) = \qquad \{2.71\} \text{ and } \{2.69\}$$

$$= \frac{6 \cdot 3 \cdot 10^4 \cdot 0.05625\left((2+2)^2 + (2+3)^2\right)}{2^3 \cdot 3\left(1 + 12\dfrac{1.2 \cdot 3 \cdot 10^4 \cdot 0.05625}{2^2 \cdot 1.25 \cdot 10^4 \cdot 0.3}\right)}2 = 13204\,\text{MN}$$

The part of shear stiffness that depends on the wall sections is

$$K_c = \sum_{i=1}^{n} \frac{^2EI_{c,i}}{h^2} = \frac{^2 \cdot 3 \cdot 10^4 (2 \cdot 2^3 + 3^3) 0.2}{12 \cdot 3^2} = 23577 \text{ MN} \qquad \{2.53\}$$

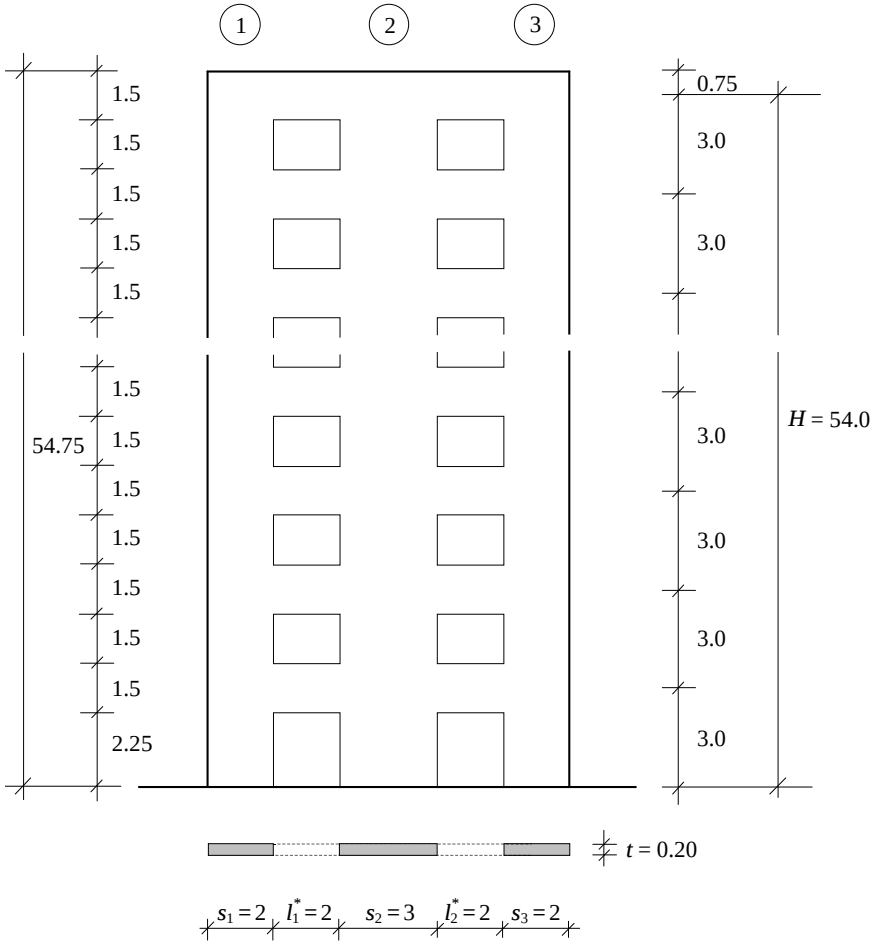

Figure 7.5 Eighteen-storey coupled shear walls CSWSH3.

With the two components, the shear stiffness is

$$K = K_b r = K_b \frac{K_c}{K_b + K_c} = 13204 \frac{23577}{13204 + 23577} = 8464 \text{ MN} \qquad \{2.54\}$$

where the reduction factor r is

$$r = \frac{K_c}{K_b + K_c} = \frac{23577}{13204 + 23577} = 0.641 \qquad \{2.55\}$$

The global second moment of area is

$$I_g = \sum_1^n A_{c,i} t_i^2 = 0.2 \cdot 2.0 \cdot 4.5^2 \cdot 2 = 16.2 \text{ m}^4 \qquad \{2.56\}$$

The local second moment of area of the coupled shear walls, amended by r, is

$$I = r \sum_1^n I_{c,i} = 0.641 \frac{0.2(2^3 \cdot 2 + 3^3)}{12} = 0.4594 \text{ m}^4 \qquad \{2.57\}$$

Load distribution factor r_s is obtained from Table 5.1 as $r_s = 0.919$.

Parameter c_1 is needed for the calculation of the critical load. Its value is obtained from Table 2.3 as a function of

$$\frac{I}{I + I_g} = \frac{0.4594}{0.4594 + 16.2} = 0.02758 \qquad \{2.59\}$$

and

$$\frac{KH^2}{E(I + I_g) r_s} = \frac{8464 \cdot 54^2}{3 \cdot 10^4 (16.2 + 0.4594) 0.919} = 53.74 \qquad \{2.60\}$$

With the relevant values from Table 2.3

	0.01	0.05
50	7.298	7.344
100	7.560	7.583

parameter c_1 is obtained either as an "intelligent guess", based on the four "surrounding" values above as $c_1 = 7.3$, for example, or after three interpolations as

1: $$7.298 + \frac{7.344 - 7.298}{0.05 - 0.01}(0.02758 - 0.01) = 7.318$$

2: $$7.56 + \frac{7.583 - 7.56}{0.05 - 0.01}(0.02758 - 0.01) = 7.570$$

3: $$c_1 = 7.318 + \frac{7.57 - 7.318}{100 - 50}(53.74 - 50.0) = 7.337$$

The critical load of the coupled shear walls can now be calculated:

$$N_{cr} = c_1 \frac{E(I + I_g)r_s}{H^2} = 7.337 \frac{3 \cdot 10^4 \cdot 16.6594 \cdot 0.919}{54^2} = 1156 \text{ MN} \qquad \{2.58\}$$

The "exact" (FEM) solution (Axis, 2003) is:

$$N_{cr} = 1207 \text{ MN}$$

The continuum solution is conservative and the difference between the continuum and FEM solutions is 4.2%.

It is mentioned in Section 2.3.1 that when the local second moment of area of the columns/shear wall sections is small compared to the global second moment of area, then an even simpler method, presented in Section 2.4.1, can be used for the determination of the critical load. This is the case now, as ratio {2.59} above is very small, so the method in Section 2.4.1 can safely be used.

The global bending part critical load is

$$N_g = \frac{7.837 E I_g r_s}{H^2} = \frac{7.837 \cdot 3 \cdot 10^4 \cdot 16.62 \cdot 0.919}{54^2} = 1200.4 \text{ MN} \qquad \{2.63\}$$

As a function of the shear critical load and the global bending critical load

$$_s = \frac{K}{N_g} = \frac{8464}{1200.4} = 7.05 \qquad \{2.62\}$$

the critical load parameter is obtained from Table 2.5

$$_s = 0.1253 + \frac{0.1337 - 0.1253}{7.5 - 7.0}(7.5 - 7.05) = 0.1329 \qquad \{\text{Table 2.5}\}$$

and the critical load of the structure emerges as

$$N_{cr} = \ _s K = 0.1329 \cdot 8464 = 1125 \text{ MN} \qquad \{2.61\}$$

The difference between the continuum and FEM solutions is now 6.8%.

8

The maximum rotation and deflection of buildings under horizontal load

Two worked examples are given here for the calculation of the maximum deflection and rotation of buildings under horizontal load, braced by frameworks, shear walls and cores. The calculations are based on the material presented in Chapters 2 and 3, and the numbers of the equations used will be given on the right-hand side in curly brackets.

8.1 THE MAXIMUM DEFLECTION OF A SIXTEEN-STOREY SYMMETRIC CROSS-WALL SYSTEM BUILDING

Calculate the top deflection of the sixteen-storey building whose layout is shown in Figure 8.1, subjected to a uniformly distributed lateral load of intensity $w^* = 1.3333$ kN/m^2 in direction y. The building is braced by two two-bay concrete frameworks (F5), two two-bay steel frameworks with cross-bracing (F11) and two concrete shear walls (W3) in direction y. The same bracing units were used in Chapter 2 for the accuracy analysis of single bracing units (Figure 2.7). The storey height is $h = 3$ m. The "exact" (FEM) computer analysis resulted in $y_{max} = 56.3$ mm and this result is to be checked. The stiffness of the four shear walls lying in direction x is so small in direction y that—in line with structural engineering practice—their contribution is ignored.

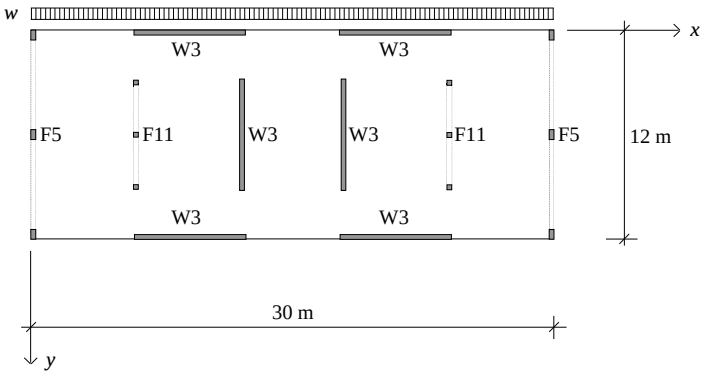

Figure 8.1 Layout of symmetric building for the deflection analysis.

In making use of symmetry, it is enough to consider half of the structure. The horizontal load on half of the structure is

$$w = 1.3333 \cdot 15 = 20 \text{ kN/m}$$

Because of the symmetric arrangement, the rotation of the building is zero.

The bracing system for half of the structure consists of framework F11, framework F5 and shear wall W3 (Figure 8.2). The calculation consists of two parts: first, the three individual bracing units will be considered, based on the relevant sections in Sections 2.1 and 2.6, then, having identified the base unit, the top deflection of the building will be determined using the equations given in Section 3.1.

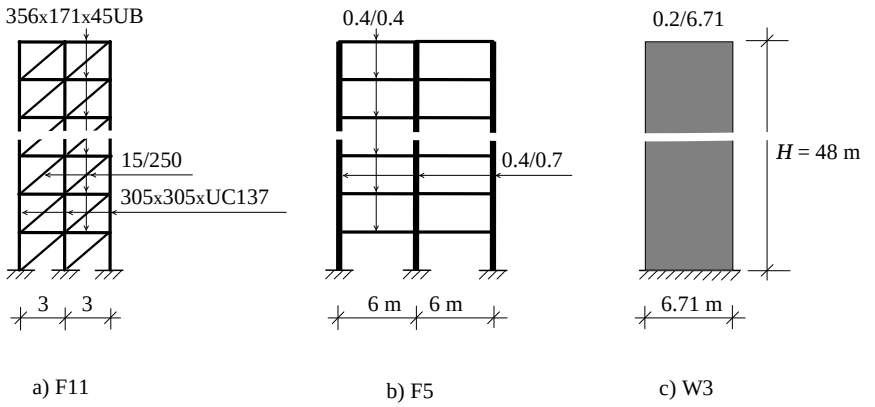

Figure 8.2 Bracing units for the sixteen-storey building.

8.1.1 Individual bracing units

The stiffness characteristics of the three different bracing units are determined first.

Bracing Unit 1: F11

The modulus of elasticity for the two-bay steel framework with cross-bracing is $E = 2 \cdot 10^8$ kN/m^2. General data for the columns, beams and diagonals are given in Figure 8.2/a and in Table 8.1.

The shear stiffness of the structure is

$$K = (n-1)\left(\frac{d^3}{A_d E_d h l^2} + \frac{l}{A_h E_h h}\right)^{-1} = \qquad \{\text{Table 2.6}\} \ \& \ \{2.69\}$$

$$= 2\left(\frac{4.243^3}{0.00375 \cdot 2 \cdot 10^8 \cdot 3 \cdot 3^2} + \frac{3}{0.00573 \cdot 2 \cdot 10^8 \cdot 3} \right)^{-1} = 430590 \text{ kN}$$

Table 8.1 Cross-sectional characteristics for framework F11.

Characteristics	Columns	Beams	Diagonals
Cross-section	305×305UC137	356×171×45UB	15/250
Area [m^2]	0.0174	0.00573	0.00375
Second moment of area [m^4]	0.0003281	0.0001207	0.00001953

The global second moment of area is

$$I_g = \sum_1^n A_{c,i} t_i^2 = 0.0174 \cdot 3^2 \cdot 2 = 0.3132 \text{ m}^4 \qquad \{2.32\}$$

The local second moment of area (with $r = 1$, because of the cross-bracing) is

$$I = r \sum_1^n I_{c,i} = 0.0003281 \cdot 3 = 0.0009843 \text{ m}^4 \qquad \{2.31\}$$

The total second moment of area for the bending stiffness is

$$I_f = I + I_g = 0.3132 + 0.0009843 = 0.3142 \text{ m}^4 \qquad \{2.23\}$$

Auxiliary parameters a, b, s, and H are also needed for the calculation of the deflection:

$$a = \frac{K}{EI_g} = \frac{430590}{2 \cdot 10^8 \cdot 0.3132} = 0.00687, \qquad b = \frac{K}{EI} = \frac{430590}{2 \cdot 10^8 \cdot 0.0009843} = 2.1873$$

$$s = 1 + \frac{I}{I_g} = 1 + \frac{0.0009843}{0.3132} = 1.00314 \cong 1.0 \qquad \{2.14\}$$

$$= \sqrt{a+b} = \sqrt{0.00687 + 2.1873} = 1.4813 \qquad \text{and} \qquad H = 71.1$$

With the above auxiliary quantities, the maximum top deflection of the framework can now be calculated:

$$y_{\max} = y(H) = \frac{wH^4}{8EI_f} + \frac{wH^2}{2Ks^2} - \frac{wEI}{K^2 s^3}\left(\frac{1 + H\sinh H}{\cosh H} - 1\right) \qquad \{2.24\}$$

$$= \frac{20 \cdot 48^4}{8 \cdot 2 \cdot 10^8 \cdot 0.3142} + \frac{20 \cdot 48^2}{2 \cdot 430590} - \frac{20 \cdot 2 \cdot 10^8 \cdot 0.0009843}{430590^2}\left(\frac{1 + 71.1\sinh 71.1}{\cosh 71.1} - 1\right)$$

$$y_{\max} = 0.2112 + 0.0535 - 0.0015 = 0.263\,\text{m}$$

The stiffness of Bracing Unit 1 is:

$$S_1 = \frac{1}{y_{\max}} = \frac{1}{0.263} = 3.80\,\frac{1}{\text{m}} \qquad \{3.2\}$$

Bracing Unit 2: F5

The modulus of elasticity for the two-bay concrete framework is $E = 25 \cdot 10^6$ kN/m^2. General data for the columns and beams are given in Figure 8.2/b.

The part of the shear stiffness which is associated with the beams is

$$K_b = \sum_{i=1}^{n-1} \frac{12EI_{b,i}}{l_i h} = 2\frac{12 \cdot 25 \cdot 10^6 \cdot 0.4^4}{12 \cdot 6 \cdot 3} = 71111\,\text{kN} \qquad \{2.28\}$$

The part of the shear stiffness which is associated with the columns is

$$K_c = \sum_{i=1}^{n} \frac{12EI_{c,i}}{h^2} = 3\frac{12 \cdot 25 \cdot 10^6 \cdot 0.4 \cdot 0.7^3}{12 \cdot 3^2} = 1143333\,\text{kN} \qquad \{2.29\}$$

The above two parts define reduction factor r as

$$r = \frac{K_c}{K_b + K_c} = \frac{1143333}{71111 + 1143333} = 0.9414 \qquad \{2.30\}$$

The shear stiffness of the framework can now be determined:

$$K = K_b \frac{K_c}{K_b + K_c} = 71111\frac{1143333}{71111 + 1143333} = 66947\,\text{kN} \qquad \{2.27\}$$

For the local bending stiffness (EI=$EI_c r$), the sum of the second moments of area of the columns should be produced (and multiplied by reduction factor r). As the bays of the framework are identical, the second moment of area of one column is simply multiplied by n and r (the reduction factor):

$$I = r\sum_{1}^{n} I_{c,i} = 0.9414 \cdot 3 \cdot \frac{0.4 \cdot 0.7^3}{12} = 0.03229\ \mathrm{m}^4 \qquad \{2.31\}$$

The global second moment of area is

$$I_g = \sum_{1}^{n} A_{c,i} t_i^2 = 0.4 \cdot 0.7 \cdot 6^2 \cdot 2 = 20.16\,\mathrm{m}^4 \qquad \{2.32\}$$

The total second moment of area for the bending stiffness is

$$I_f = I + I_g = I_c r + I_g = 0.03229 + 20.16 = 20.1923\,\mathrm{m}^4 \qquad \{2.23\}$$

Auxiliary parameters *a*, *b*, *s*, and *H* are also needed for the calculation of the deflection:

$$a = \frac{K}{EI_g} = \frac{66947}{25 \cdot 10^6 \cdot 20.16} = 0.0001328\,, \quad b = \frac{K}{EI} = \frac{66947}{25 \cdot 10^6 \cdot 0.03229} = 0.0829$$

$$s = 1 + \frac{I}{I_g} = 1 + \frac{0.03229}{20.16} = 1.0016 \cong 1.0 \qquad \{2.14\}$$

$$= \sqrt{a+b} = \sqrt{0.0001328 + 0.0829} = 0.2882 \qquad \text{and} \qquad H\text{=}13.83$$

With the above auxiliary quantities, the maximum top deflection of the framework can now be calculated:

$$y_{\max} = y(H) = \frac{wH^4}{8EI_f} + \frac{wH^2}{2Ks^2} - \frac{wEI}{K^2 s^3}\left(\frac{1 + H\sinh H}{\cosh H} - 1\right) \qquad \{2.24\}$$

$$= \frac{20 \cdot 48^4}{8 \cdot 25 \cdot 10^6 \cdot 20.1923} + \frac{20 \cdot 48^2}{2 \cdot 66947} - \frac{20 \cdot 25 \cdot 10^6 \cdot 0.03229}{66947^2}\left(\frac{1 + 13.83\sinh 13.83}{\cosh 13.83} - 1\right)$$

$$y_{\max} = 0.0263 + 0.3441 - 0.0462 = 0.3242\,\mathrm{m}$$

The stiffness of Bracing Unit 2 is:

$$S_2 = \frac{1}{y_{\max}} = \frac{1}{0.3242} = 3.09\,\frac{1}{\mathrm{m}} \qquad \{3.2\}$$

Bracing Unit 3: W3

The modulus of elasticity for the concrete shear wall is $E = 25{\cdot}10^6$ kN/m^2. Its geometrical characteristics are given in Figure 8.2/c. The maximum deflection of the shear wall is

$$y_{\max} = y(H) = \frac{wH^4}{8EI} = \frac{20 \cdot 48^4}{8 \cdot 25 \cdot 10^6 \dfrac{0.2 \cdot 6.71^3}{12}} = 0.1054 \text{ m} \qquad \{2.72\}$$

Its stiffness is

$$S_3 = \frac{1}{y_{\max}} = \frac{1}{0.1054} = 9.485 \frac{1}{\text{m}} \qquad \{3.2\}$$

8.1.2 Base unit. Maximum deflection

As the shear wall cannot be a base unit and the *b*-value of framework F11 is greater then the *b*-value of framework F5 (2.1873 > 0.0829), the base unit is framework F11 with $EI = EI_1$, $EI_g = EI_{g,1}$ and $K = K_1$.

The apportioner for the base unit is

$$q_1 = \frac{S_1}{S_1 + S_2 + S_3} = \frac{3.8}{3.8 + 3.09 + 9.485} = 0.232 \qquad \{3.3\}$$

The load on the base unit is

$$w_1 = q_1 w = 0.232 \cdot 20 = 4.64 \text{ kN/m} \qquad \{3.1\}$$

The following stiffness ratios and coefficients are needed:

$$a_1 = \frac{EI_2}{EI_1} = \frac{25{\cdot}10^6 \cdot 0.03229}{2{\cdot}10^8 \cdot 0.0009843} = 4.1, \qquad b_1 = \frac{K_2}{K_1} = \frac{66947}{430590} = 0.1555$$

$$c_1 = \frac{EI_{g,2}}{EI_{g,1}} = \frac{25{\cdot}10^6 \cdot 20.16}{2{\cdot}10^8 \cdot 0.3132} = 8.046 \qquad \{3.16\}$$

$$\bar{a} = \frac{K}{EI_g} \frac{1 + \sum_{j=1}^{f-1} \dfrac{a_j}{c_j}}{1 + \sum_{j=1}^{f-1} \dfrac{a_j}{b_j}} = \frac{430590}{2{\cdot}10^8 \cdot 0.3132} \frac{1 + \dfrac{4.1}{8.046}}{1 + \dfrac{4.1}{0.1555}} = 0.000379$$

$$\bar{b} = \frac{K}{EI}\frac{f}{1+\sum_{j=1}^{f-1}\frac{a_j}{b_j}} = \frac{430590}{2\cdot 10^8 \cdot 0.0009843}\frac{2}{1+\frac{4.1}{0.1555}} = 0.1599$$

$$\bar{s} = 1+\frac{\bar{a}}{\bar{b}} = 1+\frac{0.000379}{0.1599} = 1.0024 \cong 1.0$$

$$\bar{\ } = \sqrt{\bar{a}+\bar{b}} = \sqrt{0.000379+0.1599} = 0.40\,, \qquad H = 0.40\cdot 48 = 19.22 \qquad \{3.13\}$$

The maximum deflection of the building at H = 48 m can now be determined:

$$y_{\max} = y(H) = \frac{\bar{w}H^4}{8EI_f} + \frac{\bar{w}H^2}{2K\bar{s}^2} - \frac{\bar{w}EI}{K^2\bar{s}^3}\left(\frac{1+\bar{\ }H\sinh\bar{\ }H}{\cosh\bar{\ }H}-1\right) \qquad \{3.14\}$$

$$= \frac{4.64\cdot 48^4}{8\cdot 2\cdot 10^8\cdot 0.3142} + \frac{4.64\cdot 48^2}{2\cdot 430590} - \frac{4.64\cdot 2\cdot 10^8\cdot 0.0009843}{430590^2}\left(\frac{1+19.22\sinh 19.22}{\cosh 19.22}-1\right)$$

$$y_{\max} = 0.049+0.012-0.000 = 0.061\text{ m} = 61\text{ mm}$$

The continuum solution is conservative. The difference between the continuum and FEM solutions is 8.3%.

8.2 THE MAXIMUM DEFLECTION OF A TWENTY-EIGHT STOREY ASYMMETRIC BUILDING BRACED BY FRAMEWORKS, SHEAR WALLS AND A CORE

Calculate the top rotation and deflection of the twenty-eight storey building whose layout is shown in Figure 8.3, subjected to a uniformly distributed lateral load of intensity w^* = 1.0 kN/m^2 in direction y. The size of the layout is given by L = 24 m and B = 12 m. The building is braced by two one-bay frameworks (F1), one two-bay framework (F5), two shear walls (W4) and a U-core (U). The modulus of elasticity of the concrete bracing units is $25\cdot 10^6$ kN/m^2. The storey height is h = 3 m. The FE computer analysis resulted in $y_{\max}$ = 404 mm and this result is to be checked. The bracing units are numbered as shown in Figure 8.3. General data for the bracing units are given in Figure 8.4.

Following the establishment of the stiffnesses of the units, the maximum deflection of the building is calculated in two parts. The deflection of the shear centre axis is determined first, then the additional deflection due to the rotation around the shear centre is added.

8.2.1 Individual bracing units

The stiffness characteristics of the four different bracing units are determined first.

Bracing Unit 1 (identical to Bracing Unit 6): F1

Both the width and the depth of both the beams and the columns are 0.4 m/0.4 m (Figure 8.4/a).

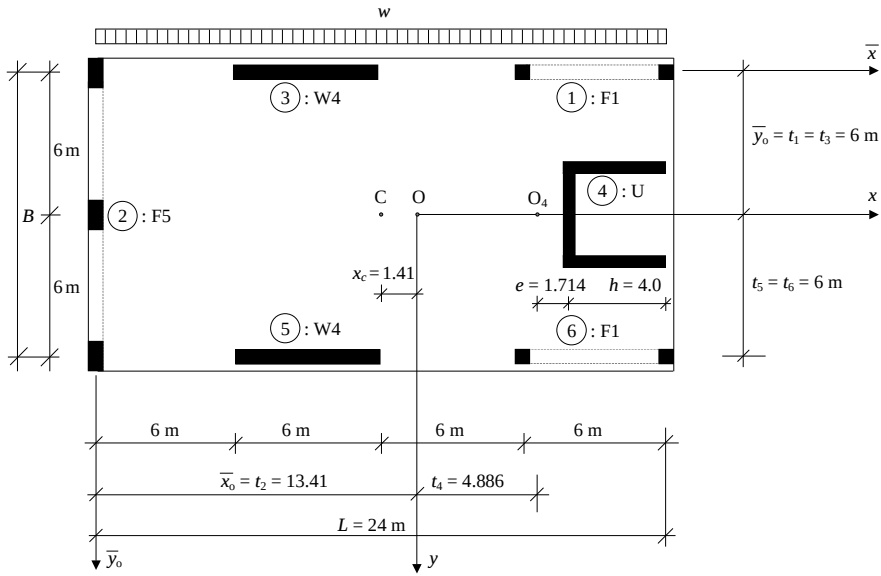

Figure 8.3 Layout for the deflection analysis.

The part of the shear stiffness which is associated with the beams is

$$K_b = \sum_{i=1}^{n-1} \frac{12EI_{b,i}}{l_i h} = 1\frac{12 \cdot 25 \cdot 10^6 \cdot 0.4^4}{12 \cdot 6 \cdot 3} = 35556 \text{ kN} \qquad \{2.28\}$$

The part of the shear stiffness which is associated with the columns is

$$K_c = \sum_{i=1}^{n} \frac{12EI_{c,i}}{h^2} = 2\frac{12 \cdot 25 \cdot 10^6 \cdot 0.4^4}{12 \cdot 3^2} = 142222 \text{ kN} \qquad \{2.29\}$$

The above two parts define reduction factor r as

$$r = \frac{K_c}{K_b + K_c} = \frac{142222}{35556 + 142222} = 0.8 \qquad \{2.30\}$$

The shear stiffness of the framework can now be determined:

$$K = K_b \frac{K_c}{K_b + K_c} = 35556 \cdot 0.8 = 28445\,\text{kN} \qquad \{2.27\}$$

For the local bending stiffness (EI=$EI_c r$), the sum of the second moments of area of the columns should be produced (and multiplied by reduction factor r):

$$I = r\sum_{1}^{n} I_{c,i} = 0.8 \cdot 2 \cdot \frac{0.4^4}{12} = 0.00341333\,\text{m}^4 \qquad \{2.31\}$$

The global second moment of area is

$$I_g = \sum_{1}^{n} A_{c,i} t_i^2 = 0.4 \cdot 0.4 \cdot 3^2 \cdot 2 = 2.88\,\text{m}^4 \qquad \{2.32\}$$

The total second moment of area for the bending stiffness is

$$I_f = I + I_g = 0.00341333 + 2.88 = 2.8834\,\text{m}^4 \qquad \{2.23\}$$

Auxiliary parameters a, b, s, and H are also needed for the calculation of the deflection:

$$a = \frac{K}{EI_g} = \frac{28445}{25 \cdot 10^6 \cdot 2.88} = 0.000395\,,\ b = \frac{K}{EI} = \frac{28445}{25 \cdot 10^6 \cdot 0.00341333} = 0.33334$$

$$s = 1 + \frac{I}{I_g} = 1 + \frac{0.00341333}{2.88} = 1.0012 \cong 1.0$$

$$= \sqrt{a + b} = \sqrt{0.000395 + 0.33334} = 0.5777 \qquad \text{and} \qquad H = 48.53 \qquad \{2.14\}$$

With the above auxiliary quantities, the maximum top deflection of framework F1 can now be calculated:

$$y_{\max} = y(H) = \frac{wH^4}{8EI_f} + \frac{wH^2}{2Ks^2} - \frac{wEI}{K^2 s^3}\left(\frac{1 + H\sinh H}{\cosh H} - 1\right) = \qquad \{2.24\}$$

$$= \frac{24 \cdot 84^4}{8 \cdot 25 \cdot 10^6 \cdot 2.8834} + \frac{24 \cdot 84^2}{2 \cdot 28445} - \frac{24 \cdot 25 \cdot 10^6 \cdot 0.003413}{28445^2}\left(\frac{1 + 48.53 \sinh 48.53}{\cosh 48.53} - 1\right)$$

$$y_{\max} = 2.072 + 2.977 - 0.120 = 4.929 \text{ m}$$

The stiffness of Bracing Unit 1 (and Bracing Unit 6) is:

$$S_1 = S_6 = \frac{1}{y_{\max}} = \frac{1}{4.929} = 0.2029 \frac{1}{\text{m}} \qquad \{3.2\}$$

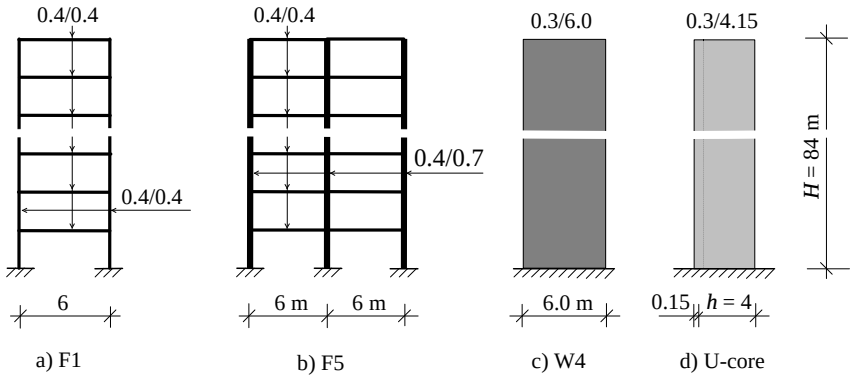

Figure 8.4 Bracing units for the twenty-eight storey building.

Bracing Unit 2: F5

The width and the depth of the beams and the columns are 0.4 m/0.4 m and 0.4 m/0.7 m (Figure 8.4/b).

The part of the shear stiffness which is associated with the beams is

$$K_b = \sum_{i=1}^{n-1} \frac{12EI_{b,i}}{l_i h} = 2\frac{12 \cdot 25 \cdot 10^6 \cdot 0.4^4}{12 \cdot 6 \cdot 3} = 71111 \text{ kN} \qquad \{2.28\}$$

The part of the shear stiffness which is associated with the columns is

$$K_c = \sum_{i=1}^{n} \frac{12EI_{c,i}}{h^2} = 3\frac{12 \cdot 25 \cdot 10^6 \cdot 0.4 \cdot 0.7^3}{12 \cdot 3^2} = 1143333 \text{ kN} \qquad \{2.29\}$$

The above two parts define reduction factor r as

$$r = \frac{K_c}{K_b + K_c} = \frac{1143333}{71111 + 1143333} = 0.9414 \qquad \{2.30\}$$

The shear stiffness of the framework can now be determined:

$$K = K_b \frac{K_c}{K_b + K_c} = 71111 \frac{1143333}{71111 + 1143333} = 66947\,\text{kN} \qquad \{2.27\}$$

For the local bending stiffness ($EI = EI_c r$), the sum of the second moments of area of the columns should be produced (and multiplied by reduction factor r). As the bays of the framework are identical, the second moment of area of one column is simply multiplied by n and r (the reduction factor):

$$I = r \sum_{1}^{n} I_{c,i} = 0.9414 \cdot 3 \cdot \frac{0.4 \cdot 0.7^3}{12} = 0.03229\ \text{m}^4 \qquad \{2.31\}$$

The global second moment of area is

$$I_g = \sum_{1}^{n} A_{c,i} t_i^2 = 0.4 \cdot 0.7 \cdot 6^2 \cdot 2 = 20.16\,\text{m}^4 \qquad \{2.32\}$$

The total second moment of area for the bending stiffness is

$$I_f = I + I_g = I_c r + I_g = 0.03229 + 20.16 = 20.1923\,\text{m}^4 \qquad \{2.23\}$$

Auxiliary parameters a, b, s, and H are also needed for the calculation of the deflection:

$$a = \frac{K}{EI_g} = \frac{66947}{25 \cdot 10^6 \cdot 20.16} = 0.0001328\,, \quad b = \frac{K}{EI} = \frac{66947}{25 \cdot 10^6 \cdot 0.03229} = 0.0829$$

$$s = 1 + \frac{I}{I_g} = 1 + \frac{0.03229}{20.16} = 1.0016 \cong 1.0$$

$$= \sqrt{a + b} = \sqrt{0.0001328 + 0.0829} = 0.2882 \qquad \text{and} \qquad H = 24.21 \qquad \{2.14\}$$

With the above auxiliary quantities, the maximum top deflection of the framework can now be calculated:

$$y_{\max} = y(H) = \frac{wH^4}{8EI_f} + \frac{wH^2}{2Ks^2} - \frac{wEI}{K^2 s^3}\left(\frac{1 + H \sinh H}{\cosh H} - 1\right) = \qquad \{2.24\}$$

$$= \frac{24 \cdot 84^4}{8 \cdot 25 \cdot 10^6 \cdot 20.1923} + \frac{24 \cdot 84^2}{2 \cdot 66947} - \frac{24 \cdot 25 \cdot 10^6 \cdot 0.03229}{66947^2}\left(\frac{1 + 24.21 \sinh 24.21}{\cosh 24.21} - 1\right)$$

$$y_{\max} = 0.2959 + 1.2648 - 0.1003 = 1.460 \text{ m}$$

The stiffness of Bracing Unit 2 is:

$$S_2 = \frac{1}{y_{\max}} = \frac{1}{1.46} = 0.6849 \frac{1}{\text{m}} \qquad \{3.2\}$$

Bracing Unit 3 (identical to Bracing Unit 5): W4

The thickness and the width of the shear wall are 0.3 m and 6.0 m (Figure 8.4/c). The maximum deflection of the shear wall is

$$y_{\max} = y(H) = \frac{wH^4}{8EI} = \frac{24 \cdot 84^4}{8 \cdot 25 \cdot 10^6 \frac{0.3 \cdot 6^3}{12}} = 1.106 \text{ m} \qquad \{2.72\}$$

Its stiffness is

$$S_3 = \frac{1}{y_{\max}} = \frac{1}{1.106} = 0.904 \frac{1}{\text{m}} \qquad \{3.2\}$$

Bracing Unit 4: U-core

The dimensions for the core are: $b = 4.0$ m, $h = 4.0$ m and $t_f = t_w = 0.3$ m (Figure 8.4/d). Its stiffness characteristics are calculated using Table 2.7:

The torsional constant:

$$J = \frac{1}{3}(2ht_f^3 + bt_w^3) = \frac{0.3^3}{3}(2 \cdot 4.0 + 4.0) = 0.108 \text{ m}^4 \qquad \{\text{Table 2.7}\}$$

The warping constant:

$$I_\Omega = \frac{t_f h^3 b^2}{12} \frac{3t_f h + 2t_w b}{6t_f h + t_w b} = \frac{0.3 \cdot 4^3 \cdot 4^2}{12} \frac{3 \cdot 4 + 2 \cdot 4}{6 \cdot 4 + 4} = 18.29 \text{ m}^6 \qquad \{\text{Table 2.7}\}$$

Location of shear centre:

$$e = \frac{3t_f h^2}{6t_f h + t_w b} = \frac{3 \cdot 4^2}{6 \cdot 4 + 4} = 1.714 \text{ m} \qquad \{\text{Table 2.7}\}$$

Second moment of area with respect to local axis *x*:

$$I_x = \frac{4.15 \cdot 4.3^3}{12} - \frac{3.85 \cdot 3.7^3}{12} = 11.245\ \text{m}^4$$

The maximum deflection of the core in direction *y* is

$$y_{\max} = y(H) = \frac{wH^4}{8EI_x} = \frac{24 \cdot 84^4}{8 \cdot 25 \cdot 10^6 \cdot 11.245} = 0.531\ \text{m} \qquad \{2.76\}$$

Its stiffness is

$$S_4 = \frac{1}{y_{\max}} = \frac{1}{0.531} = 1.883\,\frac{1}{\text{m}} \qquad \{3.2\}$$

The total horizontal load in direction *y* is transferred to the shear centre in the form of a force and a torque. The force results in the uniform translation v_o of the building while the torque develops rotation around the shear centre, which then causes additional translations v_φ as shown in Figure 8.5. The uniform translation is determined first.

8.2.2 Deflection of the shear centre axis

To balance the horizontal load in direction *y*, Bracing Unit 2 (F5) and Bracing Unit 4 (U) offer resistance. The contribution of the other four units, being effective in the perpendicular direction, is negligible and is ignored. In using the relevant stiffnesses calculated above, the location of the shear centre (Figure 8.3) from the left-hand side of the layout is

$$\bar{x}_o = \frac{\sum_1^{f+m} S_i \bar{x}_i}{\sum_1^{f+m} S_i} = \frac{S_4(L - h_4 - e)}{S_2 + S_4} = \frac{1.883(24.0 - 4.0 - 1.714)}{0.6849 + 1.883} = 13.41\ \text{m} \qquad \{3.17\}$$

where h_4 is the size of the flange of the U-core.

Because of symmetry, the location of the shear centre in the vertical direction is known without any calculation as

$$\bar{y}_o = 6.0\ \text{m} \qquad \{3.17\}$$

Of the two participating bracing units, Unit 2 (F5) is the base unit (as the U-core cannot be a base unit).

The apportioner for the base unit is

$$q_2 = \frac{S_2}{S_2 + S_4} = \frac{0.6849}{0.6849 + 1.883} = 0.2667 \qquad \{3.3\}$$

and the load on the base unit is

$$w_2 = wq_2 = 0.2667 \cdot 24 = 6.40 \text{ kN/m} \qquad \{3.1\}$$

Auxiliary parameters a, b, s, and H are needed for the calculation of the deflection:

$$\bar{a} = \frac{K}{EI_g} = \frac{66947}{25 \cdot 10^6 \cdot 20.16} = 0.0001328 \qquad \{3.16\}$$

$$\bar{b} = \frac{K}{EI} f = \frac{66947}{25 \cdot 10^6 \cdot 0.03229} 1 = 0.083$$

$$\bar{s} = 1 + \frac{\bar{a}}{\bar{b}} = 1 + \frac{0.0001328}{0.083} = 1.0016 \cong 1.0 \qquad \{3.13\}$$

$$\bar{} = \sqrt{\bar{a} + \bar{b}} = \sqrt{0.0001328 + 0.083} = 0.288 \quad \text{and} \quad H=24.22 \qquad \{3.13\}$$

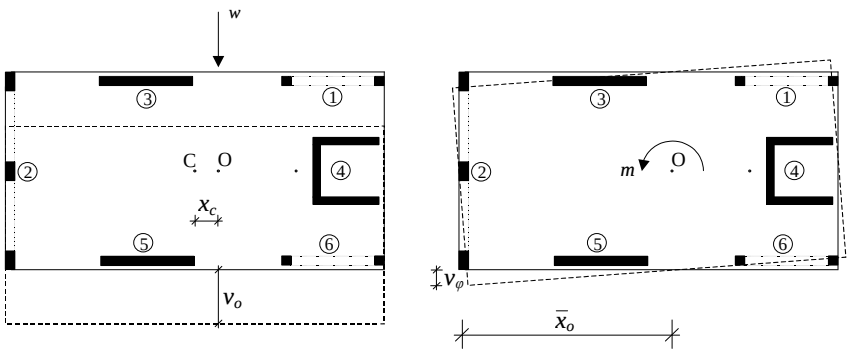

a) uniform translation b) rotation around the shear centre

Figure 8.5 Deflection of building. a) uniform part, b) due to rotation around the shear centre.

With the above auxiliary quantities, the maximum top deflection of the shear centre axis can now be calculated (Figure 8.5/a):

$$v_o = y(H) = \frac{\bar{w}H^4}{8EI_f} + \frac{\bar{w}H^2}{2K\bar{s}^2} - \frac{\bar{w}EI}{K^2\bar{s}^3}\left(\frac{1+\bar{}H\sinh\bar{}H}{\cosh\bar{}H} - 1\right) \qquad \{3.14\}$$

$$= \frac{6.4\cdot 84^4}{8\cdot 25\cdot 10^6\cdot 20.1923} + \frac{6.4\cdot 84^2}{2\cdot 66947} - \frac{6.4\cdot 25\cdot 10^6\cdot 0.03229}{66947^2}\left(\frac{1+24.22\sinh 24.22}{\cosh 24.22} - 1\right)$$

$$v_o = 0.079 + 0.337 - 0.027 = 0.389 \text{ m}$$

8.2.3 Rotation around the shear centre. Maximum deflection

Rotation around the shear centre causes additional translations and the left-hand corner of the building will develop the greatest deflection. The distance between the shear centre and the centroid of the layout (Figure 8.3) is

$$x_c = \bar{x}_o - \frac{L}{2} = 13.41 - \frac{24.0}{2} = 1.41\,\text{m}$$

and the torsional moment per unit length therefore is

$$m_t = wx_c = 24\cdot 1.41 = 33.84\,\frac{\text{kNm}}{\text{m}} \qquad \{3.29\}$$

All six bracing units (F1+F5+W4+U+W5+F1) take part in resisting torsion and to determine the rotation of the building, the perpendicular distances of the bracing units from the shear centre are needed. In the coordinate system whose origin is in the shear centre and whose axes are parallel with the sides of the building (Figure 8.3), these are:

$$t_1 = \bar{y}_o = 6.0\,\text{m} \qquad t_2 = \bar{x}_o = 13.41\,\text{m} \qquad t_3 = \bar{y}_o = 6.0\,\text{m}$$

$$t_4 = L - \bar{x}_o - h_4 - e = 4.876\,\text{m} \qquad t_5 = B - \bar{y}_o = 6.0\,\text{m} \qquad t_6 = B - \bar{y}_o = 6.0\,\text{m}$$

Of the frameworks, potential base units, Unit 1 (F1) is the base unit (as its *b*-value is greater than that of Unit 2: 0.33 > 0.08).

The rotational stiffnesses are needed to establish the moment share on the base unit:

$$S_{\Omega 1} = t_1^2 S_1 = 6^2\cdot 0.2029 = 7.304\,\text{m}\,,\quad S_{\Omega 2} = t_2^2 S_2 = 13.41^2\cdot 0.6849 = 123.2\,\text{m} \quad \{3.25\}$$

$$S_{\Omega 3} = t_3^2 S_3 = 6^2\cdot 0.904 = 32.54\,\text{m}\,,\quad S_{\Omega 4} = t_4^2 S_4 = 4.876^2\cdot 1.883 = 44.77\,\text{m} \quad \{3.25\}$$

$$S_{\Omega 5} = t_5^2 S_5 = 6^2 \cdot 0.904 = 32.54\,\text{m}\,, \quad S_{\Omega 6} = t_6^2 S_6 = 6^2 \cdot 0.2029 = 7.304\,\text{m} \qquad \{3.25\}$$

The torsional apportioner related to the base unit (F1) is

$$q_\Omega = \frac{S_\Omega}{\sum_{i=1}^{f+m} S_{\Omega,i}} = \frac{7.304}{7.304 + 123.2 + 32.54 + 44.77 + 32.54 + 7.304} = 0.0295 \qquad \{3.26\}$$

and, with the apportioner, the torsional moment share on the base unit is

$$\overline{m} = m_t q_\Omega = 33.84 \cdot 0.0295 = 0.998\,\frac{\text{kNm}}{\text{m}} \qquad \{3.28\}$$

The torsional stiffness characteristics of the base unit are:

$$EI_\Omega = EIt^2 = 25 \cdot 10^6 \cdot 0.00341333 \cdot 6^2 = 3.072 \cdot 10^6\,\text{kNm}^4 \qquad \{3.19\}$$

$$EI_{g\Omega} = EI_g t^2 = 25 \cdot 10^6 \cdot 2.88 \cdot 6^2 = 2592 \cdot 10^6\,\text{kNm}^4 \qquad \{3.20\}$$

$$E(I_\Omega + I_{g\Omega}) = (3.072 + 2592)10^6 = 2595 \cdot 10^6\,\text{kNm}^4$$

$$(GJ) = Kt^2 = 28445 \cdot 6^2 = 1.024 \cdot 10^6\,\text{kNm}^2 \qquad \{3.21\}$$

The following stiffness ratios and coefficients are needed:

$$a_1 = \frac{EI_2}{EI_1} = \frac{0.03229}{0.00341333} = 9.46\,, \qquad b_1 = \frac{K_2}{K_1} = \frac{66947}{28445} = 2.353$$

$$c_1 = \frac{EI_{g,2}}{EI_{g,1}} = \frac{20.16}{2.88} = 7.0\,, \qquad a_2 = \frac{EI_3}{EI_1} = \frac{0.00341333}{0.00341333} = 1.0 \qquad \{3.16\}$$

$$b_2 = \frac{K_3}{K_1} = \frac{28445}{28445} = 1.0\,, \qquad c_2 = \frac{EI_{g,3}}{EI_{g,1}} = \frac{2.88}{2.88} = 1.0$$

$$\overline{a} = \frac{K}{EI_g} \frac{1 + \sum_{j=1}^{f-1} \frac{a_j}{c_j}}{1 + \sum_{j=1}^{f-1} \frac{a_j}{b_j}} = \frac{28445}{25 \cdot 10^6 \cdot 2.88} \frac{1 + \frac{9.46}{7.0} + 1}{1 + \frac{9.46}{2.353} + 1} = 0.00022$$

$$\bar{b} = \frac{K}{EI}\frac{f}{1+\sum_{j=1}^{f-1}\frac{a_j}{b_j}} = \frac{28445}{25\cdot 10^6 \cdot 0.00341333}\frac{3}{1+\frac{9.46}{2.353}+1} = 0.1661$$

$$\bar{s} = 1+\frac{\bar{a}}{\bar{b}} = 1+\frac{0.00022}{0.1661} = 1.0013 \cong 1.0$$

$$\bar{} = \sqrt{\bar{a}+\bar{b}} = \sqrt{0.00022+0.1661} = 0.408\,, \qquad \bar{H} = 0.408\cdot 84 = 34.26 \quad \{3.13\}$$

The maximum rotation of the building at H = 84 m can now be determined:

$$_{\max} = \quad (H) = \frac{\bar{m}H^4}{8E(I_{\Omega}+I_{g\Omega})} + \frac{\bar{m}H^2}{2(GJ)\bar{s}^2} - \frac{\bar{m}EI_{\Omega}}{(GJ)^2\bar{s}^3}\left(\frac{1+\bar{H}\sinh\bar{H}}{\cosh\bar{H}}-1\right) \{3.24\}$$

$$= \frac{0.998\cdot 84^4}{8\cdot 2595\cdot 10^6} + \frac{0.998\cdot 84^2}{2\cdot 1.024\cdot 10^6} - \frac{0.998\cdot 3.072\cdot 10^6}{(1.024\cdot 10^6)^2}\left(\frac{1+34.26\sinh 34.26}{\cosh 34.26}-1\right)$$

$$= 0.00239+0.00344-0.00010 = 0.00573 \text{ rad}$$

This rotation causes additional deflection, in proportion to the distance from the shear centre. Maximum deflection develops at the left-hand side of the building (Figure 8.5/b), where this deflection is added to the uniform deflection, resulting in the overall maximum deflection of the building as

$$v_{\max} = v_o + v \quad = v_o + \quad \bar{x}_o = 0.389 + 0.00573\cdot 13.41 = 0.466 \text{ m}$$

The continuum solution for the maximum deflection of the building is conservative. The difference between continuum and FEM solutions is 15.3%.

9

The fundamental frequency of buildings

Two worked examples are presented in this chapter for the calculation of the fundamental frequency of buildings under uniformly distributed mass over the floors, braced by frameworks and shear walls. The calculations are based on the material presented in Chapter 4, and the numbers of the equations used will be given on the right-hand side in curly brackets.

9.1 THIRTY-STOREY DOUBLY SYMMETRIC BUILDING BRACED BY SHEAR WALLS AND FRAMEWORKS

Calculate the fundamental frequency of the thirty-storey reinforced concrete building (Figure 9.1) subjected to uniformly distributed mass over the floors. The modulus of elasticity is $E = 25000$ MN/m^2, the modulus of elasticity in shear is $G = 10400$ MN/m^2, the storey height is $h = 3$ m and the total height of the building is $H = 90$ m. The thickness of the shear walls is 0.35 m. The weight per unit volume of the building is assumed to be $\gamma = 2.5$ kN/m^3.

Before the whole system of four frameworks and four shear walls is investigated, it is advantageous to establish the basic characteristics of the two types of bracing unit.

9.1.1 Individual bracing units

Bracing Unit 1 (framework, identical to Bracing Units 2, 5 and 6 – Figure 9.2/a)

The cross-sections of the columns and beams of the four identical frameworks are 0.35/0.35 and 0.35/0.50 (metres), respectively.

The shear stiffness that is associated with the beams of the framework is

$$K_{b,1} = \sum_{j=1}^{n-1} \frac{12 E_b I_{b,j}}{l_j h} = 2 \frac{12 \cdot 25 \cdot 10^6 \cdot 0.35 \cdot 0.50^3}{12 \cdot 5 \cdot 3} = 145833 \text{ kN} \qquad \{4.2\}$$

The shear stiffness that is associated with the columns of the framework is

$$K_{c,1} = \sum_{j=1}^{n} \frac{12 E_c I_{c,j}}{h^2} = 3 \frac{12 \cdot 25 \cdot 10^6 \cdot 0.35^4}{12 \cdot 3^2} = 125052 \text{ kN} \qquad \{4.3\}$$

The combination of the two part shear stiffnesses gives the "original" shear stiffness of the framework:

$$K_1 = K_{b,1}\frac{K_{c,1}}{K_{b,1}+K_{c,1}} = 145833\frac{125052}{145833+125052} = 67323\,\text{kN} \qquad \{4.1\}$$

where the reduction factor

$$r_1 = \frac{K_{c,1}}{K_{b,1}+K_{c,1}} = \frac{125052}{145833+125052} = 0.4616 \qquad \{4.4\}$$

is introduced.

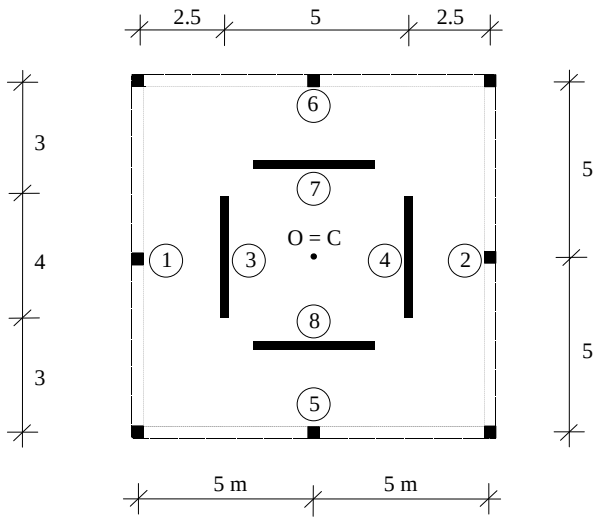

Figure 9.1 Layout of thirty-storey building for the frequency analysis.

Mass distribution factor r_f is obtained from Table 4.1 as a function of the number of storeys:

$$r_f = 0.967 \qquad \{\text{Table 4.1}\}$$

The mass density per unit length is calculated using Equation (4.7):

$$m = \frac{A}{g}LB = \frac{2.5}{9.81}10\cdot 10 = 25.48\,\text{kg/m} \qquad \{4.7\}$$

The square of the fundamental frequency associated with the "original" shear stiffness of Bracing Unit 1 is

$$f_{s',1}^2 = \frac{1}{(4H)^2}\frac{r_f^2 K_1}{m} = \frac{0.967^2 \cdot 67323}{(4 \cdot 90)^2 \cdot 25.48} = 0.01906\ \text{Hz}^2 \qquad \{4.6\}$$

The global second moment of area of the cross-sections of the columns is:

$$I_{g,1} = \sum_{j=1}^{n} A_{c,j} t_j^2 = 0.35 \cdot 0.35 \cdot 5^2 \cdot 2 = 6.125\ \text{m}^4 \qquad \{4.9\}$$

The square of the fundamental frequency that is associated with the global full-height bending vibration of the framework is

$$f_{g,1}^2 = \frac{0.313 r_f^2 E_c I_{g,1}}{H^4 m} = \frac{0.313 \cdot 0.967^2 \cdot 25 \cdot 10^6 \cdot 6.125}{90^4 \cdot 25.48} = 0.0268\ \text{Hz}^2 \qquad \{4.8\}$$

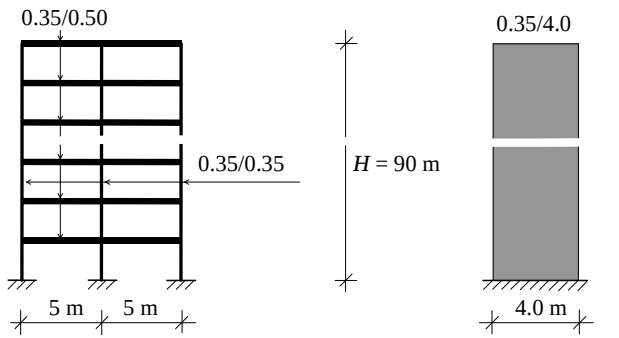

Figure 9.2 Bracing units for the building.

There is an interaction between the "original" shear and global bending modes that reduces the effectiveness of the shear stiffness. The factor of effectiveness can be calculated using the squares of the two relevant frequencies as

$$s_{f,1}^2 = \frac{f_{g,1}^2}{f_{g,1}^2 + f_{s',1}^2} = \frac{0.0268}{0.0268 + 0.01906} = 0.5844 \qquad \{4.10\}$$

Bracing Unit 3 (shear wall, identical to Bracing Units 4, 7 and 8 – Figure 9.2/b)

The size of the shear wall is 4.0 metres with a thickness of 0.35 m. It only has bending stiffness which will directly be incorporated into the lateral model.

9.1.2 Lateral vibration in direction *y* (Bracing Units 1, 2, 3 and 4)

Because of double symmetry, the behaviour (and the fundamental frequency of lateral vibration) of the building is identical in directions *x* and *y*.

The effective shear stiffness for the whole system (that contains two frameworks) is obtained as

$$K_e = \sum_1^f s_{f,i}^2 K_i = 0.5844 \cdot 67323 \cdot 2 = 78687 \text{ kN} \qquad \{4.11\}$$

The "original" shear stiffness:

$$K = \sum_{i=1}^f K_i = 67323 \cdot 2 = 134646 \text{ kN} \qquad \{4.5\}$$

The effectiveness factor for the lateral system can now be established:

$$s_f = \sqrt{\frac{K_e}{K}} = \sqrt{\frac{78687}{134646}} = 0.7644 \qquad \{4.12\}$$

The square of the frequency that belongs to the effective shear stiffness is:

$$f_s^2 = \frac{1}{(4H)^2} \frac{r_f^2 K_e}{m} = \frac{0.967^2 \cdot 78687}{(4 \cdot 90)^2 \cdot 25.48} = 0.02228 \text{ Hz}^2 \qquad \{4.13\}$$

The bending stiffness for the system (Bracing Units 1, 2, 3 and 4) is:

$$EI = E_c I_c + E_w I_w = E_c \sum_1^f I_{c,i} r_i + E_w \sum_1^m I_{w,k} = \qquad \{4.14\}$$

$$= 25 \cdot 10^6 \left(\frac{0.35^4}{12} 0.4616 + \frac{0.35 \cdot 4.0^3}{12} \right) 2 = 93362195 \text{ kNm}^2$$

The square of the lateral frequency that is associated with this bending stiffness is

$$f_b^2 = \frac{0.313 r_f^2 EI}{H^4 m} = \frac{0.313 \cdot 0.967^2 \cdot 93362195}{90^4 \cdot 25.48} = 0.01635\,\text{Hz}^2 \qquad \{4.15\}$$

With the non-dimensional parameter

$$k = H\sqrt{\frac{K_e}{EI}} = 90\sqrt{\frac{78687}{93362195}} = 2.613 \qquad \{4.17\}$$

the frequency parameter is obtained from Table 4.2 as

$$= 0.9809 + \frac{1.1014 - 0.9809}{0.50}(k - 2.50) = 1.0081 \qquad \{\text{Table 4.2}\}$$

The lateral frequency of the system can now be calculated:

$$f_x = f_y = \sqrt{f_b^2 + f_s^2 + \left(\frac{^2}{0.313} - \frac{k^2}{5} - 1\right) s_f\, f_b^2} = \qquad \{4.18\}$$

$$= \sqrt{0.01635 + 0.02228 + \left(\frac{1.0081^2}{0.313} - \frac{2.613^2}{5} - 1\right) 0.7644 \cdot 0.01635} = 0.223\,\text{Hz}$$

9.1.3 Pure torsional vibration (with all bracing units participating)

The calculation is made fairly simple by the fact that the system is doubly symmetric and the location of the shear centre and the location of the bracing units in relation to the shear centre are readily known.

The radius of gyration is

$$i_p = \sqrt{\frac{L^2 + B^2}{12} + t^2} = \sqrt{\frac{10^2 + 10^2}{12}} = \sqrt{16.67} = 4.08\,\text{m} \qquad \{4.20\}$$

The "original" Saint-Venant torsional stiffness is

$$(GJ) = \sum_1^m GJ_k + \sum_1^f \left((K_i)_x y_i^2 + (K_i)_y x_i^2\right)$$

$$= 4 \cdot \frac{1}{3} 0.35^3 \cdot 4.0 \cdot 10.4 \cdot 10^6 + 4 \cdot 67323 \cdot 5^2 = 9110433\,\text{kNm}^2 \qquad \{4.27\}$$

The effective shear stiffness is

$$(GJ)_e = \sum_1^m GJ_k + \sum_1^f \left((K_{e,i})_x y_i^2 + (K_{e,i})_y x_i^2 \right)$$

$$= 4 \cdot \frac{1}{3} 0.35^3 \cdot 4.0 \cdot 10.4 \cdot 10^6 + 4 \cdot 0.5844 \cdot 67323 \cdot 5^2 = 6312489 \text{ kNm}^2 \quad \{4.21\}$$

The effectiveness factor is the ratio of the effective and "original" shear stiffnesses:

$$s = \sqrt{\frac{(GJ)_e}{(GJ)}} = \sqrt{\frac{6312489}{9110433}} = 0.8324 \quad \{4.26\}$$

The warping stiffness of the system originates from the bending stiffness of the four shear walls and the bending stiffness of the columns of the four frameworks (with the own warping stiffness of the bracing units being zero):

$$EI_\Omega = E_w \sum_1^m \left(I_{\Omega,k} + (I_{w,k})_x y_k^2 + (I_{w,k})_y x_k^2 \right) + E_c \sum_1^f \left((I_{c,i} r_i)_x y_i^2 + (I_{c,i} r_i)_y x_i^2 \right)$$

$$= 25 \cdot 10^6 \left(\frac{0.35 \cdot 4^3}{12} 4 \cdot 2.5^2 + \frac{0.35^4}{12} 0.4616 \cdot 4 \cdot 5^2 \right) = 1168109768 \text{ kNm}^4 \quad \{4.22\}$$

The square of the pure torsional frequency associated with the warping stiffness is

$$f_\Omega^2 = \frac{0.313 r_f^2 EI_\Omega}{i_p^2 H^4 m} = \frac{0.313 \cdot 0.967^2 \cdot 1168 \cdot 10^6}{16.67 \cdot 90^4 \cdot 25.48} = 0.01227 \text{ Hz}^2 \quad \{4.24\}$$

and the formula for the pure torsional frequency associated with the Saint-Venant stiffness is

$$f_t^2 = \frac{r_f^2 (GJ)_e}{16 i_p^2 H^2 m} = \frac{0.967^2 \cdot 6.31 \cdot 10^6}{16 \cdot 16.67 \cdot 90^2 \cdot 25.48} = 0.1072 \text{ Hz}^2 \quad \{4.25\}$$

With the non-dimensional parameter

$$k = H \sqrt{\frac{(GJ)_e}{EI_\Omega}} = 90 \sqrt{\frac{6.31 \cdot 10^6}{1168 \cdot 10^6}} = 6.615 \quad \{4.28\}$$

the torsional frequency parameter is obtained using Table 4.2 as

$$= 1.949 + \frac{2.07 - 1.949}{7.0 - 6.5}(6.615 - 6.5) = 1.977 \qquad \{\text{Table 4.2}\}$$

The pure torsional frequency can now be determined:

$$f = \sqrt{f_\Omega^2 + f_t^2 + \left(\frac{^2}{0.313} - \frac{k^2}{5} - 1\right) s \; f_\Omega^2} \qquad \{4.23\}$$

$$= \sqrt{0.01227 + 0.1072 + \left(\frac{1.977^2}{0.313} - \frac{6.615^2}{5} - 1\right) 0.8324 \cdot 0.01227} = 0.384 \text{ Hz}$$

Because of the doubly symmetric arrangement of the bracing system, there is no coupling among the two lateral and pure torsional modes and the fundamental frequency of the building is the smallest one of the three "basic" frequencies:

$$f = \text{Min } f_x, f_y, f \; = 0.223 \text{ Hz} \qquad \{4.38\}$$

9.2 SIX-STOREY ASYMMETRIC BUILDING BRACED BY SHEAR WALLS AND INFILLED FRAMEWORKS

Calculate the fundamental frequency of the six-storey building whose layout is shown in Figure 9.3, subjected to uniformly distributed mass over the floors. The building is braced by two reinforced concrete shear walls and two infilled frameworks. The thickness of both the reinforced concrete elements and the masonry infill is 0.3 m. The depths of the columns and the beams are 0.5 m and 0.3 m, respectively. The modulus of elasticity is $E = 30000$ MN/m^2 for the shear walls and the frameworks and $E_d = 3000$ MN/m^2 for the masonry. The modulus of elasticity in shear for the shear walls is $G = 12500$ MN/m^2. The storey height is $h = 3$ m and the total height of the building is $H = 18$ m. The weight per unit volume of the building is assumed to be $\gamma = 2.5$ kN/m^3.

The basic geometrical and stiffness characteristics are collected in the first five columns in Table 9.1. Data in the last two columns can only be calculated after the location of the shear centre is determined in Section 9.2.3.

The mass density per unit length is calculated using Equation (4.7):

$$m = \; A = \frac{}{g} LB = \frac{2.5}{9.81} 24 \cdot 12 = 73.4 \text{ kg/m} \qquad \{4.7\}$$

Mass distribution factor r_f is obtained from Table 4.1 as a function of the number of storeys:

$$r_f = 0.863 \qquad \{\text{Table 4.1}\}$$

9.2.1 Lateral vibration in direction *x*

There are only the two shear walls (and no frameworks) that effectively contribute to the lateral stiffness of the building and the corresponding frequency is

$$f_b^2 = f_w^2 = \frac{0.313 r_f^2}{H^4 m} E_w \sum_1^m I_{w,k} = \frac{0.313 \cdot 0.863^2 \cdot 3 \cdot 10^7 \cdot 2.275}{18^4 \cdot 73.4} = 2.065\,\text{Hz}^2 \quad \{4.15\}$$

and

$$f_x = f_b = \sqrt{2.065} = 1.437\ \text{Hz}$$

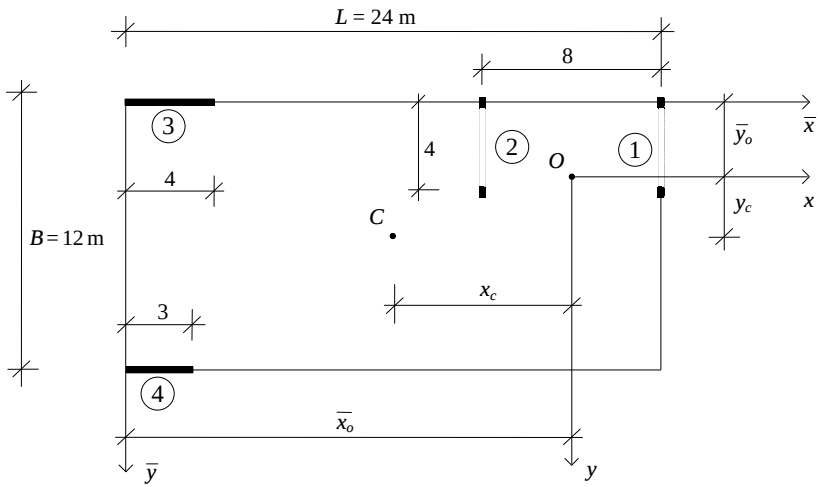

Figure 9.3 Layout of six-storey building.

9.2.2 Lateral vibration in direction *y*

The two infilled frameworks are modelled by replacing the masonry panels with diagonal struts of cross-sectional area

$$A_d = 0.15dt$$

where t is the thickness of the masonry wall and $0.15d$ is the effective width of the masonry infill (b_w in Figure 9.4/a). Equation (2.68) can now be used to determine the shear stiffness of Unit 1:

$$K_1 = \left(\frac{d^3}{A_d E_d h l^2} + \frac{l}{A_h E_h h} \right)^{-1}$$

$$= \left(\frac{5^3}{0.3 \cdot 0.15 \cdot 5 \cdot 3 \cdot 10^6 \cdot 3 \cdot 4^2} + \frac{4}{0.09 \cdot 3 \cdot 10^7 \cdot 3} \right)^{-1} = 229787 \text{ kN} \qquad \{2.68\}$$

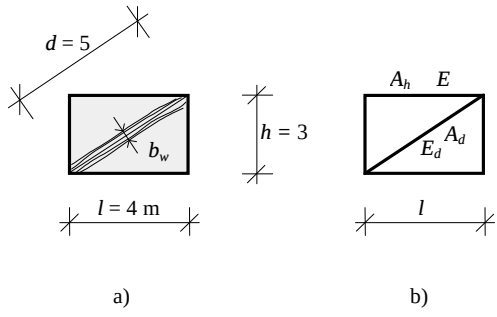

Figure 9.4 Modelling of masonry infill.

The total "original" shear stiffness of the system is

$$K = \sum_{i=1}^{f} K_i = 2 \cdot 229787 = 459574 \text{ kN} \qquad \{4.5\}$$

Table 9.1 Basic characteristics of the bracing units.

Bracing Unit	$\bar{x}_i$	$\bar{y}_i$	$I_{x,i}$	$I_{y,i}$	J	$x_i = \bar{x}_i - \bar{x}_o$	$y_i = \bar{y}_i - \bar{y}_o$
1	24.00		0.00625			4.0	
2	16.00		0.00625			-4.0	
3		0.0		1.6	0.036		-3.56
4		12.0		0.675	0.027		8.44
Σ			0.0125	2.275	0.063		

The frequency that belongs to the original shear stiffness of Unit 1 is

$$f_{s',1}^2 = \frac{1}{(4H)^2} \frac{r_f^2 K_1}{m} = \frac{0.863^2 \cdot 229787}{(4 \cdot 18)^2 \cdot 73.4} = 0.4498 \text{ Hz}^2 \qquad \{4.6\}$$

The global second moment of area of the cross-sections of the columns

$$I_{g,1} = \sum_{j=1}^{n} A_{c,j} t_j^2 = 0.3 \cdot 0.5 \cdot 2^2 \cdot 2 = 1.2 \text{ m}^4 \qquad \{4.9\}$$

is needed for the calculation of the corresponding frequency:

$$f_{g,1}^2 = \frac{0.313 r_f^2 E I_{g,1}}{H^4 m} = \frac{0.313 \cdot 0.863^2 \cdot 3 \cdot 10^7 \cdot 1.2}{18^4 \cdot 73.4} = 1.0891 \text{ Hz}^2 \qquad \{4.8\}$$

With the above part frequencies the effectiveness factor of Unit 1 can be determined

$$s_{f,1}^2 = \frac{f_{g,1}^2}{f_{g,1}^2 + f_{s',1}^2} = \frac{1.0891}{1.0891 + 0.4498} = 0.7077 \qquad \{4.10\}$$

with which the effective shear stiffness of the whole system is

$$K_e = \sum_{1}^{2} s_{f,i}^2 K_i = 0.7077 \cdot 229787 \cdot 2 = 325241 \text{ kN} \qquad \{4.11\}$$

The effectiveness factor of the whole system is

$$s_f = \sqrt{\frac{K_e}{K}} = \sqrt{\frac{325241}{459574}} = 0.8412 \qquad \{4.12\}$$

The frequency that belongs to the effective shear stiffness is

$$f_s^2 = \frac{1}{(4H)^2} \frac{r_f^2 K_e}{m} = \frac{0.863^2 \cdot 325241}{(4 \cdot 18)^2 \cdot 73.4} = 0.6366 \text{ Hz}^2 \qquad \{4.13\}$$

The local bending stiffness of the frameworks

$$EI = 3 \cdot 10^7 \cdot 0.0125 = 375000 \text{ kNm}^2 \qquad \{4.14\}$$

is needed for the determination of the other component of the frequency:

$$f_b^2 = \frac{0.313 r_f^2 EI}{H^4 m} = \frac{0.313 \cdot 0.863^2 \cdot 375000}{18^4 \cdot 73.4} = 0.011345 \text{ Hz}^2 \qquad \{4.15\}$$

With the non-dimensional parameter

$$k = H\sqrt{\frac{K_e}{EI}} = 18\sqrt{\frac{325241}{375000}} = 16.76 \qquad \{4.17\}$$

the frequency parameter is obtained using Table 4.2 as

$$= 4.408 + \frac{4.532 - 4.408}{17 - 16.5}(16.76 - 16.5) = 4.472 \qquad \{\text{Table 4.2}\}$$

The lateral frequency in direction *y* can now be determined:

$$f_y = \sqrt{f_b^2 + f_s^2 + \left(\frac{^2}{0.313} - \frac{k^2}{5} - 1\right) s_f\, f_b^2} \qquad \{4.18\}$$

$$= \sqrt{0.011345 + 0.6366 + \left(\frac{4.472^2}{0.313} - \frac{16.76^2}{5} - 1\right) 0.8412 \cdot 0.011345} = 0.844\ \text{Hz}$$

9.2.3 Pure torsional vibration

The calculation starts with the determination of the shear centre. The basic geometrical and stiffness characteristics of the four bracing units are collected in Table 9.1.

Compared to the two identical Bracing Units 1 and 2, Units 3 and 4 have negligible stiffness with regard to axis *x*, and so the shear centre is in the middle of the two frameworks in direction *x*:

$$\bar{x}_o = 20\ \text{m}$$

In direction *y*, the position of the shear centre is in proportion to the stiffnesses of the two shear walls:

$$\bar{y}_o = \frac{\sum_1^m I_{y,i}\bar{y}_i}{\sum_1^m I_{y,i}} = \frac{0.625 \cdot 12}{2.275} = 3.56\,\text{m} \qquad \{3.18\}$$

When the location of the shear centre is known, the data can be entered into the last two columns in Table 9.1 and the radius of gyration of the plan area of the building can be determined, using the distance of the shear centre and the centroid, as

$$x_c = \frac{L}{2} - \bar{x}_o = \frac{24}{2} - 20 = -8\,\text{m} \qquad \{4.34\}$$

$$y_c = \frac{B}{2} - \bar{y}_o = \frac{12}{2} - 3.56 = 2.44\,\text{m} \qquad \{4.34\}$$

The radius of gyration is

$$i_p = \sqrt{\frac{L^2 + B^2}{12} + t^2} = \sqrt{\frac{24^2 + 12^2}{12} + 8^2 + 2.44^2} = \sqrt{129.95} = 11.4\,\text{m} \qquad \{4.20\}$$

The torsional stiffness characteristics are calculated using the stiffnesses and the perpendicular distances of the bracing units from the shear centre ($I_{x,i}$, $I_{y,i}$, J_i, x_i and y_i in Table 9.1).

The "original" Saint-Venant torsional stiffness is

$$(GJ) = \sum_1^2 GJ_k + \sum_1^2 (K_i)_y x_i^2 = 0.063 \cdot 1.25 \cdot 10^7 +$$

$$+ 229787 \cdot 4^2 \cdot 2 = 787500 + 7353184 = 8140684\,\text{kNm}^2 \qquad \{4.27\}$$

The effective Saint-Venant torsional stiffness is obtained using the (identical) effectiveness factors of the two frameworks:

$$(GJ)_e = \sum_1^2 GJ_k + \sum_1^2 (K_{e,i})_y x_i^2 = 0.063 \cdot 1.25 \cdot 10^7 +$$

$$+ 229787 \cdot 0.7077 \cdot 4^2 \cdot 2 = 787500 + 5203848 = 5991348\,\text{kNm}^2 \qquad \{4.21\}$$

With the original and effective Saint-Venant torsional stiffnesses, the effectiveness factor is expressed as

$$s = \sqrt{\frac{(GJ)_e}{(GJ)}} = \sqrt{\frac{5991348}{8140684}} = 0.8579 \qquad \{4.26\}$$

When the warping stiffness of the system is considered, only the contribution of the shear walls is taken into account as that of the columns of the frameworks is negligible:

$$EI_\Omega = E \sum_1^m (I_{w,k})_x y_k^2 = 3 \cdot 10^7 (1.6 \cdot 3.56^2 + 0.675 \cdot 8.44^2) =$$

$$= 2.0508 \cdot 10^9 \text{ kNm}^4 \qquad \{4.22\}$$

The square of the frequency for pure torsional vibration that is associated with the effective Saint-Venant stiffness is

$$f_t^2 = \frac{r_f^2 (GJ)_e}{16 i_p^2 H^2 m} = \frac{0.863^2 \cdot 5991348}{16 \cdot 11.4^2 \cdot 18^2 \cdot 73.4} = 0.09024 \text{ Hz}^2 \qquad \{4.25\}$$

and the square of the pure torsional frequency associated with the warping stiffness is calculated as

$$f_\Omega^2 = \frac{0.313 r_f^2 EI_\Omega}{i_p^2 H^4 m} = \frac{0.313 \cdot 0.863^2 \cdot 2.0508 \cdot 10^9}{11.4^2 \cdot 18^4 \cdot 73.4} = 0.4774 \text{ Hz}^2 \qquad \{4.24\}$$

With the non-dimensional parameter

$$k = H \sqrt{\frac{(GJ)_e}{EI_\Omega}} = 18 \sqrt{\frac{5991348}{2.0508 \cdot 10^9}} = 0.9729 \qquad \{4.28\}$$

the vibration parameter is obtained using Table 4.2:

$$= 0.5851 + \frac{0.6542 - 0.5851}{1.0 - 0.5}(0.9729 - 0.5) = 0.650 \qquad \{\text{Table 4.2}\}$$

Finally, the frequency of pure torsional vibration is

$$f = \sqrt{f_\Omega^2 + f_t^2 + \left(\frac{^2}{0.313} - \frac{k^2}{5} - 1 \right) s \; f_\Omega^2} \qquad \{4.23\}$$

$$= \sqrt{0.4774 + 0.09024 + \left(\frac{0.65^2}{0.313} - \frac{0.9729^2}{5} - 1 \right) 0.8579 \cdot 0.4774} = 0.796 \text{ Hz}$$

9.2.4 Coupling of the basic frequencies

As the centroid of the layout does not lie on either of the principal axes, triple coupling of the basic modes occurs. Using the squares of the basic frequencies f_x, f_y and f_φ and the eccentricity parameters

$$_x = \frac{x_c}{i_p} = \frac{8.0}{11.4} = 0.7018 \qquad \text{and} \qquad _y = \frac{y_c}{i_p} = \frac{2.44}{11.4} = 0.214 \qquad \{4.33\}$$

the smallest root of the cubic equation

$$\left(f^2\right)^3 + a_2\left(f^2\right)^2 + a_1 f^2 - a_0 = 0 \qquad \{4.31\}$$

is the fundamental frequency of the building. With

$$a_0 = \frac{f_x^2 f_y^2 f^2}{1 - {}_x^2 - {}_y^2} = \frac{1.437^2 \cdot 0.844^2 \cdot 0.796^2}{1 - 0.7018^2 - 0.214^2} = 2.0188 \qquad \{4.32\}$$

$$a_1 = \frac{f_x^2 f_y^2 + f^2 f_x^2 + f^2 f_y^2}{1 - {}_x^2 - {}_y^2}$$

$$= \frac{1.437^2 \cdot 0.844^2 + 0.796^2 \cdot 1.437^2 + 0.796^2 \cdot 0.844^2}{1 - 0.7018^2 - 0.214^2} = 6.998$$

$$a_2 = \frac{f_x^2 \, {}_x^2 + f_y^2 \, {}_y^2 - f_x^2 - f_y^2 - f^2}{1 - {}_x^2 - {}_y^2}$$

$$= \frac{1.437^2 \cdot 0.7018^2 + 0.844^2 \cdot 0.214^2 - 1.437^2 - 0.844^2 - 0.796^2}{1 - 0.0277^2 - 0.0617^2} = -5.115$$

the fundamental frequency is

$$f = 0.626 \text{ Hz}$$

The approximate formula [Equation {4.35}] would result in

$$f = \left(\frac{1}{f_x^2} + \frac{1}{f_y^2} + \frac{1}{f^2}\right)^{-\frac{1}{2}} = \left(\frac{1}{1.437^2} + \frac{1}{0.844^2} + \frac{1}{0.796^2}\right)^{-\frac{1}{2}} = 0.537 \text{ Hz} \qquad \{4.35\}$$

for the fundamental frequency. This is good approximation, which can be expected as the eccentricity of the system is fairly great.

10

The global critical load of buildings

Two worked examples are given here for the calculation of the global critical load and global critical load ratio of buildings under uniformly distributed floor load, braced by frameworks, shear walls and cores. The calculations are based on the material presented in Chapters 2 and 5, and the numbers of the equations used will be given on the right-hand side in curly brackets.

10.1 THIRTY-STOREY DOUBLY SYMMETRIC BUILDING BRACED BY SHEAR WALLS AND FRAMEWORKS

Calculate the critical load and the critical load ratio of the thirty-storey building whose layout is shown in Figure 10.1, subjected to uniformly distributed vertical floor load of intensity $Q = 8.0$ kN/m^2. The modulus of elasticity is $E = 25000$ MN/m^2, the modulus of elasticity in shear is $G = 10400$ MN/m^2, the storey height is $h = 3$ m and the total height of the building is $H = 90$ m.

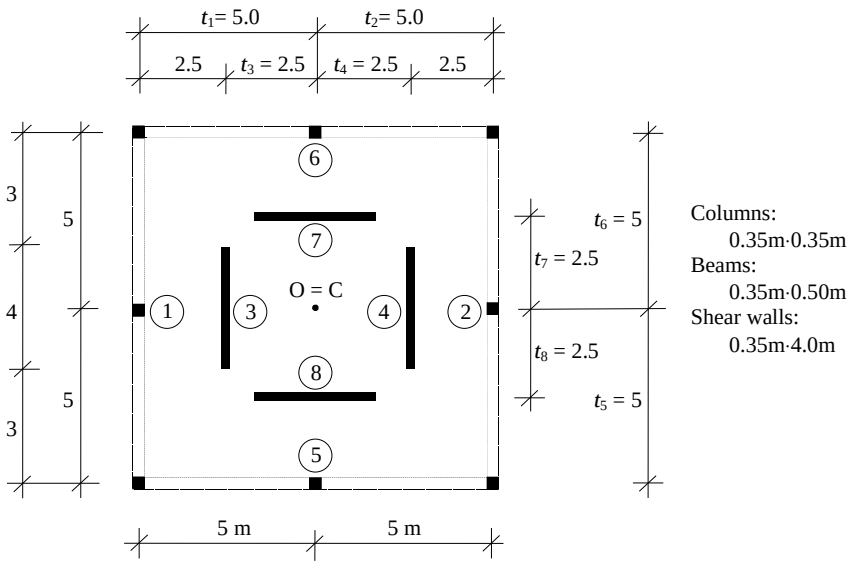

Figure 10.1 Layout of thirty-storey building for the stability analysis.

10.1.1 Individual bracing units

Before the whole system of four frameworks and four shear walls is investigated, it is advantageous to establish the basic characteristics of the two types of bracing unit. (The building is identical to the one used in Section 9.1 for the frequency analysis.)

Bracing Unit 1 (framework, identical to Bracing Units 2, 5 and 6 – Figure 9.2/a)

The cross-sections of the columns and beams of the four identical frameworks are 0.35/0.35 and 0.35/0.50 (metres), respectively.

The shear stiffness that is associated with the beams of the framework is

$$K_{b,1} = \sum_{j=1}^{n-1} \frac{12E_b I_{b,j}}{l_j h} = 2\frac{12 \cdot 25 \cdot 10^3 \cdot 0.35 \cdot 0.50^3}{12 \cdot 5 \cdot 3} = 145.83\,\text{MN} \qquad \{5.1\}$$

The shear stiffness that is associated with the columns of the framework is

$$K_{c,1} = \sum_{j=1}^{n} \frac{^2E_c I_{c,j}}{h^2} = 3\frac{^2 \cdot 25 \cdot 10^3 \cdot 0.35^4}{12 \cdot 3^2} = 102.85\,\text{kN} \qquad \{5.2\}$$

The combination of the two part shear stiffnesses gives the “original” shear stiffness of the framework:

$$K_1 = K_{b,1}\frac{K_{c,1}}{K_{b,1} + K_{c,1}} = 145.83\frac{102.85}{145.83 + 102.85} = 60.31\,\text{MN} \qquad \{5.3\}$$

where

$$r_1 = \frac{K_{c,1}}{K_{b,1} + K_{c,1}} = \frac{102.85}{145.83 + 102.85} = 0.4136 \qquad \{5.4\}$$

is the reduction factor.

Load distribution factor r_s is obtained from Table 5.1 as a function of the number of storeys:

$$r_s = 0.95 \qquad \{\text{Table 5.1}\}$$

The global second moment of area of the cross-sections of the columns is:

$$I_{g,1} = \sum_{j=1}^{n} A_{c,j} t_j^2 = 0.35 \cdot 0.35 \cdot 5^2 \cdot 2 = 6.125\,\text{m}^4 \qquad \{5.6\}$$

With the global second moment of area, the global bending critical load of the framework is

$$N_{g,1} = \frac{7.837 r_s E_c I_{g,1}}{H^2} = \frac{7.837 \cdot 0.95 \cdot 25 \cdot 10^3 \cdot 6.125}{90^2} = 140.75\,\text{MN} \qquad \{5.7\}$$

Because of the different buckling shape of the shear and global bending modes, there is an interaction between the two modes and the original shear stiffness is reduced by the effectiveness factor

$$s_1 = \frac{N_{g,1}}{K_1 + N_{g,1}} = \frac{140.75}{60.31 + 140.75} = 0.700 \qquad \{5.9\}$$

Bracing Unit 3 (shear wall, identical to Bracing Units 4, 7 and 8 – Figure 9.2/b)

The size of the shear wall is 4.0 metres with a thickness of 0.35 m. It only has bending stiffness which will directly be incorporated into the lateral model.

10.1.2 Sway buckling in directions *x* and *y*

Because of double symmetry, the behaviour (and the critical load of lateral buckling) of the building is identical in directions *x* and *y*.

The total shear stiffness of the two frameworks is

$$K = \sum_{i=1}^{f} K_i = 60.31 \cdot 2 = 120.62\ \text{MN} \qquad \{5.5\}$$

The effective shear stiffness for the whole system (that contains two frameworks) is obtained as

$$K_e = \sum_{1}^{f} K_i s_i = 60.31 \cdot 2 \cdot 0.7 = 84.43\,\text{MN} \qquad \{5.10\}$$

and the effectiveness factor for the whole system is

$$s = \frac{K_e}{K} = \frac{84.43}{120.62} = 0.7 \qquad \{5.11\}$$

The total bending stiffness of the system is obtained by adding up the local bending stiffness of the vertical structural units:

$$EI = E_c I_c + E_w I_w = E_c \sum_1^f I_{c,i} r_i + E_w \sum_1^m I_{w,i} \qquad \{5.12\}$$

$$= 25 \cdot 10^3 \left(\frac{0.35^4}{12} 0.4136 + \frac{0.35 \cdot 4.0^3}{12} \right) 2 = 93359 \text{ MN}$$

With the above bending stiffness, the local bending critical load of the system can now be presented as

$$N_l = \frac{7.837 r_s EI}{H^2} = \frac{7.837 \cdot 0.95 \cdot 93359}{90^2} = 85.81 \text{ MN} \qquad \{5.13\}$$

With the stiffness ratio

$$= \frac{K_e}{N_l} = \frac{84.43}{85.81} = 0.9839 \qquad \{5.17\}$$

the critical load parameter can be obtained from Table 5.2 as

$$= 3.3488 + \frac{3.5758 - 3.3488}{1.0 - 0.9} (0.9839 - 0.9) = 3.539 \qquad \{\text{Table 5.2}\}$$

The sway critical load (that is identical in directions *x* and *y*) can now be determined as

$$N_{cr,x} = N_{cr,y} = N_l + K_e + (\quad - \quad -1) s N_l \qquad \{5.18\}$$

$$= 85.81 + 84.43 + (3.539 - 0.9839 - 1) 0.7 \cdot 85.81$$

$$= 85.81 + 84.43 + 93.41 = 263.65 \text{ MN}$$

The effect of interaction between the bending and shear modes is considerable: the third term (93.41)—responsible for the interaction—amounts to 35.4% of the total critical load.

10.1.3 Pure torsional buckling

The radius of gyration is needed for the torsional analysis:

$$i_p = \sqrt{\frac{L^2 + B^2}{12} + t^2} = \sqrt{\frac{10^2 + 10^2}{12}} = \sqrt{16.67} = 4.08 \text{ m} \qquad \{5.28\}$$

The "original" Saint-Venant torsional stiffness is made up from two parts as both the four shear walls and the shear stiffness of the four frameworks have a contribution

$$(GJ) = \sum_{1}^{m} GJ_k + \sum_{1}^{f} \left((K_i)_x y_i^2 + (K_i)_y x_i^2 \right)$$

$$= 4\frac{4 \cdot 0.35^3}{3} 10.4 \cdot 10^3 + 4 \cdot 60.31 \cdot 5^2 = 8409 \text{ MNm}^2 \qquad \{5.35\}$$

In a similar manner, the effective Saint-Venant torsional stiffness of the system comes from two sources: the Saint-Venant torsional stiffness of the shear walls and the effective shear stiffness of the frameworks:

$$(GJ)_e = \sum_{1}^{m} GJ_k + \sum_{1}^{f} \left((K_{e,i})_x y_i^2 + (K_{e,i})_y x_i^2 \right)$$

$$= 4\frac{4 \cdot 0.35^3}{3} 10.4 \cdot 10^3 + 4 \cdot 60.31 \cdot 0.7 \cdot 5^2 = 6600 \text{ MNm}^2 \qquad \{5.29\}$$

The Saint-Venant torsional critical load that belongs to the effective Saint-Venant torsional stiffness is

$$N_t = \frac{(GJ)_e}{i_p^2} = \frac{6600}{16.67} = 395.9 \text{ MN} \qquad \{5.33\}$$

The effectiveness of the Saint-Venant torsional stiffness is expressed by the factor

$$s = \frac{(GJ)_e}{(GJ)} = \frac{6600}{8409} = 0.7849 \qquad \{5.34\}$$

There are no cores in the bracing system so the warping stiffness originates from two sources: the bending stiffness of the four shear walls and the bending stiffness of the columns of the four frameworks:

$$EI_\Omega = E_w \sum_{1}^{m} \left((I_{w,k})_x y_k^2 + (I_{w,k})_y x_k^2 \right) + E_c \sum_{1}^{f} \left((I_{c,i} r_i)_x y_i^2 + (I_{c,i} r_i)_y x_i^2 \right)$$

$$= 25 \cdot 10^3 \left(\frac{0.35 \cdot 4.0^3}{12} 2.5^2 + \frac{0.35^4}{12} 0.4136 \cdot 5^2 \right) 4 = 1.168 \cdot 10^6 \text{ MNm}^4 \qquad \{5.30\}$$

The contribution of the columns of the frameworks (second term) is very small (0.1%) and can safely be ignored in Equation {5.30}.

The warping torsional critical load of the system is

$$N_{\Omega} = \frac{7.837 r_s E I_{\Omega}}{i_p^2 H^2} = \frac{7.837 \cdot 0.95 \cdot 1.168 \cdot 10^6}{16.67 \cdot 90^2} = 64.40 \text{ MN} \qquad \{5.32\}$$

With parameter

$$= \frac{N_t}{N_{\Omega}} = \frac{395.9}{64.40} = 6.148 \qquad \{5.36\}$$

the critical load parameter α_{φ} is given in Table 5.2 as a function of parameter β_{φ}:

$$= 12.241 + \frac{13.749 - 12.241}{7.0 - 6.0}(6.148 - 6.0) = 12.46 \qquad \{\text{Table 5.2}\}$$

The critical load of pure torsional buckling is now obtained as:

$$N_{cr,} = N_{\Omega} + N_t + (\quad - \quad -1)s \;\; N_{\Omega} \qquad \{5.31\}$$

$$= 64.4 + 395.9 + (12.46 - 6.148 - 1)0.7849 \cdot 64.4 =$$

$$= 64.4 + 395.9 + 268.5 = 729 \text{ MN}$$

The effect of interaction between the warping torsional and Saint-Venant torsional modes is considerable: the third term (268.5)—responsible for the interaction—amounts to 36.8% of the total torsional critical load.

10.1.4 The global critical load and critical load ratio of the building

Because of double symmetry, there is no coupling among the three basic modes ($N_{cr,x}$, $N_{cr,y}$ and $N_{cr,\varphi}$) and the global critical load of the building is the smallest one of the three:

$$N_{cr} = N_{cr,x} = 263.65 \text{ MN}$$

Assuming a uniformly distributed floor load of $Q = 8$ kN/m^2, the total vertical load on the building is

$$N = nLBQ = 30 \cdot 10 \cdot 10 \cdot 0.008 = 24 \text{ MN} \qquad \{6.2\}$$

and the global critical load ratio is

$$= \frac{N_{cr}}{N} = \frac{263.65}{24} = 11 > 10 \qquad \{6.3\} \text{ and } \{6.5\}$$

indicating an adequate bracing system.

10.2 SIX-STOREY ASYMMETRIC BUILDING BRACED BY A CORE AND AN INFILLED FRAMEWORK

The six-storey building in London has undergone refurbishment during which some bracing walls have been removed resulting in some reduction in stiffness. The task is to investigate the structural adequacy of the building.

Figure 10.2 shows a simplified typical floor layout. The lateral and torsional stiffness of the building is provided by a reinforced concrete U-core and a four-bay infilled framework. The wall thickness of the core is $t = 0.15$ m. The location of the U-core (defined by its shear centre) is given in Table 10.1. The cross-sections of the beams and columns of the framework are 0.3 m/0.3 m and 0.3 m/0.5 m, respectively. The four bays are identical at $l = 3.75$ m. The modulus of elasticity is $E = 20000$ MN/m^2, the modulus of elasticity in shear is $G = 8333$ MN/m^2 for the concrete structures. The modulus of elasticity is $E_d = 3000$ MN/m^2 for the masonry infill whose thickness is $t = 0.3$ m. A ratio of $b_w/d = 0.30$ is assumed for the effective width of the infill when the equivalent diagonal strut is established.

The storey height is $h = 3.417$ m and the total height of the building is $H = 20.5$ m.

The global critical load and critical load ratio will be determined to show if the building has adequate stiffness. The intensity of the vertical floor load is assumed to be $Q = 10.0$ kN/m^2.

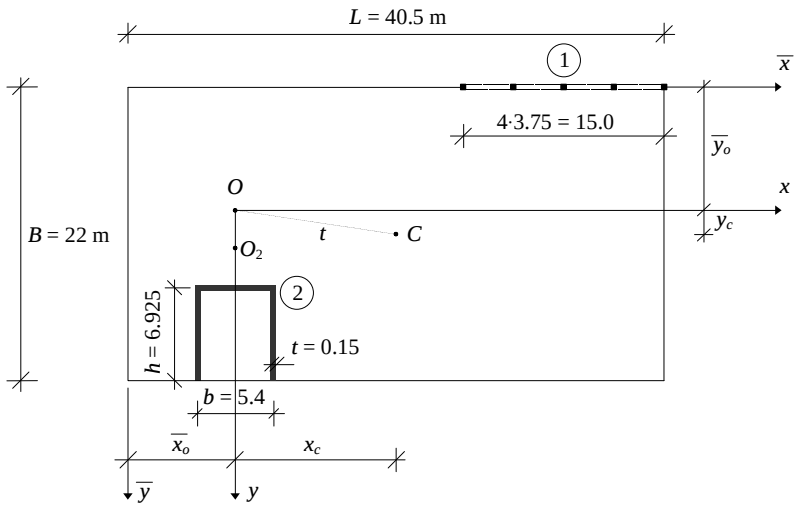

Figure 10.2 Layout of six-storey building for the stability analysis.

As a function of the number of storeys, the load distribution factor for the six-storey building is

$$r_s = 0.791 \qquad \{\text{Table 5.1}\}$$

Before the whole building is investigated, the basic characteristics of the two bracing units are determined.

10.2.1 Individual bracing units

Bracing Unit 1 (infilled framework)

With b_w/d = 0.30, the effective cross-sectional area of the diagonal is

$$A_d = tb_w = t \cdot 0.3 \cdot d = 0.3 \cdot 0.3 \cdot 5.073 = 0.4566\,\text{m}^2 \qquad \{2.66\}$$

and with four identical bays, the shear stiffness of Unit 1 is

$$K_1 = 4\left(\frac{d^3}{A_d E_d h l^2} + \frac{l}{A_h E_h h}\right)^{-1} \qquad \{2.68\}$$

$$= 4\left(\frac{5.073^3}{0.4566 \cdot 3000 \cdot 3.417 \cdot 3.75^2} + \frac{3.75}{0.09 \cdot 2 \cdot 10^4 \cdot 3.417}\right)^{-1} = 1542.5\,\text{MN}$$

With the cross-sections of the columns of the four-bay framework, the global second moment of area is

$$I_{g,1} = \sum_{j=1}^{n} A_{c,j} t_j^2 = 0.3 \cdot 0.5(7.5^2 + 3.75^2)2 = 21.09\,\text{m}^2 \qquad \{5.6\}$$

The global bending critical load of the framework is

$$N_{g,1} = \frac{7.837 r_s E_c I_{g,1}}{H^2} = \frac{7.837 \cdot 0.791 \cdot 2 \cdot 10^4 \cdot 21.09}{20.5^2} = 6221.9\,\text{MN} \qquad \{5.7\}$$

As a function of part critical load ratio $_s$, defined by

$$_s = \frac{K_1}{N_{g,1}} = \frac{1542.5}{6221.9} = 0.248 \qquad \{2.62\}$$

critical load parameter $_s$ is obtained from Table 2.5 as

$$_s = 1.0 \qquad \{\text{Table 2.5}\}$$

and the critical load of the infilled frame is

$$N_{x,1} = \ _sK_1 = 1542.5\,\text{MN} \qquad \{2.61\}$$

The sum of the second moments of area of the five columns will also be needed later on:

$$I_{y,1} = 5\frac{0.3\cdot 0.5^3}{12} = 0.0156\ \text{m}^4$$

Table 10.1 Basic characteristics of the bracing units.

Bracing Unit	$\bar{x}_i$	$\bar{y}_i$	$I_{x,i}$	$I_{y,i}$	J	I_ω	$x_i = \bar{x}_i - \bar{x}_o$	$y_i = \bar{y}_i - \bar{y}_o$
1	33.00	0	0	0.0156			24.9	-9.2
2	8.10	12.011	15.29	17.12	0.0217	81.41	0	2.811

Bracing Unit 2 (U-core)

The torsional stiffness characteristics of the U-core can be calculated using the Equations given in Table 2.7. The warping constant, the Saint-Venant constant and the location of its shear centre are

$$I_\Omega = \frac{t_f h^3 b^2}{12}\frac{3t_f h + 2t_w b}{6t_f h + t_w b} = \frac{0.15\cdot 6.925^3\cdot 5.4^2}{12}\frac{3\cdot 6.925 + 2\cdot 5.4}{6\cdot 6.925 + 5.4} = 81.41\ \text{m}^6$$

$$J = \frac{1}{3}(2ht_f^3 + bt_w^3) = \frac{0.15^3(2\cdot 6.925 + 5.4)}{3} = 0.0217\ \text{m}^4 \qquad \{\text{Table 2.7}\}$$

$$e = \frac{3t_f h^2}{6t_f h + t_w b} = \frac{3\cdot 6.925^2}{6\cdot 6.925 + 5.4} = 3.064\ \text{m} \qquad \{\text{Table 2.7}\}$$

The basic characteristics are tabulated in Table 10.1 where the last two columns are only completed after the location of the shear centre is established below.

The critical loads of the core in the two principal directions are:

$$N_{x,2} = \frac{7.837EI_y r_s}{H^2} = \frac{7.837\cdot 2\cdot 10^4\cdot 17.12\cdot 0.791}{20.5^2} = 5051\,\text{MN} \qquad \{2.92\}$$

and

$$N_{y,2} = \frac{7.837 EI_x r_s}{H^2} = \frac{7.837 \cdot 2 \cdot 10^4 \cdot 15.29 \cdot 0.791}{20.5^2} = 4511 \text{ MN} \qquad \{2.92\}$$

The coordinates of the shear centre can now be calculated:

$$\bar{x}_o = \frac{\sum_1^{f+m} N_{y,i} \bar{x}_i}{\sum_1^{f+m} N_{y,i}} = \frac{4511 \cdot 8.1 + 0}{4511 + 0} = 8.10 \text{ m} \qquad \{5.37\}$$

$$\bar{y}_o = \frac{\sum_1^{f+m} N_{x,i} \bar{y}_i}{\sum_1^{f+m} N_{x,i}} = \frac{5051 \cdot 12.011 + 0}{5051 + 1542.5} = 9.20 \text{ m} \qquad \{5.37\}$$

10.2.2 Sway buckling in directions *x* and *y*

There is an interaction in direction *x* between the core and the infilled frame. The original shear stiffness of the system originates from the infilled frame:

$$K = \sum_{i=1}^{f} K_i = K_1 = 1542.5 \text{ MN} \qquad \{5.5\}$$

The global bending critical load of the framework (calculated above in Section 10.2.1) and the original shear stiffness define the effectiveness factor as

$$s_1 = \frac{N_{g,1}}{K_1 + N_{g,1}} = \frac{6221.9}{1542.5 + 6221.9} = 0.8014 \qquad \{5.9\}$$

and the effective shear stiffness is

$$K_e = \sum_1^f K_i s_i = K_1 s_1 = 1542.5 \cdot 0.8014 = 1236 \text{ MN} \qquad \{5.10\}$$

With the bending stiffness coming from the columns of the framework and the core (Table 10.1)

$$EI = E_c I_c + E_w I_w = 2 \cdot 10^4 (0.0156 + 17.12) = 342712 \text{ MNm}^2 \quad \{5.12\}$$

the bending critical load is

$$N_l = \frac{7.837 r_s EI}{H^2} = \frac{7.837 \cdot 0.791 \cdot 342712}{20.5^2} = 5055 \text{ MN} \quad \{5.13\}$$

As a function of the ratio of the part critical loads

$$= \frac{K_e}{N_l} = \frac{1236}{5055} = 0.2445 \quad \{5.17\}$$

the critical load factor is obtained from Table 5.2:

$$= 1.5798 + \frac{1.8556 - 1.5798}{0.3 - 0.2}(0.2445 - 0.2) = 1.7 \quad \{\text{Table 5.2}\}$$

The critical load in direction *x* is

$$N_{cr,x} = N_l + K_e + (\quad - \quad - 1) s N_l \quad \{5.18\}$$

$$= 5055 + 1236 + (1.7 - 0.2445 - 1) 0.8014 \cdot 5055$$

$$= 5055 + 1236 + 1845 = 8136 \text{ MN}$$

The effect of interaction between the bending and shear modes (1845 MN) now amounts to 23% of the total critical load.

The situation in direction *y* is much simpler as the infilled frame only has negligible stiffness perpendicular to its plane that is safely ignored compared to the stiffness of the core. The critical load hence is

$$N_{cr,y} = N_{y,2} = 4511 \text{MN} \quad \{2.92\}$$

10.2.3 Pure torsional buckling

With the coordinates of the geometrical centre

$$x_c = \frac{L}{2} - \bar{x}_o = \frac{40.5}{2} - 8.1 = 12.15 \text{ m} \quad \{5.42\}$$

and

$$y_c = \frac{B}{2} - \bar{y}_o = \frac{22}{2} - 9.2 = 1.8 \text{ m}$$

the radius of gyration of the ground plan is

$$i_p = \sqrt{\frac{L^2 + B^2}{12} + t^2} = \sqrt{\frac{40.5^2 + 22^2}{12} + 12.15^2 + 1.8^2} = 18.1\,\text{m} \qquad \{5.28\}$$

The "original" Saint-Venant torsional stiffness consists of two parts: the own contribution of the core and that of the infilled frame:

$$(GJ) = \sum_1^m GJ_k + \sum_1^f \left((K_i)_x y_i^2 + (K_i)_y x_i^2\right) = GJ_2 + K_1 y_1^2 \qquad \{5.35\}$$

$$= 8333 \cdot 0.0217 + 1542.5 \cdot 9.2^2 = 130738\,\text{MNm}^2$$

The contribution of the core—first term—is only 0.13% and can safely be ignored.

The effective Saint-Venant torsional stiffness is obtained by replacing the original shear stiffness with the effective one above:

$$(GJ)_e = \sum_1^m GJ_k + \sum_1^f \left((K_{e,i})_x y_i^2 + (K_{e,i})_y x_i^2\right) = GJ_2 + K_{e1} y_1^2 \qquad \{5.29\}$$

$$= 8333 \cdot 0.0217 + 1236 \cdot 9.2^2 = 104796\,\text{MNm}^2$$

The effectiveness factor is

$$s = \frac{(GJ)_e}{(GJ)} = \frac{104796}{130738} = 0.8016 \qquad \{5.34\}$$

The warping stiffness of the system originates from three sources: the own warping stiffness of the core, the bending stiffness of the core and the bending stiffness of the columns of the framework:

$$EI_\Omega = E_w \sum_1^m \left(I_{\Omega,k} + (I_{w,k})_x y_k^2 + (I_{w,k})_y x_k^2\right) + E_c \sum_1^f (I_{c,i} r_i)_x y_i^2 \qquad \{5.30\}$$

$$= 2 \cdot 10^4 (81.41 + 17.12 \cdot 2.811^2 + 0.0156 \cdot 9.2^2) = 4.36 \cdot 10^6\,\text{MNm}^4$$

The contribution of the columns—last term—is only 0.6% and therefore can safely be ignored.

Using the effective Saint-Venant torsional stiffness and warping torsional stiffness, the two part critical loads can now be determined. The warping torsional

critical load of the system is

$$N_{\Omega} = \frac{7.837 r_s E I_{\Omega}}{i_p^2 H^2} = \frac{7.837 \cdot 0.791 \cdot 4.36 \cdot 10^6}{18.1^2 \cdot 20.5^2} = 196.3\,\text{MN} \qquad \{5.32\}$$

and the Saint-Venant torsional critical load is

$$N_t = \frac{(GJ)_e}{i_p^2} = \frac{104796}{18.1^2} = 319.9\,\text{MN} \qquad \{5.33\}$$

The ratio of the two part critical loads

$$= \frac{N_t}{N_{\Omega}} = \frac{319.9}{196.3} = 1.63 \qquad \{5.36\}$$

is needed for getting the critical load factor. Its value is obtained from Table 5.2 as

$$= 3.5758 + \frac{5.624 - 3.5758}{2.0 - 1.0}(1.63 - 1.0) = 4.866 \qquad \{\text{Table 5.2}\}$$

The critical load of pure torsional buckling can now be calculated:

$$N_{cr,} = N_{\Omega} + N_t + (\quad - \quad - 1)s\ N_{\Omega} \qquad \{5.31\}$$

$$= 196.3 + 319.9 + (4.866 - 1.63 - 1)0.8016 \cdot 196.3$$

$$= 196.3 + 319.9 + 351.8 = 868\,\text{MN}$$

The effect of interaction between the warping torsional and Saint-Venant torsional modes is considerable: the third term (351.8 MN)—responsible for the interaction—amounts to 40.5% of the total torsional critical load.

10.2.4 The global critical load and critical load ratio of the building

The centroid of the layout does not lie on either of the principal axes and therefore there is a triple coupling of the basic critical loads $N_{cr,x}$, $N_{cr,y}$ and $N_{cr,\varphi}$. The effect of coupling is always detrimental and its magnitude (partly) depends on the eccentricity of the system:

$$_x = \frac{x_c}{i_p} = \frac{12.15}{18.1} = 0.671 \qquad \text{and} \qquad _y = \frac{y_c}{i_p} = \frac{1.8}{18.1} = 0.0994 \qquad \{5.41\}$$

Once the part critical loads and the eccentricity parameters are available, the critical load is obtained by solving the cubic equation

$$(N)^3 + b_2(N)^2 + b_1 N - b_0 = 0 \qquad \{5.39\}$$

In the above equation the coefficients are

$$b_0 = \frac{N_{cr,x} N_{cr,y} N_{cr,}}{1 - {}^2_x - {}^2_y} = \frac{8136 \cdot 4511 \cdot 868}{1 - 0.671^2 - 0.0994^2} = 5.9 \cdot 10^{10} \qquad \{5.40\}$$

$$b_1 = \frac{N_{cr,x} N_{cr,y} + N_{cr,}\ N_{cr,x} + N_{cr,}\ N_{cr,y}}{1 - {}^2_x - {}^2_y}$$

$$= \frac{8136 \cdot 4511 + 868 \cdot 8136 + 868 \cdot 4511}{1 - 0.671^2 - 0.0994^2} = 8.88 \cdot 10^7$$

$$b_2 = \frac{N_{cr,x}\ {}^2_x + N_{cr,y}\ {}^2_y - N_{cr,x} - N_{cr,y} - N_{cr,}}{1 - {}^2_x - {}^2_y}$$

$$= \frac{8136 \cdot 0.671^2 + 4511 \cdot 0.0994^2 - 8136 - 4511 - 868}{1 - 0.671^2 - 0.0994^2} = -18166$$

The smallest root of the cubic equation is the global critical load of the building:

$$N_{cr} = 791\,\text{MN}$$

(A simpler, faster, albeit approximate way of obtaining the combined critical load is using the Föppl-Papkovich formula

$$N_{cr} = \left(\frac{1}{N_{cr,x}} + \frac{1}{N_{cr,y}} + \frac{1}{N_{cr,}} \right)^{-1} \qquad \{5.43\}$$

which gives N_{cr} = 668 MN.)

Assuming a uniformly distributed floor load of Q = 10 kN/m^2, the total vertical load on the building is

$$N = nLBQ = 6 \cdot 40.5 \cdot 22 \cdot 0.01 = 53.46\,\text{MN} \qquad \{6.2\}$$

and the global critical load ratio (using the exact figure) is

$$= \frac{N_{cr}}{N} = \frac{791}{53.46} = 14.8 > 10 \qquad \{6.3\} \text{ and } \{6.5\}$$

indicating an adequate bracing system.

11

Global structural analysis of a twenty-two storey building

Individual types of analysis have been carried out so far. However, the structural engineer is normally responsible for the building as a whole, not only for certain units or individual aspects of its behaviour. Before the building is constructed, all areas relating to structural behaviour have to be looked at. This chapter shows how such global analysis is carried out using a real building. The investigation normally starts with the stability analysis and then moves on to determine the fundamental frequency of the building. The maximum deflection of the building under horizontal load concludes the global analysis. Many stiffness characteristics needed for the individual investigations are identical, and they only have to be established once and then can be reused. Hence the resulting global analysis covering the three different areas requires much less work than three individual analyses separately.

The case study is based on and uses a simplified version of the structure of the Sheffield Arts Tower, seen on the cover of the book. The twenty-three storey structure is braced by four reinforced concrete cores and four perimeter frames. The perimeter frames are replaced by 16 bulky columns on ground floor level making this region much stiffer than the superstructure. The simplified static model of the twenty-two storey superstructure is the subject of the analysis, whose layout is shown in Figure 11.1. The basic data of the superstructure is given below.

Size of ground plan: $L = 36.0$ m and $B = 20.0$ m.
Storey height: $h = 3$ m. Number of storeys: 22. Height of structure: 66 m.
Modulus of elasticity: $E = 23 \cdot 10^3$ MN/m^2.
Shear modulus: $G = 9.583 \cdot 10^3$ MN/m^2.
Cross-sections of both the beams and the columns of the frames: 0.4 m/0.4 m.

In addition to the eight bracing units, concrete columns are also part of the vertical load carrying system but their contribution to the lateral and torsional stiffness is small compared to that of the bracing units and is therefore ignored for the calculation. It is assumed for the analysis that the cores only develop bending deformation.

The weight per unit volume of the building (for the dynamic analysis) is assumed to be $\gamma = 3$ kN/m^3. A vertical load of $Q = 10$ kN/m^2 is considered for the stability analysis and for the determination of the global critical load ratio. When the structure is subjected to lateral load and the top rotation and deflection are calculated, a uniformly distributed horizontal load of intensity 1.3 kN/m^2 is considered in direction y, which results in a wind load of $w_y = 46.8$ kN/m.

It will be seen that—as far as stiffnesses are concerned—the building is almost doubly symmetric and the eccentricity of the bracing system (see distance OC in Figure 11.1) plays a very little role in the behaviour of the structure. Nevertheless, for the sake of completeness, a comprehensive and full global analysis will be carried out. The numbers of the Equations used for the calculations (derived in Part I) will be given on the right-hand side in curly brackets. The investigation starts with the stability analysis.

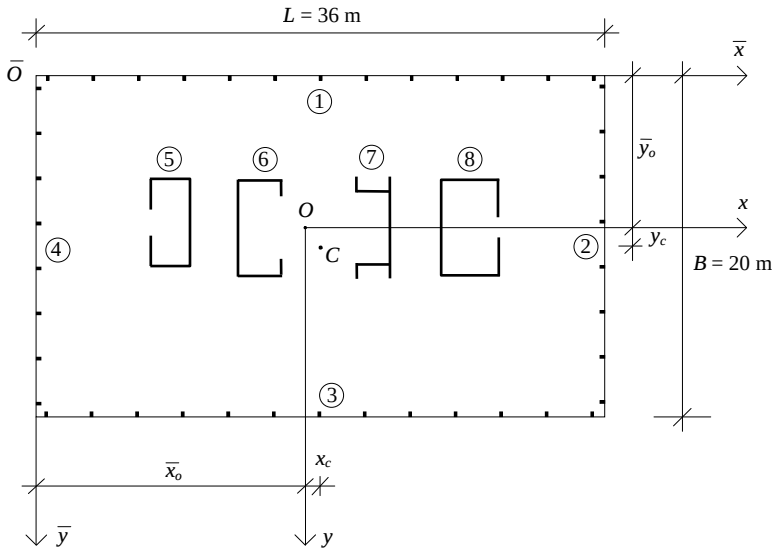

Figure 11.1 Typical layout of superstructure above ground floor level.

11.1 THE CRITICAL LOAD

The load distribution factor is obtained from Table 5.1 as a function of the number of storeys:

$$r_s = \frac{n}{n+1.588} = \frac{22}{22+1.588} = 0.933 \qquad \{\text{Table 5.1}\}$$

Before the structural analysis is carried out, the basic characteristics of the individual bracing units are given in the next section.

11.1.1 Individual bracing units

Bracing Unit 1 (framework, identical to Bracing Unit 3)

The cross-sections of the columns and beams of the framework are 0.40/0.40 (metres). With twelve bays and a bay-size of $l = 3$ m, the shear stiffness that is

associated with the beams of the framework is

$$K_{b,1} = \sum_{j=1}^{n-1} \frac{12 E_b I_{b,j}}{l_j h} = 12 \frac{12 \cdot 23 \cdot 10^6 \cdot 0.40^4}{12 \cdot 3 \cdot 3} = 785067 \text{ kN} \qquad \{5.1\}$$

The shear stiffness that is associated with the columns of the framework is

$$K_{c,1} = \sum_{j=1}^{n} \frac{^2 E_c I_{c,j}}{h^2} = 13 \frac{^2 \cdot 23 \cdot 10^6 \cdot 0.40^4}{12 \cdot 3^2} = 699499 \text{ kN} \qquad \{5.2\}$$

The combination of the two part shear stiffnesses gives the “original” shear stiffness of the framework:

$$K_1 = K_{b,1} \frac{K_{c,1}}{K_{b,1} + K_{c,1}} = 785067 \frac{699499}{785067 + 699499} = 369908 \text{ kN} \qquad \{5.3\}$$

where the reduction factor

$$r_1 = \frac{K_{c,1}}{K_{b,1} + K_{c,1}} = \frac{699499}{785067 + 699499} = 0.471 \qquad \{5.4\}$$

is used.

The local second moment of area of the cross-sections of the columns is a simple sum of the second moments of areas of the individual columns (amended by *r*):

$$I_1 = r \sum_{1}^{n} I_{c,j} = 0.471 \cdot 13 \cdot \frac{0.4^4}{12} = 0.01306 \text{ m}^4 \qquad \{2.57\}$$

The global second moment of area of the cross-sections of the columns is:

$$I_{g,1} = \sum_{j=1}^{n} A_{c,j} t_j^2 = 0.4^2 \cdot 2(18^2 + 15^2 + 12^2 + 9^2 + 6^2 + 3^2) = 262.08 \text{ m}^4 \qquad \{5.6\}$$

The framework is very wide and the local effect of the columns is very small and the ratio defined by Equation (2.59) is also very small. In such cases the simpler method presented in Section 2.4.1 can be used for the determination of the critical load.

With the global second moment of area, the global bending critical load of the framework is

$$N_{g,1} = \frac{7.837 r_s E_c I_{g,1}}{H^2} = \frac{7.837 \cdot 0.933 \cdot 23 \cdot 10^6 \cdot 262.08}{66^2} = 10118248\,\text{kN} \qquad \{2.63\}$$

With

$$_s = \frac{K_1}{N_{g,1}} = \frac{369908}{10118248} = 0.0365 \qquad \{2.62\}$$

critical load parameter $_s$ is obtained using Figure 2.17 as

$$_s = 1.0 \qquad \{\text{Figure 2.17}\}$$

and the critical load of the framework is

$$N_{cr,1} = \ _s K_1 = 1.0 \cdot 369.9 = 369.9\ \text{MN} \qquad \{2.61\}$$

The effectiveness factor is

$$s_1 = \frac{N_{g,1}}{K_1 + N_{g,1}} = \frac{10118}{369.9 + 10118} = 0.9647 \qquad \{5.9\}$$

Bracing Unit 2 (framework, identical to Bracing Unit 4)

The cross-sections of the columns and beams of the framework are 0.40/0.40 (metres). With seven bays and a bay-size of l = 2.85 m, the shear stiffness that is associated with the beams of the framework is

$$K_{b,2} = \sum_{j=1}^{n-1} \frac{12 E_b I_{b,j}}{l_j h} = 7 \frac{12 \cdot 23 \cdot 10^6 \cdot 0.40^4}{12 \cdot 2.85 \cdot 3} = 482058\,\text{kN} \qquad \{5.1\}$$

The shear stiffness that is associated with the columns of the framework is

$$K_{c,2} = \sum_{j=1}^{n} \frac{^2 E_c I_{c,j}}{h^2} = 8 \frac{^2 \cdot 23 \cdot 10^6 \cdot 0.40^4}{12 \cdot 3^2} = 430461\,\text{kN} \qquad \{5.2\}$$

The combination of the two part shear stiffnesses gives the “original” shear stiffness of the framework:

$$K_2 = K_{b,2} \frac{K_{c,2}}{K_{b,2} + K_{c,2}} = 482058 \frac{430461}{482058 + 430461} = 227400\,\text{kN} \qquad \{5.3\}$$

where the reduction factor

$$r_2 = \frac{K_{c,2}}{K_{b,2} + K_{c,2}} = \frac{430461}{482058 + 430461} = 0.472 \qquad \{5.4\}$$

is introduced.

The local second moment of area of the cross-sections of the columns is a simple sum of the second moments of areas of the individual columns (amended by *r*):

$$I_2 = r\sum_{1}^{n} I_{c,j} = 0.472 \cdot 8 \cdot \frac{0.4^4}{12} = 0.008055\,\text{m}^4 \qquad \{2.57\}$$

The global second moment of area of the cross-sections of the columns is:

$$I_{g,2} = \sum_{j=1}^{n} A_{c,j} t_j^2 = 0.4^2 \cdot 2(9.975^2 + 7.125^2 + 4.275^2 + 1.425^2) = 54.58\,\text{m}^4 \qquad \{5.6\}$$

The framework is very wide and the local effect of the columns is very small and the ratio defined by Equation (2.59) is also very small. In such cases the simpler method presented in Section 2.4.1 can be used for the determination of the critical load.

With the global second moment of area, the global bending critical load of the framework is

$$N_{g,2} = \frac{7.837 r_s E_c I_{g,2}}{H^2} = \frac{7.837 \cdot 0.933 \cdot 23 \cdot 10^6 \cdot 54.58}{66^2} = 2107196\,\text{kN} \qquad \{2.63\}$$

With

$$_s = \frac{K_2}{N_{g,2}} = \frac{227400}{2107196} = 0.11 \qquad \{2.62\}$$

critical load parameter $_s$ is obtained using Figure 2.17 as

$$_s = 1.0 \qquad \{\text{Figure 2.17}\}$$

and the critical load of the framework is

$$N_{cr,2} = \ _s K_2 = 1.0 \cdot 227.4 = 227.4\,\text{MN} \qquad \{2.61\}$$

The effectiveness factor is

$$s_2 = \frac{N_{g,2}}{K_2 + N_{g,2}} = \frac{2107.2}{227.4 + 2107.2} = 0.9026 \qquad \{5.9\}$$

Bracing Units 5, 6, 7 and 8

The basic geometric characteristics of the four U-cores (a, b, c, d, h, t_1, t_2 and t_3) are given in Table 11.1. The last column in Table 11.1 contains the location of the shear centre of the cores, in relation to their centroid, according to the relevant formula in Table 2.8. The rest of the formulae in Table 2.8 enable the determination of the bending and torsional characteristics of the cores. These data, as well as the location of the cores in the $\bar{x}-\bar{y}$ coordinate system (Figure 11.1) are collected in Table 11.2. The critical loads of the cores in directions x and y (N_x and N_y) are calculated using Equations (2.92) with the corresponding second moment of area of the core. Table 11.2 also contains the relevant data related to the four frameworks.

Table 11.1 Cross-sectional characteristics for the bracing cores.

Bracing core	a	b	c	d	h	t_1=t_2=t_3	y_o
5	0.15	5.0	0.15	2.00	2.5	0.3	-2.85
6	0.15	5.3	0.15	0.90	2.5	0.3	-2.20
7	0.80	3.9	0.80	0.15	1.6	0.3	-1.07
8	0.15	5.3	0.15	2.00	3.4	0.3	-3.74

With the coordinates ($\bar{x}_i$ and $\bar{y}_i$ in the second and third columns in Table 11.2 refer to the shear centre of the cores) and the critical loads (ninth and tenth columns in Table 11.2) of the bracing units, the location of the shear centre of the bracing system can now be calculated:

$$\bar{x}_o = \frac{\sum_{1}^{f+m} N_{y,i}\bar{x}_i}{\sum_{1}^{f+m} N_{y,i}} = \qquad \{5.37\}$$

$$\frac{227.4(36+0)+193.8\cdot 12.59+142.2\cdot 12.49+50.1\cdot 23.16+386.1\cdot 23.12}{1227.0} = 18.329 \text{ m}$$

and

$$\bar{y}_o = \frac{\sum_{1}^{f+m} N_{x,i}\bar{y}_i}{\sum_{1}^{f+m} N_{x,i}} = \qquad \{5.37\}$$

$$= \frac{369.9(0+20)+605.1\cdot 8.9+655.7\cdot 9.05+390.7\cdot 9.05+841.4\cdot 9.15}{3232.7} = 9.265 \text{ m}$$

A new *x-y* coordinate system is now established whose *O* origin is in the shear centre (Figure 11.1). The location of the bracing units has to be determined in this coordinate system using

$$x_i = \bar{x}_i - \bar{x}_o \qquad \text{and} \qquad y_i = \bar{y}_i - \bar{y}_o$$

These new coordinates are given in the last two columns in Table 11.2.

Table 11.2 Basic characteristics of the bracing units.

Bracing unit	$\bar{x}_i$	$\bar{y}_i$	I_x	I_y	J	I_ω	K	N_x	N_y	x_i	y_i
1	18.00	0.00	-	0.013	-	-	369.9	-	369.9	-0.329	-9.265
2	36.00	10.0	0.008	-	-	-	227.4	227.4	-	17.67	0.735
3	18.00	20.0	-	0.013	-	-	369.9	-	369.9	-0.329	10.74
4	0.00	10.0	0.008	-	-	-	227.4	227.4	-	-18.33	0.735
5	12.59	8.90	15.68	5.021	0.126	69.4	-	193.8	605.1	-5.74	-0.365
6	12.49	9.05	16.99	3.685	0.109	25.5	-	142.2	655.7	-5.84	-0.215
7	23.16	9.05	10.12	1.299	0.090	3.2	-	50.1	390.7	4.83	-0.215
8	23.12	9.15	21.80	10.00	0.145	140.9	-	386.1	841.4	4.79	-0.115
Σ			64.61	20.03	0.470	239.0		1227.0	3232.7		

11.1.2 Sway buckling in direction *y*

The participating bracing units in direction *y* are Units 2, 4, 5, 6, 7 and 8.

The original shear stiffness originates from the two frameworks (Units 2 and 4):

$$K = \sum_{i=1}^{f} K_i = K_2 + K_4 = 2 \cdot 227.4 = 454.8 \text{ MN} \qquad \{5.5\}$$

With the effectiveness factors of Unit 2 and 4 [Equation {5.9} in the previous Section], the effective shear stiffness is

$$K_e = \sum_{1}^{f} K_i s_i = 2 \cdot 227.4 \cdot 0.9026 = 410.502 \text{ MN} \qquad \{5.10\}$$

The effectiveness factor for the whole system is

$$s = \frac{K_e}{K} = \frac{410.502}{454.8} = 0.9026 \qquad \{5.11\}$$

The bending stiffness of the system is

$$EI = E_c I_c + E_w I_w = E_c \sum_{1}^{f} I_{c,i} r_i + E_w \sum_{1}^{m} I_{w,i}$$

$$= 23 \cdot 10^3 \left(8 \frac{0.4^4}{12} 0.472 \cdot 2 + 64.59 \right) = 1.486 \cdot 10^6 \text{ MNm}^2 \qquad \{5.12\}$$

where the first term stands for the contribution of the columns of the frameworks. It amounts to 0.02% and can safely be neglected. The second term represents the four cores, according to the fourth column in Table 11.2.

The local bending critical load can now be calculated:

$$N_l = \frac{7.837 r_s EI}{H^2} = \frac{7.837 \cdot 0.933 \cdot 1.486 \cdot 10^6}{66^2} = 2494 \text{ MN} \qquad \{5.13\}$$

Using the part critical load ratio

$$= \frac{K_e}{N_l} = \frac{410.5}{2494} = 0.1646 \qquad \{5.17\}$$

the critical load parameter is obtained from Table 5.2

$$= 1.2949 + \frac{1.5798 - 1.2949}{0.2 - 0.1} (0.1646 - 0.1) = 1.479 \qquad \{\text{Table 5.2}\}$$

and the sway critical load in direction *y* is

$$N_{cr,y} = N_l + K_e + (\quad - \quad - 1) s N_l$$

$$= 2494 + 410.5 + (1.479 - 0.1646 - 1) 0.9026 \cdot 2494 = 3612 \text{ MN} \qquad \{5.18\}$$

The third term represents the effect of the interaction between the bending and shear modes and it amounts to 19.6% of the total critical load.

11.1.3 Sway buckling in direction *x*

The participating bracing units in direction *x* are Units 1, 3, 5, 6, 7 and 8.

The original shear stiffness originates from the two frameworks (Units 1 and 3):

$$K = \sum_{i=1}^{f} K_i = K_1 + K_3 = 2 \cdot 369.9 = 739.8 \text{ MN} \qquad \{5.5\}$$

With the effectiveness factors of Units 1 and 3 [Equation {5.9} at Unit 1 in Section 11.1.1], the effective shear stiffness is

$$K_e = \sum_1^f K_i s_i = 2 \cdot 369.9 \cdot 0.9647 = 713.7 \text{ MN} \qquad \{5.10\}$$

The effectiveness factor for the whole system is

$$s = \frac{K_e}{K} = \frac{713.7}{739.8} = 0.9647 \qquad \{5.11\}$$

The bending stiffness of the system is

$$EI = E_c I_c + E_w I_w = E_c \sum_1^f I_{c,i} r_i + E_w \sum_1^m I_{w,i}$$

$$= 23 \cdot 10^3 \left(13 \cdot \frac{0.4^4}{12} 0.471 \cdot 2 + 20.01 \right) = 4.607 \cdot 10^5 \text{ MNm}^2 \qquad \{5.12\}$$

where the first term stands for the contribution of the columns of the frameworks. It amounts to 0.13% and can safely be neglected. The second term represents the four cores, according to the fifth column in Table 11.2.

The local bending critical load can now be calculated:

$$N_l = \frac{7.837 r_s EI}{H^2} = \frac{7.837 \cdot 0.933 \cdot 4.607 \cdot 10^5}{66^2} = 773.3 \text{ MN} \qquad \{5.13\}$$

Using the part critical load ratio

$$= \frac{K_e}{N_l} = \frac{713.7}{773.3} = 0.923 \qquad \{5.17\}$$

the critical load parameter is obtained from Table 5.2 as

$$= 3.3488 + \frac{3.5758 - 3.3488}{1.0 - 0.9} (0.923 - 0.9) = 3.40 \qquad \{\text{Table 5.2}\}$$

and the sway critical load in direction x is

$$N_{cr,x} = N_l + K_e + (\quad - \quad - 1) s N_l$$

$$= 773.3 + 713.7 + (3.4 - 0.923 - 1) 0.9647 \cdot 773.3 = 2589 \text{ MN} \qquad \{5.18\}$$

The third term represents the effect of the interaction between the bending and shear modes and it amounts to 42.6% of the total critical load.

11.1.4 Pure torsional buckling

With the coordinates of the centroid in the coordinate system *x*-*y* (Figure 11.1)

$$x_c = \frac{L}{2} - \bar{x}_o = \frac{36}{2} - 18.329 = 0.329 \text{ m} \qquad \{5.42\}$$

and

$$y_c = \frac{B}{2} - \bar{y}_o = \frac{20}{2} - 9.265 = 0.735 \text{ m} \qquad \{5.42\}$$

the distance between the shear centre and the centroid is

$$t = \sqrt{x_c^2 + y_c^2} = \sqrt{0.329^2 + 0.735^2} = 0.805 \text{ m}$$

With the above data, the radius of gyration is

$$i_p = \sqrt{\frac{L^2 + B^2}{12} + t^2} = \sqrt{\frac{36^2 + 20^2}{12} + 0.805^2} = 11.91 \text{ m} \qquad \{5.28\}$$

The "original" Saint-Venant torsional stiffness consists of two parts. In addition to the Saint-Venant torsional stiffness of the individual bracing cores, those units that have shear stiffness (i.e. the frameworks) also contribute:

$$(GJ) = \sum_1^m GJ_k + \sum_1^f \left((K_i)_x y_i^2 + (K_i)_y x_i^2 \right) \qquad \{5.35\}$$

$$= 9583 \cdot 0.47 + 369.9(9.265^2 + 10.74^2) + 227.4(17.67^2 + 18.33^2) = 226328 \text{ MNm}^2$$

The first term represents the "own" contribution of the cores and it amounts to 2% of the total Saint-Venant torsional stiffness.

The real (effective) Saint-Venant stiffness is always smaller than the "original" one as the effect of the frameworks is limited by their effectiveness factor:

$$(GJ)_e = \sum_1^m GJ_k + \sum_1^f \left((K_{e,i})_x y_i^2 + (K_{e,i})_y x_i^2 \right) =$$

$$= 9583 \cdot 0.47 + 369.9 \cdot 0.9647(9.265^2 + 10.74^2) + 227.4 \cdot 0.9026(17.67^2 + 18.33^2)$$

$$= 209344 \text{ MNm}^2 \qquad \{5.29\}$$

The effectiveness of the Saint-Venant torsional stiffness for the whole system can now be determined:

$$s = \frac{(GJ)_e}{(GJ)} = \frac{209344}{226328} = 0.925 \qquad \{5.34\}$$

The warping stiffness of the system comes from three sources: the own warping stiffness of the cores, the bending stiffness of the walls and the bending stiffness of the columns of the frameworks [Equation (5.30)]. When the first two items exist, the contribution of the third is normally negligible. This is the case now and the third source is neglected below. In addition, in this special case, the vertical distance between the shear centre of the cores and the shear centre of the system is very small (last column in Table 11.2) and the contribution of the second moment of area of the cores with respect to axis x is also ignored. Hence, the warping stiffness is calculated as:

$$EI_\Omega = E_w \sum_1^m \left(I_{\Omega k} + (I_{w,k})_x y_k^2 + (I_{w,k})_y x_k^2 \right) \qquad \{5.30\}$$

$$= 23 \cdot 10^3 \left((239 + (15.68 \cdot 5.74^2 + 16.99 \cdot 5.84^2 + 10.12 \cdot 4.83^2 + 21.8 \cdot 4.79^2) \right)$$

$$= 47640874 \text{ MNm}^4$$

The first term represents the "own" contribution of the cores and it amounts to 11.5% of the total warping torsional stiffness.

With the above stiffnesses, the part torsional critical loads can now be determined.

The warping torsional critical load of the system is

$$N_\Omega = \frac{7.837 r_s EI_\Omega}{i_p^2 H^2} = \frac{7.837 \cdot 0.933 \cdot 47640874}{11.91^2 \cdot 66^2} = 563.8 \text{ MN} \qquad \{5.32\}$$

and the Saint-Venant torsional critical load is

$$N_t = \frac{(GJ)_e}{i_p^2} = \frac{209344}{11.91^2} = 1476 \text{ MN} \qquad \{5.33\}$$

As a function of the ratio of the above part critical loads

$$= \frac{N_t}{N_\Omega} = \frac{1476}{563.8} = 2.618 \qquad \{5.36\}$$

the critical load parameter is obtained from Table 5.2:

$$= 5.624 + \frac{7.427 - 5.624}{3.0 - 2.0}(2.618 - 2.0) = 6.738 \qquad \{\text{Table 5.2}\}$$

Finally, the critical load of pure torsional buckling is

$$N_{cr,} = N_\Omega + N_t + (\quad - \quad -1)s \; N_\Omega$$

$$= 563.8 + 1476 + (6.738 - 2.618 - 1)0.925 \cdot 563.8 = 3667 \text{ MN} \qquad \{5.31\}$$

The third term represents the effect of the interaction between the Saint-Venant and warping torsional modes. It amounts to a considerable 44% of the total torsional critical load.

11.1.5 Coupling of the basic critical loads: the global critical load of the building

The centroid of the layout does not coincide with the shear centre so there is a coupling of basic critical loads $N_{cr,x}$, $N_{cr,y}$ and $N_{cr,\varphi}$. As the centroid does not even lie on one of the principal axes, this coupling is a triple one. Any coupling reduces the value of the critical load so, theoretically, the effect of coupling must be taken into account. Eccentricity parameters τ_x and τ_y are needed for the exact calculation of the coupling of the critical loads:

$$_x = \frac{x_c}{i_p} = \frac{0.329}{11.91} = 0.0276 \qquad \text{and} \qquad _y = \frac{y_c}{i_p} = \frac{0.735}{11.91} = 0.0617 \qquad \{5.41\}$$

With the eccentricity parameters, the smallest root of the cubic equation

$$(N)^3 + b_2(N)^2 + b_1 N - b_0 = 0 \qquad \{5.39\}$$

is the critical load, where

$$b_0 = \frac{N_{cr,x}N_{cr,y}N_{cr,}}{1 - {}^2_x - {}^2_y} = \frac{2589 \cdot 3612 \cdot 3667}{1 - 0.0276^2 - 0.0617^2} = 3.445 \cdot 10^{10} \qquad \{5.40\}$$

$$b_1 = \frac{N_{cr,x}N_{cr,y} + N_{cr,}\;N_{cr,x} + N_{cr,}\;N_{cr,y}}{1 - {}^2_x - {}^2_y} \qquad \{5.40\}$$

$$= \frac{2589 \cdot 3612 + 3667 \cdot 2592 + 3667 \cdot 3612}{1 - 0.0276^2 - 0.0617^2} = 3.225 \cdot 10^7$$

$$b_2 = \frac{N_{cr,x}\ {}^2_x + N_{cr,y}\ {}^2_y - N_{cr,x} - N_{cr,y} - N_{cr,}}{1 - {}^2_x - {}^2_y} = -9897 \qquad \{5.40\}$$

The critical load (the smallest root of the above cubic equation) is

$$N_{cr} = 2567 \text{ MN}$$

As the very small values of eccentricity parameters τ_x and τ_y indicated, the coupling of the basic modes only had a small effect on the global critical load: the reduction (from 2589 MN to 2567 MN) is less than 1%.

The approximate formula [Equation {5.43}] would result in

$$N_{cr} = \left(\frac{1}{N_{cr,x}} + \frac{1}{N_{cr,y}} + \frac{1}{N_{cr,}} \right)^{-1} = \left(\frac{1}{2589} + \frac{1}{3612} + \frac{1}{3667} \right)^{-1} = 1069 \text{ MN}$$

for the critical load. It is a very conservative value, due to the fact that the eccentricity of the system is very small.

11.1.6 The global critical load ratio

Assuming a uniformly distributed vertical floor load of $Q = 10$ kN/m^2, the total vertical load on the building is

$$N = LBQn = 36 \cdot 20 \cdot 0.01 \cdot 22 = 158.4 \text{ MN} \qquad \{6.2\}$$

The global critical load ratio is therefore

$$= \frac{N_{cr}}{N} = \frac{2567}{158.4} = 16.2 \qquad \{6.3\}$$

indicating a satisfactory bracing system.

The condition

$$\geq 10 \qquad \{6.5\}$$

is satisfied, so any vertical load bearing element can be considered as braced (by the bracing system) and the second-order effects (due to sway and torsion) can be neglected.

11.2 THE FUNDAMENTAL FREQUENCY

The mass distribution factor is obtained from Table 4.1 as a function of the number of storeys:

$$r_f = \sqrt{\frac{n}{n+2.06}} = \sqrt{\frac{22}{22+2.06}} = 0.956 \qquad \{\text{Table 4.1}\}$$

With $\gamma = 3.0$, the mass density per unit length for the building is

$$m = \quad A = \frac{A}{g} = \frac{3 \cdot 36 \cdot 20}{9.81} = 220.2 \text{ kg/m} \qquad \{4.7\}$$

11.2.1 Individual bracing units

The basic shear and bending stiffness characteristics of the two different frameworks are determined in this section for later use. The stiffness characteristics of the four cores will be incorporated into the continuum model directly.

Bracing Unit 1 (framework, identical to Bracing Unit 3)

The shear stiffness that is associated with the beams of the framework is unchanged [or, if a stability analysis had not been carried out, given by (4.2)]:

$$K_{b,1} = \sum_{j=1}^{n-1} \frac{12 E_b I_{b,j}}{l_j h} = 12 \frac{12 \cdot 23 \cdot 10^6 \cdot 0.40^4}{12 \cdot 3 \cdot 3} = 785067 \text{ kN} \qquad \{5.1\} \text{ or } \{4.2\}$$

The shear stiffness that is associated with the columns of the framework is

$$K_{c,1} = \sum_{j=1}^{n} \frac{12 E_c I_{c,j}}{h^2} = 13 \frac{12 \cdot 23 \cdot 10^6 \cdot 0.40^4}{12 \cdot 3^2} = 850489 \text{ kN} \qquad \{4.3\}$$

The combination of the two part shear stiffnesses gives the “original” shear stiffness of the framework:

$$K_1 = K_{b,1} \frac{K_{c,1}}{K_{b,1} + K_{c,1}} = 785067 \frac{850489}{785067 + 850489} = 408235 \text{ kN} \qquad \{4.1\}$$

where

$$r_1 = \frac{K_{c,1}}{K_{b,1} + K_{c,1}} = \frac{850489}{785067 + 850489} = 0.520 \qquad \{4.4\}$$

is the reduction factor.

The square of the frequency associated with the "original" shear stiffness of Unit 1 is

$$f_{s',1}^2 = \frac{1}{(4H)^2}\frac{r_f^2 K_1}{m} = \frac{0.956^2 \cdot 408235}{(4 \cdot 66)^2 \cdot 220.2} = 0.0243\,\text{Hz}^2 \qquad \{4.6\}$$

The global second moment of area of the cross-sections of the columns is unchanged [or, if a stability analysis had not been carried out, given by (4.9)]:

$$I_{g,1} = \sum_{j=1}^{n} A_{c,j} t_j^2 = 0.4^2 \cdot 2(18^2 + 15^2 + 12^2 + 9^2 + 6^2 + 3^2) = 262.08\,\text{m}^4 \qquad \{4.9\}$$

The square of the frequency associated with the global full-height bending vibration of the framework is

$$f_{g,1}^2 = \frac{0.313 r_f^2 E_c I_{g,1}}{H^4 m} = \frac{0.313 \cdot 0.956^2 \cdot 23 \cdot 10^6 \cdot 262.08}{66^4 \cdot 220.2} = 0.4127\,\text{Hz}^2 \qquad \{4.8\}$$

The factor of effectiveness for the first bracing unit is

$$s_{f,1}^2 = \frac{f_{g,1}^2}{f_{g,1}^2 + f_{s',1}^2} = \frac{0.4127}{0.4127 + 0.0243} = 0.9444 \qquad \{4.10\}$$

Bracing Unit 2 (framework, identical to Bracing Unit 4)

The shear stiffness that is associated with the beams of the framework is unchanged [or, if a stability analysis had not been carried out, given by (4.2)]:

$$K_{b,2} = \sum_{j=1}^{n-1} \frac{12 E_b I_{b,j}}{l_j h} = 7\frac{12 \cdot 23 \cdot 10^6 \cdot 0.40^4}{12 \cdot 2.85 \cdot 3} = 482058\,\text{kN} \qquad \{5.1\} \text{ or } \{4.2\}$$

The shear stiffness that is associated with the columns of the framework is

$$K_{c,2} = \sum_{j=1}^{n} \frac{12 E_c I_{c,j}}{h^2} = 8\frac{12 \cdot 23 \cdot 10^6 \cdot 0.40^4}{12 \cdot 3^2} = 523378\,\text{kN} \qquad \{4.3\}$$

The combination of the two part shear stiffnesses gives the "original" shear stiffness of the framework:

$$K_2 = K_{b,2}\frac{K_{c,2}}{K_{b,2} + K_{c,2}} = 482058\frac{523378}{482058 + 523378} = 250934\,\text{kN} \qquad \{4.1\}$$

where the reduction factor

$$r_2 = \frac{K_{c,2}}{K_{b,2} + K_{c,2}} = \frac{523378}{482058 + 523378} = 0.5205 \qquad \{4.4\}$$

is used.

The square of the frequency associated with the "original" shear stiffness of Unit 2 is

$$f_{s',2}^2 = \frac{1}{(4H)^2} \frac{r_f^2 K_2}{m} = \frac{0.956^2 \cdot 250934}{(4 \cdot 66)^2 \cdot 220.2} = 0.01494 \text{ Hz}^2 \qquad \{4.6\}$$

The global second moment of area of the cross-sections of the columns is unchanged [or, if a stability analysis had not been carried out, given by (4.9)]:

$$I_{g,2} = \sum_{j=1}^{n} A_{c,j} t_j^2 = 0.4^2 \cdot 2(9.975^2 + 7.125^2 + 4.275^2 + 1.425^2) = 54.58 \text{ m}^4 \qquad \{4.9\}$$

The square of the frequency associated with the global full-height bending vibration of the framework is

$$f_{g,2}^2 = \frac{0.313 r_f^2 E_c I_{g,2}}{H^4 m} = \frac{0.313 \cdot 0.956^2 \cdot 23 \cdot 10^6 \cdot 54.58}{66^4 \cdot 220.2} = 0.08595 \text{ Hz}^2 \qquad \{4.8\}$$

The factor of effectiveness for Bracing Unit 2 is

$$s_{f,2}^2 = \frac{f_{g,2}^2}{f_{g,2}^2 + f_{s',2}^2} = \frac{0.08595}{0.08595 + 0.01494} = 0.8519 \qquad \{4.10\}$$

11.2.2 Lateral vibration in direction *y*

The participating bracing units in direction *y* are Units 2, 4, 5, 6, 7 and 8.

The original shear stiffness originates from the two frameworks (Units 2 and 4):

$$K = \sum_{i=1}^{f} K_i = K_2 + K_4 = 2 \cdot 250934 = 501868 \text{ kN} \qquad \{4.5\}$$

With the effectiveness factors of Unit 2 and 4 [{4.10} above], the effective shear stiffness is

$$K_e = \sum_1^f K_i s_i^2 = 2 \cdot 250934 \cdot 0.8519 = 427541 \text{ kN} \qquad \{4.11\}$$

The effectiveness factor for the whole system is

$$s_f = \sqrt{\frac{K_e}{K}} = \sqrt{\frac{427541}{501868}} = 0.923 \qquad \{4.12\}$$

The square of the frequency which is associated with shear deformation can now be determined using the effective shear stiffness:

$$f_s^2 = \frac{1}{(4H)^2} \frac{r_f^2 K_e}{m} = \frac{0.956^2 \cdot 427541}{(4 \cdot 66)^2 \cdot 220.2} = 0.02546 \text{ Hz}^2 \qquad \{4.13\}$$

With EI already available from the stability analysis, the square of the frequency of the system in bending is obtained from

$$f_b^2 = \frac{0.313 r_f^2 EI}{H^4 m} = \frac{0.313 \cdot 0.956^2 \cdot 1.486 \cdot 10^9}{66^4 \cdot 220.2} = 0.1017 \text{ Hz}^2 \qquad \{4.15\}$$

With the non-dimensional parameter

$$k = H\sqrt{\frac{K_e}{EI}} = 66\sqrt{\frac{427541}{1.486 \cdot 10^9}} = 1.1195 \qquad \{4.17\}$$

the frequency parameter is obtained from Table 4.2 as

$$= 0.6542 + \frac{0.7511 - 0.6542}{0.5}(1.1195 - 1) = 0.677 \qquad \{\text{Table 4.2}\}$$

The lateral frequency of the building in direction y is

$$f_y = \sqrt{f_b^2 + f_s^2 + \left(\frac{2}{0.313} - \frac{k^2}{5} - 1\right) s_f f_b^2} \qquad \{4.18\}$$

$$= \sqrt{0.1017 + 0.02546 + \left(\frac{0.677^2}{0.313} - \frac{1.1195^2}{5} - 1\right) 0.923 \cdot 0.1017} = 0.384 \text{ Hz}$$

The third term covers the effect of the interaction between the bending and shear modes and represents a 13.6% increase in the value of the lateral frequency.

11.2.3 Lateral vibration in direction *x*

The participating bracing units in direction *x* are Units 1, 3, 5, 6, 7 and 8.

The original shear stiffness originates from the two frameworks (Units 1 and 3):

$$K = \sum_{i=1}^{f} K_i = K_2 + K_4 = 2 \cdot 408235 = 816470 \text{ kN} \qquad \{4.5\}$$

With the effectiveness factors of Unit 1 and 3 [{4.10} in Section 11.2.1], the effective shear stiffness is

$$K_e = \sum_{1}^{f} K_i s_i^2 = 2 \cdot 408235 \cdot 0.9444 = 771074 \text{ kN} \qquad \{4.11\}$$

The effectiveness factor for the whole system is

$$s_f = \sqrt{\frac{K_e}{K}} = \sqrt{\frac{771074}{816470}} = 0.9718 \qquad \{4.12\}$$

The square of the frequency which is associated with shear deformation can now be determined using the effective shear stiffness:

$$f_s^2 = \frac{1}{(4H)^2} \frac{r_f^2 K_e}{m} = \frac{0.956^2 \cdot 771074}{(4 \cdot 66)^2 \cdot 220.2} = 0.0459 \text{ Hz}^2 \qquad \{4.13\}$$

With using bending stiffness *EI* from the stability analysis, the square of the frequency of the system in bending is obtained from

$$f_b^2 = \frac{0.313 r_f^2 EI}{H^4 m} = \frac{0.313 \cdot 0.956^2 \cdot 4.607 \cdot 10^8}{66^4 \cdot 220.2} = 0.0315 \text{ Hz}^2 \qquad \{4.15\}$$

With the non-dimensional parameter

$$k = H\sqrt{\frac{K_e}{EI}} = 66\sqrt{\frac{771074}{4.607 \cdot 10^8}} = 2.70 \qquad \{4.17\}$$

the frequency parameter is obtained from Table 4.2 as

$$= 0.9809 + \frac{1.1014 - 0.9809}{3.0 - 2.5}(2.7 - 2.5) = 1.029 \qquad \{\text{Table 4.2}\}$$

The lateral frequency of the building in direction *x* is

$$f_x = \sqrt{f_b^2 + f_s^2 + \left(\frac{^2}{0.313} - \frac{k^2}{5} - 1\right) s_f\, f_b^2} \qquad \{4.18\}$$

$$= \sqrt{0.0315 + 0.0459 + \left(\frac{1.029^2}{0.313} - \frac{2.7^2}{5} - 1\right) 0.9718 \cdot 0.0315} = 0.325 \text{ Hz}$$

The third term covers the effect of the interaction between the bending and shear modes and represents a 26.9% increase in the value of the lateral frequency.

11.2.4 Pure torsional vibration

All the bracing units participate in torsional vibration.

The effective Saint-Venant torsional stiffness of the system comes from the Saint-Venant torsional stiffness of the cores and the effective shear stiffness of the frameworks:

$$(GJ)_e = \sum_1^m GJ_k + \sum_1^f \left((K_{e,i})_x y_i^2 + (K_{e,i})_y x_i^2\right) = 9.583 \cdot 10^6 \cdot 0.47 + \qquad \{4.21\}$$

$$+ 408235 \cdot 0.9444(9.265^2 + 10.74^2) + 250934 \cdot 0.8519(17.67^2 + 18.33^2)$$

$$= 220.6 \cdot 10^6 \text{ kNm}^2$$

The original Saint-Venant torsional stiffness is

$$(GJ) = \sum_1^m GJ_k + \sum_1^f \left((K_i)_x y_i^2 + (K_i)_y x_i^2\right) \qquad \{4.27\}$$

$$= 9.583 \cdot 10^6 \cdot 0.47 + 408235(9.265^2 + 10.74^2) + 250934(17.67^2 + 18.33^2)$$

$$= 249.3 \cdot 10^6 \text{ kNm}^2$$

The effectiveness of the Saint-Venant torsional stiffness is

$$s = \sqrt{\frac{(GJ)_e}{(GJ)}} = \sqrt{\frac{220.6}{249.3}} = \sqrt{0.8849} = 0.9407 \qquad \{4.26\}$$

The square of the pure torsional frequency associated with the Saint-Venant torsional stiffness is

$$f_t^2 = \frac{r_f^2 (GJ)_e}{16 i_p^2 H^2 m} = \frac{0.956^2 \cdot 220.6 \cdot 10^6}{16 \cdot 11.91^2 \cdot 66^2 \cdot 220.2} = 0.0926 \text{ Hz}^2 \qquad \{4.25\}$$

With the value of EI_ω already available from the stability analysis, the square of the pure torsional frequency associated with the warping torsional stiffness is

$$f_\Omega^2 = \frac{0.313 r_f^2 EI_\Omega}{i_p^2 H^4 m} = \frac{0.313 \cdot 0.956^2 \cdot 4.764 \cdot 10^{10}}{11.91^2 \cdot 66^4 \cdot 220.2} = 0.0230 \text{ Hz}^2 \qquad \{4.24\}$$

As a function of torsion parameter

$$k = H \sqrt{\frac{(GJ)_e}{EI_\Omega}} = 66 \sqrt{\frac{220.6 \cdot 10^6}{4.764 \cdot 10^{10}}} = 4.49 \qquad (4.28)$$

the frequency parameter is obtained from Table 4.2:

$$= 1.3437 + \frac{1.465 - 1.3437}{4.5 - 4.0}(4.49 - 4.0) = 1.463 \qquad \{\text{Table 4.2}\}$$

With the above part frequencies and stiffness characteristics, the fundamental frequency for pure torsional vibration is

$$f = \sqrt{f_\Omega^2 + f_t^2 + \left(\frac{^2}{0.313} - \frac{k^2}{5} - 1 \right) s \; f_\Omega^2} \qquad \{4.23\}$$

$$= \sqrt{0.023 + 0.0926 + \left(\frac{1.463^2}{0.313} - \frac{4.49^2}{5} - 1 \right) 0.9407 \cdot 0.023} = 0.393 \text{ Hz}^2$$

The interaction between the Saint-Venant and warping torsional modes—third term—amounts to a 25.3% increase in the value of the torsional frequency.

11.2.5 Coupling of the basic frequencies: the fundamental frequency of the building

As the centroid of the layout does not coincide with the shear centre, the coupling of the basic frequencies has to be considered. Using the values of the basic frequencies f_x, f_y and f_φ—or rather their squares—and the eccentricity parameters τ_x

and τ_y, the smallest root of the cubic equation

$$\left(f^2\right)^3 + a_2\left(f^2\right)^2 + a_1 f^2 - a_0 = 0 \qquad \{4.31\}$$

is the fundamental frequency of the building. With

$$a_0 = \frac{f_x^2 f_y^2 f^2}{1 - \frac{2}{x} - \frac{2}{y}} = \frac{0.384^2 \cdot 0.325^2 \cdot 0.393^2}{1 - 0.0276^2 - 0.0617^2} = 0.00242 \qquad \{4.32\}$$

$$a_1 = \frac{f_x^2 f_y^2 + f^2 f_x^2 + f^2 f_y^2}{1 - \frac{2}{x} - \frac{2}{y}}$$

$$= \frac{0.384^2 \cdot 0.325^2 + 0.393^2 \cdot 0.384^2 + 0.393^2 \cdot 0.325^2}{1 - 0.0276^2 - 0.0617^2} = 0.0549$$

$$a_2 = \frac{f_x^2 \frac{2}{x} + f_y^2 \frac{2}{y} - f_x^2 - f_y^2 - f^2}{1 - \frac{2}{x} - \frac{2}{y}}$$

$$= \frac{0.384^2 \cdot 0.0276^2 + 0.325^2 \cdot 0.0617^2 - 0.384^2 - 0.325^2 - 0.393^2}{1 - 0.0276^2 - 0.0617^2} = -0.4089$$

the fundamental frequency is

$$f = 0.303 \text{ Hz}$$

The interaction among the basic modes results in a 6.7% reduction in the value of the fundamental frequency. This relatively small amount is due to the fact that the eccentricity of the bracing system is very small.

The approximate formula [Equation {4.35}] would result in

$$f = \left(\frac{1}{f_x^2} + \frac{1}{f_y^2} + \frac{1}{f^2}\right)^{-\frac{1}{2}} = \left(\frac{1}{0.384^2} + \frac{1}{0.325^2} + \frac{1}{0.393^2}\right)^{-\frac{1}{2}} = 0.210 \text{ Hz} \qquad \{4.35\}$$

for the fundamental frequency. This is a very conservative value, again, due to the fact that the eccentricity of the system is very small.

11.3 MAXIMUM DEFLECTION OF THE BUILDING

The building is subjected to a uniformly distributed horizontal load of intensity 1.3 kN/m^2 in direction y, which results in a wind load of w_y = 46.8 kN/m. Due to this load, the top of the building undergoes a uniform translation (defined by the translation of the shear centre) and an "uneven" translation (due to the rotation of the building around the shear centre). Accordingly, the maximum translation is determined in two steps.

11.3.1 Deflection of the shear centre axis

The participating bracing units in direction y are Units 2, 4, 5, 6, 7 and 8. The stiffnesses of these units are needed first.

Bracing Unit 2 (identical to Bracing Unit 4)

Stiffness characteristics K, I_g and I calculated earlier for the frequency analysis can be used here for establishing the following auxiliary quantities needed for the calculation of the top deflection of the framework:

$$a = \frac{K}{EI_g} = \frac{250934}{23\cdot 10^6 \cdot 54.58} = 0.0002 \qquad \{2.14\}$$

$$b = \frac{K}{EI} = \frac{250934}{23\cdot 10^6 \cdot 0.008055} = 1.3544$$

$$s = 1 + \frac{a}{b} = 1 + \frac{0.0002}{1.3544} \cong 1.0$$

$$= \sqrt{a+b} = 1.164\,, \qquad H = 1.164 \cdot 66 = 76.8$$

$$I_f = I + I_g = 0.008055 + 54.58 = 54.59\ \text{m}^4 \qquad \{2.23\}$$

With the above auxiliary quantities, the top deflection of the framework is

$$y_2 = \frac{wH^4}{8EI_f} + \frac{wH^2}{2Ks^2} - \frac{wEI}{K^2 s^3}\left(\frac{1 + H\sinh H}{\cosh H} - 1\right) = \frac{46.8\cdot 66^4}{8\cdot 23\cdot 10^6 \cdot 54.59} + \frac{46.8\cdot 66^2}{2\cdot 250934}$$

$$- \frac{46.8\cdot 23\cdot 10^6 \cdot 0.008055}{250934^2}\left(\frac{1 + 76.8\sinh(76.8)}{\cosh(76.8)} - 1\right) = 0.4842\ \text{m} \qquad \{2.24\}$$

and the stiffness of Units 2 and 4 is

$$S_{2y} = S_{4y} = \frac{1}{y_2} = \frac{1}{0.4842} = 2.065 \frac{1}{\text{m}} \qquad \{3.2\}$$

The top deflections of Units 5, 6, 7 and 8 in direction *y* are

$$y_5 = \frac{wH^4}{8EI_x} = \frac{46.8 \cdot 66^4}{8 \cdot 23 \cdot 10^6 \cdot 15.68} = 0.3078\,\text{m} \qquad \{2.83\}$$

$$y_6 = \frac{wH^4}{8EI_x} = \frac{46.8 \cdot 66^4}{8 \cdot 23 \cdot 10^6 \cdot 16.99} = 0.2841\,\text{m} \qquad \{2.83\}$$

$$y_7 = \frac{wH^4}{8EI_x} = \frac{46.8 \cdot 66^4}{8 \cdot 23 \cdot 10^6 \cdot 10.12} = 0.4769\,\text{m} \qquad \{2.83\}$$

$$y_8 = \frac{wH^4}{8EI_x} = \frac{46.8 \cdot 66^4}{8 \cdot 23 \cdot 10^6 \cdot 21.8} = 0.2214\,\text{m} \qquad \{2.83\}$$

and the corresponding stiffnesses are

$$S_{5y} = \frac{1}{y_5} = \frac{1}{0.3078} = 3.249 \frac{1}{\text{m}}, \qquad S_{6y} = \frac{1}{y_6} = \frac{1}{0.2841} = 3.520 \frac{1}{\text{m}} \qquad \{3.2\}$$

$$S_{7y} = \frac{1}{y_7} = \frac{1}{0.4769} = 2.097 \frac{1}{\text{m}}, \qquad S_{8y} = \frac{1}{y_8} = \frac{1}{0.2214} = 4.517 \frac{1}{\text{m}} \qquad \{3.2\}$$

The sum of the stiffnesses is

$$\sum_{i=1}^{6} S_{i,y} = 17.513 \frac{1}{\text{m}}$$

Bracing Unit 2 is the base unit (as there are only two—identical—frameworks in the system). The apportioner related to Unit 2 is

$$q_2 = \frac{S_{2y}}{\sum S_{i,y}} = \frac{2.065}{17.513} = 0.1179 \qquad \{3.3\}$$

and the load share on the Base Unit (Bracing Unit 2) is

$$\overline{w} = w_y q_2 = 46.8 \cdot 0.1179 = 5.518\ \text{kN/m} \qquad \{3.16\}$$

With

$$a_1 = \frac{EI_4}{EI} = 1, \qquad b_1 = \frac{K_4}{K} = 1 \qquad \text{and} \qquad c_1 = \frac{EI_{g,4}}{EI_g} = 1 \qquad \{3.16\}$$

$$\bar{a} = \frac{K}{EI_g} \frac{1 + \sum_{j=1}^{f-1} \frac{a_j}{c_j}}{1 + \sum_{j=1}^{f-1} \frac{a_j}{b_j}} = \frac{250934}{23 \cdot 10^6 \cdot 54.58} \frac{1+1}{1+1} = 0.0002$$

$$\bar{b} = \frac{K}{EI} \frac{f}{1 + \sum_{j=1}^{f-1} \frac{a_j}{b_j}} = \frac{250934}{23 \cdot 10^6 \cdot 0.008055} \frac{2}{1+1} = 1.35$$

$$\bar{s} = 1 + \frac{\bar{a}}{\bar{b}} = 1 + \frac{0.0002}{1.35} = 1.00015 \cong 1.0 \qquad \{3.13\}$$

$$\bar{} = \sqrt{\bar{a} + \bar{b}} = \sqrt{0.0002 + 1.35} = 1.162, \qquad \bar{H} = 1.162 \cdot 66 = 76.7$$

the top deflection of the shear centre axis is

$$v_o = \frac{\bar{w} H^4}{8EI_f} + \frac{\bar{w} H^2}{2K\bar{s}^2} - \frac{\bar{w} EI}{K^2 \bar{s}^3} \left(\frac{1 + \bar{H} \sinh \bar{H}}{\cosh \bar{H}} - 1 \right) = \frac{5.518 \cdot 66^4}{8 \cdot 23 \cdot 10^6 \cdot 54.59} + \frac{5.518 \cdot 66^2}{2 \cdot 250934}$$

$$- \frac{5.518 \cdot 23 \cdot 10^6 \cdot 0.008055}{250934^2} \left(\frac{1 + 76.7 \sinh(76.7)}{\cosh(76.7)} - 1 \right) = 0.0571 \text{ m} \qquad \{3.14\}$$

The second part of the maximum deflection of the building comes from the rotation of the building around the shear centre, which causes additional deflection, in this case, at the right-hand size of the building. This additional deflection can be very great in many practical cases. However, in this particular case, because of the closeness of the centroid and the shear centre (x_c = 0.329 m, calculated in Section 11.1.4), structural engineering common sense says that this additional deflection is very small and is probably negligible. For the sake of completeness, however, the calculation of this additional deflection is presented in the following.

The rotation of the building around the shear centre is determined first.

11.3.2 Rotation around the shear centre axis

The torsional moment that causes this rotation is

$$m_t = w_y x_c = 46.8 \cdot 0.329 = 15.4 \text{ kNm/m} \qquad \{3.29\}$$

The participating bracing units are Units 1, 2, 3, 4, 5, 6, 7 and 8. The missing stiffness characteristics are calculated first.

Bracing Unit 1 (identical to Bracing Unit 3)

Stiffness characteristics K, I_g and I calculated earlier for the frequency analysis can be used here for establishing the following auxiliary quantities needed for the calculation of the top deflection of the framework:

$$a = \frac{K}{EI_g} = \frac{408235}{23 \cdot 10^6 \cdot 262.08} = 0.000068 \qquad \{2.14\}$$

$$b = \frac{K}{EI} = \frac{408235}{23 \cdot 10^6 \cdot 0.01306} = 1.3591, \qquad s = 1 + \frac{a}{b} = 1 + \frac{0.000068}{1.3591} \cong 1.0$$

$$= \sqrt{a + b} = 1.166, \qquad H = 1.166 \cdot 66 = 76.9$$

$$I_f = I + I_g = 0.01306 + 262.08 = 262.09 \text{ m}^4 \qquad \{2.23\}$$

With the above auxiliary quantities, the top deflection of the framework is

$$x_1 = \frac{wH^4}{8EI_f} + \frac{wH^2}{2Ks^2} - \frac{wEI}{K^2 s^3}\left(\frac{1 + H \sinh H}{\cosh H} - 1\right) = \frac{46.8 \cdot 66^4}{8 \cdot 23 \cdot 10^6 \cdot 262.09} + \frac{46.8 \cdot 66^2}{2 \cdot 408235}$$

$$- \frac{46.8 \cdot 23 \cdot 10^6 \cdot 0.01306}{408235^2}\left(\frac{1 + 76.9 \sinh(76.9)}{\cosh(76.9)} - 1\right) = 0.2617 \text{ m} \qquad \{2.24\}$$

and the stiffness of Units 1 and 3 is

$$S_{1x} = S_{3x} = \frac{1}{x_1} = \frac{1}{0.2617} = 3.821 \frac{1}{\text{m}} \qquad \{3.2\}$$

The stiffnesses of the four cores in direction x are also needed. Based on their maximum deflection in direction x

$$x_5 = \frac{wH^4}{8EI_y} = \frac{46.8 \cdot 66^4}{8 \cdot 23 \cdot 10^6 \cdot 5.021} = 0.9612 \text{ m} \qquad \{2.82\}$$

$$x_6 = \frac{wH^4}{8EI_y} = \frac{46.8 \cdot 66^4}{8 \cdot 23 \cdot 10^6 \cdot 3.685} = 1.3097\,\text{m} \qquad \{2.82\}$$

$$x_7 = \frac{wH^4}{8EI_y} = \frac{46.8 \cdot 66^4}{8 \cdot 23 \cdot 10^6 \cdot 1.296} = 3.7239\,\text{m} \qquad \{2.82\}$$

$$x_8 = \frac{wH^4}{8EI_y} = \frac{46.8 \cdot 66^4}{8 \cdot 23 \cdot 10^6 \cdot 10.00} = 0.4826\,\text{m} \qquad \{2.82\}$$

the corresponding stiffnesses are

$$S_{5x} = \frac{1}{x_5} = \frac{1}{0.9612} = 1.040\,\frac{1}{\text{m}}, \qquad S_{6x} = \frac{1}{x_6} = \frac{1}{1.3097} = 0.7635\,\frac{1}{\text{m}} \qquad \{3.2\}$$

$$S_{7x} = \frac{1}{x_7} = \frac{1}{3.7239} = 0.2685\,\frac{1}{\text{m}}, \qquad S_{8x} = \frac{1}{x_8} = \frac{1}{0.4826} = 2.072\,\frac{1}{\text{m}} \qquad \{3.2\}$$

Using the lateral stiffnesses and the distances of the bracing units from the shear centre, it is now possible to determine the torsional stiffnesses:

$$S_{\Omega 1x} = y_1^2 S_{1x} = 9.265^2 \cdot 3.821 = 328.00\,\text{m} \qquad \{3.25\}$$

$$S_{\Omega 2y} = x_2^2 S_{2y} = 17.67^2 \cdot 2.065 = 644.75\,\text{m} \qquad \{3.25\}$$

$$S_{\Omega 3x} = y_3^2 S_{3x} = 10.74^2 \cdot 3.821 = 440.74\,\text{m} \qquad \{3.25\}$$

$$S_{\Omega 4y} = x_4^2 S_{4y} = 18.33^2 \cdot 2.065 = 693.82\,\text{m} \qquad \{3.25\}$$

$$S_{\Omega 5x} = x_5^2 S_{5x} = 5.74^2 \cdot 1.040 = 34.27\,\text{m} \qquad \{3.25\}$$

$$S_{\Omega 5y} = y_5^2 S_{5y} = 0.365^2 \cdot 3.249 = 0.43\,\text{m} \qquad \{3.25\}$$

$$S_{\Omega 6x} = x_6^2 S_{6x} = 5.84^2 \cdot 0.7635 = 26.04\,\text{m} \qquad \{3.25\}$$

$$S_{\Omega 6y} = y_6^2 S_{6y} = 0.215^2 \cdot 3.52 = 0.16\,\text{m} \qquad \{3.25\}$$

$$S_{\Omega 7x} = x_7^2 S_{7x} = 4.83^2 \cdot 0.2685 = 6.26\,\text{m} \qquad \{3.25\}$$

$$S_{\Omega 7y} = y_7^2 S_{7y} = 0.215^2 \cdot 2.097 = 0.10\,\text{m} \qquad \{3.25\}$$

$$S_{\Omega 8x} = x_8^2 S_{8x} = 4.79^2 \cdot 2.072 = 47.54\,\text{m} \qquad \{3.25\}$$

$$S_{\Omega 8y} = y_8^2 S_{8y} = 0.115^2 \cdot 4.517 = 0.06\,\text{m} \qquad \{3.25\}$$

The sum of the torsional stiffnesses is

$$\sum_{i=1}^{12} S_{\Omega,i} = 2222.17$$

Bracing Unit 1 is the base unit as it has a (slightly) greater b-value than Bracing Unit 2.

The apportioner related to Unit 1 is

$$q_{\Omega,1} = \frac{S_{\Omega,1}}{\sum_{i=1}^{f+m} S_{\Omega,i}} = \frac{328.00}{2222.17} = 0.1476 \qquad \{3.26\}$$

and the moment share on Unit 1 is

$$\overline{m} = m_t q_{\Omega,1} = w x_c q_{\Omega,1} = 46.8 \cdot 0.329 \cdot 0.1476 = 2.2726\,\text{kNm/m} \qquad \{3.28\}$$

The stiffness characteristics of the base unit are:

$$EI_{\Omega} = EIy_1^2 = 23 \cdot 10^6 \cdot 0.01306 \cdot 9.265^2 = 25.785 \cdot 10^6\,\text{kNm}^4 \qquad \{3.19\}$$

$$EI_{g\Omega} = EI_g y_1^2 = 23 \cdot 10^6 \cdot 262.08 \cdot 9.265^2 = 517431 \cdot 10^6\,\text{kNm}^4 \qquad \{3.20\}$$

$$(GJ) = Ky_1^2 = 408235 \cdot 9.265^2 = 35.04 \cdot 10^6\,\text{kNm}^2 \qquad \{3.21\}$$

With stiffness ratios $\bar{a}$ and $\bar{b}$ from Equations {3.16}

$$\bar{a} = \frac{K}{EI_g} \frac{1 + \sum_{j=1}^{f-1} \frac{a_j}{c_j}}{1 + \sum_{j=1}^{f-1} \frac{a_j}{b_j}} = \frac{408235}{23 \cdot 10^6 \cdot 262.08} \frac{1 + 1 + \frac{0.008055}{0.01306} \frac{262.08}{54.58} 2}{1 + 1 + \frac{0.008055}{0.01306} \frac{408235}{250934} 2} = 0.000134$$

$$\bar{b} = \frac{K}{EI}\frac{f}{1+\sum_{j=1}^{f-1}\frac{a_j}{b_j}} = \frac{408235}{23\cdot 10^6\cdot 0.01306}\frac{4}{1+1+\frac{0.008055}{0.01306}\frac{408235}{250934}2} = 1.3567$$

and

$$s = 1+\frac{\bar{a}}{\bar{b}} = 1+\frac{0.000134}{1.3567} = 1.0001 \cong 1.0 \qquad \{3.13\}$$

$$= \sqrt{\bar{a}+\bar{b}} = \sqrt{1.357} = 1.165 \qquad \text{and} \qquad H = 76.9 \qquad \{3.13\}$$

the maximum rotation of the building is

$$_{\max} = \frac{\bar{m}H^4}{8E(I_\Omega + I_{g\Omega})} + \frac{\bar{m}H^2}{2K_\Omega \bar{s}^2} - \frac{\bar{m}EI_\Omega}{K_\Omega^2 \bar{s}^3}\left(\frac{1+\bar{H}\sinh\bar{H}}{\cosh\bar{H}} - 1\right)$$

$$= \frac{2.2726\cdot 66^4}{8\cdot 517457\cdot 10^6} + \frac{2.2726\cdot 66^2}{2\cdot 35.04\cdot 10^6} - \frac{2.2726\cdot 25.85\cdot 10^6}{(35.04\cdot 10^6)^2}\left(\frac{1+76.9\sinh(76.9)}{\cosh(76.9)} - 1\right)$$

$$= 0.0000104 + 0.0001413 - 0.0000036 = 0.0001481 \text{ rad} \qquad \{3.24\}$$

11.3.3 The maximum deflection of the building

The maximum deflection occurs at the right-hand corner of the building where the uniform translation and the additional translation due to the rotation of the building add up as:

$$v_{\max} = v(H) = v_o + \quad x_{\max} = 0.0571 + 0.0001481\cdot 17.67 =$$

$$= 0.0571 + 0.0026 = 0.0597 \text{ m} \qquad \{3.36\}$$

As structural engineering common sense indicated, the additional deflection due to the rotation of the building around the shear centre is small—4.3% of the total—compared to the uniform translation. This is due to the fact that the distance between the shear centre and the centroid of the layout is very short.

The recommended maximum deflection of the building is

$$v_{ASCE} = \frac{H}{500} = 0.132 \text{ m}$$

12

The global critical load ratio: a performance indicator

Chapter 6 introduced the global critical load ratio as the ratio of the global critical load to the total vertical load of the building. Through two sets of comprehensive series of worked examples involving different bracing system arrangements of the same building, it is shown in this chapter how the global critical load ratio is calculated in different situations. In addition, it is also shown here that the global critical load ratio is more than a simple ratio of two quantities; it also gives a strong indication regarding the performance of the structure. The greater the global critical load ratio, the better the performance of the bracing system, as far as the maximum top deflection, the fundamental frequency and the stability of the building are concerned.

The numbers of the equations used for the calculations are given in curly brackets on the right-hand side.

12.1 TEN-STOREY BUILDING BRACED BY TWO REINFORCED CONCRETE SHEAR WALLS AND TWO STEEL FRAMEWORKS

A ten-storey building with a storey height of $h = 3$ m will be considered for the case study. The length and breadth of the building are $L = 15$ m and $B = 9$ m. Two steel braced frameworks and two reinforced concrete shear walls are available for providing the building with sufficient stability. The modulus of elasticity for the columns, beams and diagonals of the steel frameworks is $E = 2 \cdot 10^5$ MN/m^2. The modulus of elasticity and the modulus of elasticity in shear for the reinforced concrete shear walls are $E = 25 \cdot 10^3$ MN/m^2 and $G = 10.42 \cdot 10^3$ MN/m^2, respectively. In addition to the four bracing units, concrete columns are also part of the vertical load carrying system but their contribution to the lateral and torsional stiffness is small compared to that of the bracing units and is therefore ignored for the calculation. It is assumed for the analysis that the shear walls only develop bending deformation.

Assume that the arrangement of the bracing units is up to the designer. Three different arrangements will be examined in order to show how the critical load ratio is able to monitor the performance of the bracing system and to find an optimum solution. The weight per unit volume of the building (for the dynamic analysis) is $\gamma = 3$ kN/m^3. A vertical floor load intensity of $Q = 10$ kN/m^2 is considered for the stability analysis and for the determination of the global critical load ratio. When the structures are subjected to lateral load and the top rotation and deflection are calculated, a uniformly distributed horizontal load of intensity

$q = 17.0$ kN/m is considered, whose resultant makes 50° with axis x. The load components of this wind load are

$$q_x = -17 \cdot \cos 50^\circ = -10.9 \text{ kN/m} \qquad \text{and} \qquad q_y = -17 \cdot \sin 50^\circ = -13.0 \text{ kN/m}$$

representing a total horizontal load with a resultant of $F = 510$ kN, whose components are

$$F_x = -327 \text{ kN} \qquad \text{and} \qquad F_y = -390 \text{ kN}$$

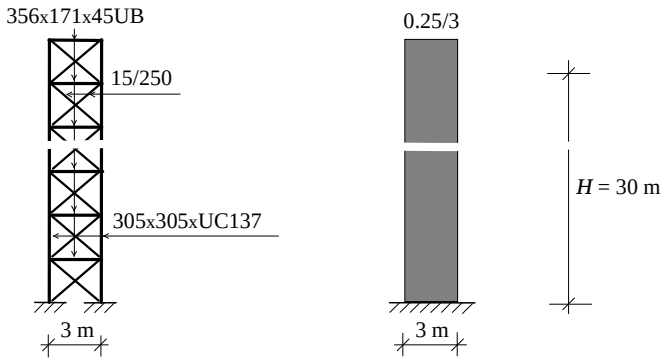

a) Steel braced frame b) Reinforced concrete shear wall

Figure 12.1 Bracing units for the ten-storey building.

The basic characteristics of the bracing units are summarised in Table 12.1.

Table 12.1 Cross-sectional characteristics for the bracing units.

Characteristics	Steel framework with double cross-bracing			Shear wall
	Columns	Beams	Diagonals	
Cross-section	305×305UC137	356×171×45UB	15/250	0.25 m×3 m
A [m^2]	$1.74 \cdot 10^{-2}$	$5.73 \cdot 10^{-3}$	$3.75 \cdot 10^{-3}$	0.75
I_1 [m^4]	$3.281 \cdot 10^{-4}$	$1.207 \cdot 10^{-4}$	$1.953 \cdot 10^{-5}$	0.5625
I_2 [m^4]	-	-	-	$3.906 \cdot 10^{-3}$
J [m^4]	-	-	-	$1.5625 \cdot 10^{-2}$

12.1.1 The critical load of the individual bracing units

Before the three different arrangements are investigated, the critical load of the shear wall and of the framework with double cross-bracing is calculated. For both structures, the load distribution factor is obtained from Table 5.1 as

$$r_s = 0.863 \qquad \{\text{Table 5.1}\}$$

Shear wall

The critical load of the shear wall is

$$N_{cr} = \frac{7.837 EIr_s}{H^2} = \frac{7.837 \cdot 25 \cdot 10^3 \cdot 0.5625 \cdot 0.863}{30^2} = 105.7 \text{ MN} \qquad \{2.74\}$$

Framework with double cross-bracing

The procedure for the calculation of the critical load of the braced frame is presented in Section 2.4.1. The shear stiffness of the framework is needed first:

$$K = 2A_d E_d \frac{hl^2}{d^3} = 2 \cdot 3.75 \cdot 10^{-3} \cdot 2 \cdot 10^5 \frac{3 \cdot 3^2}{4.243^3} = 530.2 \text{ MN} \qquad \{\text{Table 2.6}\}$$

The global second moment of area

$$I_g = \sum_1^n A_{c,i} t_i^2 = 1.74 \cdot 10^{-2} \cdot 1.5^2 \cdot 2 = 0.0783 \text{ m}^4 \qquad \{2.32\}$$

is needed for the full-height global bending buckling of the framework. This critical load is

$$N_g = \frac{7.837 r_s EI_g}{H^2} = \frac{7.837 \cdot 0.863 \cdot 2 \cdot 10^5 \cdot 7.83 \cdot 10^{-2}}{30^2} = 117.7 \text{ MN} \qquad \{2.63\}$$

With

$$_s = \frac{K}{N_g} = \frac{530.2}{117.7} = 4.5 \qquad \{2.62\}$$

the critical load parameter is obtained from Table 2.5 as

$$_s = 0.2006 \qquad \{\text{Table 2.5}\}$$

and the critical load of the framework is

$$N_{cr} = \ _s K = 0.2006 \cdot 530.2 = 106.4 \text{ MN} \qquad \{2.61\}$$

The effectiveness of the shear stiffness is given by

$$s = \frac{N_g}{K + N_g} = \frac{117.7}{530.2 + 117.7} = 0.1817 \qquad \{5.9\}$$

12.1.2 Case 1: an unacceptable bracing system arrangement

The bracing arrangement shown in Figure 12.2 is deliberately chosen as one obviously not appropriate for a ten-storey building. Nevertheless, it is included in the investigation as it illustrates spectacularly how the critical load ratio pinpoints the weakness(es) of the bracing system.

With the critical loads of the individual bracing units now available, the first step is to establish the location of the shear centre. Because of symmetry, only direction *x* requires calculation:

$$\bar{x}_o = \frac{\sum_{1}^{f+m} N_{y,i}\bar{x}_i}{\sum_{1}^{f+m} N_{y,i}} = \frac{2\cdot 106.4\cdot 7.5 + 2\cdot 105.7\cdot 15}{2\cdot 106.4 + 2\cdot 105.7} = 11.24\ \text{m}, \qquad \bar{y}_o = 4.5\,\text{m} \qquad \{5.37\}$$

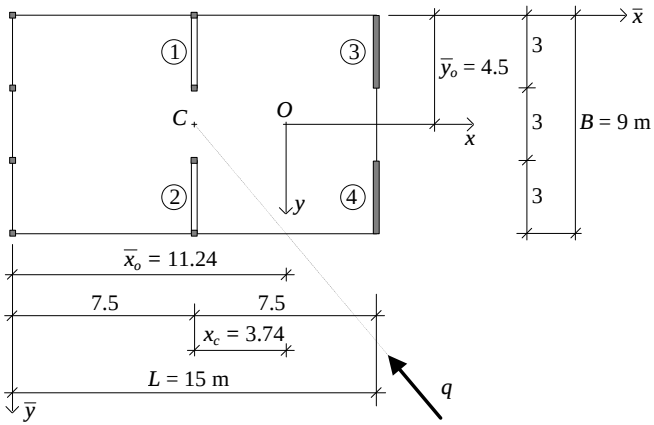

Figure 12.2 Case 1: An unacceptable bracing arrangement.

12.1.2.1 Stability analysis

The three basic (sway in directions *x* and *y* and pure torsional) critical loads will be calculated then the coupling of the modes will be considered.

Direction y

The effective shear stiffness of the system (with two frameworks) is

$$K_e = \sum_{1}^{f} K_i s_i = 2\cdot 530.2\cdot 0.1817 = 192.7\ \text{MN} \qquad \{5.10\}$$

The effectiveness factor for the whole system is

$$s = \frac{K_e}{K} = \frac{192.7}{2 \cdot 530.2} = 0.1817 \qquad \{5.11\}$$

The total bending stiffness of the system is obtained by adding up the local bending stiffness of the vertical structural units:

$$EI = E_c I_c + E_w I_w = \left(2 \cdot 3.281 \cdot 10^{-4} \cdot 2 \cdot 10^5 + 0.5625 \cdot 25 \cdot 10^3\right) 2$$

$$= 28387 \text{ MNm}^2 \qquad \{5.12\}$$

The contribution of the four columns (first term) is less than 1%.
The local bending critical load of the system is

$$N_l = \frac{7.837 r_s EI}{H^2} = \frac{7.837 \cdot 0.863 \cdot 28387}{30^2} = 213.3 \text{ MN} \qquad \{5.13\}$$

With

$$= \frac{K_e}{N_l} = \frac{192.7}{213.3} = 0.90 \qquad \{5.17\}$$

the critical load parameter is

$$= 3.3448 \qquad \{\text{Table } 5.2\}$$

The critical load in direction *y* is now obtained as

$$N_{cr,y} = N_l + K_e + (\quad - \quad - 1) s N_l \qquad \{5.18\}$$

$$= 213.3 + 192.7 + (3.3448 - 0.9 - 1) 0.1817 \cdot 213.3 = 462.2 \text{ MN}$$

The effect of the interaction between the bending and shear modes (third term) amounts to 12.1%.

Direction x
No bracing is provided for lateral stability in direction *x* and only the shear walls (normally ignored in the direction perpendicular to their plane) offer nominal resistance:

$$N_{cr,x} = \frac{7.837 EI r_s}{H^2} = \frac{7.837 \cdot 25 \cdot 10^3 \cdot 2 \cdot 0.003906 \cdot 0.863}{30^2} = 1.5 \text{ MN} \qquad \{2.74\}$$

Before pure torsional buckling can be investigated, the distance between the

shear centre and the centroid of the layout is needed:

$$t = x_c = \frac{L}{2} - \bar{x}_o = \frac{15}{2} - 11.24 = -3.74 \text{ m} \qquad \{5.42\}$$

Pure torsional buckling
The radius of gyration is needed first:

$$i_p = \sqrt{\frac{L^2 + B^2}{12} + t^2} = \sqrt{\frac{15^2 + 9^2}{12} + 3.74^2} = \sqrt{39.49} = 6.28 \text{ m} \qquad \{5.28\}$$

The "original" Saint-Venant torsional stiffness originates from the shear walls and the frameworks as

$$(GJ) = \sum_1^m GJ_k + \sum_1^f \left((K_i)_x y_i^2 + (K_i)_y x_i^2 \right) \qquad \{5.35\}$$

$$= 2 \cdot 10.42 \cdot 10^3 \cdot 0.015625 + 2 \cdot 530.2 \cdot 3.74^2 = 15158 \text{ MN}$$

The contribution of the own Saint-Venant stiffness of the shear walls (first term) is very little: 2.1%.

The effective Saint-Venant torsional stiffness is

$$(GJ)_e = \sum_1^m GJ_k + \sum_1^f \left((K_{e,i})_x y_i^2 + (K_{e,i})_y x_i^2 \right) \qquad \{5.29\}$$

$$= 2 \cdot 10.42 \cdot 10^3 \cdot 0.015625 + 2 \cdot 530.2 \cdot 0.1817 \cdot 3.74^2 = 3021 \text{ MNm}^2$$

The Saint-Venant torsional critical load that is associated with this stiffness is

$$N_t = \frac{(GJ)_e}{i_p^2} = \frac{3021}{39.49} = 76.50 \text{ MN} \qquad \{5.33\}$$

The effectiveness factor is

$$s = \frac{(GJ)_e}{(GJ)} = \frac{3021}{15158} = 0.1993 \qquad \{5.34\}$$

The warping torsional stiffness of the system originates from the two shear walls and the columns of the frameworks. In neglecting the contribution of the columns, it is

$$EI_{\Omega} = E_w \sum_{1}^{m} \left((I_{w,k})_x y_k^2 + (I_{w,k})_y x_k^2 \right)$$

$$= 25000 \cdot 0.5625 \cdot 3.76^2 \cdot 2 = 397620 \text{ MNm}^4 \qquad \{5.30\}$$

The warping torsional critical load of the system is

$$N_{\Omega} = \frac{7.837 r_s EI_{\Omega}}{i_p^2 H^2} = \frac{7.837 \cdot 0.863 \cdot 397620}{39.49 \cdot 30^2} = 75.7 \text{ MN} \qquad \{5.32\}$$

With

$$= \frac{N_t}{N_{\Omega}} = \frac{76.50}{75.7} = 1.01 \qquad \{5.36\}$$

the critical load parameter is obtained from Table (5.2) as

$$= 3.5758 + \frac{5.624 - 3.5758}{2.0 - 1.0}(1.01 - 1.0) = 3.596 \qquad \{\text{Table 5.2}\}$$

and the critical load for pure torsional buckling is

$$N_{cr,} = N_{\Omega} + N_t + (\quad - \quad - 1)s \; N_{\Omega} \qquad \{5.31\}$$

$$= 75.7 + 76.5 + (3.596 - 1.01 - 1)0.1993 \cdot 75.7 = 176.1 \text{ MN}$$

The effect of the interaction between the Saint-Venant and warping torsional modes (third term) is 13.6%.

With the three basic modes, their coupling must be considered.

Mode coupling

The arrangement of the bracing system is monosymmetric and the centroid of the vertical load of the building lies on axis *x*. Two things may happen. Sway buckling may develop in direction *x* (defined by $N_{cr,x}$) or buckling in direction *y* ($N_{cr,y}$) couples with pure torsional buckling ($N_{cr,\varphi}$). The critical load of this coupled buckling is obtained approximately as

$$N_y = \left(\frac{1}{N_{cr,y}} + \frac{1}{N_{cr,}} \right)^{-1} = \left(\frac{1}{462.2} + \frac{1}{176.1} \right)^{-1} = 127.5 \text{ MN} \qquad \{5.44\}$$

The critical load of the building is the smaller one of $N_{cr,x}$ and $N_{y\varphi}$, i.e.:

$$N_{cr} = \text{Min! } N_{cr,x}, N_y = 1.5 \text{ MN} \qquad \{5.45\}$$

The total load on the building is

$$N = LBQn = 15 \cdot 9 \cdot 0.01 \cdot 10 = 13.5\,\text{MN} \qquad \{6.2\}$$

and the global critical load ratio is

$$= \frac{N_{cr}}{N} = \frac{1.5}{13.5} = 0.11 \qquad \{6.3\}$$

showing a totally unacceptable, unstable bracing system.

12.1.2.2 Frequency analysis

As with the stability analysis, the three basic (lateral in directions *x* and *y* and pure torsional) frequencies will be calculated then the coupling of the modes will be considered. (For practical reasons, instead of the basic frequencies themselves, their squares will be used.)

Mass distribution factor r_f is obtained from Table 4.1 as a function of the number of storeys as

$$r_f = 0.911 \qquad \{\text{Table 4.1}\}$$

The mass density per unit length is needed for each basic frequency:

$$m = \quad A = \frac{}{g} A = \frac{3}{9.81} 15 \cdot 9 = 41.28\,\text{kg/m} \qquad \{4.7\}$$

The above value is related to the whole building. Nevertheless, it can also be used for the calculation of the frequencies of the individual bracing units as, eventually, the frequency values of the individual bracing units will be used for the determination of the fundamental frequency of the whole building.

Before the whole system is investigated, it is useful to determine the effectiveness factor for the framework (which is different from the effectiveness factor relating to stability). To this end, the frequencies that belong to both the original shear stiffness and the global bending stiffness are needed. These are:

$$f_{s'}^2 = \frac{1}{(4H)^2} \frac{r_f^2 K}{m} = \frac{0.911^2 \cdot 530200}{(4 \cdot 30)^2 \cdot 41.28} = 0.7402\ \text{Hz}^2 \qquad \{4.6\}$$

and

$$f_g^2 = \frac{0.313 r_f^2 E_c I_g}{H^4 m} = \frac{0.313 \cdot 0.911^2 \cdot 2 \cdot 10^8 \cdot 7.83 \cdot 10^{-2}}{30^4 \cdot 41.28} = 0.1217\ \text{Hz}^2 \qquad \{4.8\}$$

The effectiveness factor is now obtained as

$$s_f^2 = \frac{f_g^2}{f_g^2 + f_s^2} = \frac{0.1217}{0.1217 + 0.7402} = 0.1412 \qquad \{4.10\}$$

The lateral frequencies can now be investigated.

Direction y
With the total bending stiffness of the system [{5.12} in the beginning of Section 12.1.2], the lateral frequency of the system in bending is obtained from

$$f_b^2 = \frac{0.313 r_f^2 EI}{H^4 m} = \frac{0.313 \cdot 0.911^2 \cdot 28387 \cdot 10^3}{30^4 \cdot 41.28} = 0.2205\,\text{Hz}^2 \qquad \{4.15\}$$

The total effective shear stiffness is

$$K_e = \sum_1^f s_{f,i}^2 K_i = 0.1412 \cdot 530200 \cdot 2 = 149728\ \text{kN} \qquad \{4.11\}$$

and the effectiveness factor for the system is

$$s_f = \sqrt{\frac{K_e}{K}} = \sqrt{\frac{149728}{2 \cdot 530200}} = 0.3758 \qquad \{4.12\}$$

The lateral frequency which is associated with shear deformation can now be determined using the effective shear stiffness:

$$f_s^2 = \frac{1}{(4H)^2} \frac{r_f^2 K_e}{m} = \frac{0.911^2 \cdot 149728}{(4 \cdot 30)^2 \cdot 41.28} = 0.2090\ \text{Hz}^2 \qquad \{4.13\}$$

With the non-dimensional parameter

$$k = H\sqrt{\frac{K_e}{EI}} = 30\sqrt{\frac{149728}{28387 \cdot 10^3}} = 2.179 \qquad \{4.17\}$$

the frequency parameter is obtained as

$$= 0.8628 + \frac{0.9809 - 0.8628}{2.5 - 2.0}(2.179 - 2.0) = 0.905 \qquad \{\text{Table } 4.2\}$$

and the lateral frequency in direction *y* is

$$f_y = \sqrt{f_b^2 + f_s^2 + \left(\frac{^2}{0.313} - \frac{k^2}{5} - 1\right) s_f\, f_b^2} \qquad \{4.18\}$$

$$= \sqrt{0.2205 + 0.2090 + \left(\frac{0.905^2}{0.313} - \frac{2.179^2}{5} - 1\right) 0.3758 \cdot 0.2205} = 0.696 \text{ Hz}$$

Direction x

As with the stability analysis, the system is very weak in direction *x* and the lateral frequency is determined by the small stiffness of the shear walls perpendicular to their plane. (This stiffness is normally neglected in practical structural engineering calculations.)

The lateral frequency is

$$f_x = \frac{0.56 r_f}{H^2} \sqrt{\frac{EI_y}{m}} = \frac{0.56 \cdot 0.911}{30^2} \sqrt{\frac{25 \cdot 10^6 \cdot 2 \cdot 0.003906}{41.28}} = 0.0039 \text{ Hz} \qquad \{2.73\}$$

Pure torsional vibration

The "original" Saint-Venant torsional stiffness originates from the shear walls and the frameworks. Its value is now identical for both the stability and the frequency analyses

$$(GJ) = \sum_1^m GJ_k + \sum_1^f \left((K_i)_x y_i^2 + (K_i)_y x_i^2 \right) \qquad \{5.35\} \text{ or } \{4.27\}$$

$$= 2 \cdot 10.42 \cdot 10^3 \cdot 0.015625 + 2 \cdot 530.2 \cdot 3.74^2 = 15158 \text{ MNm}^2$$

With the effectiveness factor of the frameworks for the frequency analysis [see {4.10} above], the effective Saint-Venant torsional stiffness of the system is

$$(GJ)_e = \sum_1^m GJ_k + \sum_1^f \left((K_{e,i})_x y_i^2 + (K_{e,i})_y x_i^2 \right) \qquad \{4.21\}$$

$$= 2 \cdot 10.42 \cdot 10^3 \cdot 0.015625 + 2 \cdot 530.2 \cdot 0.1412 \cdot 3.74^2 = 2420 \text{ MNm}^2$$

The effectiveness of the Saint-Venant torsional stiffness is expressed by the factor

$$s = \sqrt{\frac{(GJ)_e}{(GJ)}} = \sqrt{\frac{2420}{15158}} = 0.3996 \qquad \{4.26\}$$

The warping torsional stiffness of the system is again identical for both the stability and the frequency analyses. In neglecting the contribution of the columns again, it is

$$EI_\Omega = E_w \sum_1^m \left((I_{w,k})_x y_k^2 + (I_{w,k})_y x_k^2 \right) \qquad \{4.22\} \text{ or } \{5.30\}$$

$$= 25000 \cdot 0.5625 \cdot 3.76^2 \cdot 2 = 397620 \,\text{MNm}^4$$

With the radius of gyration from the stability analysis, the two contributors to the pure torsional frequency can now be produced:

$$f_\Omega^2 = \frac{0.313 r_f^2 EI_\Omega}{i_p^2 H^4 m} = \frac{0.313 \cdot 0.911^2 \cdot 3.9762 \cdot 10^8}{39.49 \cdot 30^4 \cdot 41.28} = 0.0782 \text{ Hz}^2 \qquad \{4.24\}$$

and

$$f_t^2 = \frac{r_f^2 (GJ)_e}{16 i_p^2 H^2 m} = \frac{0.911^2 \cdot 2420 \cdot 10^3}{16 \cdot 39.49 \cdot 30^2 \cdot 41.28} = 0.0856 \,\text{Hz}^2 \qquad \{4.25\}$$

With torsion parameter

$$k = H \sqrt{\frac{(GJ)_e}{EI_\Omega}} = 30 \sqrt{\frac{2420}{397620}} = 2.34 \qquad \{4.28\}$$

the vibration parameter can now be obtained using Table 4.2:

$$= 0.8628 + \frac{0.9809 - 0.8628}{2.5 - 2.0}(2.34 - 2.0) = 0.943 \qquad \{\text{Table 4.2}\}$$

The frequency for pure torsional vibration is

$$f = \sqrt{f_\Omega^2 + f_t^2 + \left(\frac{^2}{0.313} - \frac{k^2}{5} - 1 \right) s \; f_\Omega^2} \qquad \{4.23\}$$

$$= \sqrt{0.0782 + 0.0856 + \left(\frac{0.943^2}{0.313} - \frac{2.34^2}{5} - 1 \right) 0.3996 \cdot 0.0782} = 0.433 \,\text{Hz}$$

Coupling of the vibration modes

Pure torsional vibration and lateral vibration in direction *y* combine. The value of the combined frequency can be approximated as

$$f_y = \left(\frac{1}{f_y^2} + \frac{1}{f^2} \right)^{-\frac{1}{2}} = \left(\frac{1}{0.696^2} + \frac{1}{0.433^2} \right)^{-\frac{1}{2}} = 0.368 \,\text{Hz} \qquad \{4.36\}$$

As the frequency of lateral vibration in direction x is (much) smaller, the fundamental frequency of the building is this smaller value:

$$f_x = 0.039 \text{ Hz} \qquad \{2.73\}$$

12.1.2.3 Maximum deflection

Based on the results in the previous two sections, it can be safely stated that the building is much more vulnerable in direction x and, as an approximation, only direction x is considered. Compared to the shear walls, the two frameworks offer negligible resistance and—in line with structural engineering common practice—their contribution is ignored.

The maximum deflection of the building is calculated as

$$x_{\max} = x(H) = \frac{q_x H^4}{8EI_y} = \frac{10.9 \cdot 30^4}{8 \cdot 25 \cdot 10^6 \cdot 2 \cdot 3.906 \cdot 10^{-3}} = 5.65 \text{ m} \qquad \{2.72\}$$

In summary, the bracing system is clearly unacceptable: the maximum deflection is far too great, the fundamental frequency is very small and, above all, the building is not stable. The inadequacy of the system is clearly indicated by the value of the critical load ratio ($\lambda = 0.11$). For a theoretically stable bracing system, this value must be greater than 1.0 and, preferably, it should be greater than 10.0.

The main weakness of the bracing system lies in the lack of bracing in direction x. To improve the performance of the building, the two frameworks are rotated by 90 degrees and are moved to the left-hand side of the building to create a more balanced arrangement (Figure 12.3).

12.1.3 Case 2: a more balanced bracing system arrangement

The arrangement shown in Figure 12.3 remedies a fatal problem with Case 1, namely, this time the system has considerable stiffness in direction x as well. It remains to be seen if the improvement is great enough to result in an adequate bracing system.

12.1.3.1 Stability analysis

The three basic (sway in directions x and y and pure torsional) critical loads will be calculated then the coupling of the modes will be considered.

Direction y

Buckling in direction y is resisted by the two shear walls. The corresponding critical load is

$$N_{cr,y} = 2 \cdot 105.7 = 211.4 \text{ MN} \qquad \{2.74 \text{ in Section } 12.1.1\}$$

Direction x

Buckling in direction x is resisted by the two frameworks. The corresponding critical load is

$$N_{cr,x} = 2 \cdot 106.4 = 212.8 \text{ MN} \qquad \{2.61 \text{ in Section } 12.1.1\}$$

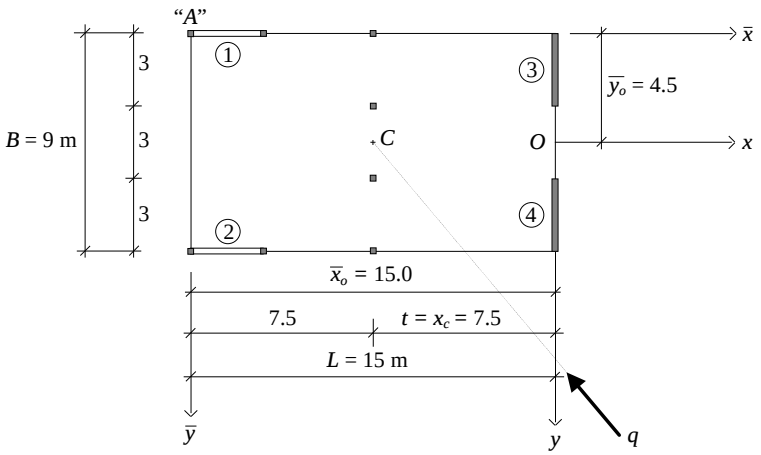

Figure 12.3 Case 2: A more balanced bracing arrangement.

Pure torsional buckling

Because of the symmetric arrangement of the two shear walls and of the two frameworks, the location of the shear centre is readily available:

$$\bar{x}_o = 15.0 \text{ m} \qquad \bar{y}_o = 4.5 \text{ m}$$

The radius of gyration is

$$i_p = \sqrt{\frac{L^2 + B^2}{12} + t^2} = \sqrt{\frac{15^2 + 9^2}{12} + 7.5^2} = \sqrt{81.75} = 9.04 \text{ m} \qquad \{5.28\}$$

In addition to the own Saint-Venant torsional stiffness of the shear walls, only the two frameworks contribute to the torsional resistance (as the shear walls has zero perpendicular distance from the shear centre).

The "original" Saint-Venant torsional stiffness of the system is

$$(GJ) = \sum_1^m GJ_k + \sum_1^f \left((K_i)_x y_i^2 + (K_i)_y x_i^2 \right) \qquad \{5.35\}$$

$$= 2 \cdot 10.42 \cdot 10^3 \cdot 0.015625 + 2 \cdot 530.2 \cdot 4.5^2 = 21799 \text{ MNm}^2$$

The contribution of the shear walls (first term) is only 1.5%.

With the effectiveness factor [{5.9} in Section 12.1.1] the effective Saint-Venant torsional stiffness is

$$(GJ)_e = \sum_1^m GJ_k + \sum_1^f \left((K_{e,i})_x y_i^2 + (K_{e,i})_y x_i^2 \right) \qquad \{5.29\}$$

$$= 2 \cdot 10.42 \cdot 10^3 \cdot 0.015625 + 2 \cdot 530.2 \cdot 0.1817 \cdot 4.5^2 = 4227 \text{ MNm}^2$$

As the contribution of the columns of the frameworks is negligible and the perpendicular distance of the shear walls from the shear centre is zero, the warping torsional stiffness is

$$EI_\Omega \cong 0 \qquad \{5.30\}$$

and the critical load for pure torsional buckling is defined by the Saint-Venant torsional critical load as

$$N_{cr,} = N_t = \frac{(GJ)_e}{i_p^2} = \frac{4227}{81.75} = 51.7 \text{ MN} \qquad \{5.31\} \text{ \& } \{5.33\}$$

As the arrangement of the bracing system is monosymmetric and the centroid of the vertical load of the building lies on axis x, buckling in direction y ($N_{cr,y}$) couples with pure torsional buckling ($N_{cr,\varphi}$). The critical load of this combined buckling is obtained from

$$N_y = \left(\frac{1}{N_{cr,y}} + \frac{1}{N_{cr,}} \right)^{-1} = \left(\frac{1}{211.4} + \frac{1}{51.7} \right)^{-1} = 41.5 \text{ MN} \qquad \{5.44\}$$

The critical load of the building is the smaller one of $N_{cr,x}$ and $N_{y\varphi}$, i.e.:

$$N_{cr} = \text{Min! } N_{cr,x}, N_y = 41.5 \text{ MN} \qquad \{5.45\}$$

With the total vertical load on the building (N = 13.5MN), the global critical load ratio is now

$$= \frac{N_{cr}}{N} = \frac{41.5}{13.5} = 3.1 \qquad \{6.3\}$$

indicating a stable building and a big improvement on Case 1, as far as stability is concerned. The situation regarding the fundamental frequency and the maximum

deflection of the building will be looked at in the next two sections.

The above values of the basic critical loads indicate that the stability of the system is limited by the relatively small value of pure torsional buckling.

12.1.3.2 Frequency analysis

The three basic (sway in directions *x* and *y* and pure torsional) frequencies will be calculated then the coupling of the modes will be considered. The behaviour of the building is very similar to that with the stability analysis.

Direction y

Vibration in direction *y* is resisted by the two shear walls. The corresponding lateral frequency is

$$f_y = \frac{0.56 r_f}{H^2}\sqrt{\frac{EI_x}{m}} = \frac{0.56 \cdot 0.911}{30^2}\sqrt{\frac{25 \cdot 10^6 \cdot 2 \cdot 0.5625}{41.28}} = 0.468 \text{ Hz} \qquad \{2.73\}$$

Direction x

Vibration in direction *x* is resisted by the two frameworks of identical characteristics. The effectiveness factor is needed first. With the squares of the two participating frequencies

$$f_{s'}^2 = \frac{1}{(4H)^2}\frac{r_f^2 K}{m} = \frac{0.911^2 \cdot 530200}{(4 \cdot 30)^2 \cdot 41.28} = 0.7402 \text{ Hz}^2 \qquad \{4.6\}$$

and

$$f_g^2 = \frac{0.313 r_f^2 E_c I_g}{H^4 m} = \frac{0.313 \cdot 0.911^2 \cdot 2 \cdot 10^8 \cdot 7.83 \cdot 10^{-2}}{30^4 \cdot 41.28} = 0.1217 \text{ Hz}^2 \qquad \{4.8\}$$

the effectiveness factor assumes the value

$$s_f^2 = \frac{f_g^2}{f_g^2 + f_{s'}^2} = \frac{0.1217}{0.1217 + 0.7402} = 0.1412 \qquad \{4.10\}$$

and the combined effective shear stiffness of Unit 1 and Unit 2 is

$$K_e = \sum_1^f s_{f,i}^2 K_i = 0.1412 \cdot 530.2 \cdot 2 = 149.728 \text{ MN} \qquad \{4.11\}$$

The lateral frequency which is associated with shear deformation can now be determined using the effective shear stiffness:

$$f_s^2 = \frac{1}{(4H)^2}\frac{r_f^2 K_e}{m} = \frac{0.911^2 \cdot 149728}{(4 \cdot 30)^2 \cdot 41.28} = 0.2090 \text{ Hz}^2 \qquad \{4.13\}$$

Using the "original" and the effective shear stiffnesses, the effectiveness for the whole system is obtained as

$$s_f = \sqrt{\frac{K_e}{K}} = \sqrt{\frac{149.728}{2 \cdot 530.2}} = 0.3758 \qquad \{4.12\}$$

The local bending stiffness of the two frameworks is

$$EI = E_c I_c = 2(2 \cdot 10^8 \cdot 2 \cdot 3.281 \cdot 10^{-4}) = 262480 \text{ kNm}^2 \qquad \{4.14\}$$

With the above bending stiffness, the lateral frequency of the system in bending is

$$f_b^2 = \frac{0.313 r_f^2 EI}{H^4 m} = \frac{0.313 \cdot 0.911^2 \cdot 262480}{30^4 \cdot 41.28} = 0.00204 \text{ Hz}^2 \qquad \{4.15\}$$

With the non-dimensional parameter

$$k = H\sqrt{\frac{K_e}{EI}} = 30\sqrt{\frac{149728}{262480}} = 22.66 \qquad \{4.17\}$$

the frequency parameter is obtained using Table 4.2 as

$$= 5.278 + \frac{7.769 - 5.278}{10}(22.66 - 20.0) = 5.942 \qquad \{\text{Table 4.2}\}$$

Finally, the frequency for lateral vibration in direction *x* is

$$f_x = \sqrt{f_b^2 + f_s^2 + \left(\frac{^2}{0.313} - \frac{k^2}{5} - 1\right) s_f f_b^2} \qquad \{4.18\}$$

$$= \sqrt{0.00204 + 0.209 + \left(\frac{5.942^2}{0.313} - \frac{22.66^2}{5} - 1\right) 0.3758 \cdot 0.00204} = 0.467 \text{ Hz}$$

Pure torsional vibration

The situation is similar to the stability analysis in that only the two frameworks contribute to the resistance against torsional vibration. The "original" Saint-Venant

torsional stiffness is

$$(GJ) = \sum_{1}^{m} GJ_k + \sum_{1}^{f} \left((K_i)_x y_i^2 + (K_i)_y x_i^2 \right) \qquad \{4.27\}$$

$$= 2 \cdot 10.42 \cdot 10^3 \cdot 0.015625 + 2 \cdot 530.2 \cdot 4.5^2 = 21799 \text{ MNm}^2$$

(that can also be taken from the stability analysis), and the effective Saint-Venant torsional stiffness [using {4.11} above] is

$$(GJ)_e = \sum_{1}^{m} GJ_k + \sum_{1}^{f} \left((K_{e,i})_x y_i^2 + (K_{e,i})_y x_i^2 \right) \qquad \{4.21\}$$

$$= 2 \cdot 10.42 \cdot 10^3 \cdot 0.015625 + 149.728 \cdot 4.5^2 = 3358 \text{ MNm}^2$$

As with the stability analysis, the contribution of the columns of the frameworks is negligible and the perpendicular distance of the shear walls from the shear centre is zero, so the warping torsional stiffness is

$$EI_\Omega \cong 0 \qquad \{4.22\}$$

The frequency for pure torsional vibration simplifies to

$$f = f_t = \frac{r_f}{4 i_p H} \sqrt{\frac{(GJ)_e}{m}} = \frac{0.911}{4 \cdot 9.04 \cdot 30} \sqrt{\frac{3358000}{41.28}} = 0.2395 \text{ Hz} \qquad \{4.23 \ \& \ 4.25\}$$

Assuming uniform mass distribution, the centroid of the mass lies on axis *x*, and therefore lateral vibration in direction *y* couples with pure torsional vibration. The resulting coupled vibration is obtained as

$$f_y = \left(\frac{1}{f_y^2} + \frac{1}{f^2} \right)^{-\frac{1}{2}} = \left(\frac{1}{0.468^2} + \frac{1}{0.2395^2} \right)^{-\frac{1}{2}} = 0.213 \text{ Hz} \qquad \{4.36\}$$

This combined frequency is smaller than $f_x = 0.469$, so the fundamental frequency of the building is

$$f = \text{Min!} \ f_x, \ f_y = 0.213 \text{ Hz} \qquad \{4.37\}$$

It is clear from the above values that resistance to torsion is relatively small.

12.1.3.3 Maximum deflection

The two components of the wind load will be treated separately. When wind load in direction x is considered, the arrangement is symmetric and the wind is resisted by two identical frameworks. It is enough to work with half of the structure (one framework) and half of the load:

$$w_x = \frac{1}{2}(17 \cdot \cos 50^\circ) = 5.46 \text{ kN/m}$$

With auxiliary quantities

$$a = \frac{K}{EI_g} = \frac{530.2}{2 \cdot 10^5 \cdot 7.83 \cdot 10^{-2}} = 0.033857, \quad b = \frac{K}{EI} = \frac{530.2}{2 \cdot 10^5 \cdot 2 \cdot 3.281 \cdot 10^{-4}} = 4.04$$

$$s = 1 + \frac{a}{b} = 1 + \frac{0.033857}{4.4} = 1.00838 \cong 1.0, \qquad H = H\sqrt{a+b} = 60.6 \qquad \{2.14\}$$

$$I_f = I + I_g = 2 \cdot 3.281 \cdot 10^{-4} + 7.83 \cdot 10^{-2} = 0.079 \text{ m}^4 \qquad \{2.23\}$$

the maximum deflection is

$$x_{\max} = y(H) = \frac{wH^4}{8EI_f} + \frac{wH^2}{2Ks^2} - \frac{wEI}{K^2 s^3}\left(\frac{1 + H \sinh H}{\cosh H} - 1\right) \qquad \{2.24\}$$

$$= \frac{5.46 \cdot 30^4}{8 \cdot 2 \cdot 10^8 \cdot 0.079} + \frac{5.46 \cdot 30^2}{2 \cdot 530200} - \frac{5.46 \cdot 2 \cdot 10^8 \cdot 2 \cdot 3.281 \cdot 10^{-4}}{530200^2}\left(\frac{1 + 60.6 \sinh 60.6}{\cosh 60.6} - 1\right)$$

$$= 0.0350 + 0.0046 - 0.00015 = 0.0395 \text{ m}$$

When the component of the wind in direction y is considered (w_y = 13 kN/m), the maximum deflection is obtained in two steps. First, the deflection of the shear centre has to be determined, caused by the wind load acting through the shear centre, then the additional deflection due to the rotation of the building around the shear centre has to be added.

In the first case the load is resisted by the two shear walls and the maximum deflection is

$$v_o = \frac{13 \cdot 30^4}{8 \cdot 25 \cdot 10^6 \cdot 2 \cdot 0.5625} = 0.0468 \text{ m} \qquad \{2.72\}$$

In addition to this uniform deflection, the torsional moment

$$\overline{m} = w_y x_c = 17 \cdot \sin 50^\circ \cdot 7.5 = 97.67 \text{ kNm/m} \qquad \{3.28\}$$

develops rotation around the shear centre, which leads to additional deflection. The torsional moment is balanced by the torsional resistance of the two frameworks. (The two shear walls have zero perpendicular distance from the shear centre so they cannot take part.)

The global warping torsional stiffness of the frameworks is

$$EI_{g\Omega} = EI_g t^2 = 2 \cdot 10^5 \cdot 7.83 \cdot 10^{-2} \cdot 4.5^2 \cdot 2 = 634230 \,\text{MNm}^4 \qquad \{3.20\}$$

The Saint-Venant torsional stiffness of the frameworks is

$$(GJ) = Kt^2 = 530.2 \cdot 4.5^2 \cdot 2 = 21473.1 \,\text{MNm}^2 \qquad \{3.21\}$$

The local warping torsional stiffness of the frameworks is negligible and is therefore ignored so the warping torsional stiffness of the system is

$$EI_\Omega \cong 0 \qquad \{3.19\}$$

With the above torsional stiffnesses, the rotation of the building around the shear centre can now be determined:

$$_{\max} = \quad (H) = \frac{\overline{m} H^4}{8E(I_\Omega + I_{g\Omega})} + \frac{\overline{m} H^2}{2(GJ)\bar{s}^2} - \frac{\overline{m} EI_\Omega}{(GJ)^2 \bar{s}^3}\left(\frac{1 + \overline{\ } H \sinh \overline{\ } H}{\cosh \overline{\ } H} - 1\right)$$

$$= \frac{97.67 \cdot 30^4}{8 \cdot 634230000} + \frac{97.67 \cdot 30^2}{2 \cdot 21473100} = 0.0156 + 0.0020 = 0.0176 \text{ rad} \qquad \{3.24\}$$

The maximum displacement of the building develops at the top at the left-hand side corner of the plan of the building (point "*A*" in Figure 12.3) and, making use of the angle of rotation, is obtained from

$$v_{\max} = v(H) = v_o + \quad x_{\max} = 0.0468 + 0.0176 \cdot 15 = 0.311 \,\text{m} \qquad \{3.36\}$$

where $x_{\max}$ is the distance of the corner point (where maximum deflection occurs) from the shear centre. It is clear from Equation {3.36} that the overwhelming majority of the maximum deflection of the building is caused by the rotation of the system.

The maximum deflection in the wind direction is

$$d_{\max} = \sqrt{0.0468^2 + 0.311^2} = 0.315 \,\text{m}$$

As the increase in the value of the critical load ratio indicated, the performance of "Case 2" improved drastically, compared to "Case 1": the critical load and the fundamental frequency increased considerably and the maximum

deflection decreased. However, further improvements are possible as the next section will demonstrate.

12.1.4 Case 3: an effective bracing system arrangement

As the results in the previous section show, the efficiency of "Case 2" was limited mainly because of its relatively poor performance in torsion. It is therefore the torsional resistance of the system that is improved in this section by rearranging the bracing units again in such a way that Bracing Units 1 and 3 are exchanged (Figure 12.4). The resulting bracing system is doubly symmetric, still has considerable lateral stiffness in both principal directions and its torsional resistance is increased by the fact that all four bracing units now have "torsion arms" (i.e. perpendicular distances from the shear centre).

12.1.4.1 Stability analysis

The three basic (sway in directions *x* and *y* and pure torsional) critical loads will be calculated then the coupling of the modes will be considered.

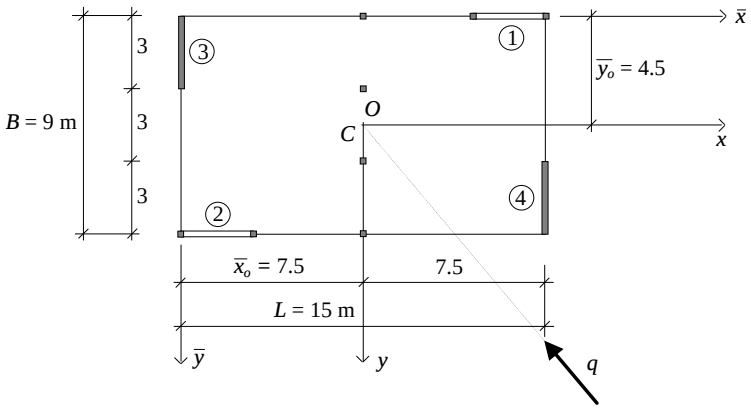

Figure 12.4 Case 3: A doubly symmetric arrangement.

Direction y
Buckling in direction *y* is resisted by the two shear walls. The corresponding critical load is identical to that of "Case 2":

$$N_{cr,y} = 2 \cdot 105.7 = 211.4 \text{ MN} \qquad \{2.74 \text{ in Section } 12.1.1\}$$

Direction x
Buckling in direction *x* is resisted by the two frameworks. The corresponding critical load is again identical to that of "Case 2":

$$N_{cr,x} = 2 \cdot 106.4 = 212.8 \text{ MN} \qquad \{2.61 \text{ in Section } 12.1.1\}$$

Pure torsional buckling
Because of the doubly symmetric arrangement of the two shear walls and of the two frameworks, the location of the shear centre is readily available:

$$\bar{x}_o = 7.5 \text{ m}, \qquad \bar{y}_o = 4.5 \text{ m}$$

The radius of gyration is

$$i_p = \sqrt{\frac{L^2 + B^2}{12} + t^2} = \sqrt{\frac{15^2 + 9^2}{12}} = \sqrt{25.5} = 5.05 \text{ m} \qquad \{5.28\}$$

The "original" and effective Saint-Venant torsional stiffnesses of the two frameworks are identical to that of "Case 2" (Section 12.1.3):

$$(GJ) = 2 \cdot 10.42 \cdot 10^3 \cdot 0.015625 + 2 \cdot 530.2 \cdot 4.5^2 = 21799 \text{ MNm}^2 \qquad \{5.35\}$$

and

$$(GJ)_e = 2 \cdot 10.42 \cdot 10^3 \cdot 0.015625 + 2 \cdot 530.2 \cdot 0.1817 \cdot 4.5^2 = 4227 \text{ MNm}^2 \qquad \{5.29\}$$

The effectiveness of the Saint-Venant torsional stiffness is expressed by the factor

$$s = \frac{(GJ)_e}{(GJ)} = \frac{4227}{21799} = 0.194 \qquad \{5.34\}$$

With the contribution of the shear walls, the warping torsional stiffness is:

$$EI_\Omega = E_w \sum_1^m \left(I_{\Omega k} + (I_{w,k})_x y_k^2 + (I_{w,k})_y x_k^2 \right) \qquad \{5.30\}$$

$$= 25 \cdot 10^3 \cdot 0.5625 \cdot 7.5^2 \cdot 2 = 1582031 \text{ MNm}^4$$

With the part critical loads

$$N_\Omega = \frac{7.837 r_s EI_\Omega}{i_p^2 H^2} = \frac{7.837 \cdot 0.863 \cdot 1582031}{25.5 \cdot 30^2} = 466.2 \text{ MN} \qquad \{5.32\}$$

and

$$N_t = \frac{(GJ)_e}{i_p^2} = \frac{4227}{25.5} = 165.8\,\text{MN} \qquad \{5.33\}$$

the critical load parameter can be obtained as a function of

$$= \frac{N_t}{N_\Omega} = \frac{165.8}{466.2} = 0.3556 \qquad \{5.36\}$$

from Table 5.2 as

$$= 1.8556 + \frac{2.1226 - 1.8556}{0.4 - 0.3}(0.3556 - 0.3) = 2.00 \qquad \{\text{Table 5.2}\}$$

The critical load for pure torsional buckling is

$$N_{cr,} = N_\Omega + N_t + (\quad - \quad -1)s\ N_\Omega \qquad \{5.31\}$$

$$= 466.2 + 165.8 + (2.0 - 0.3556 - 1)0.194 \cdot 466.2 = 690.3\,\text{MN}$$

As the arrangement of the bracing system is doubly symmetric and the centroid of the vertical load of the building coincides with the shear centre of the bracing system, the critical load of the building is the smallest one of the three basic critical loads:

$$N_{cr} = \text{Min!}\, N_{cr,x}, N_{cr,y}, N_{cr,} = 211.4\,\text{MN} \qquad \{5.46\}$$

With the total vertical load on the building (N = 13.5MN), the global critical load ratio is now

$$= \frac{N_{cr}}{N} = \frac{211.4}{13.5} = 15.7 > 10 \qquad \{6.3\} \text{ and } \{6.5\}$$

indicating a stable building and a big improvement on “Case 2”. Its value also exceeds the recommended value. The situation regarding the fundamental frequency and the maximum deflection of the building will be looked at in the next two sections.

12.1.4.2 Frequency analysis

The three basic frequencies will be determined and then their coupling will be considered.

Lateral vibration

The situation is similar to that with the stability analysis in that the lateral frequencies are unchanged (i.e. identical to those of “Case 2”):

$f_x = 0.467$ Hz {Section 12.1.3}

$f_y = 0.468$ Hz {Section 12.1.3}

Pure torsional vibration
The "original" Saint-Venant torsional stiffness is

$$(GJ) = \sum_1^m GJ_k + \sum_1^f \left((K_i)_x y_i^2 + (K_i)_y x_i^2\right) \quad \{4.27\}$$

$$= 2 \cdot 10.42 \cdot 10^3 \cdot 0.015625 + 2 \cdot 530.2 \cdot 4.5^2 = 21799 \text{ MNm}^2$$

(that can also be taken from the stability analysis), and the effective Saint-Venant torsional stiffness [using {4.11} above] is

$$(GJ)_e = \sum_1^m GJ_k + \sum_1^f \left((K_{e,i})_x y_i^2 + (K_{e,i})_y x_i^2\right) \quad \{4.21\}$$

$$= 2 \cdot 10.42 \cdot 10^3 \cdot 0.015625 + 149.728 \cdot 4.5^2 = 3358 \text{ MNm}^2$$

The effectiveness of the Saint-Venant torsional stiffness is expressed by the factor

$$s = \sqrt{\frac{(GJ)_e}{(GJ)}} = \sqrt{\frac{3358}{21799}} = 0.392 \quad \{4.26\}$$

With the contribution of the two shear walls, the warping torsional stiffness is:

$$EI_\Omega = E_w \sum_1^m \left(I_{\Omega k} + (I_{w,k})_x y_k^2 + (I_{w,k})_y x_k^2\right) \quad \{4.22\}$$

$$= 25 \cdot 10^3 \cdot 0.5625 \cdot 7.5^2 \cdot 2 = 1582031 \text{ MNm}^4$$

(which can also be taken from the stability analysis).

The two contributors to the pure torsional frequency are:

$$f_\Omega^2 = \frac{0.313 r_f^2 EI_\Omega}{i_p^2 H^4 m} = \frac{0.313 \cdot 0.911^2 \cdot 1.582 \cdot 10^9}{25.5 \cdot 30^4 \cdot 41.28} = 0.482 \text{ Hz}^2 \quad \{4.24\}$$

and

$$f_t^2 = \frac{r_f^2 (GJ)_e}{16 i_p^2 H^2 m} = \frac{0.911^2 \cdot 3358000}{16 \cdot 25.5 \cdot 30^2 \cdot 41.28} = 0.184 \text{ Hz}^2 \qquad \{4.25\}$$

With torsion parameter

$$k = H\sqrt{\frac{(GJ)_e}{EI_\Omega}} = 30\sqrt{\frac{3358}{1582031}} = 1.382 \qquad \{4.28\}$$

the frequency parameter is obtained using Table 4.2:

$$= 0.6542 + \frac{0.7511 - 0.6542}{1.5 - 1.0}(1.382 - 1.0) = 0.728 \qquad \{\text{Table 4.2}\}$$

The frequency for pure torsional vibration can now be determined:

$$f = \sqrt{f_\Omega^2 + f_t^2 + \left(\frac{^2}{0.313} - \frac{k^2}{5} - 1\right) s \; f_\Omega^2} \qquad (4.23)$$

$$= \sqrt{0.482 + 0.184 + \left(\frac{0.728^2}{0.313} - \frac{1.382^2}{5} - 1\right) 0.392 \cdot 0.482} = 0.851 \text{ Hz}$$

As the arrangement of the bracing system is doubly symmetric and the centroid of the mass of the building coincides with the shear centre of the bracing system, no coupling occurs and the fundamental frequency of the building is the smallest one of f_x, f_y and f_φ, i.e.:

$$f = \text{Min! } f_x,\ f_y,\ f = 0.467 \text{ Hz} \qquad \{4.38\}$$

12.1.4.3 Maximum deflection

The wind load in direction y is resisted by the two shear walls in a symmetric arrangement and the corresponding deflection is

$$y_{\max} = x(H) = \frac{q_y H^4}{8EI_x} = \frac{13.0 \cdot 30^4}{8 \cdot 25 \cdot 10^6 \cdot 2 \cdot 0.5625} = 0.0468 \text{ m} \qquad \{2.72\}$$

When wind load in direction x is considered, the arrangement is also symmetric and the wind is resisted by two identical frameworks. The situation is identical to that discussed in detail in Section 12.1.3 with “Case 2” and the corresponding deflection is

$$x_{max} = 0.0395 \text{ m} \qquad \{2.24 \text{ in Section } 12.1.3\}$$

The maximum deflection in the wind direction is

$$d_{max} = \sqrt{0.0468^2 + 0.0395^2} = 0.0612 \text{ m}$$

The two weaknesses of the original bracing arrangement have been eliminated in two steps: the problem of the practically non-existent lateral stiffness was addressed with "Case 2" and then the still poor torsional behaviour was improved with "Case 3". The change in the value of the global critical load ratio spectacularly shows its usefulness in monitoring the efficiency of the bracing system.

12.2 FIVE-STOREY BUILDING BRACED BY A SINGLE CORE

Kollár's (1977) classic five-storey building was first used to show how a single core is best used to be effective against torsional buckling. The worked example here will demonstrate that, in addition to stability, the global critical load ratio also "handles" frequencies, rotations and deflections and identifies efficient and inefficient bracing system arrangements.

The vertical load of the building is carried by columns but their lateral and torsional stiffness is very small and is therefore ignored is the calculations. It is assumed that the lateral and torsional stiffness of the building is provided by a U-core (Figure 12.5/b). The basic geometrical, stiffness and loading characteristics are as follows:

Size of ground plan: L = 26 m, B = 14 m
Storey height: h = 3.0 m, number of storeys: 5
Height of building: H = 15 m
Modulus of elasticity: E = 23000 MN/m^2
Modulus of elasticity in shear: G = 9580 MN/m^2
Floor load (for the stability analysis): Q = 8 kN/m^2
Wind load (for the deflection analysis): w = 1.0 kN/m^2 in direction y
Weight per unit volume of the building (for the frequency analysis):
γ = 3.0 kN/m^3

The load distribution factor for the stability analysis is

$$r_s = 0.759 \qquad \{\text{Table } 5.1\}$$

and the mass distribution factor for the frequency analysis is

$$r_f = 0.842 \qquad \{\text{Table } 4.1\}$$

As the size of the building and of the sole bracing unit is given, the structural performance of the building is governed by the location of the core. Two locations

will be considered with and without taking into consideration the possibility that the open U-core can partially be closed. This results in four cases. In the four cases the maximum rotation and the maximum deflection, the fundamental frequency, the global critical load and the global critical load ratio of the building will be determined.

The equations related to U-cores given in Tables 2.7 and 2.8 are used for determining the stiffness characteristics of the U-core.

12.2.1 Layout A: open core in the right-hand side of the layout

The bracing core is first placed in the lower right-hand corner of the layout in such a way that the shear centre of the core is in the middle of size B of the building (Figure 12.5/a). The geometrical and stiffness characteristics of this case are collected in the first row in Table 12.2.

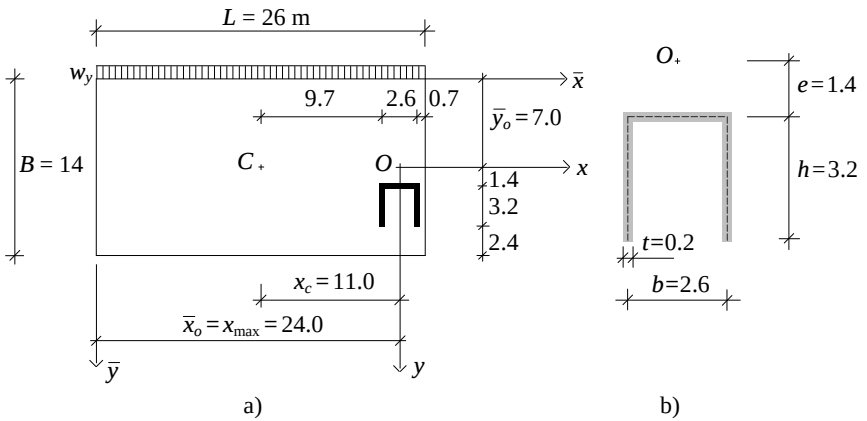

Figure 12.5 Kollár's building. a) Layout A, b) bracing core.

Table 12.2 Geometrical and stiffness characteristics.

Layout	I_x	I_y	J	I_ω	$\bar{x}_o$	$\bar{y}_o$	x_c	y_c	i_p
"A"	2.045	2.466	0.024	2.51	24.0	7.00	11.0	0.00	13.92
"B"	2.045	2.466	0.024	2.51	13.0	7.00	0.0	0.00	8.52
"C"	2.479	2.599	1.450	0.00	24.0	8.70	11.0	1.70	14.00
"D"	2.479	2.599	1.450	0.00	13.0	7.00	0.0	0.00	8.52

12.2.1.1 Maximum rotation and deflection

The w = 1 kN/m^2 wind load intensity represents a $w_y = Lw$ = 26.0 kN/m wind load per unit height in direction y. The total torsional moment is

$$m_t = w_y x_c = 26 \cdot 11 = 286 \text{ kNm/m} \qquad \{3.29\}$$

With torsion parameter

$$k = H\sqrt{\frac{GJ}{EI_\Omega}} = 15\sqrt{\frac{9580 \cdot 0.024}{23000 \cdot 2.51}} = 0.947 \qquad \{2.88\}$$

the maximum rotation of the building can be calculated as

$$_{\max} = \quad (H) = \frac{m_z H^2}{GJ}\left(\frac{\cosh k - 1}{k^2 \cosh k} - \frac{\tanh k}{k} + \frac{1}{2}\right) \qquad \{2.89\}$$

$$= \frac{286 \cdot 15^2}{9.58 \cdot 10^6 \cdot 0.024}\left(\frac{\cosh(0.947) - 1}{0.947^2 \cosh(0.947)} - \frac{\tanh(0.947)}{0.947} + \frac{1}{2}\right) = 0.02335 \text{ rad}$$

Maximum deflection develops at the left-hand side of the building at $x_{\max} = 24.0$. It consists of two parts. The top layout of the building undergoes a uniform translation of

$$v_o = v(H) = \frac{w_y H^4}{8EI_x} = \frac{26 \cdot 15^4}{8 \cdot 23 \cdot 10^6 \cdot 2.045} = 0.0035 \text{ m} \qquad \{2.83\}$$

The rotation around the shear centre causes additional deflection and the total maximum deflection is calculated as

$$v_{\max} = v(H) = v_o + \quad x_{\max} = 0.0035 + 0.02335 \cdot 24$$

$$= 0.0035 + 0.5604 = 0.564 \text{ m} \qquad \{3.36\}$$

As the recommended maximum deflection is

$$v_{\text{ASCE}} = \frac{H}{500} = \frac{15}{500} = 0.030 \text{ m}$$

the bracing of the building is clearly unacceptable.

12.2.1.2 Fundamental frequency

The mass density per unit length for the building is

$$m = \quad A = \frac{}{g} A = \frac{3}{9.81} 26 \cdot 14 = 111.3 \text{ kg/m} \qquad \{4.7\}$$

The lateral frequencies in directions *x* and y are calculated using the formulae given for cores but with the above mass density (which relates to the whole building):

$$f_x = \frac{0.56 r_f}{H^2}\sqrt{\frac{EI_y}{m}} = \frac{0.56 \cdot 0.842}{15^2}\sqrt{\frac{23 \cdot 10^6 \cdot 2.466}{111.3}} = 1.50 \text{ Hz} \qquad \{2.97\}$$

and

$$f_y = \frac{0.56 r_f}{H^2}\sqrt{\frac{EI_x}{m}} = \frac{0.56 \cdot 0.842}{15^2}\sqrt{\frac{23 \cdot 10^6 \cdot 2.045}{111.3}} = 1.36 \text{ Hz} \qquad \{2.97\}$$

The frequency of pure torsional vibration of the building is obtained using the formula given for a single core but with the radius gyration that relates to the whole layout area as the mass is distributed over the whole floor area of the building:

$$i_p = \sqrt{\frac{L^2 + B^2}{12} + t^2} = \sqrt{\frac{L^2 + B^2}{12} + x_c^2} = \sqrt{\frac{26^2 + 14^2}{12} + 11^2} = 13.92 \text{ m} \qquad \{4.20\}$$

With using the torsion parameter calculated earlier, the frequency parameter for pure torsional vibration is obtained from Table 4.2:

$$= 0.5851 + \frac{0.6542 - 0.5851}{1.0 - 0.5}(0.947 - 0.5) = 0.647 \qquad \{\text{Table 4.2}\}$$

and the pure torsional frequency is

$$f = \frac{r_f}{i_p H^2}\sqrt{\frac{EI_\Omega}{m}} = \frac{0.647 \cdot 0.842}{13.92 \cdot 15^2}\sqrt{\frac{23 \cdot 10^6 \cdot 2.51}{111.3}} = 0.125 \text{ Hz} \qquad \{2.98\}$$

The centroid of the layout lies on axis *x* of the coordinate system whose origin is the shear centre of the core—which now is the whole bracing system—and therefore there is a coupling of lateral vibration in direction *y* and pure torsional vibration. One of the frequencies (f_φ) is much smaller than the other. In such cases it is favourable to use the approximate formulae for taking into account the effect of coupling as they offer a very simple solution with good accuracy. Hence

$$f_y = \left(\frac{1}{f_y^2} + \frac{1}{f^2}\right)^{-\frac{1}{2}} = \left(\frac{1}{1.36^2} + \frac{1}{0.125^2}\right)^{-\frac{1}{2}} = 0.124 \text{ Hz} \qquad \{4.36\}$$

This frequency is smaller than that of lateral vibration in direction *x*, so the fundamental frequency of the building is

$$f = \text{Min!}\ f_x,\ f_y\ = 0.124\ \text{Hz} \qquad \{4.37\}$$

This is a very small value considering other buildings of similar size and mass.

12.2.1.3 Global critical load and critical load ratio

The critical load for sway buckling in direction *x* is calculated using the relevant second moment of area of the core:

$$N_{cr,x} = \frac{7.837 EI_y r_s}{H^2} = \frac{7.837 \cdot 23 \cdot 10^3 \cdot 2.466 \cdot 0.759}{15^2} = 1499\ \text{MN} \qquad \{2.92\}$$

In a similar way, the sway buckling load in direction *y* is

$$N_{cr,y} = \frac{7.837 EI_x r_s}{H^2} = \frac{7.837 \cdot 23 \cdot 10^3 \cdot 2.045 \cdot 0.759}{15^2} = 1244\ \text{MN} \qquad \{2.92\}$$

The critical load of pure torsional buckling is obtained using the formula given for a single core but with the radius gyration that relates to the whole layout area as the load is distributed over the whole floor area of the building. The radius of gyration is

$$i_p = \sqrt{\frac{L^2 + B^2}{12} + t^2} = \sqrt{\frac{L^2 + B^2}{12} + x_c^2} = \sqrt{\frac{26^2 + 14^2}{12} + 11^2} = 13.92\ \text{m} \qquad \{5.28\}$$

The non-dimensional parameter

$$k_s = H\sqrt{\frac{GJ}{r_s EI_\Omega}} = 15\sqrt{\frac{9580 \cdot 0.024}{0.759 \cdot 23000 \cdot 2.51}} = 1.086 \qquad \{2.95\}$$

is also needed as the critical load parameter α is obtained as a function of k_s:

$$= 10.77 + \frac{11.37 - 10.77}{1.1 - 1.0}(1.086 - 1.0) = 11.286 \qquad \{\text{Table 2.10}\}$$

The critical load for pure torsional buckling is now obtained as

$$N_{cr,} = \frac{r_s EI_\Omega}{i_p^2 H^2} = \frac{11.286 \cdot 0.759 \cdot 23 \cdot 10^3 \cdot 2.51}{13.92^2 \cdot 15^2} = 11.3\ \text{MN} \qquad \{2.94\}$$

When the coupling of the basic critical loads is considered, the situation is similar to that of vibration. There is a coupling of sway buckling in direction *y* and pure torsional buckling. One of the critical loads ($N_{cr,\varphi}$) is much smaller than the other one and the relevant summation formula is used:

$$N_y = \left(\frac{1}{N_{cr,y}} + \frac{1}{N_{cr,}} \right)^{-1} = \left(\frac{1}{1244} + \frac{1}{11.3} \right)^{-1} = 11.2 \text{ MN} \qquad \{5.44\}$$

This critical load is smaller than that of sway buckling in direction *x*, so the critical load of the building is

$$N_{cr} = \text{Min! } N_{cr,x}, N_y = 11.2 \text{ MN} \qquad \{5.45\}$$

The total vertical load on the five floors is

$$N = LBQn = 26 \cdot 14 \cdot 0.008 \cdot 5 = 14.56 \text{ MN} \qquad \{6.2\}$$

and the global critical load ratio

$$= \frac{N_{cr}}{N} = \frac{11.2}{14.56} = 0.8 \qquad \{6.3\}$$

reveals an unstable building.

The bracing of the building is totally unacceptable and the examination of the relevant figures related to the top deflection, fundamental frequency and stability points to a weak torsional performance. The torsional resistance of the building is small, for two reasons. One, the torsional stiffness of the core is small and two, the distance between the centroid of the layout and the shear centre is great.

In the following section an attempt is made to remedy the situation by moving the core to a more favourable position.

12.2.2 Layout B: open core in the centre of the layout

The bracing core is moved to the centre in such a way that its shear centre and the centroid of the layout coincide (Figure 12.6).

The geometrical and stiffness characteristics of this case are collected in the second row in Table 12.2 in the previous section.

12.2.2.1 Maximum rotation and deflection

As the resultant of the wind load passes through the shear centre, there is no rotation around the shear centre:

$$= 0 \qquad \{2.89\}$$

It also follows that the deflection of the building is entirely made up from the uniform part of the deflection. This was calculated in the previous case so the top deflection of the building is readily available as

$$v_{\max} = v_o + \quad x_{\max} = 0.0035 + 0 = 0.0035\,\text{m} \qquad \{3.36\}$$

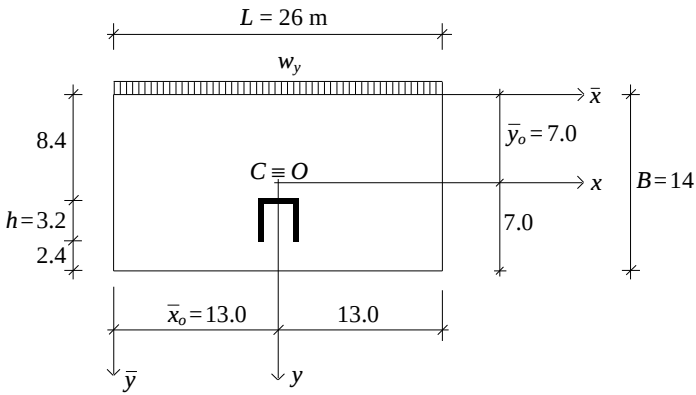

Figure 12.6 Kollár's building. Layout B: bracing core in the centre.

12.2.2.2 Fundamental frequency

By moving the core to the centre, the values of the lateral vibration in the principal directions do not change and the results obtained in the previous section hold:

$$f_x = \frac{0.56 r_f}{H^2}\sqrt{\frac{EI_y}{m}} = 1.50\,\text{Hz} \qquad \{2.97\}$$

and

$$f_y = \frac{0.56 r_f}{H^2}\sqrt{\frac{EI_x}{m}} = 1.36\,\text{Hz} \qquad \{2.97\}$$

The situation is different when the torsional behaviour is considered. The distance between the shear centre and the centroid of the mass is now reduced to zero and this fact alters the value of the radius of gyration:

$$i_p = \sqrt{\frac{L^2 + B^2}{12} + t^2} = \sqrt{\frac{26^2 + 14^2}{12} + 0} = 8.52\,\text{m} \qquad \{4.20\}$$

The frequency parameter is unchanged at $\eta_\varphi = 0.647$ and the pure torsional frequency is

$$f_{\Omega} = \frac{r_f}{i_p H^2}\sqrt{\frac{EI_{\Omega}}{m}} = \frac{0.647 \cdot 0.842}{8.52 \cdot 15^2}\sqrt{\frac{23 \cdot 10^6 \cdot 2.51}{111.3}} = 0.205\,\text{Hz} \qquad \{2.98\}$$

As the centroid and the shear centre coincide, there is no coupling among the two lateral and pure torsional vibrations and the fundamental frequency is the smallest one of the three:

$$f = \text{Min!}\ f_x,\ f_y,\ f_{\Omega} = 0.205\,\text{Hz} \qquad \{4.38\}$$

12.2.2.3 Global critical load and critical load ratio

The situation concerning stability is very similar to that of vibration. The sway critical loads are unchanged from the previous case at

$$N_{cr,x} = \frac{7.837 EI_y r_s}{H^2} = 1499\,\text{MN} \qquad \{2.92\}$$

and

$$N_{cr,y} = \frac{7.837 EI_x r_s}{H^2} = 1244\,\text{MN} \qquad \{2.92\}$$

but, due to the change in the value of the radius of gyration, the value of pure torsional buckling changes. With $\alpha = 11.286$, determined in the previous case, the pure torsional critical load is

$$N_{cr,\Omega} = \frac{r_s EI_{\Omega}}{i_p^2 H^2} = \frac{11.286 \cdot 0.759 \cdot 23 \cdot 10^3 \cdot 2.51}{8.52^2 \cdot 15^2} = 30.3\,\text{MN} \qquad \{2.94\}$$

As there is no coupling, this is also the global critical load of the building:

$$N_{cr} = \text{Min!}\ N_{cr,x}, N_{cr,y}, N_{cr,\Omega} = N_{cr,\Omega} = 30.3\,\text{MN} \qquad \{5.46\}$$

To sum it up, everything has improved compared to the previous case: the maximum deflection decreased enormously, the fundamental frequency increased and the critical load also increased nearly three-fold. The global critical load ratio reflects these favourable changes:

$$= \frac{N_{cr}}{N} = \frac{30.3}{14.56} = 2.1 \qquad \{6.3\}$$

However, although the building is now theoretically stable, the value of the global critical load ratio is far from the recommended value of $\lambda = 10$ [Equation (6.5)].

As mentioned above in connection with Layout A, the poor torsional performance of the building was caused by the small torsional stiffness of the core and the relatively great distance between the centroid of the layout and the shear centre.

The situation has improved by moving the core to the centre but the improvement is not big enough. In the following section another attempt is made to remedy the original situation by increasing the torsional stiffness of the core (while leaving the core at its original position).

12.2.3 Layout C: partially closed core in the right-hand side of the layout

In practical situations it is normally possible and feasible to close the U-core partially. It is done in this case by adding small lip-sections and connecting the wall sections at the opening by beams at floor levels (Figure 12.7/b). The thickness and the depth of the connecting beams are t_b = 0.20 m and d = 0.65 m. The distance of the connecting beams is equal to the storey height: s = 3 m.

Due to this alteration, the value of the second moments of area of the core slightly changes. The value of the warping constant dramatically decreases and, as a conservative estimate, it is ignored in the following calculation. The lips add a little to the value of the original Saint-Venant torsional constant:

$$J = \frac{1}{3}\sum_{i=1}^{m} h_i t_i^3 = \frac{0.2^3}{3}(2 \cdot 3.1 + 2.6 + 2 \cdot 0.4) = 0.026\,\mathrm{m}^4 \qquad \{2.75\}$$

Because of the partial closure, however, the value of the Saint-Venant torsional constant drastically increases. This increase is calculated according to Vlasov (1961) as

$$\bar{J} = \frac{4A_o^2}{\dfrac{l^3 sG}{12EI_b} + \dfrac{1.2ls}{A_b}} = \frac{4 \cdot 3.1^2 \cdot 2.6^2}{\dfrac{1.8^3 \cdot 3 \cdot 9580}{12 \cdot 23000 \cdot 0.004577} + \dfrac{1.2 \cdot 1.8 \cdot 3}{0.13}} = 1.424\,\mathrm{m}^4 \qquad \{2.79\}$$

where

$$A_b = t_b d = 0.2 \cdot 0.65 = 0.13\,\mathrm{m}^2$$

and

$$I_b = \frac{t_b d^3}{12} = \frac{0.2 \cdot 0.65^3}{12} = 0.004577 \text{ m}^4$$

are the cross-sectional area and the second moment of area of the connecting beams.

The value of the total Saint-Venant constant is

$$J + \bar{J} = 0.026 + 1.424 = 1.45 \text{ m}^4$$

Because of the partial closure, the location of the shear centre of the core also changes. It is a move "backwards", definitely towards the centre of the core, but its exact value is very difficult to establish. Using an equivalent thickness of

$$t_w^* = \frac{d}{s} t_b = \frac{0.65}{3.0} 0.2 \cong 0.04 \text{ m} \qquad \{2.81\}$$

the computer program PROSEC (1994) gives

$$e = 0.30 \text{ m}$$

for the location of the shear centre (Figure 12.7/b). The geometrical and stiffness characteristics related to Layout C are collected in the third row of Table 12.2 in Section 12.2.1.

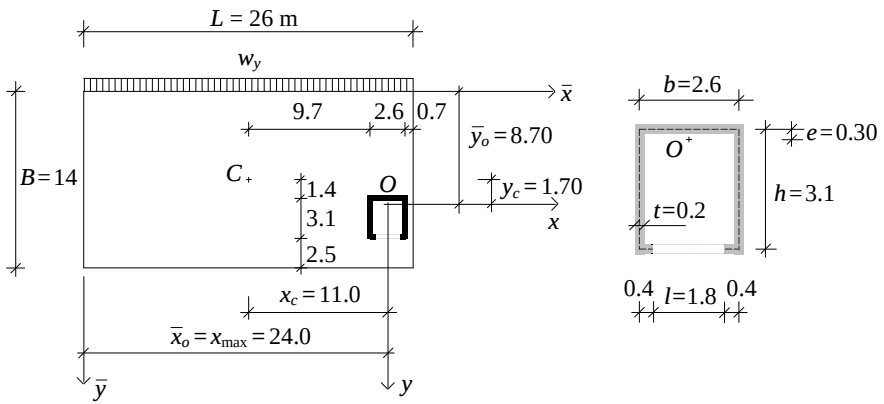

Figure 12.7 Kollár's building. a) Layout C, b) Partially closed core.

12.2.3.1 Maximum rotation and deflection

The situation is similar to the one with Layout A. Maximum deflection develops at the left-hand side of the building at $x_{max} = 24.0$. It consists of two parts. The building undergoes a uniform deflection of

$$v_o = v(H) = \frac{w_y H^4}{8EI_x} = \frac{26 \cdot 15^4}{8 \cdot 23 \cdot 10^6 \cdot 2.479} = 0.0029 \text{ m} \qquad \{2.83\}$$

The rotation around the shear centre

$$_{max} = \quad (H) = \frac{m_z H^2}{2GJ} = \frac{286 \cdot 15^2}{2 \cdot 9.58 \cdot 10^6 \cdot 1.45} = 0.00232 \qquad \{2.91\}$$

causes the second part of the deflection with a "torsion arm" of $x_{max} = 24.0$. The total deflection is

$$v_{max} = v(H) = v_o + \quad x_{max} = 0.0029 + 0.00232 \cdot 24$$

$$= 0.0029 + 0.0557 = 0.059 \text{ m} \qquad \{3.36\}$$

The recommended maximum deflection of the building is

$$v_{ASCE} = \frac{H}{500} = \frac{15}{500} = 0.030 \text{ m}$$

12.2.3.2 Fundamental frequency

The three basic frequencies are needed first.

The lateral frequencies in directions *x* and y are calculated using the formulae given for cores but with the mass density which relates to the whole building:

$$f_x = \frac{0.56 r_f}{H^2} \sqrt{\frac{EI_y}{m}} = \frac{0.56 \cdot 0.842}{15^2} \sqrt{\frac{23 \cdot 10^6 \cdot 2.599}{111.3}} = 1.536 \text{ Hz} \qquad \{2.97\}$$

and

$$f_y = \frac{0.56 r_f}{H^2} \sqrt{\frac{EI_x}{m}} = \frac{0.56 \cdot 0.842}{15^2} \sqrt{\frac{23 \cdot 10^6 \cdot 2.479}{111.3}} = 1.50 \text{ Hz} \qquad \{2.97\}$$

The radius of gyration is

$$i_p = \sqrt{\frac{L^2 + B^2}{12} + t^2} = \sqrt{\frac{26^2 + 14^2}{12} + 11^2 + 1.70^2} = 14.0\,\text{m} \qquad \{4.20\}$$

The frequency of pure torsional vibration of the building is obtained using the formula given for a single core (with *GJ* only) but with the radius gyration that relates to the whole layout area as the mass is distributed over the whole floor area of the building:

$$f = \frac{1}{4Hi_p}\sqrt{\frac{GJ}{m}} = \frac{1}{4 \cdot 15 \cdot 14.0}\sqrt{\frac{9.58 \cdot 10^6 \cdot 1.45}{111.3}} = 0.421\,\text{Hz} \qquad \{2.99\}$$

There is a triple coupling and, as one of the basic frequencies is much smaller than the others, its effect can be approximated with good accuracy using the Föppl-Papkovich formula:

$$f = \left(\frac{1}{f_x^2} + \frac{1}{f_y^2} + \frac{1}{f^2}\right)^{-\frac{1}{2}} = \left(\frac{1}{1.536^2} + \frac{1}{1.50^2} + \frac{1}{0.421^2}\right)^{-\frac{1}{2}} = 0.392\,\text{Hz} \qquad \{4.35\}$$

12.2.3.3 Global critical load and critical load ratio

The critical load for sway buckling in direction *x* is calculated using the relevant second moment of area of the core:

$$N_{cr,x} = \frac{7.837EI_y r_s}{H^2} = \frac{7.837 \cdot 23 \cdot 10^3 \cdot 2.599 \cdot 0.759}{15^2} = 1580\,\text{MN} \qquad \{2.92\}$$

In a similar way, the sway buckling load in direction *y* is

$$N_{cr,y} = \frac{7.837EI_x r_s}{H^2} = \frac{7.837 \cdot 23 \cdot 10^3 \cdot 2.479 \cdot 0.759}{15^2} = 1507\,\text{MN} \qquad \{2.92\}$$

Torsion is resisted by the Saint-Venant torsional stiffness and the critical load of pure torsional buckling is

$$N_{cr,} = \frac{GJ}{i_p^2} = \frac{9580 \cdot 1.45}{14.0^2} = 70.9\,\text{MN} \qquad \{2.96\}$$

Because of the triple coupling, this critical load is reduced and the global critical load of the building is

$$N_{cr} = \left(\frac{1}{N_{cr,x}} + \frac{1}{N_{cr,y}} + \frac{1}{N_{cr,}} \right)^{-1} = \left(\frac{1}{1580} + \frac{1}{1507} + \frac{1}{70.9} \right)^{-1} = 64.9 \text{ MN} \quad \{5.43\}$$

The global critical load ratio

$$= \frac{N_{cr}}{N} = \frac{64.9}{14.56} = 4.5 \quad \{6.3\}$$

shows a stable structure but the recommended margin is not yet achieved. (The maximum deflection also exceeds the recommended value.) However, the situation can further be improved.

12.2.4 Layout D: partially closed core in the centre of the layout

In combining the previous two actions, the partially closed core is now moved to the centre in such a way that its shear centre and the centroid of the layout coincide (Figure 12.8).

The geometrical and stiffness characteristics of this case are collected in the fourth row in Table 12.2 in Section 12.2.1.

12.2.4.1 Maximum rotation and deflection

As the resultant of the wind load passes through the shear centre, there is no rotation around the shear centre:

$$= 0 \quad \{2.89\}$$

It also follows that the deflection of the building is entirely made up from the uniform part of the deflection. This was calculated in the previous case so the top deflection of the building is readily available as

$$v_{\max} = v_o + \quad x_{\max} = 0.0029 + 0.0 = 0.0029 \text{ m} \quad \{3.36\}$$

12.2.4.2 Fundamental frequency

By moving the core to the centre, the values of the lateral vibration do not change and the results obtained in the previous section hold:

$$f_x = \frac{0.56 r_f}{H^2} \sqrt{\frac{EI_y}{m}} = 1.536 \text{ Hz} \quad \{2.97\}$$

and

$$f_y = \frac{0.56 r_f}{H^2}\sqrt{\frac{EI_x}{m}} = 1.50 \text{ Hz} \qquad \{2.97\}$$

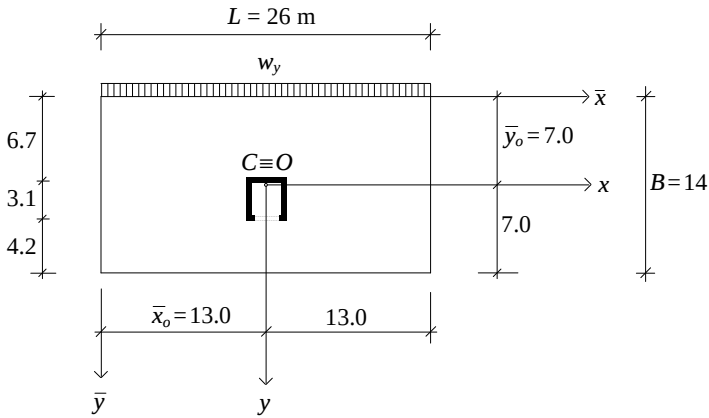

Figure 12.8 Kollár's building. Layout D: partially closed core in the centre.

The situation is different when the torsional behaviour is considered. The distance between the shear centre and the centroid of the mass is now reduced to zero and this fact alters the value of the radius of gyration:

$$i_p = \sqrt{\frac{L^2 + B^2}{12} + t^2} = \sqrt{\frac{26^2 + 14^2}{12} + 0} = 8.52 \text{ m} \qquad \{4.20\}$$

The pure torsional frequency is

$$f = \frac{1}{4Hi_p}\sqrt{\frac{GJ}{m}} = \frac{1}{4 \cdot 15 \cdot 8.52}\sqrt{\frac{9.58 \cdot 10^6 \cdot 1.45}{111.3}} = 0.691 \text{ Hz} \qquad \{2.99\}$$

As the centroid and the shear centre coincide, there is no coupling among the two lateral and pure torsional vibrations and the fundamental frequency is the smallest of the three:

$$f = \text{Min!}\ f_x,\ f_y,\ f = 0.691 \text{ Hz} \qquad \{4.38\}$$

12.2.4.3 Global critical load and critical load ratio

The situation concerning stability is very similar to that of vibration. The sway critical loads are unchanged from the previous case at

$$N_{cr,x} = \frac{7.837 EI_y r_s}{H^2} = 1580 \text{ MN} \qquad \{2.92\}$$

and

$$N_{cr,y} = \frac{7.837 EI_x r_s}{H^2} = 1507 \text{ MN} \qquad \{2.92\}$$

but, due to the change in the value of the radius of gyration, the value of pure torsional buckling changes:

$$N_{cr,} = \frac{GJ}{i_p^2} = \frac{9580 \cdot 1.45}{8.52^2} = 191 \text{ MN} \qquad \{2.96\}$$

As there is no coupling, this, being the smallest one of the three basic critical loads, is also the global critical load of the building:

$$N_{cr} = \text{Min!}\, N_{cr,x}, N_{cr,y}, N_{cr,} = N_{cr,} = 191 \text{ MN} \qquad \{5.46\}$$

To sum it up, everything has improved compared to the previous case: the maximum deflection decreased enormously, the fundamental frequency increased and the critical load also increased nearly three-fold. The global critical load ratio reflects these favourable changes:

$$= \frac{N_{cr}}{N} = \frac{191}{14.56} = 13 \qquad \{6.3\}$$

The results of the four arrangements are collected in Table 12.3.

Table 12.3 Kollár's building: a summary.

Layout	maximum rotation [°]	maximum deflection [mm]	fundamental frequency [Hz]	global critical load [MN]	global critical load ratio [-]
"A"	1.3	564	0.124	11.2	0.8
"B"	0	3.5	0.205	30.3	2.1
"C"	0.13	59	0.391	64.9	4.5
"D"	0	2.9	0.691	191	13

Appendix:

List of worksheets

The following sixteen downloadable Mathcad worksheets accompany the book and can be downloaded at www.crcpress.com/product/isbn/9780415595735. The worksheets cover the worked examples in Chapters 7, 8, 9, 10, 11 and 12. Mathcad Plus 6.0 (MathSoft, 1995) was used for producing the Filename.mcd files. According to support staff at Adept Scientific in June 2011, all versions (6.0 and higher) of Mathcad can open these Mathcad 6.0 files and will update them for ongoing use.

7_1DeflectionF6.mcd (Maximum deflection of 34-storey frame F6)
The worksheet calculates the maximum deflection of a three-bay sway frame under uniformly distributed horizontal load. In modifying the input data (modulus of elasticity, number/size of bays, number of storeys, storey height, size of the cross-sections of the columns/beams, intensity of the horizontal load), the maximum deflection of any multi-storey framework on fixed supports can be determined at once. The worksheet also produces the deflection shape of the structure.

7_2FrequencyF5.mcd (Fundamental frequency of 40-storey frame F5)
The worksheet calculates the fundamental frequency of a two-bay sway frame subjected to uniformly distributed mass on floor levels. In modifying the input data (modulus of elasticity, number/size of bays, number of storeys, storey height, size of the cross-sections of the columns/beams, magnitude of mass), the fundamental frequency of any multi-storey framework on fixed supports can be determined at once.

7_3StabFFSH1.mcd (Critical load of 7-bay, 12-storey framework FFSH1)
The worksheet calculates the global critical load and global critical load ratio of a seven-bay sway frame subjected to uniformly distributed vertical load on floor levels. In modifying the input data (modulus of elasticity, number/size of bays, number of storeys, storey height, size of the cross-sections of the columns/beams, intensity of vertical load), the global critical load and global critical load ratio of any multi-storey framework on fixed supports can be determined at once.

7_4StabSRX.mcd (Critical load of 8-storey framework SR-X with cross-bracing)
The worksheet calculates the global critical load of a single-bay framework with

cross-bracing subjected to uniformly distributed vertical load on floor levels. In modifying the input data (modulus of elasticity, number/size of bays, number of storeys, storey height, size of the cross-sections of the columns/beams/diagonals, type of cross-bracing), the global critical load of any multi-storey framework with cross-bracing can be determined at once.

7_5StabCSWSH3.mcd (Critical load of 18-storey, 2-bay coupled shear walls CSWSH3)
The worksheet calculates the global critical load of the eighteen storey, two-bay coupled shear walls subjected to uniformly distributed vertical load on floor levels. In modifying the input data (modulus of elasticity, number/size of bays, number of storeys, storey height, size of the cross-sections of the wall-sections/beams), the global critical load of any multi-storey, multi-bay coupled shear walls can be determined at once. When modifying the input data, attention should be paid to the calculation of the shear stiffness (K_b and K_c) as the structure in the worked example has wall sections of different size.

8_1DeflBuildF5F11W3.mcd (Maximum deflection of 16-storey symmetric cross wall building 2F11+2F5+2W3)
The worksheet calculates the maximum deflection of a sixteen-storey symmetric building braced by two two-bay frameworks with cross-bracing, two two-bay sway frames and two shear walls, under uniformly distributed horizontal load. In modifying the input data (modulus of elasticity, number/size of bays, number of storeys, storey height, size of the cross-sections of the columns/beams/diagonals, size of shear wall, intensity of the horizontal load), and adding any number of new bracing units, the maximum deflection of any symmetric planar system of frameworks, coupled shear walls and shear walls can be determined at once.

8_2DeflBuildF1F5W4U.mcd (Maximum deflection of 28-storey building braced by 2F1+F5+2W4+U)
The worksheet calculates the deflection of and the rotation around the shear centre axis, then the maximum deflection of a twenty-eight storey building braced by two one-bay frameworks, one two-bay sway framework, two shear walls and one U-core, under uniformly distributed horizontal load. In modifying the input data (modulus of elasticity, number/size of bays, number of storeys, storey height, size of the cross-sections of the columns/beams, size of shear wall, size of U-core, size of layout, location of bracing units, intensity of the horizontal load), and adding any number of new bracing units, the maximum deflection of any system of frameworks, coupled shear walls, shear walls and cores can be determined at once.

9_1FreqSymmBuild.mcd (Fundamental frequency of doubly symmetric building)
The worksheet calculates the fundamental frequency of a thirty-storey doubly symmetric building braced by four two-bay frameworks and four shear walls. In modifying the input data (modulus of elasticity, number/size of bays, number of storeys, storey height, size of the cross-sections of the columns/beams, size of shear walls, size of layout, magnitude of mass), and adding new bracing units in a doubly symmetric arrangement, the fundamental frequency of any doubly symmetric building can be determined at once.

9_2FreqBuild.mcd (Fundamental frequency of 6-storey asymmetric building)
The worksheet calculates the fundamental frequency of a six-storey building braced by two infilled frameworks and two shear walls, vibrating in a three-dimensional manner. In modifying the input data (modulus of elasticity, number/size of bays, number of storeys, storey height, size of the cross-sections of the columns/beams, characteristics of the infill, size of shear walls, size of layout, location of bracing units, magnitude of mass), and adding any number of new bracing units, the fundamental frequency of any asymmetric building can be determined at once.

10_1StabSymmBuild.mcd (Stability of 30-storey doubly symmetric building)
The worksheet calculates the global critical load and the global critical load ratio of a thirty-storey doubly symmetric building braced by four two-bay frameworks and four shear walls. In modifying the input data (modulus of elasticity, number/size of bays, number of storeys, storey height, size of the cross-sections of the columns/beams, size of shear walls, size of layout, intensity of vertical load on floor levels), and adding any number of new bracing units in a doubly symmetric arrangement, the critical load of any doubly symmetric building can be determined at once.

10_2StabBuild.mcd (Stability of 6-storey Premier House)
The worksheet calculates the global critical load and the global critical load ratio of a six-storey asymmetric building braced by an infilled framework and a U-core, developing three-dimensional sway-torsional buckling. In modifying the input data (modulus of elasticity, characteristics of the infill, number/size of bays, number of storeys, storey height, size of the cross-sections of the columns/beams, size of U-core, size of layout, intensity of vertical load on floor levels), and adding any number of new bracing units, the global critical load and the global critical load ratio of any building can be determined at once.

11_Sheffield.mcd (Global structural analysis of 22-storey building braced by 4 cores and 4 frames)
The worksheet presents a comprehensive, global, three-dimensional structural analysis. It calculates the global critical load, the global critical load ratio, the fundamental frequency and the maximum rotation and deflection of the building. In modifying the input data (modulus of elasticity, number/size of bays, number of storeys, storey height, size of the cross-sections of the columns/beams, size of U-cores, size of layout, location of bracing units, intensity of vertical load on floor levels, intensity of horizontal load, magnitude of mass), and adding any number of new bracing units, the comprehensive analysis can be repeated for any multi-storey building in minutes.

12_1GlobalCase1.mcd; 12_1GlobalCase2.mcd; 12_1GlobalCase3.mcd
The three worksheets carry out a comprehensive global structural analysis of the same building. In the three cases the bracing system consists of the same bracing units (two one-bay steel frameworks with double bracing and two shear walls) but their arrangement is different. The global critical load, the fundamental frequency and the maximum rotation and deflection of the ten-storey building are calculated.

The global critical load ratio is used as a performance indicator to characterize the overall behaviour of the building. The worksheets can be used as templates for the global structural analysis of similar buildings.

12_2GlobalKollar.mcd (Kollár's 5-storey building)
The worksheet carries out four comprehensive global structural analyses. The five-storey building is the same, the bracing system—a single U-core—is nearly the same: in two cases it is open and in the other two cases it is partially closed. The other difference is the location of the core. The maximum rotation and deflection, the fundamental frequency, global critical load and the global critical load ratio are determined. The global critical load ratio is used as a performance indicator to characterize the overall behaviour and structural suitability of the building.

References

Achyutha, H., Injaganeri, S.S., Satyanarayanan, S. and Krishnamoorthy, C.S., 1994, Inelastic behaviour of brick infilled reinforced concrete frames. *Journal of Structural Engineering*, **21**, No. 2, pp. 107–115.

Allen, H.G., 1969, *Analysis and design of structural sandwich panels*, (Oxford: Pergamon Press).

Armer, G.S.T. and Moore, D.B., 1994, Full-scale testing on complete multi-storey structures. *The Structural Engineer*, **72**, (2), pp. 30–31.

AXIS VM., 2003, Finite Element Program for Structural Analysis. Version 7. User's Manual, (Highlands Ranch (CO): Civilex, Inc.).

Barkan, D.D., 1962, *Dynamics of bases and foundations*, (London: McGraw-Hill).

Beck, H., 1956, Ein neues Berechnungsverfahren für gegliederte Scheiben, dargestellt am Beispiel des Vierendelträgers. *Der Bauingenieur*, **31**, pp. 436–443.

Brohn, D.M., 1996, Avoiding CAD: The Computer Aided Disaster. Symposium: Safer computing. *The Institution of Structural Engineers*, 30 January 1996.

Chitty, L., 1947, On the cantilever composed of a number of parallel beams interconnected by cross bars. *Philosophical Magazine*, London. Ser. 7, Vol. XXXVIII, pp. 685–699.

Chitty, L. and Wan, W.Y., 1948, Tall building structures under wind load. *Proceedings of the 7th International Congress for Applied Mechanics*. London, 22 January 1948, pp. 254–268.

Chwalla, E., 1959, Die neuen Hilfstafeln zur Berechnung von Spannungs-problemen der Theorie zweiter Ordnung und von Knickproblemen. *Bauingenieur*, **34**, (4, 6 and 8), p128, p240 and p299.

Coull, A., 1975, Free vibrations of regular symmetrical shear wall buildings. *Building Science*, **10**, pp. 127–133.

Coull, A., 1990, Analysis for structural design. In *Tall Buildings: 2000 and Beyond*. Council on Tall Buildings and Urban Habitat, pp. 1031–1047.

Coull, A. and Wahab, A.F.A., 1993, Lateral load distribution in asymmetrical tall building structures. *Journal of Structural Engineering, ASCE*, **119**, pp. 1032–1047.

Council on Tall Buildings, 1978, *Planning and Design of Tall Buildings*, a Monograph in 5 volumes, (New York: ASCE).

Csonka, P., 1950, *Eljárás elmozduló sarkú derékszögű keretek számítására* (*Procedure for rectangular sway frames*). (Budapest: Tudományos Könyvkiadó Vállalat).

Danay, A., Glück, J. and Gellert, M., 1975, A generalized continuum method for dynamic analysis of asymmetric tall buildings. *Earthquake Engineering and Structural Dynamics*, **4**, pp. 179–203.

Despeyroux, J., 1972, Analyse statique et dynamique des contraventments par consoles. *Annales de l'Institut Technique du Bâtiment et des Travaux Publics*, No. 290.

Dowrick, D.J., 1976, Overall stability of structures. *The Structural Engineer*, **54**, pp. 399–409.

Ellis, R.B., 1980, An assessment of the accuracy of predicting the fundamental natural frequencies of buildings. *Proceedings of The Institution of Civil Engineers*, **69**, Part 2, September, pp. 763–776.

Ellis, R.B., 1986, The significance of dynamic soil-structure interaction in tall buildings. *Proceedings of The Institution of Civil Engineers*, **81**, Part 2, pp. 221–242.

EN 1992 (Eurocode 2), 2004, *Design of concrete structures*. (European Committee of Standardization).

EN 1993 (Eurocode 3), 2004, *Design of steel structures*. (European Committee of Standardization).

Fintel, M. (editor), 1974, *Handbook of concrete engineering*, (London: Van Nostrand Reinhold).

Gluck, J. and Gellert, M., 1971, On the stability of elastically supported cantilever with continuous lateral restraint. *International Journal of Mechanical Sciences*, **13**, pp. 887–891.

Glück, J., Reinhorn, A. and Rutenberg, A., 1979, Dynamic torsional coupling in tall building structures. *Proceedings of The Institution of Civil Engineers*, **67**, Part 2, pp. 411–424.

Goldberg, J.E., 1973, Approximate methods for stability and frequency analysis of tall buildings. *Regional Conference on Planning and Design of Tall Buildings*, Madrid, pp. 123–146.

Goschy, B., 1970. Räumliche Stabilität von Groβtafelbauten (Spatial stability of system buildings). *Die Bautechnik*, **47**, pp. 416–425.

Halldorsson, O.P. and Wang, C.K., 1968, Stability analysis of frameworks by matrix methods. *Journal of the Structural Division, ASCE*, **94**, ST7, p. 1745.

Hegedűs, I. and Kollár, L.P., 1984, Buckling of sandwich columns with thick faces subjecting to axial loads of arbitrary distribution. *Acta Technica Scientiarum Hungaricae*, **97**, pp. 123–132.

Hegedűs, I. and Kollár, L.P., 1999, Application of the sandwich theory in the stability analysis of structures. In *Structural stability in engineering practice*, edited by Kollár, L., (London: E & FN Spon), pp. 187–241.

Hoenderkamp, J.C.D., 1995, Approximate deflection analysis of non-symmetric high-rise structures. In *Habitat and the high-rise – Tradition and innovation. Proceedings of the Fifth World Congress*, edited by Lynn S. Beedle, (Bethlehem: Council on Tall Buildings and Urban Habitat, Lehigh University), pp. 1185–1209.

Hoenderkamp, J.C.D. and Stafford Smith, B., 1984, Simplified analysis of symmetric tall building structures subject to lateral loads. *Proceedings of the 3rd International Conference on Tall Buildings*, Hong Kong and Gaungzhou, pp. 28–36.

Howson, P., 2006, Global analysis: Back to the future. *The Structural Engineer*, **84**, (3), pp. 18–21.

Howson, W.P. and Rafezy, B., 2002, Torsional analysis of asymmetric

proportional building structures using substitute plane frames. *Proceedings of the 3rd International Conference on Advances in Steel Structures*, Volume II, (Hong Kong: Elsevier), pp. 1177–1184.

Irwin, A.W., 1984, *Design of shear wall buildings*, Report 102, (London: Construction Industry Research and Information Association).

Jeary, A.P. and Ellis, B.R., 1981, The accuracy of mathematical models of structural dynamics. *International Seminar on Dynamic Modelling*, (Watford, UK: Building Research Establishment/The Institution of Civil Engineers), PD112/81.

Kollár, L., 1977, Épületek merevítése elcsavarodó kihajlás ellen (Bracing of buildings against torsional buckling), *Magyar Építőipar*, pp. 150–154.

Kollár, L. (editor), 1999, *Structural stability in engineering practice*, (London: E & FN Spon).

Kollár, L.P., 1986, Buckling analysis of coupled shear walls by the multi-layer sandwich model. *Acta Technica Scientiarum Hungaricae*, **99**, pp. 317–332.

Kollár, L.P., 1992, Calculation of plane frames braced by shear walls for seismic load. *Acta Technica Scientiarum Hungaricae*, **104**, (1–3), pp. 187–209.

Kollbrunner, C.F. and Basler, K., 1969, *Torsion in structures*, (Berlin, New York: Springer-Verlag).

MacLeod, I.A., 1971, *Shear wall – frame interaction*. Special Publication. (Stokie, IL: Portland Cement Association).

MacLeod, I.A., 1990, *Analytical modelling of structural systems*, (London: Ellis Horwood).

MacLeod, I.A., 2005, *Modern structural analysis. Modelling process and guidance*, (London: Thomas Telford).

MacLeod, I.A. and Marshall, J., 1983, Elastic stability of building structures. *Proceedings of 'The Michael R. Horne Conference: Instability and plastic collapse of steel structures'*, edited by Morris, L.J. (London: Granada), pp. 75–85.

MacLeod, I.A. and Zalka, K.A., 1996, The global critical load ratio approach to stability of building structures. *The Structural Engineer*, **74**, (15), pp. 249–254.

Madan, A., Reinhorn, A.M., Mander, J.B. and Valles, R.E., 1997, Modeling of masonry infill panels for structural analysis. *Journal of Structural Engineering, ASCE*, **123**, (10), pp. 1295–1302.

Martin, L. and Purkiss, J., 2008, *Structural design of steelwork to EN 1993 and EN 1994*, (Oxford: Butterworth-Heinemann).

Mainstone, R.J. and Weeks, G.A., 1972, *The influence of a bounding frame on the racking stiffness and strengths of brick walls*, (Watford: Building Research Station, Current Paper 3/72).

MathSoft, 1995, Mathcad Plus 6.0.

Nadjai, A. and Johnson, D., 1998, Torsion in tall buildings by a discrete force method. *Structural Design of Tall Buildings*, **7**, (3), pp. 217–231.

Ng, S.C. and Kuang, J.S., 2000, Triply coupled vibration of asymmetric wall-frame structures. *Journal of Structural Engineering, ASCE*, **126**, No. 8, pp. 982–987.

Pearce, D.J. and Matthews, D.D., 1971, *Shear walls. An appraisal of their design in box-frame structures*, (London: Property Services Agency, Department of the Environment).

Plantema, F.J., 1961, *Sandwich construction. The bending and buckling of sandwich beams, plates and shells*, (London: McGraw-Hill).

Polyakov, S.V., 1956, *Kamennaya Kladka v Karkasnykh zdaniyakh. Issledovanie prochnosti i zhestkosti kamennogo zapolneniya,* (Moscow). (*Masonry in framed buildings. An investigation into the strength and stiffness of masonry infilling*). English translation by G. L. Cairns, National Lending Library for Science and Technology, Boston, Yorkshire, England, 1963.

Potzta, G. and Kollár, L.P., 2003, Analysis of building structures by replacement sandwich beams. *Solids and Structures*, **40**, pp. 535–553.

PROSEC, 1994, Section Properties, version 4.05 or higher, (London: PROKON Software Consultants Ltd).

Riddington, J.R. and Stafford Smith, B., 1977, Analysis of infilled frames subject to racking with design recommendations. *The Structural Engineer*, **55**, pp. 263–268.

Rosman, R., 1960, Beitrag zur statischen Berechnung waagerecht belasteter Querwände bei Hochbauten (On the structural analysis of tall cross-wall buildings under horizontal load). *Der Bauingenieur*, **4**, pp. 133–141.

Rosman, R., 1973, Dynamics and stability of shear wall building structures. *Proceedings of The Institution of Civil Engineers*, Part 2, **55**, pp. 411–423.

Rosman, R., 1974, Stability and dynamics of shear-wall frame structures. *Building Science*, **9**, pp. 55–63.

Rosman, R., 1981, Buckling and vibrations of spatial building structures. *Engineering Structures*, **3**, (4), pp. 194–202.

Rutenberg, A., 1975, Approximate natural frequencies of coupled shear walls. *Earthquake Engineering and Structural Dynamics*, **4**, pp. 95–100.

Schueller, W., 1977, *High-rise building structures,* (New York: John Wiley & Sons).

Schueller, W., 1990, *The vertical building structure*, (New York: Van Nostrand Reinhold).

Seaburg, P.A. and Carter, C.J., 2003, *Torsional analysis of structural steel members (Design Guide 9)*, (Chicago, IL: American Institute of Steel Construction).

Smart, R.A., 1997, Computers in the design office: boon or bane. *The Structural Engineer*, **75**, (3), p. 52.

Southwell, R.V., 1922, On the free transverse vibration of a uniform circular disc clamped at its centre; and on the effects of rotation. *Proceedings of the Royal Society of London. Ser. A*, **101**, pp. 133–153.

Stafford Smith, B., 1966, The composite behaviour of infilled frames. In *Proceedings of a Symposium on Tall Buildings with particular reference to shear wall structures*, edited by Coull, A. and Stafford Smith, B., University of Southampton, Department of Civil Engineering. (Oxford: Pergamon Press), pp. 481–492.

Stafford Smith, B. and Carter, C., 1969, A method of analysis for infilled frames. *Proceedings of the Institution of Civil Engineers*, **44**, pp. 31–48.

Stafford Smith, B. and Coull, A., 1991, *Tall building structures. Analysis and design*, (New York: John Wiley & Sons), pp. 213–282 and 372–387.

Stafford Smith, B., Kuster, M. and Hoenderkamp, J.C.D., 1981, Generalized approach to the deflection analysis of braced frame, rigid frame and coupled

shear wall structures. *Canadian Journal of Civil Engineers*, **8**, (2), pp. 230–240.
Stevens, L.K., 1983, The practical significance of the elastic critical load in the design of frames. *Proceedings of 'The Michael R. Horne Conference: Instability and plastic collapse of steel structures'*, edited by Morris, L.J., (London: Granada), pp. 36–46.
Tarnai, T., 1999, Summation theorems concerning critical loads of bifurcation. In *Structural stability in engineering practice*, edited by Kollár, L., (London: E & FN Spon), pp. 23–58.
Timoshenko, S., 1928, *Vibration problems in engineering*, (London: D. Van Nostrand Company, Inc).
Vértes, G., 1985, *Structural dynamics*, (New York: Elsevier).
Vlasov, V.Z., 1961, *Tonkostennye uprugie sterzhni* (*Thin-walled elastic beams*), (Jerusalem: Israeli Program for Scientific Translations).
Zalka, K.A., 1994, *Dynamic analysis of core supported buildings*, N127/94, (Watford, UK: Building Research Establishment).
Zalka, K.A., 1999, Full-height buckling of frameworks with cross-bracing. *Structures and Buildings. Proceedings of The Institution of Civil Engineers*, **134**, pp. 181–191.
Zalka, K.A., 2000, *Global structural analysis of buildings*, (London: E & FN Spon).
Zalka, K.A., 2001, A simplified method for the calculation of the natural frequencies of wall-frame buildings. *Engineering Structures*, **23**, No. 12, pp. 1544–1555.
Zalka, K.A., 2002, Buckling analysis of buildings braced by frameworks, shear walls and cores. *The Structural Design of Tall Buildings*, **11**, No. 3, 197–219.
Zalka, K.A., 2009, A simple method for the deflection analysis of tall wall-frame building structures under horizontal load. *The Structural Design of Tall and Special Buildings*, **18**, No. 3, 291–311.
Zalka, K.A., 2010, Torsional analysis of multi-storey building structures under horizontal load. *The Structural Design of Tall and Special Buildings*, online: 1 Dec 2010, doi:10.1002/tal.665.
Zalka, K.A. and Armer, G.S.T., 1992, *Stability of large structures*, (Oxford: Butterworth-Heinemann).
Zbirohowski-Koscia, K., 1967, *Thin walled beams. From theory to practice*, (London: Crosby Lockwood and Son).

A sound and more modern Eurocode-based approach to design is the global approach, as opposed to the traditional element-based design procedures. The global approach considers the structures as whole units. Although large frameworks and even whole buildings are now routinely analysed using computer packages, structural engineers do not always understand complex three-dimensional behaviour, which is essential to manipulate the stiffness and the location of the bracing units to achieve an optimum structural arrangement.

With coverage of theoretical background and worked examples, **Structural Analysis of Regular Multi-Storey Buildings** offers useful tools to researchers and practicing structural engineers. It can be used to carry out the planar stress, stability and frequency analysis of individual bracing units such as frameworks, coupled shear walls and cores. In addition, and perhaps more importantly, it can be used for the three-dimensional stress, stability and frequency analysis of whole buildings consisting of such bracing units.

The book includes closed-form solutions useful at the preliminary design stage when quick checks are needed with different structural arrangements. Their usefulness cannot be overemphasized for checking the results of a finite element (computer-based) analysis when the input procedure involves tens of thousands of items of data and where mishandling one item of data may have catastrophic consequences.

In addition to the critical load, the fundamental frequency, the maximum stresses, and the top deflection of frameworks, coupled shear walls, cores and their spatial assemblies, the book discusses the *global safety factor* of the structure, which also acts as the performance indicator of the structure. MathCAD worksheets can be downloaded from the book's accompanying website **(www.crcpress.com/product/isbn/9780415595735)**. These one- to eight-page-long worksheets cover a very wide range of practical application and can also be used as templates for other similar structural engineering situations.

CRC Press
Taylor & Francis Group
an **informa** business
www.taylorandfrancisgroup.com

6000 Broken Sound Parkway, NW
Suite 300, Boca Raton, FL 33487
711 Third Avenue
New York, NY 10017
2 Park Square, Milton Park
Abingdon, Oxon OX14 4RN, UK

Y111194
ISBN: 978-0-415-59573-5
90000
9 780415 595735
www.crcpress.com